

**Scheduling, Spectrum Sensing and  
Cooperation in MU-MIMO Broadcast  
and Cognitive Radio Systems**

A thesis submitted to The University of Manchester for the

degree of

PhD

in the Faculty of Engineering and Physical Sciences

**2011**

**LINA JIN**

**SCHOOL OF ELECTRICAL AND  
ELECTRONIC ENGINEERING**

## Content

Content .....	2
List of tables .....	5
List of figures .....	6
Abstract .....	8
Declaration .....	9
Copyright statement .....	10
Acknowledgement .....	11
List of abbreviations .....	12
List of notations .....	14
Chapter 1 Introduction .....	16
1.1 Background .....	17
1.1.1 Communication channel, MIMO and MU-MIMO .....	17
1.1.2 Spectrum utilization – cognitive radio technique .....	24
1.2 Motivation .....	27
1.3 Outline of the thesis .....	29
Chapter 2 Literature review on wireless channel, MU-MIMO system and cognitive radio technology .....	31
2.1 Wireless radio channel and fading .....	31
2.1.1 Large-scale path loss .....	33
2.1.2 Small-scale fading and multipath .....	36
2.1.3 Rayleigh fading and Ricean fading .....	40
2.2 Performance measure of wireless communication systems .....	47
2.2.1 Capacity of wireless channel .....	47
2.2.2 Probability of message error and Bit Error Rate (BER) .....	48
2.3 Single user – MIMO system and channel capacity .....	49
2.3.1 Multiplexing gain and capacity of the MIMO channel .....	49
2.3.2 Space diversity gain and the capacity of MIMO beamforming 54	54
2.4 Multiuser MIMO channel capacity .....	60
2.4.1 Capacity of multiuser MIMO uplink channel .....	61
2.4.2 Capacity of multiuser MIMO broadcast (BC) downlink channel 64	64
2.4.3 Scheduling and linear transmission scheme in MU-MIMO BC systems .....	67
2.5 Cognitive radio technique in wireless network .....	70
2.5.1 Underlay .....	73
2.5.2 Overlay .....	73
2.5.3 Interweave .....	74
2.6 Summary .....	75
Chapter 3 Volume-based scheduling algorithm of MU-MIMO downlink channel 76	76
3.1 Introduction .....	76
3.2 System model, block diagonalisation (BD) and sum-rate capacity 78	78
3.3 Novel low complexity scheduling algorithms .....	81

## Contents

---

3.3.1	QR factorization procedures and complexity analysis.....	81
3.3.2	Details of the volume-based scheduling algorithm.....	84
3.4	Computational complexity analysis on volume-based, SUS and capacity-based scheduling algorithms.....	87
3.4.1	Complexity of five matrix operations .....	87
3.4.2	Complexity of volume-based, SUS and capacity-based scheduling algorithms .....	88
3.5	Simulation results.....	91
3.6	Summary .....	99
Chapter 4	Sum-rate gain for MU-MIMO downlink system with limited feedback and feedback resource constraint.....	100
4.1	Introduction .....	100
4.2	System model.....	105
4.2.1	Perfect channel information at the transmitter and the receiver	106
4.2.2	Perfect channel information at the receiver and the channel knowledge is available to the transmitter via feedback channel from the receiver to the transmitter.....	108
4.2.3	The two-step scheduling algorithm proposed for MU-MIMO downlink system with limited feedback and power allocation .....	110
4.3	The details of new two-step scheduling algorithm .....	111
4.3.1	Codebook design method: Random Vector Quantization (RVQ) and dominant eigenvector based LBG (DE-LBG) algorithm	112
4.3.2	The new proposed scheduling algorithm .....	115
4.4	Performance analysis .....	116
4.4.1	Sum-rate capacity analysis.....	117
4.5	Numerical results .....	123
4.6	Summary .....	128
Chapter 5	Signal detection scheme based on free probability theory in MIMO cognitive radio systems.....	129
5.1	Introduction.....	129
5.1.1	Energy detector based sensing .....	130
5.1.2	Waveform based sensing.....	133
5.1.3	Matched-filtering .....	134
5.2	A new signal detection scheme based on free probability theory for multiple-input multiple-output cognitive radio systems.....	135
5.2.1	MIMO cognitive radio system model and free probability theory	136
5.2.2	Free probability theory signal detection algorithm for MIMO cognitive radio systems .....	142
5.2.3	Simulation results.....	145
5.2.4	Summary .....	149
5.3	Cooperative FPT spectrum sensing technique in MIMO cognitive radio system .....	149
5.3.1	Introduction .....	149
5.3.2	System model.....	152
5.3.3	FPT detection and binary hypothesis test .....	154
5.3.4	Cooperative detection with false alarm rate constraint.....	156

## Contents

---

5.3.5	Simulation result .....	159
5.3.6	Summary .....	164
Chapter 6	Spectrum sensing based on higher-order statistics and receiver diversity in SIMO cognitive radio systems.....	165
6.1	Introduction.....	166
6.2	Spectrum sensing based on HOS .....	168
6.2.1	SIMO cognitive radio system model .....	168
6.2.2	Higher-order statistics .....	170
6.2.3	Proposed spectrum sensing based on third-order spectrum and receiver diversity .....	177
6.2.4	Simulation result .....	178
6.2.5	Summary .....	181
6.3	Cooperative detection based on HOS in SIMO cognitive radio systems .....	181
6.3.1	Multiuser cognitive radio system model.....	183
6.3.2	Hypothesis test at each secondary user .....	188
6.3.3	Cooperative detection.....	189
6.3.4	Simulation Result.....	194
6.3.5	Summary .....	198
Chapter 7	Conclusions & future work .....	200
Appendix	.....	208
Reference	.....	209

Word count: 48595

## List of tables

Table 3.1 Comparison of $QR$ procedures .....	82
Table 3.2 Complexity analysis on five matrix operations .....	88
Table 4.1 Summary of feedback load .....	127

## List of figures

Figure 1.1 General communication system.....	19
Figure 1.2 Wireless cellular system.....	19
Figure 1.3 A point-to-point MIMO wireless system.....	20
Figure 1.4 Multiuser MIMO downlink.....	24
Figure 1.5 Multiuser MIMO uplink. ....	24
Figure 1.6 Spectrum occupancy measurements [Ofcom, “Cognitive Radio,] in a rural area (top), near Heathrow airport (middle) and in central London (bottom).....	26
Figure 2.1 A wireless radio channel and signal multipath transmission. ....	31
Figure 2.2 Path loss in wireless radio channel. ....	34
Figure 2.3 Path loss and shadow fading in wireless radio channel .....	36
Figure 2.4 Channel characteristics in terms of channel impulse response: (a) Input signal $x(t)$ , output signal $y(t)$ and channel impulse response $h(t, \tau)$ , (b) Characteristics on time scale for flat fading, (c) Characteristics on time scale for frequency selective fading. ....	38
Figure 2.5 Diagram to demonstrate the Doppler Effect.....	39
Figure 2.6 Illustration of Rayleigh fading in wireless radio channel. Signal sample period is 1/10000 second, maximum Doppler shift is 100Hz and average path delay is 1.0000e-006 second.....	45
Figure 2.7 Illustration of Ricean fading in wireless radio channel. Signal sample period is 1/10000 second, Maximum Doppler Shift is 100Hz and K factor is 3...46	46
Figure 2.8 Decomposition of MIMO channel under the condition of perfect CSIT and CSIR.....	54
Figure 2.9 MIMO beamforming. ....	60
Figure 2.10 MU-MIMO channel: (a) Uplink, (b) Downlink.....	61
Figure 2.11 Capacity region of MIMO MAC system for two users. ....	63
Figure 2.12 Gaussian Shannon channel with Gaussian interference.....	65
Figure 2.13 Cognitive radio cycle.....	72
Figure 3.1 Sum-rate capacity versus the number of users. $8 \times 1$ MISO configuration. ....	93
Figure 3.2 Sum-rate capacity versus number of users. $4 \times 1$ MISO configuration. ....	93
Figure 3.3 Sum-rate capacity versus the number of users. $4 \times 2$ MIMO configuration.....	95
Figure 3.4 Sum-rate capacity versus the number of users. $6 \times 2$ MIMO configuration.....	95
Figure 3.5 Sum-rate capacity versus the number of users. $6 \times 3$ MIMO configuration.....	96
Figure 3.6 Average simulation time versus the number of users. $6 \times 3$ MIMO configuration. ....	98
Figure 4.1 MU-MIMO downlink system with limited feedback. The transmitter has $M$ antennas and each user terminal has one antenna. Each user has $B$ feedback bits.....	109
Figure 4.2 MU-MIMO downlink system with limited feedback. Two versions of the codebook are stored at the transmitter and the receiver.....	111
Figure 4.3 The sum-rate capacity versus SNR. There is total number of 4 users in the system and the user selection algorithm is not needed. 4 transmit antenna and 1 receive antenna per user terminal. BD precoding is applied. ....	124
Figure 4.4 Total number of 50 users is in the MISO downlink system. Antenna combination is 4 transmit antennas and 1 receive antenna per user terminal. The volume-based scheduling algorithm is applied. Maximum supportable users are 4. ....	125
Figure 4.5 Sum-rate capacity versus SNR. Total number of 50 users is in the MISO downlink system. Antenna combination is 4 transmit antennas and 1 receive antenna per user terminal. The two-step scheduling algorithm is applied. Maximum supportable users are 4.....	128
Figure 5.1 Cognitive radio system.....	137
Figure 5.2 Density function of Marčhenko-Pastur law. ....	140
Figure 5.3 The probability of detection versus SNR(dB) via FPT detection algorithm for MIMO cognitive radio system. Thresholds values $V_T$ are set to 0.90, 0.93,	

List of figures

---

0.95, 1.0 and 1.05. Corresponding $P_f$ values to $V_T$ are 0.655, 0.368, 0.204, 0.024, and 0.001.....	147
Figure 5.4 Performance comparison between FPT detector and energy detector when probabilities of false alarm are 0.2 and 0.66.....	148
Figure 5.5 Cognitive radio system.....	153
Figure 5.6 A cognitive radio parallel fusion network.....	157
Figure 5.7 ROC graph of FPT detector.....	160
Figure 5.8 Probability of detection versus SNR at transmitter (PU) in a cooperative cognitive radio system. ....	161
Figure 5.9 System false alarm rate versus number of secondary users. The false alarm rate for each SU is 0.0228 when the threshold for FPT detector is set to 1. ....	162
Figure 5.10 Probability of detection $P_d$ versus SNR at the transmitter (PU). ....	164
Figure 6.1 Cognitive radio system.....	169
Figure 6.2 SIMO system and receiver diversity.....	170
Figure 6.3 Probability of detection $P_d$ versus SNR at receiver, $P_f=0.04$ .....	179
Figure 6.4 Image of bispectrum magnitude of BPSK signal, carrier frequency is 4MHz. ....	180
Figure 6.5 Cognitive radio network with one primary user and a small number of secondary users.....	185
Figure 6.6 Cognitive Radio system with a large number of users. The SUs form a cluster in each sub-region and the cluster head in a sub-region serves as local fusion centre. ....	188
Figure 6.7 A cognitive radio parallel fusion network.....	190
Figure 6.8 A cognitive radio parallel fusion network, each SU sends his detection decision and detected SNR to central fusion centre. ....	192
Figure 6.9 CR network with a large number of users. $CH_i$ for $1 \leq i \leq Z$ - cluster head. $\delta_i = \{0,1\}$ for $1 \leq i \leq K$ - detect decision from $i$ th SU. $\delta_{CH_i} = \{0,1\}$ for $1 \leq i \leq Z$ - detect decision from $i$ th cluster head. $\delta_s = \{0,1\}$ - final detection decision from central fusion centre. ....	194
Figure 6.10 Probability of detection versus transmit power at transmitter (PU) in a CR network with a small number of users. All SUs detects and contributes to the final system-level detect decision. ....	196
Figure 6.11 Probability of detection versus transmit power at transmitter (PU) in the CR network with 2, 4, 8 secondary users. 2 users with highest received SNR are selected and contributed to the final system-level detect decision. ....	197
Figure 6.12 System-level $P_d$ versus transmit power at PU in a multiuser network with a large number of users.....	198

## Abstract

In this thesis we investigate how to improve the performance of MU-MIMO wireless system in terms of achieving Shannon capacity limit and efficient use of precious resource of radio spectrum in wireless communication.

First a new suboptimal volume-based scheduling algorithm is presented, which can be applied in MU-MIMO downlink system to transmit signals concurrently to multiple users under the assumption of perfect channel information at transmitter and receiver. The volume-based scheduling algorithm utilises Block Diagonalisation precoding and *Householder reduction* procedure of  $QR$  factorisation. In comparison with capacity-based suboptimal scheduling algorithm, the volume-based algorithm has much reduced computational complexity with only a fraction of sum-rate capacity penalty from the upper bound of system capacity limit. In comparison with semi-orthogonal user selection suboptimal scheduling algorithm, the volume-based scheduling algorithm can be implemented with less computational complexity. Furthermore, the sum-rate capacity achieved via volume-based scheduling algorithm is higher than that achieved by SUS scheduling algorithm in the MIMO case.

Then, a two-step scheduling algorithm is proposed, which can be used in the MU-MIMO system and under the assumption that channel state information is known to the receiver, but it is not known to the transmitter and the system under the feedback resource constraint. Assume that low bits codebook and high bits codebook are stored at the transmitter and receiver. The users are selected by using the low bits codebook; subsequently the BD precoding vectors for selected users are designed by employing high bits codebook. The first step of the algorithm can alleviate the load on feedback uplink channel in the MU-MIMO wireless system while the second step can aid precoding design to improve system sum-rate capacity.

Next, a MU-MIMO cognitive radio (CR) wireless system has been studied. In such system, a primary wireless network and secondary wireless network coexist and the transmitters and receivers are equipped with multiple antennas. Spectrum sensing methods by which a portion of spectrum can be utilised by a secondary user when the spectrum is detected not in use by a primary user were investigated. A Free Probability Theory (FPT) spectrum sensing method that is a blind spectrum sensing method is proposed. By utilizing the asymptotic behaviour of random matrix based on FPT, the covariance matrix of transmitted signals can be estimated through a large number of observations of the received signals. The method performs better than traditional energy spectrum sensing method. We also consider cooperative spectrum sensing by using the FPT method in MU-MIMO CR system. Cooperative spectrum sensing can improve the performance of signal detection. Furthermore, with the selective cooperative spectrum sensing approach, high probability of detection can be achieved when the system is under false alarm constraint.

Finally, spectrum sensing method based on the bispectrum of high-order statistics (HOS) and receive diversity in SIMO CR system is proposed. Multiple antennas on the receiver can improve received SNR value and therefore enhance spectrum sensing performance in terms of increase of system-level probability of detection. Discussions on cooperative spectrum sensing by using the spectrum sensing method based on HOS and receive diversity are presented.

## Declaration

I, the named author of the thesis confirm that no portion of the work referred to in the thesis has been submitted in support of an application for another degree or qualification of this or any other university or other institute of learning.

Signature .....

Name.....

## Copyright statement

- i. The author of this thesis (including any appendices and/or schedules to this thesis) owns certain copyright or related rights in it (the “Copyright”) and s/he has given The University of Manchester certain rights to use such Copyright, including for administrative purposes.
- ii. Copies of this thesis, either in full or in extracts and whether in hard or electronic copy, may be made only in accordance with the Copyright, Designs and Patents Act 1988 (as amended) and regulations issued under it or, where appropriate, in accordance with licensing agreements which the University has from time to time. This page must form part of any such copies made.
- iii. The ownership of certain Copyright, patents, designs, trade marks and other intellectual property (the “Intellectual Property”) and any reproductions of copyright works in the thesis, for example graphs and tables (“Reproductions”), which may be described in this thesis, may not be owned by the author and may be owned by third parties. Such Intellectual Property and Reproductions cannot and must not be made available for use without the prior written permission of the owner(s) of the relevant Intellectual Property and/or Reproductions.
- iv. Further information on the conditions under which disclosure, publication and commercialisation of this thesis, the Copyright and any Intellectual Property and/or Reproductions described in it may take place is available in the University IP Policy (see <http://www.campus.manchester.ac.uk/medialibrary/policies/intellectual-property.pdf>), in any relevant Thesis restriction declarations deposited in the University Library, The University Library’s regulations (see <http://www.manchester.ac.uk/library/aboutus/regulations>) and in The University’s policy on presentation of Theses.

## **Acknowledgement**

I would like to express my gratitude to people who guided and supported me during whole period of my graduate study. First of all, I would like to thank my supervisor Dr. Zhirun Hu for his continual support and guidance over the years. His kindness, knowledge, rigorous style and continual encouragement have been great inspirational. I am also grateful Professor Tony Brown for serving as my PhD advisor.

I would like to thank my industrial supervisor in BT Dr Xuanye Gu who supported and guided me with his great patience. His knowledge in the area of wireless communication has been great resource to me. I also appreciate the EPSRC funding and BT sponsorship which has facilitated my graduate study.

Finally, I am indebted to my family. My mum's encouragement is always great strength for me to deal with any difficulties that I come across. My children are inspirational since they have shown me their enthusiasm to learn. Studying in parallel with my children has brought lots of enjoyment to my life. I am also thankful to my husband for his hard work to look after family while I have to spend more time on my study.

## List of abbreviations

AWGN	Additive White Gaussian Noise
BC	Broadcast
BD	Block Diagonalisation
BER	Bit Error Rate
BF	Beamforming
BPS	Bits Per Second
BPSK	Binary Phase-shift Keying
BS	Base Station
CDMA	Code-Division Multiple Access
CR	Cognitive Radio
CSI	Channel State/Side Information
CSIR	Channel State/Side Information at Receiver
CSIT	Channel State/Side Information at Transmitter
DE-LBG	Dominant Eigenvector based LBG
DPC	Dirty Paper Coding
DSA	Dynamic Spectrum Access
ED	Energy Detector
EGC	Equal Gain Combination
FCC	Federal Communications Commission
FDMA	Frequency-Division Multiple Access
FPT	Free Probability Theory
GLA	Generalized Lloyds Algorithm
HOS	High-order Statistics
LAN	Local Area Network
LOS	Line-of-Sight
MAC	Multiple Access Channel
MIMO	Multiple-Input Multiple-Output
MISO	Multiple-Input Single-Output
MPAM	Pulse Amplitude Modulation
MPSK	Phase-Shift Keying
MRC	Maximal Ratio Combination
MU-MIMO	Multiple-User Multiple-Input Multiple-Output
NTIA	National Telecommunications and Information Administration
OFDM	Orthogonal Frequency Division Multiplexing
PFS	Proportional Fair Scheduling
PSD	Power Spectral Density

## List of abbreviations

---

PU	Primary User
ROC	Receiver Operating Characteristic
RR	Round-Robin
RVQ	Random Vector Quantization
SDMA	Space-Division Multiple Access
SIMO	Single-Input and Multiple-Output
SINR	Signal-to-Interference-plus-Noise Ratio
SISO	Single-Input Single-Output
SNR	Signal-to-Noise Ratio
ST	Space Time
SU	Secondary User
SU-MIMO	Single-User Multiple-Input Multiple-Output
SUs	Secondary Users
SUS	Semi-orthogonal User Selection
SVD	Singular Value Decomposition
TDMA	Time-Division Multiple Access
TS	Time Sharing
TV	Television
ZFBF	Zero-Forcing Beamforming

## List of notations

$\ll$	much greater than
$\gg$	much less than
$\neq$	not equal to
$\approx$	approximately equal to
$\geq$	great than and equal
$\leq$	less than and equal
$\Delta x$	the difference between two points of $x$
$\sum_n^m [\cdot]$ or $\sum_i [\cdot]$	sum of $n$ th item to $m$ th item, or sum of $i$ items
$\prod$	product
$\emptyset$	empty set
$\exp(x)$	exponential function of $x$
$\int$	integration operator
$\arctan$	inverse tan
$I_0(\cdot)$	modified Bessel function of the first kind and zero order
$\rightarrow$	approach to
$\infty$	infinite
$\Sigma$	diagonal matrix
$A^T$	transpose of matrix $A$
$A^H$	Hermitian of matrix $A$
$\mathbf{x}^*$	complex conjugate of vector $\mathbf{x}$
$\mathbf{x}^T$	transpose of vector $\mathbf{x}$
$\mathbf{x}^H$	Hermitian of vector $\mathbf{x}$
$I(X;Y)$	mutual information between random variables $X$ and $Y$
$\max_x f(x)$	maximum value of $f(x)$ maximized over all $x$
$\log_x(y)$	the log, base $x$ of $y$
$\ln(x)$	natural log of $x$
$Tr(\mathbf{A})$	trace of matrix $\mathbf{A}$
$E(\cdot)$	expectation operator
$\det[\mathbf{A}]$	determinant of matrix $\mathbf{A}$
$\mathbf{I}$	identity matrix
$\ \mathbf{x}\ _F$	Frobenius norm of vector $\mathbf{x}$
$\ \mathbf{x}\ $	norm of vector $\mathbf{x}$
$\sqrt{x}$	square root of $x$
$x^*$	complex conjugate of $x$
$\mathcal{CN}(\mu, \sigma^2)$	complex Gaussian distribution with mean $\mu$ and variance $\sigma^2$

## List of notations

---

$\mathbb{C}$	field of all complex numbers
$N \times M$ matrix	a matrix with $N$ rows and $M$ columns
$\mathfrak{U}(M, N)$	class of $M \times N$ unitary matrix
$\arg \max [f(x)]$	value of $x$ that maximizes the function $f(x)$
$\arg \min [f(x)]$	value of $x$ that minimizes the function $f(x)$
$O(\cdot)$	big $O$ notation
$E(\mathbf{x}, \mathbf{x}^H)$	covariance matrix of vector $\mathbf{x}$
$\langle \mathbf{x}, \mathbf{y} \rangle$	inner product of vectors $\mathbf{x}$ and $\mathbf{y}$
$\text{Re}[x]$	real part of $x$
$\frac{\partial^2 [f(x, y)]}{\partial x \partial y}$	partial derivatives of $f(x, y)$ with respect to $x$ and $y$
$\text{cum}(\cdot)$	cumulant
$\min(\cdot)$	minimum
$\max(\cdot)$	maximum
$\text{prob}(\cdot)$	probability of

In this thesis, we use upper case boldface letters for matrices and lower case boldface letters for vectors.

## Chapter 1 Introduction

In the past two decades, mankind has witnessed the fast development of the wireless communication industry. The examples of the wireless application and service are the use of mobile phone, Internet access, wireless Local Area Network (LAN) access, gaming, message forwarding and downloading, file retrieving and transfer, large volume data transfers between mobile handsets or laptop, video downloading to a handheld entertainment product, voice exchange on mobile phones and the multimedia communication to and from other mobile devices. The consequence of this expansion of the wireless communication industry is that the demand for capacity and frequency bandwidth has become increasingly high. Therefore, the available resources such as spectrum and system capacity become limited. To address these issues and to allocate these precious resources to different applications and services efficiently, multiuser Multiple-Input Multiple-Output (MU-MIMO) and Cognitive Radio (CR) are hot research areas in last decade. MU-MIMO and CR are two techniques that are the main focus of this thesis.

In a point-to-point Multiple-Input Multiple-Output (MIMO) system, multiple antennas are equipped at the transmitter and receiver. Two special cases of the MIMO system are Single-Input and Multiple-Output (SIMO) and Multiple-Input and Single-Output (MISO), where multiple-antennas are equipped at the receiver for SIMO system and multiple-antennas are equipped at the transmitter for MISO system. Multiple antennas in MIMO system introduce a new space dimension to the wireless system. It is recognized that MIMO technology in wireless system can increase system capacity and improve system performance by utilizing the space dimension and applying advanced coding techniques [A. Goldsmith, 2005, E. Larsson and P. Stoica, 2003 and A. Paulraj et al., 2003]. Each transmitter-receiver pair in MU-MIMO system forms a MIMO communication channels, the

users share the receive antennas in the uplink case and transmit antennas in the downlink case. Since different users have different channels that experience various degrees of channel fading, the channel information of different users can be exploited. The system resource can be allocated to a best channel or several users with good channel conditions in order to maximize system data rate. In the case of serving more than one users, the methodology of signal transmission is to minimize inter-user interference [D. Gesbert et al., 2007 and D. Tse and P. Viswanath, 2005]. It is recognized that the MU-MIMO technology plays a very important part in current commercial wireless systems and future generation mobile systems [M. Jiang and L. Hanzo, 2007].

Cognitive radio is an emergent technology for improving the utilization of radio spectrum resource [I. Mitola, J. and J. Maguire, G. Q., 1999, J. Mitola, 2000]. The cognitive radio is built on a software-defined radio, which is considered as an intelligent wireless communication system that is aware of its environment and learns from its setting, and therefore is able to adapt the system parameters to its surrounding for signal transmission. The utmost goals of the cognitive radio technology are to utilize the radio spectrum efficiently and to ensure reliable communication as the radio spectrum becomes a scarce resource with the emergence of new applications and services of wireless communication in recent years.

This thesis provides some suggestions and solutions to deal with the fundamental limits of wireless networks, such as capacity limits and radio spectrum shortage problem. The remainder of this chapter provides necessary background material and outlines the specific contributions of this thesis.

### **1.1 Background**

#### **1.1.1 Communication channel, MIMO and MU-MIMO**

In 1948, Claude Shannon [C. E. Shannon, 1948] pioneered the mathematical theory of communication which is based on the concept of mutual information between the input and output of a channel. It is evident that the theory has formed a basis for analyzing the performance of both wired and wireless communication systems. The essence of the theory is the concept of channel capacity which is defined as the maximum data rate over a channel with asymptotically small error probability. In a typical communication system with the additive white Gaussian noise (AWGN) channel as shown in Figure 1.1, the relationship between the output signal and input signal can be expressed as

$$y = x + n, \quad (1.1)$$

where  $y$  denotes the output signal,  $x$  denotes the input signal and  $n$  denotes the AWGN noise. That is, the output of the system is the summation of input  $x$  and AWGN noise  $n$ . Assume that the signal-to-noise ratio ( $SNR$ ) is the ratio of the power of the output signal in Watts to the power of the noise in Watts, and  $B$  is the channel bandwidth in Hz, Shannon capacity in bits per second (bps) of such a channel is given below

$$C = B \log_2(1 + SNR). \quad (1.2)$$

Since Shannon capacity is the maximum data rate that a communication system can achieve with near zero error probability, the data rate achieved in a practical system is inevitable lower than the Shannon capacity due to the limitation of channel bandwidth and signal power. In other words, Shannon capacity is generally used as an upper bound on the achievable data rate in a real system.

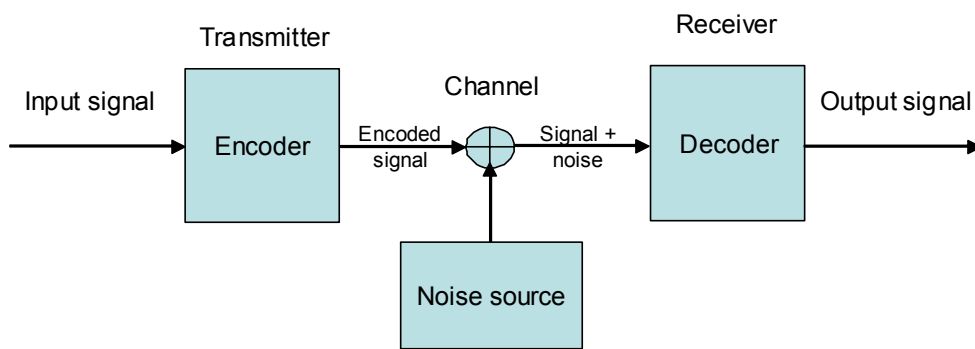


Figure 1.1 General communication system.

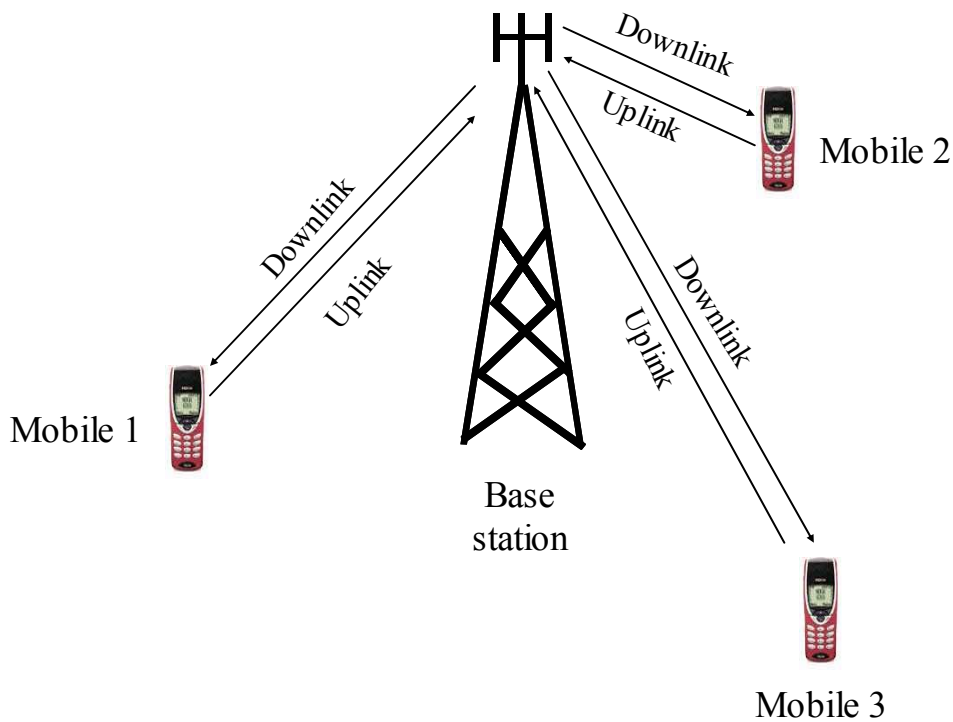
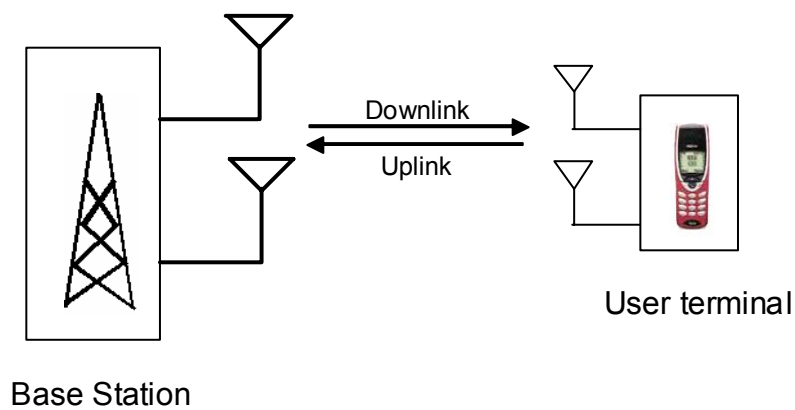


Figure 1.2 Wireless cellular system

Shannon capacity limit can be applied as the upper bound of a wireless system, such as a cellular system shown in Figure 1.2. When the base station is transmitting messages to the mobiles, the channel is referred to as a downlink or broadcast channel. The reverse link is called uplink channel where the messages from a mobile are transmitted to the base

station. In this thesis, a downlink channel in a wireless network means that the base station transmits different signals (voice, data file or multimedia streams) to different mobiles or users. A downlink channel differs from a TV or radio broadcast channel where a transmitter sends the same message to each receiver. In following chapters of this thesis, we are interested in transmission of different messages to each mobile in the context of finding a scheduling algorithm in MU-MIMO wireless system to maximize system sum-rate capacity. On the other hand, we are interested in the scenario of spectrum sensing where same message are transmitted from transmitter and reaches different receivers.

To meet the demands for higher data rate in wireless systems, MIMO technology has been utilized in various wireless standards. For example, MIMO technology is incorporated in IEEE Standard for local and metropolitan area networks IEEE standard 802.16e. The use of multiple input and multiple output antennas adds another dimension to the wireless communication system, which is known as antenna and space dimension. The MIMO technology can improve system capacity of wireless system. A typical point-to-point (single user) MIMO wireless system is shown in Figure 1. 3.



**Figure 1.3 A point-to-point MIMO wireless system.**

The earlier studies on MIMO system can be found in the pioneering works by Winter [J. Winters, 1987], Foschini and Gans [Foschini and Gans, 1998], and E. Telatar [E. Telatar, 1999]. In 1987, Winters studied fundamental limits on the data rate of multiple antenna systems in the Rayleigh fading environment. The distribution of the maximum data rate at a given error rate in the channels was investigated. His research demonstrated that large capacity in systems can be potentially achieved with limited bandwidth. In 1998, Foschini and Gans used MIMO technology to improve wireless capacities by considering Rayleigh fading channel and the receiver with full knowledge of Channel State Information (CSI). Very large capacity can be achieved by forming a channel with increased spatial dimensions under the condition of fixed bandwidth and total transmitted power. In 1999, E. Telatar investigated single user MIMO system over an additive Gaussian channel with and without fading. The mathematical formulas for the capacities as well as the error exponents of the channels are derived. His work demonstrated that the large gains of multi-antenna systems over single antenna systems can be achieved under independence assumptions for the fades and noises at different receiving antennas.

Since then, researches on MIMO technology have been pursued intensively to achieve spectral efficiency and high system capacity in wireless communication [A. J. Paulraj et al., 2004]. The advantages of MIMO systems over single-input single-output (SISO) systems are twofold: (a) system capacity and spectral efficiency can be improved significantly. The increase of the capacity of a wireless link is proportional to the minimum number of transmitter or the receiver antennas [G. G. Raleigh and J. M. Cioffi, 1996], [G. G. Raleigh and J. M. Cioffi, 1998]. The system data rate can be increased via spatial multiplexing without consuming more frequency resources and without increasing total transmit power. (b) The effects of fading can be reduced via diversity in a MIMO system.

SU-MIMO technique is theoretically understood and has been applied in the communication industry to achieve channel capacity gain and spectrum efficiency in past decades. The research emphasis on MIMO technology has shifted from SU-MIMO to multiuser-MIMO in recent years [D. Gesbert et al., 2007]. One obvious benefit of MU-MIMO system is that the space signature of users in the system can be explored to obtain high system capacity and better spectrum utilization. Research on MU-MIMO in last two decades has revealed that antennas across users in the system, such as cellular system, can be collectively exploited to achieve high multiplexing gain. This technique involves scheduling to multiple users simultaneously within same channel such as, time slot or frequency band. This technique is also called space-division multiple access (SDMA) [M. Cooper and M. Goldberg, 1996]. SDMA explores the space signatures of users and assigns to different users different spatial beams and encoding/decoding is applied to the users. Although signal transmissions to/from users within same spectrum coexist, they are separable in space. The studies in [M. Jiang and L. Hanzo, 2007] show improved system performance due to multiuser multiplexing gain in a MU-MIMO-OFDM (orthogonal frequency division multiplexing) wireless systems, where multiple users are transmitted simultaneously in orthogonal frequency band under the interference limit required. An overview of the results on Shannon capacity limits of SU and MU-MIMO channels is provided [A. Goldsmith, et al., 2003]. In the area of precoding strategy, the research has been done on the sum capacity and achievable sum rates for dirty paper coding (DPC) [D. Gesbert and M. Kountouris, 2007], coordinated beamforming [C.-B. Chae et al., 2006], and zero-forcing beamforming (ZFBE) with the dimensionality constraint [T. Yoo and A. Goldsmith, 2006]. DPC [M. Costa, 1983] combined with user scheduling and power loading algorithm [G. Caire and S. Shamai, 2003] is demonstrated as an optimum strategy in MU-MIMO BC (broadcast downlink channel) among the precoding strategies. DPC strategy in MU-MIMO BC system is a theoretical pre-interference cancellation technique. In [P. Viswanath et al., 2002], multiuser diversity is

explored in opportunistic beamforming using dumb antennas. The results show that the data rates can be increase significantly via multiuser diversity in a scheduling scheme designed to detect the channel condition of each user and only a user with the best channel conditions being served at one time.

Figure 1.4 shows the downlink channel and Figure 1.5 is the uplink channel of simple case of two users and one base station in a MU-MIMO wireless system, each user terminal having two antennas and base station having two antennas. In a MU-MIMO uplink system, the spectral sharing is typically done by dividing the signal dimensions along the time, frequency and/or code space axes, that is, frequency-division multiple access (FDMA), time-division multiple access (TDMA), code-division multiple access (CDMA) and space-division multiple access (SDMA). SDMA is generally done with directional antennas and realized with smart antennas [J. H. Winters, 1998]. In MU-MIMO downlink system, a scheduling algorithm for servicing multiple users can be designed if transmitter and receivers have perfect channel state information. However, a transmitter without channel information is common in a MU-MIMO downlink system. In this case, CSIT can be obtained via an uplink feedback channel in MU-MIMO system to aid scheduling to multiple users simultaneously and precoding design in MU-MIMO downlink system. This feedback strategy may cause a significant burden on uplink capacity. In a MU-MIMO system with a large number of users, a scheduling procedure might be complex in order to select a group of users and serve them simultaneously. Optimal scheduling involves exhaustive search whose complexity is exponential in the group size and depends on the choice of precoding, decoding, and channel state feedback technique. In this thesis, the MU-MIMO downlink system is considered. The discussions on scheduling strategy will be presented in chapter 3 and chapter 4.

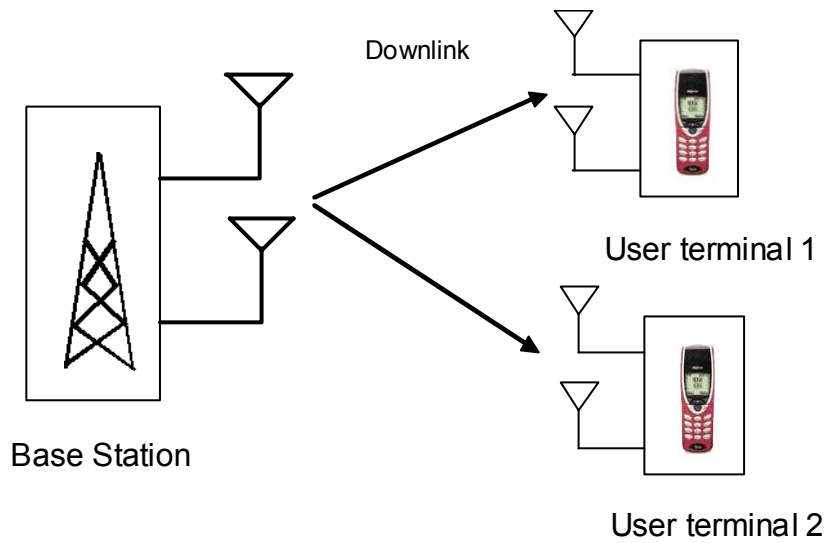


Figure 1.4 Multiuser MIMO downlink.

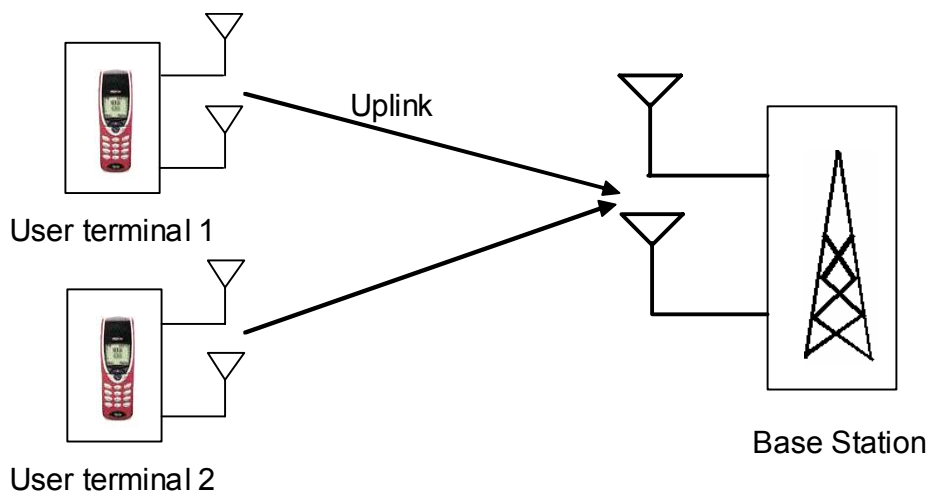


Figure 1.5 Multiuser MIMO uplink.

### 1.1.2 Spectrum utilization – cognitive radio technique

To improve spectrum utilization in MU-MIMO system, cognitive radio technique will be discussed in later chapters in this thesis. Cognitive radio (CR) is a hot research topic in recent years. The study in CR is to find a

solution to a problem that radio spectrum resources become scarce with the increasing wireless application and, at the same time, the spectrum is not efficiently utilized. Current wireless networks are normally regulated by a fixed spectrum assignment policy. The spectrum is regulated by governmental agencies and is assigned to license holders or services on a long term basis for large geographical regions. The practice of this spectrum allocation inevitably results that the spectrum usage is concentrated on certain portions of the spectrum while a significant amount of the spectrum remains unutilized. The frequency allocation chart [National Telecommunications and Information Administration, 2003] from National Telecommunications and Information Administration (NTIA) organization in USA shows that all frequencies are allocated to various applications. The UK Frequency Allocation Table [Ofcom, 2008] is published by Ofcom on behalf of the National Frequency Planning Group, a sub-committee of the Cabinet Official Committee on UK Spectrum Strategy. The table shows the position as at December 2008 and will be updated according to the modification of spectrum policy decisions to meet the demand of emerging range of applications and services. The spectrum allocation chart [Roke, 2007] also shows that the whole range of spectrum is heavily occupied by the allocated radio services.

Researches on spectrum utilisation have demonstrated that not all spectrums are in use for all of the time. Figure 1.6 [Ofcom, “Cognitive Radio,”] shows the spectrum occupancy measurements in a rural area, near Heathrow airport and in central London. The central London band has the highest degree of spectrum occupancy while the rural area measurement shows the lowest degree of occupancy and large areas of space.

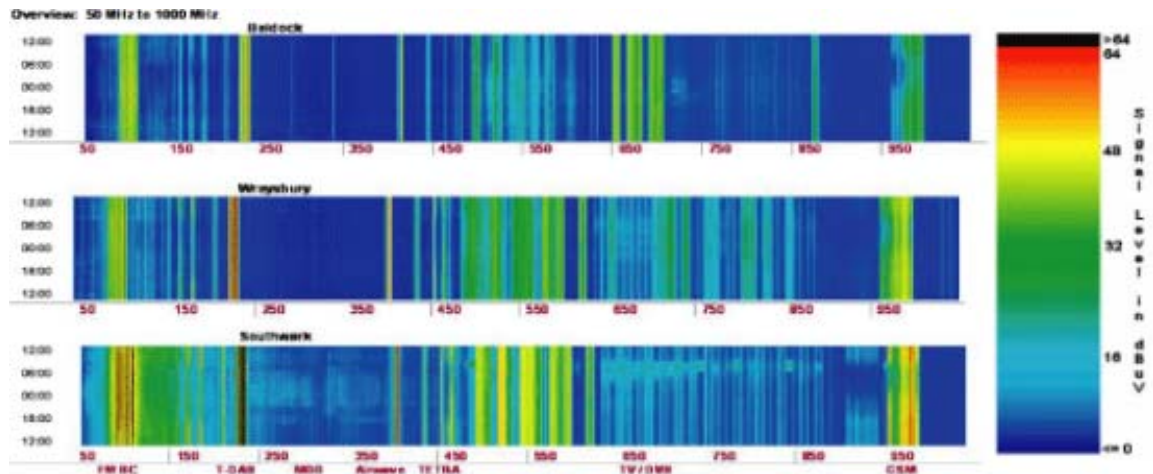


**Figure 1.6** Spectrum occupancy measurements [Ofcom, “Cognitive Radio,] in a rural area (top), near Heathrow airport (middle) and in central London (bottom).

It is obvious that the traditional fixed spectrum assignment policy can not meet the needs of ever increasing demand to access the limited spectrum for mobile services in recent years. Cognitive Radio is one technology which offers the potential to make efficient use of the unused spectrum, allowing large amounts of spectrum to become available for future high bandwidth applications. The essence of cognitive radio techniques is to allow users from different networks to use/share the spectrum in an opportunistic manner. To access dynamically to a licensed band, cognitive radio technology enables the users from unlicensed users to determine if licensed users occupy in a licensed band; to select the best available channel if unoccupied licensed bands are detected; to be able to share the bands among users, and finally to vacate the channel when a licensed user is detected. Cognitive radio technique has been included in the application initiatives, such as, the IEEE 802.22 standard wireless regional area network (WRAN) [802.22 Working Group, 2008, C. Stevenson et al., 2009] and the Wireless Innovation Alliance [Wireless Innovation Alliance, 2008] that support unleashing the potential of using “White Spaces” in the television (TV) spectrum.

Cognitive radio technique may include spectrum sensing, spectrum analysis, and spectrum decision in a typical CR cycle [I. Mitola, J. and J. Maguire, G. Q., 1999, I. Akyildiz et al., 2006, S. Haykin, 2005]. In this thesis, we will focus our discussion on spectrum sensing methods that an unlicensed user (secondary user) detects if a licensed user (primary user) occupies a portion of the spectrum. A review paper summarised various spectrum sensing methods reported in recent years (Y. Zeng et al., 2010). Examples of the proposed spectrum sensing methods are energy detection [H. Urkowitz, 1967], matched filtering detection [A. Sahai and D. Cabric, 2005], wavelet-based sensing [Z. Tian and G. B. Giannakis, 2006]. Spectrum sensing methods can be categorised into three types: (a) methods can be used when source signal and noise power information are known; (b) methods require only noise power information (semi blind), and (c) methods can be applied without information of source signal and noise power (blind). We will discuss spectrum sensing methods in chapter 5 and chapter 6. Furthermore, MIMO technique will be considered to improve the performance of spectrum sensing. In MU-MIMO system, cooperative spectrum sensing among users can also improve system sensing performance. This cooperative sensing method takes the advantage of users with different locations. Sensing decision from users close to the transmitter and/or with less external interference will greatly affect the final system sensing decision. Cooperative sensing can also increase system sensing reliability since the chance of all users sensing incorrectly due to channel fading or shadowing effect is low.

### **1.2 Motivation**

Two main streams of studies on MU-MIMO are: (a) Concerning achieving upper bound of Shannon capacities or optimal capacity regions for a given MU-MIMO system regardless how the capacity might be achieved and how complex the solution to a problem formulation is. (b) The emphasis is on the

practical implementation of any transmission schemes in the MU-MIMO system. The consequence of this strategy may result that the performance measure in terms of achievable rates is far from theoretical Shannon capacity. Our work in this thesis will be focused on developing transmission schemes that are not only feasible but also can approach Shannon capacity limit, i.e., to build a transmission strategy achieving high data rate with less complex. The MIMO downlink system will be considered in our study.

Most of scheduling algorithms function under the assumption of perfect channel state information at the transmitter and receiver. However, variable nature of wireless channel might cause difficulties of obtaining exact channel state information at transmitter (CSIT) and channel state information at the receiver (CSIR). It might be relatively straightforward to directly measure the wireless channel at the receiver. However, it is normally the case that the transmitter is not aware of any channel information. In this thesis, we also consider a situation that perfect CSIR and transmitter obtains the channel state information through uplink feedback channel. To ease feedback load, we propose a two-step scheduling algorithm to deal with the system under feedback resource constraint. Using low bits feedback to select users in the first stage of the algorithm can significantly alleviate system feedback load.

Final motivation is to solve the problem of scarce spectrum resource and increase spectrum utilisation in MU-MIMO wireless system. In particular, we focus on exploring efficient spectrum sensing methods which are essential in cognitive radio technique to detect if a portion of spectrum allocated to a licensed user is in use. User cooperation in a MU-MIMO system can reduce hidden node problem and shadowing effect. Therefore, we also investigate how cooperative spectrum sensing can improve system performance in terms of probability of detection enhancement.

### **1.3 Outline of the thesis**

In following chapters, chapter 2 presents literature review on wireless channel and fading phenomenon existed in the wireless channel, system capacity as one of performance measures in MIMO system and MU-MIMO system, and cognitive radio technique in wireless network.

In chapter 3, we show a new volume-based scheduling algorithm. We describe how the algorithm works in the case of perfect channel knowledge at the transmitter and receiver. The algorithm is in the category of suboptimal scheduling method. We compare system sum-rate capacity achieved by the volume-based scheduling algorithm with other two suboptimal scheduling algorithms: capacity-based and SUS algorithms. We also compare the computational complexity of these suboptimal scheduling algorithms.

In chapter 4, we illustrate a two-step scheduling algorithm that is used for perfect channel state information at receiver and transmitter gaining channel state information via feedback uplink channel in MU-MIMO wireless system. It explains using low bits feedback to reduce feedback load and using high bits codebook for precoding vector design to improve system sum-rate capacity.

In chapter 5, a new Free Probability Theory (FPT) spectrum sensing is described. The review of Free Probability Theory is given in the chapter. The sensing performances between energy spectrum sensing method and the FPT spectrum sensing method are compared. In addition, the cooperative spectrum sensing is discussed.

In chapter 6, another spectrum sensing method based on Higher-Order Statistics (HOS) and receive diversity is presented. The review on HOS is provided. We demonstrate the sensing performance can be improved

by utilizing multiple antennas at the receiver. Cooperative spectrum sensing is also discussed in the case of MU-MIMO system with either a small number of users or a large number of users.

Finally, the conclusions and future work are presented in Chapter 7.

In this thesis, Matlab v7 software package is used for the simulation results presented in following chapters.

## Chapter 2 Literature review on wireless channel, MU-MIMO system and cognitive radio technology

### 2.1 Wireless radio channel and fading

Wireless radio channel is a dynamic channel in which the electromagnetic wave propagates. Comparing with wired radio channel, a mobile wireless channel is more complex in terms of random appearance of obstacles in a signal path from a transmitter to a receiver. In an urban area and outdoor environment, skyscrapers, trees as well as high density of the buildings can change a signal path significantly. The signal arriving at the receiver is not a simple case of a line-of-sight (LOS) path but the combination of the multipath signals arriving at the receiver. Similarly in the suburban area and countryside, the geographical surface of the earth such as mountains and hills can obstruct a signal; the received signal at a receiver is the combination of multi-path signals coming from a transmitter. In the situation of indoor environment, the objects in a wireless channel can vary extensively, such as floors, wall, partition in an office building, machinery etc. The complexity of a wireless channel media has brought challenge to the design of a wireless system and the analysis of the system performance. Because main theme of this PhD study is wireless MIMO (Multiple-Input Multiple-Output) system, the wireless radio propagation phenomena related to the wireless channel is presented next.

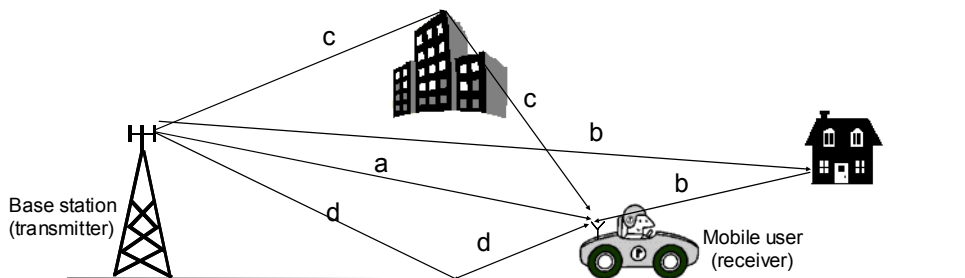


Figure 2.1 A wireless radio channel and signal multipath transmission.

Figure 2.1 shows typical signal transmission paths from a transmitter to a receiver in an outdoor environment. It is known that the signal transmission in the form of electromagnetic wave propagation experiences reflection, diffraction and scattering from various objects. As indicated in Figure 2.1, path (a) is the line-of-sight path that the signal arrives to the receiver without any obstruction. Reflection happens when a propagating electromagnetic wave impinges on an object which has large dimensions when compared to the wavelength of the propagating wave and the object has smooth surface; path (b) exhibits that an electromagnetic wave is reflected by house wall and path (d) displays that the signal is reflected by the ground surface. Diffraction occurs when the transmitted signal path from the transmitter to the receiver is obstructed by a surface that has sharp edges and the secondary waves are resulted around the obstacles. Path (c) is the case when the signal is diffracted by the top edge of a skyscraper and reaches to the recipient. The scattering situation is not shown in Figure 2.1. Scattered waves are mainly caused by many objects with small dimensions compared to the wavelength of the signal in the electromagnetic wave travelling path. These objects can be lamp posts, trees and hedges, and any rough surfaces.

There are two obvious phenomena when a radio wave propagating from a source to a destination in a wireless channel if a receiver moves away from a transmitter: (1) the average signal strength at the receiver decreases when the distance between the transmitter and receiver increases; (2) the interaction between multiple waves resulted by reflection, diffraction and scattering causes multipath fading at the destination, i.e., possible distorted signal with fast change amplitude, altered phase and frequency.

To analyze the performance of a mobile wireless channel, propagation models developed are categorized *large-scale* propagation models and *small-scale* propagation models. *Large-scale* propagation models are used to predict average signal strength at the receiver when there

exists large distance between the transmitter and the receiver, which is several hundreds or thousands metres. *Small-scale* propagation models, which are also known as fading models, deal with the circumstances when rapid fluctuations of the received signal strength occur in a short time period when the receiver moves very short distance (a few wavelengths).

There are numerous models to tackle the signal propagation in various wireless operation environments. They can be found in standard wireless communication text books and research papers, such as two-ray ground reflection model, knife-edge diffraction model [T. S. Rappaport, 2002, M. J. Feuerstein et al., 1994], practical log-distance path loss model, log-normal shadowing model and Clark's model for flat fading [Clark R. H., 1987].

## 2.1.1 Large-scale path loss

### 2.1.1.1 Log-distance Path Loss Model

Classical Log-distance Path Loss Model is used to describe large scale path loss, which specifies that average received power decreases logarithmically with distance in a wireless radio channel. Let  $PL$  denote the average path loss which is the ratio of transmit power  $P$  to receive power  $P_r$  at distance  $d$  from the transmitter, that is,  $PL = P / P_r$ ;  $d_0$  denote a close-in reference distance which is determined from the measurements close to the transmitter. The average path loss at distance  $d$  can be expressed as:

$$PL \propto (d / d_0)^n \quad , \quad (2.1)$$

where  $n$  denotes the path loss exponent which designates the rate at which the path loss increases with distance. Because of scattering phenomenon in the antenna near field, (2.1) is valid only at transmission distances  $d > d_0$ . If

average path loss is expressed in unit  $dBm$  and  $d/d_0$  is plotted in log scale, a linear relationship is found between the path loss and the separation distance of transmitter and receiver. Figure 2.2 indicates this linear trend when the parameters are taken the values  $d_0=1$ ,  $PL(d_0)=0$   $dBm$  and  $n=3$  when urban area cellular environment is considered.

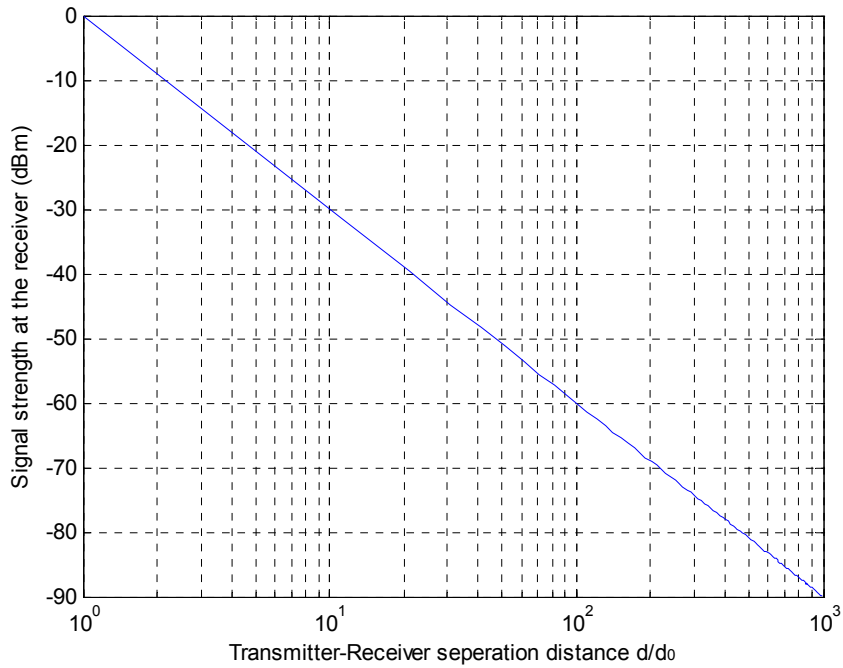


Figure 2.2 Path loss in wireless radio channel.

### 2.1.1.2 Log-normal shadowing model

In the wireless radio channel, the transmitted signal can be blocked by large objects and shadowing effect takes place. Attenuation and deflection of the transmitted signal depends on the size of the objects as well as the substance medium property. The fading due to shadowing is categorized as large scale fading. The Log-normal shadowing model is developed to describe the shadowing effect, which can be used both in outdoor and indoor environment [M. Gudmundson, 1991, V. Erceg et al., 1999]. The Log-

normal shadowing model considers that the path loss in dB at the distance  $d$  of the receiver from transmitter is contributed by the path loss solely due to the distance and the path loss due to the shadowing effect. Hence, the path loss in unit  $dB$  can be expressed as

$$PL(d) \propto 10n \log_{10} \left( \frac{d}{d_0} \right) + PL_s, \quad (2.2)$$

where  $10n \log_{10} \left( \frac{d}{d_0} \right)$  in unit  $dB$  is the Log-distance Path Loss described in section 2.1.1.1;  $PL_s$  in unit  $dB$  denotes the path loss due to the shadowing effect, which is a zero-mean Gaussian distributed random variable with standard deviation  $\sigma$  in unit  $dB$ . The value of  $\sigma$  depends on the surrounding environment. Large value of  $\sigma$  indicates that strong shadowing effect happens. The example of shadow fading is shown in Figure 2.3. The ripples on the path loss curve are contributed by shadowing effect.

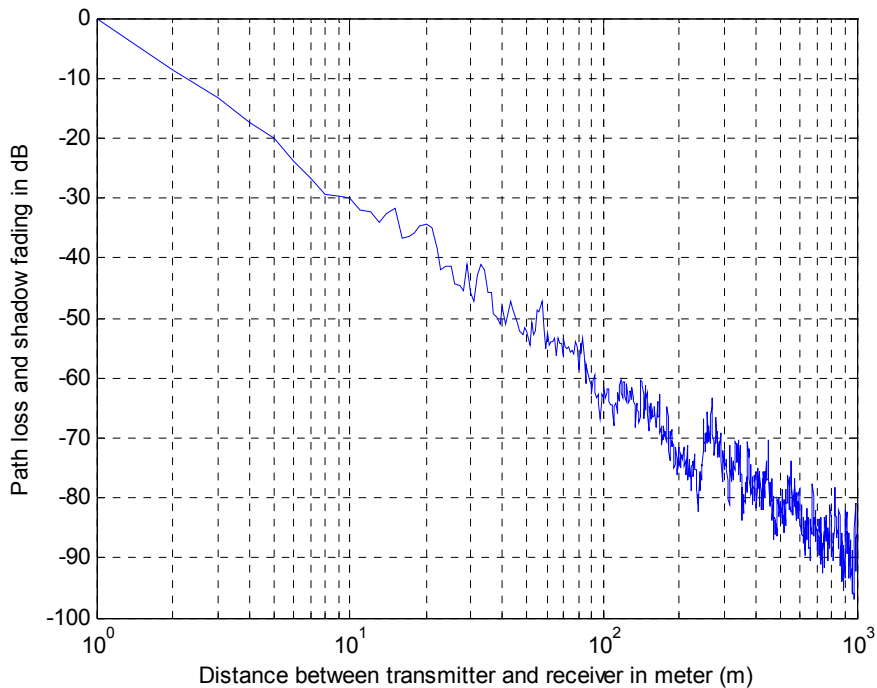


**Figure 2.3 Path loss and shadow fading in wireless radio channel**

### **2.1.2 Small-scale fading and multipath**

Apart from large-scale path loss, small-scale fading existed in a wireless radio channel can cause unstable system performance. Small-scale fading is the phenomenon that the amplitudes and phases of a received radio signal fluctuate rapidly in a short period of time. Many factors can cause small scale fading, such as, the speed of the user terminal, the speed of surrounding moving objects and the frequency bandwidth used for the signal transmission. One of the causes of small scale fading is due to the interference of two or more copies of the transmitted signal at the receiver, which is called multipath fading. In this situation, the result signals at the receiver depend on number of signal paths, the intensity of the signal from each path, time delay between multipath signals and the bandwidth of the transmitted signal.

### 2.1.2.1 Multipath time delay, flat fading and frequency selective fading

When a transmitted signal travels different paths in a mobile radio channel, each signal reaches to the receiver at slight different time. The time dispersion due to the multipath causes *flat fading* and *frequency selective fading* to the transmitted signal which depends on if all frequency components in the signal can pass through the channel.

*Flat fading* and *frequency selective fading* are two typical fading phenomena in small-scale fading, which is illustrated in Figure 2.4. In the figure,  $h(t, \tau)$  denotes a wireless channel impulse response at time  $t$ ,  $\tau$  is channel coherence time, transmitted signal is  $x(t)$  and received signal is  $y(t)$ . There are two characteristics of the channel response  $h(t, \tau)$ . Firstly the channel coherence time  $\tau$  is much less than the signal symbol length  $T_s$ , which is indicated in Figure 2.4 (b). Secondly the channel coherence time  $\tau$  is much greater than the signal symbol length  $T_s$ , as shown in Figure 2.4 (c).

Figure 2.4 (b) shows the case that the bandwidth of the input signal  $B_x = 1/T_s$  is much less than the coherence bandwidth  $B_c$  of the wireless channel, i.e.,  $B_x \ll B_c$  when the input symbol length  $T_s$  is much greater than the width of the delta function of the channel impulse response  $\tau$ . Coherence bandwidth  $B_c$  is a statistical measure of frequencies over which a channel can be considered flat i.e., a signal which can pass a channel with approximately equal gain and linear phase. In the case of multipath channel, coherence bandwidth is defined and related to rms (root mean square) delay spread of the channel [T. S. Rappaport, 2002]. If the channel is characterized with constant gain and linear phase response over a bandwidth which is greater than the bandwidth of the transmit signal, the received signal will undergo *flat fading*. In *flat fading*, the intensity of the combined

signals at the receiver due to the multipath effect in the channel will fluctuate fast with the time, however, the spectral characteristics of the transmitted signal at the receiver is not distorted.

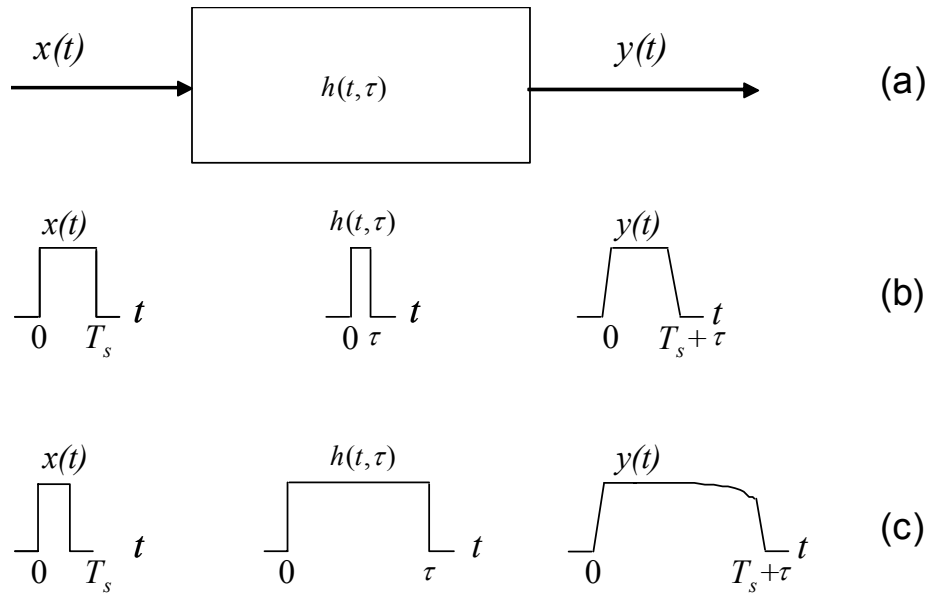


**Figure 2.4 Channel characteristics in terms of channel impulse response: (a) Input signal  $x(t)$ , output signal  $y(t)$  and channel impulse response  $h(t, \tau)$ , (b) Characteristics on time scale for flat fading, (c) Characteristics on time scale for frequency selective fading.**

On the other hand, if the input symbol length  $T_s$  is much less than the width of channel impulse response function  $\tau$  as shown in Figure 2.4 (c), the bandwidth of the input signal is much greater than the coherence bandwidth of the channel, i.e.,  $B_x \gg B_c$ . Supposing the channel has constant gain and linear phase response, a signal passing through the channel undergoes different channel gain for different frequency components. The frequency components of the signal within the coherence bandwidth have high gain and the frequency components of the signal out of range of the coherence bandwidth have much less gain. Therefore, this kind of channel generates *frequency selective fading* to the transmitted signal. The multipath signals traverse the channel and they have different time delay, large time

spread causes frequency selective fading. As a result, the received signal viewed in time domain is a distorted signal of the original transmitted signal.

### 2.1.2.2 Doppler shift and fast and slow fading

Because a mobile station normally moves in a wireless communication environment, the movement of the mobile in a short time can cause the phase change in the received signal therefore the signal frequency alteration. This effect is called Doppler shift that is illustrated in Figure 2.5.

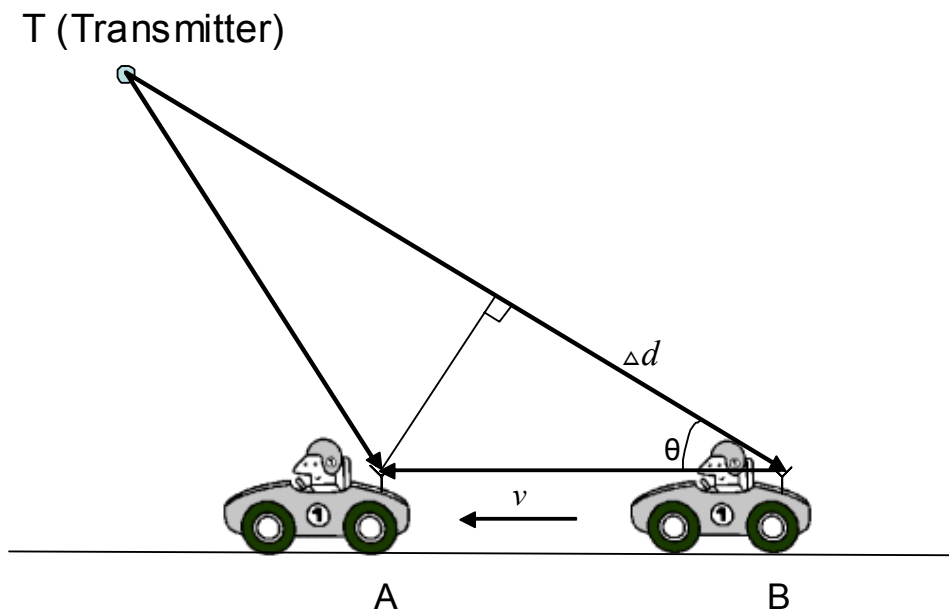


Figure 2.5 Diagram to demonstrate the Doppler Effect.

Supposing a sinusoidal carrier wave signal with carrier frequency  $f_c$  is radiated from the transmitter which is far away from the mobile station. The signal arriving angle at the mobile is  $\theta$ . The mobile station moves from position B to position A with speed  $v$  during time period that is denoted as  $\Delta t$ . Let  $\Delta d$  denote the signal travel distance variation between the path TB

and path TA, which is approximately  $\Delta d = v\Delta t \cos \theta$ . Because of this path difference, the phase change in the received signal at point A is

$$\Delta\phi = 2\pi\Delta d / \lambda = \frac{2\pi v\Delta t}{\lambda} \cos \theta , \quad (2.3)$$

where  $\lambda$  is the wavelength of the transmitted signal. Therefore, the frequency change of the received signal at point B is

$$f_d = \frac{1}{2\pi} \cdot \frac{\Delta\phi}{\Delta t} = \frac{v}{\lambda} \cos \theta . \quad (2.4)$$

The frequency  $f_d$  is called Doppler shift which is related to the mobile speed and the arrival angle of the signal wave. Hence, the frequency spectrum of the received signal will be broadened around  $f_c$  and in the range of  $f_c - f_d$  and  $f_c + f_d$ . The frequency spectrum of the received signal is also termed as Doppler spectrum because it is caused by the Doppler shift.

It is clear that the movement speed of the mobile terminal and the change of the incident angle of the transmitted signal will determine how fast a radio channel varies. The channel can be categorized as a *fast fading* channel or a *slow fading* channel which depends on if the speed of the channel variation is much faster or slower than the change rate of the transmitted base band signal.

### 2.1.3 Rayleigh fading and Ricean fading

#### 2.1.3.1 Rayleigh fading model

Rayleigh fading is a statistical model for the small scale fading in a wireless propagation environment. Rayleigh fading model assumes that the

magnitude of a signal that has passed through a wireless radio channel will vary randomly according to a Rayleigh distribution - the radial component of the sum of two uncorrelated Gaussian random variables. Rayleigh fading is most applicable when there is no dominant propagation along a line-of-sight between the transmitter and the receiver. Rayleigh fading model suites the situation when there are many objects in the environment that scatter the radio signal before it arrives at the receiver. One example of applications of Rayleigh fading model is in heavily built-up city areas where there is no line-of-sight between the transmitter and receiver.

The central limit theorem holds that, if there is sufficiently much scatter, the channel impulse response will be well-modelled as a Gaussian process irrespective of the distribution of the individual components. If there is no dominant component to the scatter, then such a process will have zero mean and phase evenly distributed between 0 and  $2\pi$  radians. The envelope of the channel response will therefore be Rayleigh distributed [J. G. Proakis, 2001]. More detailed explanation is given below in the rest of this section.

Supposing a transmitted signal  $S_0$  at time  $t$  is

$$S_0(t) = a_0 \exp(j\omega_0 t + \phi_0), \quad (2.5)$$

where  $a_0$  is the amplitude of the transmitted signal,  $\omega_0 = 2\pi f_c$ ,  $f_c$  is the frequency of the carrier wave and  $\phi_0$  is the initial radian phase of the transmitted signal. Each received signal  $S_i$  at time  $t$  from path  $i$  due to multipath can be expressed as

$$S_i(t) = a_i \exp[j(\phi_i + \frac{2\pi}{\lambda} vt \cos \theta_i)] \exp[j(\omega_0 t + \phi_0)], \quad (2.6)$$

where  $\phi_i$  is the phase change due to the time dispersion of the multipath,  $v$  is the speed of the mobile station,  $\lambda$  is the wavelength of the transmitted signal,  $\theta_i$  is the signal arriving angle and  $\frac{2\pi}{\lambda}vt \cos \theta_i$  is the phase change introduced by Doppler frequency shift.

Assume that total number of paths is  $N$ , the received signal  $S$  at the receiver is the combination of the signals from  $N$  paths:

$$S(t) = \sum_{i=1}^N S_i(t). \quad (2.7)$$

If complex form of  $\exp[j(\phi_i + \frac{2\pi}{\lambda}vt \cos \theta_i)]$  is used,  $S(t)$  can be expressed as

$$S(t) = \left[ \sum_{i=1}^N a_i \cos(\phi_i + \frac{2\pi}{\lambda}vt \cos \theta_i) + j \sum_{i=1}^N a_i \sin(\phi_i + \frac{2\pi}{\lambda}vt \cos \theta_i) \right] \times \exp[j(\omega_0 + \phi_0)] \quad (2.8)$$

Obviously, multipath effect in the wireless environment induces a real part and imaginary part of change to the transmitted signal. Let  $x_i$  designate real part and  $y_i$  designate imaginary part, i.e.,  $x_i = a_i \cos(\phi_i + \frac{2\pi}{\lambda}vt \cos \theta_i)$  and  $y_i = a_i \sin(\phi_i + \frac{2\pi}{\lambda}vt \cos \theta_i)$ ,  $S(t)$  can be expressed as

$$S(t) = (x + jy) \exp[j(\omega_0 + \phi_0)], \quad (2.9)$$

where  $x = \sum_{i=1}^N x_i$  and  $y = \sum_{i=1}^N y_i$ .

Because  $x$  is a variable of summation of  $N$  independent random variables  $x_i$  and  $y$  is a variable of summation of  $N$  independent random variables  $y_i$ , the probability density distribution of the random variables  $x$  and  $y$  should follow the normal distribution according to central limit theorem:

$$p(x) = \frac{1}{\sqrt{2\pi}\sigma_x} e^{-\frac{x^2}{2\sigma_x^2}}, \quad (2.10)$$

where  $p(x)$  is the probability distribution of variable  $x$ ,  $\sigma_x$  is the standard deviation of variable  $x$  and  $\sigma_x^2$  is the variance of  $x$ .

$$p(y) = \frac{1}{\sqrt{2\pi}\sigma_y} e^{-\frac{y^2}{2\sigma_y^2}}, \quad (2.11)$$

where  $p(y)$  is the probability distribution of variable  $y$ ,  $\sigma_y$  is the standard deviation of variable  $y$  and  $\sigma_y^2$  is the variance of  $y$ .

The joint probability density of  $x$  and  $y$  is given by:

$$p(x, y) = \frac{1}{\sqrt{2\pi}\sigma_x} e^{-\frac{x^2}{2\sigma_x^2}} \frac{1}{\sqrt{2\pi}\sigma_y} e^{-\frac{y^2}{2\sigma_y^2}}. \quad (2.12)$$

Assuming  $\sigma_x = \sigma_y = \sigma$ , the joint probability density of  $x$  and  $y$  can be expressed as:

$$p(x, y) = \frac{1}{2\pi\sigma^2} e^{-\frac{x^2+y^2}{2\sigma^2}}. \quad (2.13)$$

If we use spherical coordinates system to express the joint probability density of  $x$  and  $y$  instead of orthogonal coordinates system in space, two dimensional joint probability density of  $x$  and  $y$  can be written as

$$p(r, \theta) = \frac{r}{2\pi\sigma^2} e^{-\frac{r^2}{2\sigma^2}}, \quad (2.14)$$

where  $r^2 = x^2 + y^2$  and  $\theta = \arctan \frac{y}{x}$ .

The envelop probability density function of random radial variable  $r$  is obtained by integrating the joint probability density  $p(r, \theta)$  to  $\theta$  from 0 to  $2\pi$  :

$$p(r) = \frac{1}{2\pi\sigma^2} \int_0^{2\pi} r e^{-\frac{r^2}{2\sigma^2}} d\theta = \frac{r}{\sigma^2} e^{-\frac{r^2}{2\sigma^2}}. \quad (2.15)$$

(2.15) is Rayleigh distribution. Therefore the envelope of the multipath radio channel response without dominant line-of-sight path is Rayleigh distributed. Figure 2.6 demonstrates the simulation result of Rayleigh fading. Signal sample period is 1/10000 second, amplitude of the signal is 1 volt, maximum Doppler shift is 100Hz and average path delay is 1.0000e-006 second.

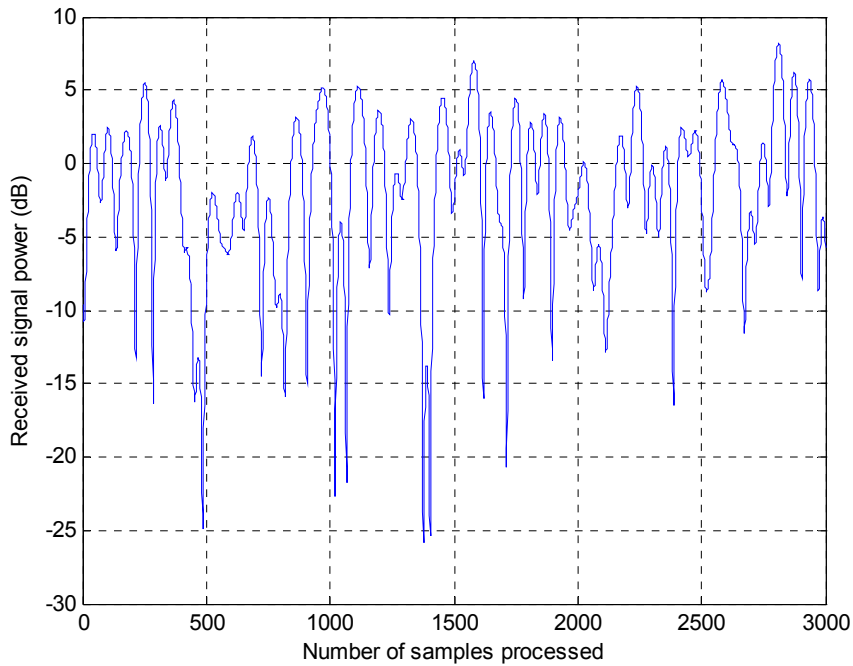


**Figure 2.6 Illustration of Rayleigh fading in wireless radio channel. Signal sample period is 1/10000 second, maximum Doppler shift is 100Hz and average path delay is 1.0000e-006 second.**

### **2.1.3.2 Rician model**

If the environment is such that, in addition to the scattering, there is a strongly dominant signal seen at the receiver, usually caused by a line-of-sight, then the mean of the random process will no longer be zero, varying instead around the power-level of the dominant path. Such a situation may be better modelled as Rician fading. Rician fading model assumes that the magnitude of a signal that has passed through a wireless radio channel will vary randomly according to a Rician distribution. The Rician distribution is given by

$$p(r) = \begin{cases} \frac{r}{\sigma^2} e^{-\frac{r^2+A^2}{2\sigma^2}} I_0\left(\frac{Ar}{\sigma^2}\right) & \text{for } (A \geq 0, r \geq 0) \\ 0 & \text{for } (r < 0) \end{cases}, \quad (2.16)$$

where  $r$  is radian variable,  $A$  denotes the peak amplitude of the dominant signal,  $\sigma$  is the standard deviation of random variable  $r$ .  $I_0(\bullet)$  is the modified Bessel function of the first kind and zero-order. The Ricean distribution becomes Rayleigh distribution if the dominant of the line-of-sight path fades away. Normally a parameter  $K = A^2 / (2\sigma^2)$  is used to describe the Ricean distribution.  $K$  is defined as Ricean factor which measures the ratio of signal power to the variance of the multipath. The Ricean distribution becomes to Rayleigh distribution when  $K \rightarrow 0$ .

Figure 2.7 shows the Ricean fading simulation result when  $K$  factor is 3, signal sample period is 1/10000 second, and maximum Doppler Shift is 100Hz.

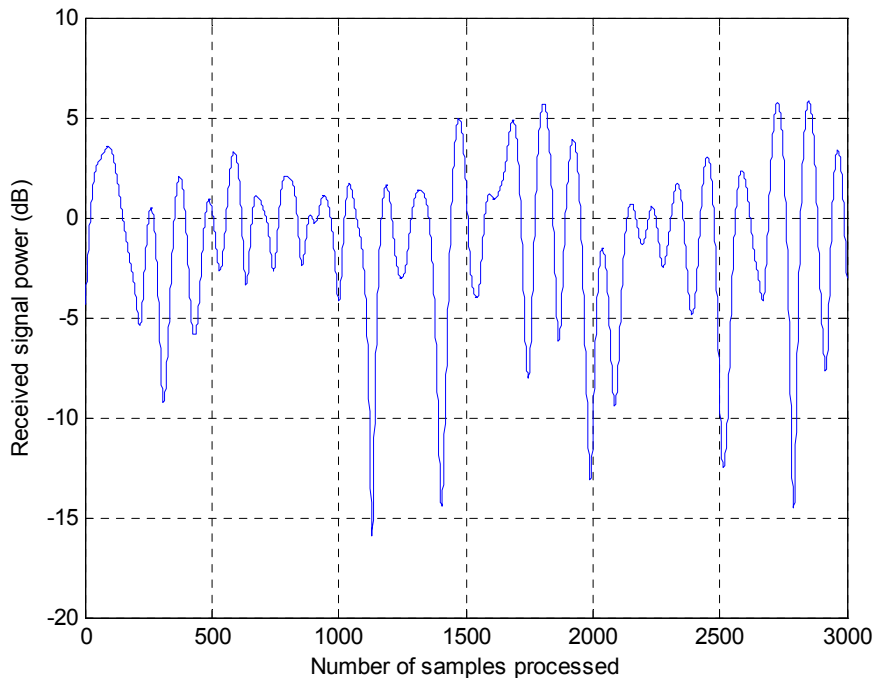


**Figure 2.7** Illustration of Ricean fading in wireless radio channel. Signal sample period is 1/10000 second, Maximum Doppler Shift is 100Hz and K factor is 3.

## **2.2 Performance measure of wireless communication systems**

### **2.2.1 Capacity of wireless channel**

It is known that Shannon capacity [C. E. Shannon, 1948] is defined as the maximum data rate over a channel with asymptotically small error probability. Figure 1.1 shows a typical communication system: the input signal is encoded by an encoder and then is transmitted from the transmitter; the signal traverses through the communication channel; the signal received at the receiver is the combination of the signal from the transmitter and the noise contributed from any sources on the way to the receiver, such as channel noise and thermal noise from the receiver; finally the output signal is the decoded signal from the receiver. The detected output signal should be realistic copy of the input signal, otherwise detection error occurs. In a typical wireless system with a discrete-time additive white Gaussian noise (AWGN) channel, the relationship between the output signal and input signal can be expressed as

$$y = x + n, \quad (2.17)$$

where  $y$  denotes the output signal at time  $t$ ,  $x$  denotes the input signal and  $n$  denotes the AWGN noise at time  $t$ . That is, the output of the system is the summation of input  $x$  and AWGN noise  $n$ . Assume that  $B$  is the channel bandwidth in  $Hz$ , the noise  $n$  is Gaussian distributed with zero mean and variance  $\sigma^2$ , average value of the received power is  $P_r$  in Watts and the received signal-to-noise ratio ( $SNR$ ) is the ratio of  $P_r B$  to the power of the noise  $\sigma^2$  in Watts, Shannon capacity in bits per second (bps) of such a channel is equal to

$$C = B \log_2(1 + SNR). \quad (2.18)$$

Shannon capacity is the maximum data rate that a communication system can achieve with near zero error probability, which is used as an upper bound on the achievable data rate in a real wired or wireless system.

### 2.2.2 Probability of message error and Bit Error Rate (BER)

In a wireless communication system, the digital signal can be sent in the form of message (or symbol) in bits [A. Goldsmith, 2005]. Assume that the total number of combination of  $K$  bits information is  $M$ , i.e.,  $M = 2^K$  and each input message  $m_i$  for  $i=1:M$  is  $K$  bits information, i.e.,  $m_i = \{b_1, b_2, \dots, b_K\}$ ;  $m_i$  is sent every  $T$  second therefore the transmission data rate of the system is  $R = K/T$  bits per second (bps). The message  $m_i$  is then modulated via signal modulation. The modulated signal  $s_i(t)$  during the time interval  $[0, T)$  is sent through the channel. The signal arriving at the receiver is then decoded and the receiver obtains the best estimation of the input message  $\hat{m}_i = \{\hat{b}_1, \hat{b}_2, \dots, \hat{b}_K\}$ . There are various modulation and demodulation methods and their usage depends on the system design requirement. The rule of thumb for the receiver design is to minimize the probability of message error  $P_e$ , which is defined as

$$P_e = \sum_{i=1}^M p(\hat{m}_i \neq m_i | m_i \text{ sent}) p(m_i \text{ sent}), \quad (2.19)$$

where  $p(m_i \text{ sent})$  is the probability of correct message estimation at the receiver  $m_i$  when the input message  $m_i$  is sent;  $p(\hat{m}_i \neq m_i | m_i \text{ sent})$  is the probability of incorrect message estimation at the receiver  $m_i$  when the input message  $m_i$  is sent. If the input signals are the binary phase-shift keying (BPSK) messages, the probability of message error is the probability of bit error that is also called bit error rate (BER). For the messages with  $K > 1$  bits information and  $M$ -signalling, that is, Pulse Amplitude Modulation (MPAM) and Phase-Shift Keying (MPSK), the relationship

between the probability of bit error  $P_b$  and the probability of message error  $P_e$  can be expressed approximately as [A. Goldsmith, 2005, p126]

$$P_b \approx \frac{P_e}{\log_2 M} . \quad (2.20)$$

Many factors can contribute to the probability of message error of wireless system; such as channel fading, transmit power, inter-symbol interference and any source of noises.

To improve the performance of the wireless system, it is desirable to attain the system capacity close to Shannon capacity and at the same time to maintain the probability of message error low in the system design. The multiple-input multiple output (MIMO) antenna technique is one of the methods to achieve these goals. The MIMO wireless system is the main focus of this thesis. The theoretic background on MIMO systems and some high capacity achieving strategies will be presented in the following sections of this chapter.

## **2.3 Single user – MIMO system and channel capacity**

### **2.3.1 Multiplexing gain and capacity of the MIMO channel**

In this section, we consider a narrowband point-to-point (single user) wireless MIMO system with  $M$  transmit antennas and  $N$  receive antennas. In a multiple antenna system, a multiplexing gain can be achieved by decomposing the MIMO channel into parallel channels and multiplexing different data streams onto these channels. The multiplexing gain can only be obtainable in the MIMO system, which is proportional to the number of transmit-antenna pairs, that is  $\min(N, M)$  [G. J. Foschini and M. J. Gans, 1998, E. Telatar, 1999]. Assume that  $\mathbf{H}(t)$  is the channel gain between the transmitter and receiver at any time instance  $t$ . The channel matrix has the

dimension of  $N \times M$  and the matrix element  $h_{ij}$  represents the gain from transmit antenna  $j$  to receive antenna  $i$ . The received signal at the receiver can be expressed as

$$\mathbf{y}(t) = \mathbf{H}(t)\mathbf{x}(t) + \mathbf{n}(t), \quad (2.21)$$

where  $\mathbf{y}(t)$  is the received signal column vector with  $N$  element,  $\mathbf{x}(t)$  is the input (transmitted) signal column vector with  $M$  dimension,  $\mathbf{n}(t)$  is the additive noise which is a column vector with  $N$  dimension. Assuming  $R$  denotes the rank of channel matrix  $\mathbf{H}$  and a MIMO channel is decomposed  $R$  parallel independent channels, an  $R$ -fold data rate increase can be achieved by multiplexing different data onto different channels in comparison with the single antenna input and single antenna output (SISO) system. In this thesis, white Gaussian noise is assumed, that is, the entries of the noise vector are independent, identically distributed (i.i.d) with zero mean and variance matrix  $\sigma^2 \mathbf{I}$ , where  $\mathbf{I}$  is the identity matrix with  $N \times N$  dimension. In the remainder of this thesis, the time index ( $t$ ) is often omitted.

A useful matrix operation used in decomposing the MIMO system is the singular value decomposition (SVD) of the channel matrix  $\mathbf{H}$ . The SVD matrix manipulation is expressed as:

$$\mathbf{H} = \mathbf{U}\mathbf{\Sigma}\mathbf{V}^H, \quad (2.22)$$

where  $\mathbf{U}$  is an  $N \times N$  unitary matrix,  $\mathbf{V}$  is an  $M \times M$  unitary matrix,  $\mathbf{V}^H$  is the Hermitian of the matrix  $\mathbf{V}$  and  $\mathbf{\Sigma}$  is an  $N \times M$  diagonal matrix of singular values  $\{\sigma_i\}$  of  $\mathbf{H}$ . Assuming  $\lambda_i$  is the  $i$ th largest eigenvalue of  $\mathbf{H}\mathbf{H}^H$ , the singular value  $\sigma_i$  is equal to  $\sqrt{\lambda_i}$  as this singular value property holds. If both transmitter and receiver have perfect channel information, the MIMO channel can be decomposed into independent parallel channels. By perform SVD to the channel matrix, we can obtain the transmit precoding

vector to the input vector  $\mathbf{x}$  and receiver shaping vector to the output vector  $\mathbf{y}$ , therefore achieve parallel decomposition of the MIMO channel, as shown in Figure 2.8. The transmit precoding can be generated by a linear transformation on input vector  $\mathbf{x}$ , that is,  $\tilde{\mathbf{x}} = \mathbf{V}\mathbf{x}$ . Similarly, the receiver shaping can be acquired by multiplying the summation of the channel output  $\tilde{\mathbf{y}}$  and the noise  $\mathbf{n}$  with  $\mathbf{U}^H$  at the receiver, i.e.,  $\mathbf{y} = \mathbf{U}^H(\tilde{\mathbf{y}} + \mathbf{n})$ . The signal and noise component after receiver shaping are  $\mathbf{U}^H \tilde{\mathbf{y}}$  and  $\tilde{\mathbf{n}} = \mathbf{U}^H \mathbf{n}$  respectively.

To estimate and optimize the channel capacity in MIMO system, parameters such as, channel bandwidth, the distribution of channel noise, the transmit power constraint are playing an important part in addition to the channel side information at the transmitter (CSIT) and channel side information at the receiver (CSIR). In general, different assumptions about channel side information (CSI) and about the distribution of the channel  $\mathbf{H}$  entries lead to different channel capacities and different approaches to space-time signalling.

The capacity of the discrete static channels in terms of the mutual information between channel input  $\mathbf{x}$  and output vector  $\mathbf{y}$  is defined as [T. Cover and J. Thomas, 1991]

$$C = \max_{p(\mathbf{x})} I(\mathbf{x}; \mathbf{y}) , \quad (2.23)$$

where  $I(\mathbf{x}; \mathbf{y})$  denotes the mutual information between channel input and channel output and  $p(\mathbf{x})$  is the input distribution. Hence the capacity is that the maximum mutual information taken over all possible input distribution  $p(\mathbf{x})$ .

Assuming that perfect channel information is known to the transmitter and receiver, the MIMO capacity can be expressed in terms of

maximizing the mutual information over all input covariance matrices  $\mathbf{R}_x$  satisfying the power constraint [A. Goldsmith et al., 2003]:

$$C = \max_{\mathbf{R}_x: \text{Tr}(\mathbf{R}_x) = \rho} B \log_2 \det[\mathbf{I}_N + \mathbf{H}\mathbf{R}_x\mathbf{H}^H], \quad (2.24)$$

where  $B$  is the channel bandwidth,  $\text{Tr}(\mathbf{R}_x)$  is the trace of input covariance matrices  $\mathbf{R}_x = \mathbf{E}[\mathbf{x}\mathbf{x}^H]$ ,  $\rho$  is the power constraint that is the ratio of the signal transmit power/noise power  $P/\sigma^2$ ,  $\mathbf{H}$  is the MIMO channel matrix,  $\mathbf{H}^H$  is the Hermitian of  $\mathbf{H}$ ,  $\mathbf{I}_N$  is the identity matrix with  $N \times N$  dimension and  $\det[\cdot]$  denotes the determinant of a matrix. It is known that maximizing MIMO channel capacity leads to the transmit power optimally allocated on each of the independent parallel channel. The capacity on this power allocation optimization can be expressed as:

$$C = \max_{P_i: \sum_i P_i \leq P} \sum_{i=1}^{R_H} B \log_2 \left(1 + \frac{P_i \gamma_i}{P}\right), \quad (2.25)$$

where  $R_H$  is the number of nonzero singular values  $\sigma_i^2$  of  $\mathbf{H}$ ,  $\gamma_i = \sigma_i^2 P / \sigma^2$  is the signal noise rate (SNR) associated with the  $i^{\text{th}}$  channel at full power.  $P_i$  is the power allocated to the  $i^{\text{th}}$  parallel channel and  $P$  is the total transmit power at the transmitter. Solving the optimization of equation (2.25) results in a well known water-filling power allocation or waterpouring algorithm for the MIMO channel [T. Cover and J. Thomas, 1991, A. Goldsmith et al., 2003]:

$$\frac{P_i}{P} = \begin{cases} 1/\gamma_0 - 1/\gamma_i & \gamma_i \geq \gamma_0 \\ 0 & \gamma_i < \gamma_0 \end{cases}, \quad (2.26)$$

for a cut off SNR value  $\gamma_0$ . The capacity under this operation can be expressed as:

$$C = \sum_{i:\gamma_i \geq \gamma_0} B \log_2 \left( \frac{\gamma_i}{\gamma_0} \right). \quad (2.27)$$

On the other hand, uniform power allocation scheme can be used if the channel information is known to the receiver and unknown to the transmitter. In this case, the mutual information for an  $M$  number of transmit antennas and  $N$  number of receive antennas of a MIMO system is as follows:

$$I(\mathbf{x}; \mathbf{y}) = B \log_2 \det \left[ \mathbf{I}_N + \frac{\rho}{M} \mathbf{H}\mathbf{H}^H \right], \quad (2.28)$$

where  $\mathbf{I}_N$  is the identity matrix with  $N$  dimension,  $\mathbf{H}$  is the MIMO channel matrix and  $\rho$  is the ratio of the signal transmit power/noise power  $P/\sigma^2$ .

In this thesis, we consider the situation of perfect CSIT and CSIR as well as the situation of perfect CSIR only. For the first case, water-filling power allocation is applied in the transmission scheme presented in the later chapters of the thesis. In the case of only channel state information known to the receiver, either equal power allocation to the transmitter is utilized or the transmitter gains the channel state information from the receiver via feedback channel and then the water-filling power allocation can be implemented.

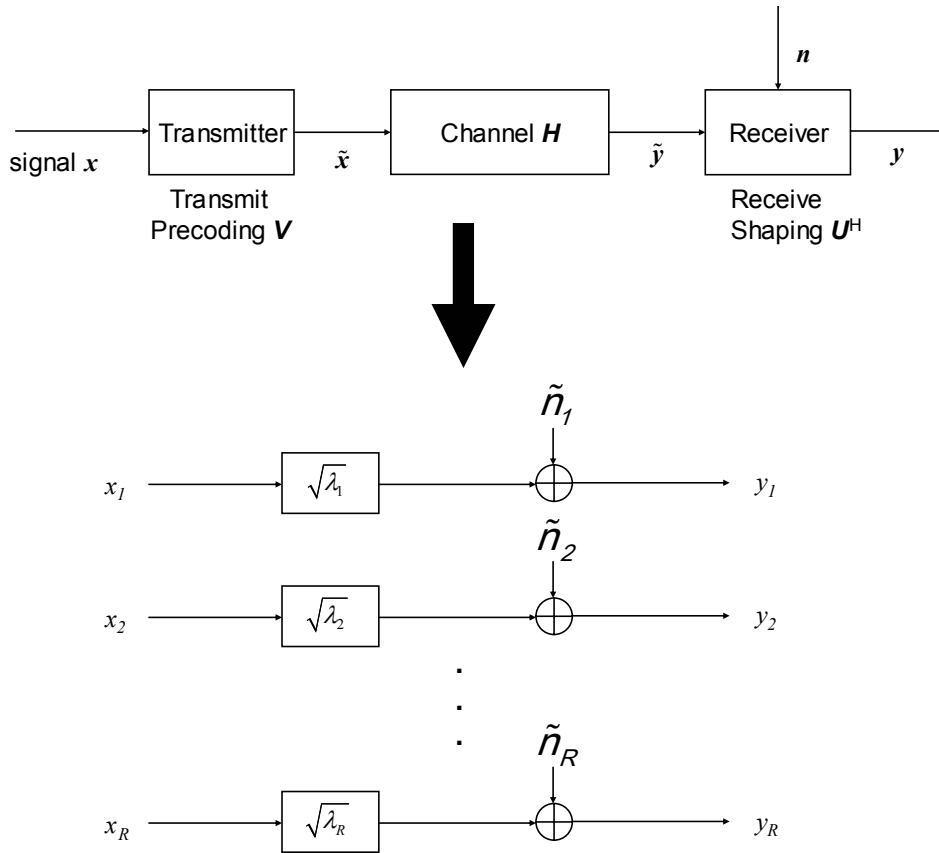


Figure 2.8 Decomposition of MIMO channel under the condition of perfect CSIT and CSIR.

### 2.3.2 Space diversity gain and the capacity of MIMO beamforming

In a wireless channel, the signal power can drop significantly across space, time and frequency due to channel fading. In the MIMO system, same copy of transmitted signal at the transmitter reaches to the receiver via different transmit-receive antenna path. Each path constitutes a diversity branch. The received signal on one path differs from the received signals on other paths since each individual path suffers from different degree of channel fading. Space diversity describes the phenomenon of multiple copies of the transmitted signal at the receiver due to the space difference of the multiple

antennas. Space diversity in a MIMO system can be used to combat fading. Space diversity gain is the increases in signal-to-interference ratio due to the space diversity scheme that can be achieved by using multiple transmit antennas and/or receive antennas. Receive antenna diversity of SIMO system and transmit antenna diversity of MISO system are two special cases of the space diversity of MIMO system. The schemes for obtaining the receive diversity gain for SIMO system and the transmit diversity gain for MISO system can be equally applied to the MIMO system. The details of the receive diversity gain of SIMO, transmit diversity gain of MISO and space diversity gain of MIMO system are following.

### 2.3.2.1 Receive diversity of SIMO system

Assuming that number of receive antennas is  $N$ , flat fading channel is considered and each transmit-receive link is Raleigh fading channel, i.e., the real and imaginary parts of element entries of the channel vector following Gaussian distributed with zero mean and unit variance. The channel vector in the SIMO system is

$$\mathbf{h}=[h_1, h_2, \dots, h_N]^T, \quad (2.29)$$

where  $[\cdot]^T$  denotes the transpose of the vector. The received signal  $\mathbf{y}$  at the receiver is

$$\mathbf{y} = \mathbf{h}s + \mathbf{n}, \quad (2.30)$$

where  $s$  is the signal that is the scalar,  $\mathbf{n}$  is the  $N \times 1$  noise vector that is the additive white Gaussian noise with zero mean and variance  $\sigma^2$ . Perfect channel information at the receiver is assumed. To maximize the received  $SNR$  and obtain the receive diversity gain; Maximum Ratio Combining

(MRC) can be implemented at the receiver. The final output after MRC operation can be expressed as

$$\mathbf{y}_{\text{MRC}} = \mathbf{h}^H \mathbf{h} s + \mathbf{h}^H \mathbf{n}, \quad (2.31)$$

where  $[\cdot]^H$  denotes the Hermitian of the vector. Assume that the transmitted signal power is  $P$ , the  $SNR$  at the receiver is

$$SNR = \|\mathbf{h}\|_F^2 \rho, \quad (2.32)$$

where  $\|\mathbf{h}\|_F^2$  denotes the Frobenius norm of  $\mathbf{h}$  and  $\rho = P / \sigma^2$  is the signal-to-noise ratio in the case of single-input and single-output (SISO) antenna link. For the Rayleigh fading channel and if the separation between the antennas at the receiver is greater than the coherence distance, which is defined as the maximum spatial separation over which the channel response can be assumed constant [T. S. Rappaport, 2002], the diversity order of such system is equal to the number of receive antennas at the receiver  $N$  [A. J. Paulraj et al., 2003]. In (2.32),  $\rho$  represents the diversity gain attained, which means that system behaves the same as the SISO system without fading. Because the mean value of  $\|\mathbf{h}\|_F^2$  is  $N$  for the flat Rayleigh fading channels under consideration, the average value of received  $SNR$  of the SIMO system is also increased by  $N$ -fold. It is known as the array gain which is defined as the average increase of  $SNR$  at the receiver due to the coherent combining effect of the multiple antennas of the MIMO antenna array.

### 2.3.2.2 Transmit diversity of MISO system

In MISO system, multiple antennas at the transmitter can be used to obtain spatial diversity and array gain. In such system, the transmitter is equipped with  $M$  antennas and one antenna at the receiver. Normally the flat Rayleigh

fading channel is considered; hence the channel vector  $\mathbf{h}$  is a row vector as follows:

$$\mathbf{h} = [h_1 \ h_2 \ \cdots \ h_M], \quad (2.33)$$

where each entry of  $\mathbf{h}$  is a complex value and the real and imaginary parts of the entries are Gaussian distributed with zero mean and unit variance. If the transmit signal is a scalar  $s$  and the transmitter has perfect channel state information, the scheme of transmit-maximal ratio combining (transmit-MRC) [T. Lo, 1999] can extract full transmit diversity gain as well as the array gain due to the transmit antenna array. The details of the scheme are given below.

Suppose that  $\mathbf{w}$  is the weight vector applied to the transmit antennas before the signal  $s$  is transmitted. The received signal at the receiver is given by

$$y = \mathbf{h}\mathbf{w}s + n, \quad (2.34)$$

where  $\mathbf{w}$  is column vector with  $M$  dimensions,  $n$  is Gaussian noise and the entries of noise are Gaussian distributed with zero mean and variance  $\sigma^2$ . If average total power of the signal is  $P$  and the weight vector is chosen as

$$\mathbf{w} = \sqrt{P} \frac{\mathbf{h}^H}{\sqrt{\|\mathbf{h}\|_F^2}}. \quad (2.35)$$

The received  $SNR$  can be maximized and given by [T. Lo, 1999]

$$SNR = \|\mathbf{h}\|_F^2 \rho. \quad (2.36)$$

For the flat Rayleigh fading channel considered and mean value  $\|\mathbf{h}\|_F^2$  of  $M$ , i.e.,  $E[\|\mathbf{h}\|_F^2] = M$  where  $E[\cdot]$  is the expectation operator, the average  $SNR$  value at the receiver can be expressed as

$$\overline{SNR} = M \rho. \quad (2.37)$$

The diversity order of such MISO system is  $M$  [A. J. Paulraj et al., 2003] and the average  $SNR$  is enhanced by a factor of  $M$  in comparison with the received signal-to-noise value  $\rho$  in the case of SISO link. Therefore, both diversity gain represented by  $\rho$  in (2.37) and array gain characterized by  $M$  can be extracted via the transmit-MRC scheme.

### 2.3.2.3 Space diversity of MIMO

For the MIMO case, space diversity and array gain can be obtained due to the multiple antenna arrays. Diversity in the MIMO channel is the combination of the transmit diversity of MISO channel and receive diversity of the SIMO channel. If the channel information is not known to the transmitter, a simple Alamouti scheme can be used to extract diversity gain [S. Alamouti, 1998]. In a simple case of two transmit and two receive antennas, the symbol transmit sequence of the Alamouti scheme is: during the first symbol period, symbol  $s_1$  is transmitted from antenna 1 and symbol  $s_2$  is transmitted from antenna 2 concurrently; then symbols  $-s_2^*$  and  $s_1^*$  are transmitted from antennas 1 and 2 respectively in the second symbol period. Since channel information is not known to the transmitter, equal transmit power  $P/2$  ( $P$  denotes the total transmit power) is applied to the transmit antennas. Assume that channel is flat fading channel and noise is white Gaussian noise with zero mean and variance  $\sigma^2$ . Alamouti scheme can extract fourth order diversity and receive array gain. In the general case of the MIMO system with  $M$  transmit antennas and  $N$  receive antennas, the

diversity order extracted by Alamouti scheme depends on the number of transmit and receive antennas and how the symbol transmit sequence designed. Alamouti scheme can be equally applied to the MISO system and extracted diversity order is related to number of transmit antenna  $M$  only.

In this thesis, we consider that the channel information is known to the transmitter in Chapter 3 where a scheduling algorithm in a multiuser MIMO (MU-MIMO) system is studied. In the MIMO system with perfect channel information, the space diversity can be extracted by a method of MIMO beamforming, as shown in Figure 2.9. In this scheme, the same symbol  $x$  is applied by a weight column vector before the signal is transmitted through the transmit antennas. To maximize the system capacity, the beamforming strategy is to use the matrix SVD operation to the channel matrix  $\mathbf{H}_{N \times M}$  and obtain the unitary matrices  $\mathbf{U}_{N \times N}$  and  $\mathbf{V}_{M \times M}^H$ , the first column vectors from  $\mathbf{U}$  and  $\mathbf{V}^H$  are selected as the precoding and shaping column vectors:  $\mathbf{v}$  and  $\mathbf{u}^H$ , where  $\mathbf{v} = [v_1, v_2, \dots, v_M]^T$  and  $\mathbf{u} = [u_1, u_2, \dots, u_N]^T$ ,  $[\cdot]^H$  denotes the Hermitian of a vector or a matrix. The vector  $\mathbf{v}$  is chosen as the transmit weight vector and  $\mathbf{u}^H$  is selected as the receive weight vector. The transmit and receive weight vectors are normalized so that  $\|\mathbf{u}\| = \|\mathbf{v}\| = 1$ . The received signal  $\mathbf{y}$  with  $N$  dimensions can be expressed as:

$$\mathbf{y} = \mathbf{u}^H \mathbf{H} \mathbf{v} x + \mathbf{u}^H \mathbf{n}, \quad (2.38)$$

where  $\mathbf{n}$  is the white Gaussian noise column vector with  $N$  dimensions and each element entry is following independent and identically distributed with zero mean and variance  $\sigma^2$ .

Since the weight vectors in the beamforming scheme corresponding to the maximum singular value  $\sigma_{\max}$  of channel matrix  $\mathbf{H}$ , the SNR at the receiver is  $\sigma_{\max}^2 \rho$  if the power constraint is  $\rho = P / \sigma^2$ . The capacity of this beamforming scheme can be expressed as

$$C = B \log_2(1 + \sigma_{\max}^2 \rho) , \quad (2.39)$$

where  $B$  is the bandwidth. Therefore, this technique is also called dominant eigenmode transmission. The beamforming scheme can extract maximum diversity order of  $NM$  (the product of number of receive and transmit antennas) and array gain is given by  $\mathcal{E}[\sigma_{\max}^2]$ .

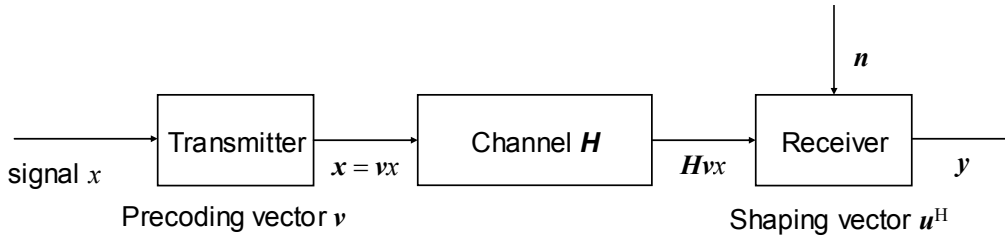


Figure 2.9 MIMO beamforming.

## 2.4 Multiuser MIMO channel capacity

We have discussed single user MIMO (SU-MIMO) case in the space time (ST) wireless system. The antenna arrays in the SU-MIMO system are deployed at one transmitter and one receiver. In a wireless application system such as cellular wireless system, one base station needs to support multiple users. If multiple antennas are equipped at the base station and user terminal having one or multiple antennas, the antenna arrays are across the base station and multiple users. The communication channel of such system is referred to as multiuser MIMO (MU-MIMO) channel. The distinct feature of MU-MIMO system is that the base station can communicate with multiple users simultaneously in the same frequency channel if a transmit scheme is designed by utilizing the space signature of the users in the system and the interference among users can be eliminated or minimized. This feature is called space division multiple access (SDMA) which refers to channel reuse within a cell due to geographical location of users.

Therefore, SDMA can improve system performance by increasing the spectral efficiency.

Assume that  $K$  users are in a cellular system, the base station is equipped with  $M$  antennas and each user terminal equipped with one or more antennas, Figure 2.10 shows two kinds of channels in the MU-MIMO system, namely uplink channel (or multiple access channels) and downlink channel (broadcast channel). The system performance analysis to MU-MIMO system is more complex than the performance analysis to the SU-MIMO system. In the case of downlink channel, the MU-MIMO channel behaves the same as SU-MIMO if the transmitter has perfect channel information from all users, although different users experience different path loss and channel fading due to the space signature of user terminals. In comparison with SU-MIMO channel, the transmit-receive pairs in MU-MIMO channel can originate from different users. In the case of uplink channel, system capacity achieved depends on if users can cooperate in encoding in the transmission stage.

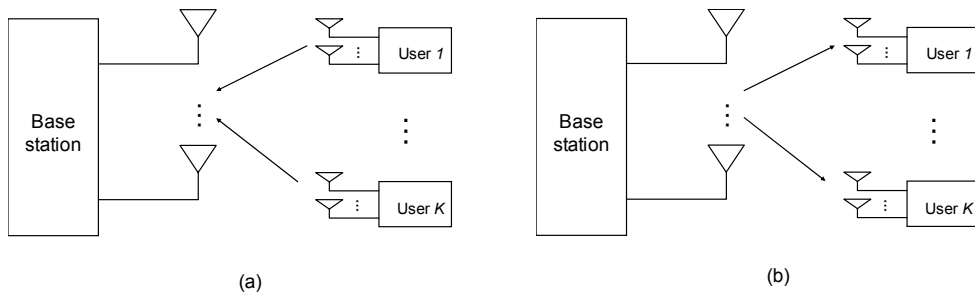


Figure 2.10 MU-MIMO channel: (a) Uplink, (b) Downlink

### 2.4.1 Capacity of multiuser MIMO uplink channel

Different from the capacity expression of SU-MIMO, MU-MIMO capacity is defined by a *rate region* [T. Cover and J. Thomas, 1991]. If there are  $K$  users in the cellular system and each user is represented by a rate vector

$R_i$  for  $i=1,\dots,K$ , the capacity region for  $K$  user MAC system is the closure of the class of achievable rate vectors. Assume that the base station is deployed with  $M$  antennas and each user terminal is equipped with  $N$  antennas; the channel matrix between the base station and user  $k$  is  $\mathbf{H}_k$ , for  $k=1,\dots,K$  with  $M \times N$  dimensions; the system MAC channel matrix including  $K$  users is  $\mathbf{H}=[\mathbf{H}_1,\dots,\mathbf{H}_K]$ ;  $\mathbf{x}_k$  for  $k=1,\dots,K$  is the input signal column vector with  $N$  dimensions for  $k$ th user and the signal follows zero mean Gaussian distributed;  $\mathbf{n}$  is zero-mean complex Gaussian noise column vector with  $M$  dimensions at receiver and  $\mathbf{E}[\mathbf{n}\mathbf{n}^H]=\mathbf{I}_{M \times M}$  where  $\mathbf{I}$  is the identity matrix. The received column signal with  $M$  dimensions at the receiver is given by

$$\mathbf{y}=[\mathbf{H}_1,\dots,\mathbf{H}_K]\begin{bmatrix} \mathbf{x}_1 \\ \vdots \\ \mathbf{x}_K \end{bmatrix}+\mathbf{n}. \quad (2.40)$$

A high sum-rate can be achieved via joint decoding than that via the independent decoding [B. Suard et al., 1998]. Joint decoding is that decoding of all signals is performed simultaneously and cooperatively and signals are processed as signals. Independent decoding is that different signals are decoded independently and in parallel and the signal from other users  $\mathbf{x}_{i \neq k}$  for  $i=1,\dots,K$  are treated as the noise when signal  $\mathbf{x}_k$  for  $k=1,\dots,K$  is decoded.

Let  $\mathbf{Q}_{x,k}=\mathbf{E}[\mathbf{x}_k\mathbf{x}_k^H]$  be the covariance matrix of input signal for user  $k$ ;  $P_k$  is the power constraint applied to the  $k$ th user terminal; and normalizing bandwidth to unity. The capacity region for joint decoding is given by

$$\sum_{k=1}^K R_k \leq \log_2 \det \left[ \mathbf{I} + \sum_{k=1}^K \mathbf{H}_k \mathbf{Q}_{x,k} \mathbf{H}_k^H \right]. \quad (2.41)$$

The capacity region of the joint decoding scheme is polyhedral when total number of user  $K > 2$ . The maximum sum-rate capacity is achievable when maximum likelihood (ML) decoding or Minimum Mean Square Error (MMSE) decoding is applied and equality of (2.41) holds. In the case of independent decoding, let  $\mathbf{Q}_{y,k} = E[\mathbf{y}\mathbf{y}^H]$  be the covariance matrix of received signal for user  $k$ , the achievable rate is given by

$$R_k \leq \log_2 \left( \frac{\det(\mathbf{Q}_{y,k})}{\det(\mathbf{Q}_{y,k} - \mathbf{Q}_{x,k})} \right) \text{ for } k=1, \dots, K, \quad (2.42)$$

since the signals from other users are considered as noise for user  $k$ . Figure 2.11 shows the capacity region of the MAC system for two users. The maximum sum-rate capacity achieved through independent decoding will be less than that via the joint decoding.

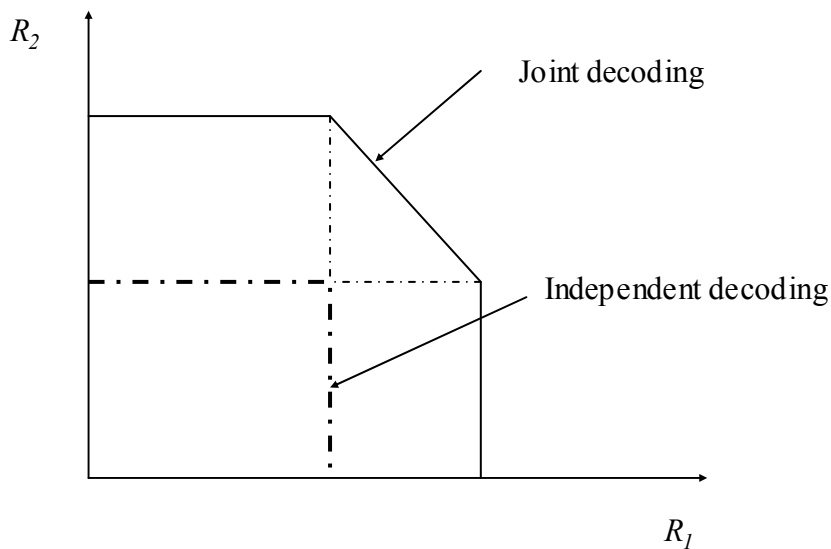


Figure 2.11 Capacity region of MIMO MAC system for two users.

## 2.4.2 Capacity of multiuser MIMO broadcast (BC) downlink channel

In a  $K$  user MIMO BC downlink cellular system, supposing the transmitter (base station) has  $M$  antennas and each user terminal (receiver) has  $N$  antennas. The  $N \times M$  channel matrix  $\mathbf{H}_k$  for  $k=1, \dots, K$  characterizes the channel gains between the transmitter and the  $k$ th receiver. Assume that the input signal is a column vector  $\mathbf{x}$  with  $M$  dimensions; a column vector  $\mathbf{n}_k$  with  $N$  dimensions represents the additive white Gaussian noise with zero mean and variance  $\sigma^2$  at  $k$ th receiver, the received signal  $\mathbf{y}_k$  for the  $k$ th user is:

$$\mathbf{y}_k = \mathbf{H}_k \mathbf{x} + \mathbf{n}_k. \quad (2.43)$$

Assume that MIMO BC channel is Gaussian distributed. In a multiuser Gaussian BC channels with one antenna at transmitter and one antenna at each receiver, it can be regarded as a degraded broadcast channel for which the capacity region is well established [T. Cover and J. Thomas, 1991]. Degraded BC channel means that one user's signal is a noisier version of the other user's signal. The capacity region for a degraded broadcast channel can be achieved by using a superposition coding and interference subtraction scheme [T. Cover and J. Thomas, 1991]. MU-MIMO downlink channel is no longer degraded channel and the capacity region for a non-degraded broadcast channel is an unsolved problem. However, the capacity region can be achieved if an interference subtraction technique based on the notion of Dirty Paper Coding (DPC) [M. Costa, 1983] is applied to the system [G. Caire and S. Shamai, 2003].

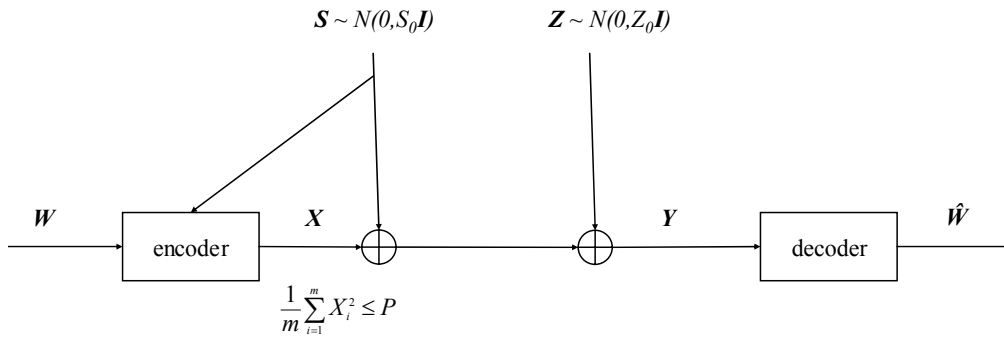


**Figure 2.12 Gaussian Shannon channel with Gaussian interference.**

In [M. Costa, 1983], a Gaussian channel is considered as shown in Figure 2.12. Assume that  $m$  sequence of codeword are sent from the transmitter and the codeword has an index  $W \in (1, \dots, M)$ . Here  $M$  is the greatest integer smaller than or equal to  $e^{mR}$  and  $R$  is the rate in nats per transmission. The interference signal  $S$  of the channel for  $m$  transmissions is assumed to be a sequence of independent identically distributed (i.i.d.) random variables with zero mean and variance  $S_0$ , i.e.,  $N(0, S_0 \mathbf{I})$  where  $\mathbf{I}$  is the identity matrix. The  $S$  is known to the transmitter but not to the receiver. The output of encoder  $X$  is the summation of the codeword input  $W$  and the interference  $S$ . Assume that the codeword  $X$  satisfies the power constraint  $\frac{1}{m} \sum_{i=1}^m X_i^2 \leq P$  where  $P$  is the transmit power. The channel output is then given by  $Y = X + S + Z$ , where the channel noise  $Z$  is Gaussian distributed with zero mean and variance  $Z_0$ , that is  $N(0, Z_0 \mathbf{I})$ . Upon receipt of  $Y$  the decoder creates an estimate  $\hat{W}$  of the index  $W$ . The idea of the transmission strategy is that it adds some extra i.i.d. interference sequence  $S$  to the output of the channel, as long as full knowledge of this extra noise sequence is known to the encoder. The optimal encoding uses codewords in the direction of  $S$ . The encoder looks at the space surrounding the vector  $S$  and chooses codewords that are compatible with the power constraint. Therefore, the encoder adapts its signal to the  $S$  instead of trying to erase it. In [M. Costa, 1983], it proves that the capacity of the Gaussian channel with this extra additive Gaussian interference and power constrained input is not

affected by the  $\mathcal{S}$  as if the channel behaves without the interference noise  $\mathcal{S}$ . The maximum capacity achieved is  $C = \log_2(1 + \frac{P}{Z_0})$ . This transmission strategy is given the name Dirty Paper Coding (DPC) because it is analogous to the problem of writing a message on a sheet of dirty paper that covered with independent dirt spots of normally distributed intensity. The writer knows the location and intensity of the dirt spots and writes; the reader read but cannot distinguish the dirt spot from the ink marks applied by the writer.

In multiuser MIMO broadcast channel, the idea of DPC can be applied at the transmitter when choosing codewords for different users in transmission [W. Yu, and J. M. Cioffi, 2004]. Assume that there exists the MU-MIMO BC system described at the beginning of this section except different users send their own codeword (input signal)  $\mathbf{x}_k$ , for  $k=1, \dots, K$ .  $K$  users is ordered as  $k=1, \dots, K$ . DPC encoding of MU-MIMO BC channel works as follows. The transmitter first transmits the codeword  $\mathbf{x}_1$  for user 1. Then the codeword for user 1 is pre-subtracted before the codeword  $\mathbf{x}_2$  for user 2 is transmitted since the transmitter has full knowledge of the codeword intended for user 1. By doing so, user 2 does not see the codeword intended for user 1 as interference. Similarly, the codeword for user  $k$  for  $k > 2, \dots, K$  does not see the codeword intended for previous  $k-1$  users as interference. Therefore following capacity region is achievable via DPC scheme in transmission:

$$(R_1, \dots, R_K): R_i \leq \log_2 \frac{\det \left[ \mathbf{I} + \sum_{k=i}^K \mathbf{H}_k \mathbf{Q}_k \mathbf{H}_k^H \right]}{\det \left[ \mathbf{I} + \sum_{k=i+1}^K \mathbf{H}_k \mathbf{Q}_k \mathbf{H}_k^H \right]} \text{ for } i=1, \dots, K, \quad (2.44)$$

where  $\mathbf{Q}_k = E[\mathbf{x}_k \mathbf{x}_k^H]$  denotes the input covariance matrix for user  $k$ .  $\mathbf{Q} = [\mathbf{Q}_1, \dots, \mathbf{Q}_K]$  is a set of positive semi-definite covariance matrices

satisfying constraint  $\sum_{i=1}^K \text{Tr}[\mathbf{Q}_i] \leq P$ , where  $\text{Tr}[\bullet]$  denotes the trace operator.

Equation (2.44) represents the capacity region for one permutation of  $K$  users. It is obvious that the capacity region expression for  $K$  user MIMO BC channel is more complex because number of full permutation of users is  $K!$ . Therefore, the capacity region is the convex hull of the union of all rate vectors over all permutations and all positive semi-definite covariance matrices satisfying the average power constraint.

As we know from [S. Vishwanath et al., 2003, P. Vishwanath and D. N. C. Tse, 2003], it is difficult to compute the MIMO downlink capacity because the rate expression in (2.44) is neither a concave nor a convex of the covariance matrices. The uplink-downlink duality is an important feature to explore in a MU-MIMO system to obtain MU-MIMO BC capacity region. By applying this duality characteristic, we can simplify calculation of the capacity region and simplify finding the corresponding optimal transmission strategy. However, this uplink-downlink duality is out of the scope of this thesis, interested reader can refer to the reference papers given for details.

### **2.4.3 Scheduling and linear transmission scheme in MU-MIMO BC systems**

In following chapters of this thesis, we consider the scheduling and linear transmission in MU-MIMO broadcast (BC) system. In MU-MIMO BC systems, the signal transmission schemes and user selection strategies (they are also called scheduling strategies) can be designed with the aim of maximizing the system capacity if the transmitter at the base station can acquire the channel information of users. The base station can broadcast the signals dedicated to multiple users simultaneously and also keep the signal interference among users to minimum via user cooperation and joint encoding. At the same time, the scheduling strategies can consider signal

transmission to the users in a fairness manner so each user can have a fair chance to be served. There are numerous research papers on scheduling in multiuser MIMO wireless systems. In [P. Viswanath et al., 2002] multiple transmit antennas are applied to induce large and fast fluctuations in a multiuser system when user channels conditions have very little change. The benefit of this scheme is to increase the dynamic range of the fluctuation so the transmitter can decide and allocate all signal power to the user with the best channel condition to exploit the multiuser diversity. T.Yoo and A. Goldsmith [T. Yoo and A GoldSmith, 2006] investigated a simple Zero-Forcing Beamforming (ZFBF) strategy to achieve suboptimal asymptotic sum capacity in a multiuser broadcast system. The scheduling strategies in the MU-MIMO BC systems can be categorized into types: (a) optimal scheduling strategies, such as Dirty Paper Coding (DPC) [M. Costa, 1983]; (b) scheduling schemes consider only the fairness to serve the users, for example, Round-Robin (RR) scheduling [R. S. Ranasinghe et al., 2001, O. S. Shin and K. B. Lee, 2003]; (c) the scheduling strategies between the categories (a) and (b), which compromise the fairness and system capacity optimization. The strategies of category (c) usually explore the user channel information and design the signal transmission scheme to achieve high system capacity limit. The examples of these strategies are Beamforming (BF) [A. Paulraj et al., 2003], Time Sharing (TS) [ P. Viswanath et al., 2002, M. Sharif and B. Hassibi, 2005], Proportional Fair Scheduling (PFS) [C. Etienne et al., 2002].

Assume that there exist  $K$  users in the MU-MIMO BC system, the transmitter has  $M$  antennas, each user terminal is equipped with  $N$  antennas and channel matrix for user  $k$  is  $\mathbf{H}_k$  with  $N \times M$  dimensions for  $k = 1, \dots, K$ . White Gaussian noise for each user  $\mathbf{n}$  is assumed, that is, the entries of the noise matrix are independent, identically distributed (i.i.d) with zero mean and variance matrix  $\sigma^2 \mathbf{I}$ , where  $\mathbf{I}$  is the identity matrix with  $N \times N$  dimension.

DPC is an optimal scheduling scheme and maximum capacity can be achieved under this scheme. DPC is also an interference cancellation technique for reducing interference in the downlink channel. By using coherent channel knowledge  $\mathbf{H}_k$ , users are ordered and user signals are sequentially encoded and transmitted. The user does not see previous user signal as interference in the DPC scheme. It has been shown theoretically DPC offers the optimal rate for MU-MIMO BC system [M. Sharif and B. Hassibi, 2007]. However, it is difficult to implement in practical systems due to the high computational complexity.

The beamforming (BF) scheduling used in a MU-MIMO downlink channel is a strategy where the transmitter transmits signals to multiple users simultaneously via a linear precoding. BF strategy assigns a beamforming weight vector to each user so that the simultaneous signals transmitted to multiple users are orthogonal to each other. In a MU-MIMO downlink system with a large number of users, a user selection algorithm can be designed by exploring user channel information. Transmitting signals to the users with the best channel conditions can assure high system capacity achieved.

Time sharing (TS) is a scheduling scheme that only one user with the best channel condition is served in any timeslot in the allocated frequency band. This scheme explores multiuser diversity by transmitting the signal to the user with the highest channel gain. However, the fairness to serve all users is not considered under this scheme.

Proportional faire scheduling (PFS) is a scheme which takes into account multiuser diversity as well as the fairness when users have varying channel conditions. In comparison with the TS scheme, PFS also serves one user in any time slot. However, the decision to serve a user of this scheme is made on if the user has the maximum ratio of  $\alpha = R_k(t)/T_k(t)$ , where  $R_k(t)$  is a requested data rate for a user  $k$  at the time  $t$  and  $T_k(t)$  is the actual

throughput at time  $t$  for the user  $k$ . The user being served in current time slot has a higher chance not to be served in next time slot because the user has the possibility of small  $\alpha$  due to high  $T_k(t)$ . Therefore, PFS is a fairer scheme than time sharing scheduling.

Round-Robin (RR) is a fair scheduling scheme and each user has a fair chance to be served in turn. However, RR scheduling does not consider whether a user has a best channel condition and therefore it does not allocate the system resource efficiently. Hence, the RR does not provide the best system capacity.

We consider a scheduling strategy in this thesis: A volume-based scheduling algorithm based on block diagonalisation (BD) precoding [Z. Shen et al., 2006]. The scheduling method is presented in the following chapter.

## ***2.5 Cognitive radio technique in wireless network***

Early idea of Cognitive Radio (CR) is proposed by Mitola and Maguire [I. Mitola, J. and J. Maguire, G. Q., 1999]. In [I. Mitola, J. and J. Maguire, G. Q., 1999], the software radios are defined as the platforms for multiband multimode personal communication systems. Cognitive radio extends the software radio with radio-domain model-based reasoning about the set of RF bands, air interfaces, protocols, and spatial and temporal patterns that moderate the use of the radio spectrum. Cognitive radio enhances the flexibility of personal services through a Radio Knowledge Representation Language (RKRL). Since then, the idea of cognitive radio has evoked much enthusiasm.

There is no agreement on formal definition of Cognitive Radio because meaning of the CR varies in different contexts [I. Akyildiz et al.,

2006, T. Yücek and H. Arslan, 2009, S. Haykin, 2005, A. Goldsmith et al., 2009]. In essence, common feature of the cognitive radio is the awareness of its environment. Following is the definition of the cognitive radio extracted from Federal Communications Commission (FCC): “A cognitive radio (CR) is a radio that can change its transmitter parameters based on interaction with the environment in which it operates. This interaction may involve active negotiation or communications with other spectrum users and/or passive sensing and decision making within the radio.” [Federal Communications Commission, 2003]. Therefore, the long term vision of cognitive radio technology is that the user terminals would automatically make use of underutilised spectrum across a broad frequency range.

A typical cognitive radio cycle [I. Mitola, J. and J. Maguire, G. Q., 1999, I. Akyildiz et al., 2006, S. Haykin, 2005] is illustrated in Figure 2.13. The cognitive radio cycle involves three main steps: spectrum sensing, spectrum analysis and spectrum decision. The spectrum sensing stage involves examining the radio environment and obtaining the spectrum holes information. Then in the spectrum analysis stage, the characteristics of the spectrum holes is determined, the channel state information is estimated and the channel capacity is predicted for the transmitter to use. In the spectrum decision step, the transmit strategy is decided, such as transmit power control, data rate, transmission mode and dynamic spectrum management.

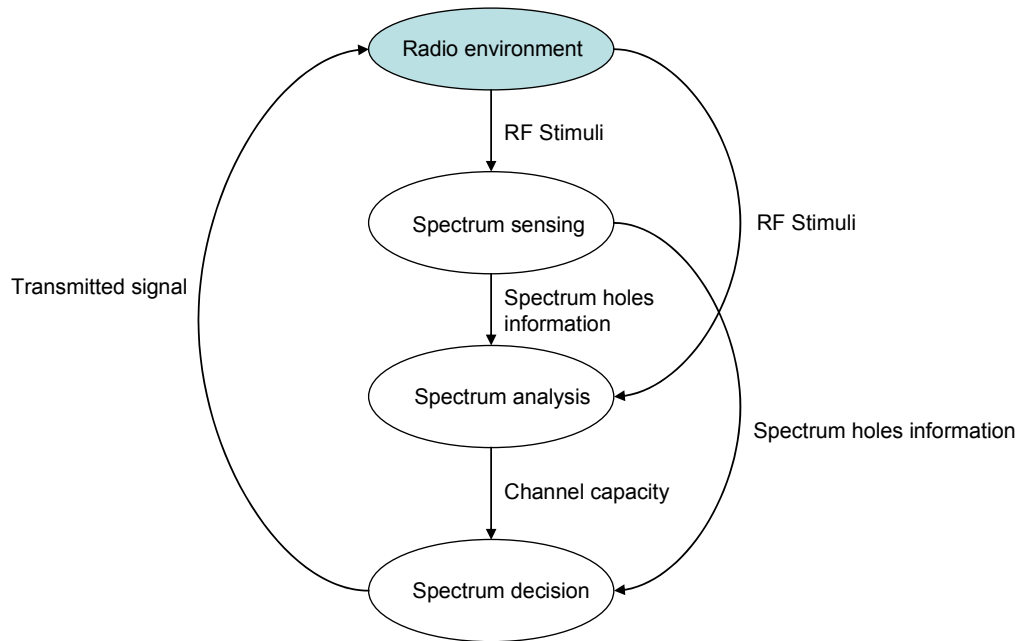


**Figure 2.13 Cognitive radio cycle.**

In early research papers on cognitive radio [I. Akyildiz et al., 2006, S. Haykin, 2005], dynamic spectrum access (DSA) networks as well as cognitive networks is predicted as the next generation wireless communication networks in view of solving scarcity of spectrum and utilizing the unused band. The heterogeneous wireless network architectures are designed for the future networks to provide high bandwidth to mobile users. It is considered that the key technology of the next generation networks is the cognitive radio which enables the unlicensed (secondary) users to use and share the spectrum with the licensed (primary) users in an opportunistic manner.

With the research development on cognitive radio, there are other ways to utilize the licensed band where both licensed and unlicensed users operate on the same band when the interference constraint to the licensed user is satisfied. In general, there are three main cognitive radio network paradigms [A. Goldsmith et al., 2009]: underlay, overlay, and interweave described as follows.

### 2.5.1 Underlay

Assuming the secondary user has knowledge of the interference caused by its transmitter to the receivers of all primary users, the *underlay paradigm* allows primary and secondary users operate simultaneously as long as the interference caused by the secondary users to the primary users is below a given threshold. For example, one of the enabling technologies, MIMO, can be used to guide the signals from the secondary users away from the primary receivers to meet the interference constraint for the primary users.

### 2.5.2 Overlay

*Overlay systems* are the systems that some signal processing and coding are applied by the secondary users to maintain or improve the communication of primary users whereas the secondary users gain the benefit of some additional bandwidth. In this case, the secondary user transmitter needs to know the primary users' codebook and its message. For example, it is recognized that there is connection between the cognitive radio channel and the broadcast channel, therefore optimality dirty paper coding (DPC) strategy for the broadcast channel can be applied to the Gaussian cognitive channel and brings capacity gain. Some form of cooperation is also required for a large network with many primary and secondary users. In general, these cooperation strategies allow nodes to relay each other's information to improve network capacity. For instance, neighbouring transmit nodes can group together, exchange their information through cooperation and mimicking a multi-antenna transmitter; similarly adjacent receive nodes can cooperate, exchange their information and form a virtual multi-antenna receiver. Then DPC strategy for a classical MIMO antenna system can be applied to this virtual MIMO transmitter/receiver to improve system performance [N. Jindal et al., 2004].

### 2.5.3 Interweave

In *interweave system*, the secondary users opportunistically exploit spectral holes to communicate without disrupting other active users (primary and secondary). The interweave paradigm reflects the original idea of the cognitive radio [I. Mitola, J. and J. Maguire, G. Q., 1999]. More details of this type of systems are described in [I. Mitola, J. and J. Maguire, G. Q., 1999, S. Haykin, 2005]. The most important feature in the interweave systems is that the secondary users need to have the knowledge of the occupancy of different frequency bands by the primary users to ensure the efficient communication through the spectral holes without causing any interference to the active primary users. Hence, successful operation of the interweave systems depends on precise primary user detection, i.e., the spectrum sensing, over a wide bandwidth. In real systems, the primary user detection might be hampered by fading and shadowing effect in the wireless channels. Other factors can also affect accurate sensing the presence of the primary users, such as, uncertainty of the noise level caused by other primary and secondary users. Furthermore, the operation of spectrum sensing is frequently required to update the information of the frequency bands occupancy to accommodate the varying nature of the primary user activity. Cooperative sensing among secondary users can certainly improve the spectrum sensing [A. Sahai et al., 2006, S. M. Mishra et al., 2006, A. Ghasemi and E. S. Sousa, 2005, G. Ganesan and Y. Li, 2005, D. Cabric et al., 2004].

It is known that the MIMO technique can improve wireless communication system performance and increase the spectral efficiency of the system [D. Tse and P. Viswanath, 2005]. Therefore, it is desirable to incorporate MIMO antenna system into a cognitive radio system to meet the goal of better spectrum utilization. In the MU-MIMO cognitive network, multiuser diversity can also add one more degree of freedom to the system and can be exploited. In this thesis, we will focus on the area of spectrum

sensing in the cognitive radio cycle of MU-MIMO systems. The details are presented in Chapter 5 and Chapter 6.

## **2.6 Summary**

In this chapter, we presented literature review in the area of wireless propagation channel, performance measure of wireless system, system capacity expression for SU-MIMO and MU-MIMO systems, scheduling algorithms for MU-MIMO system and cognitive radio technique in wireless communication network.

In the following chapters, we will focus on scheduling algorithms (Chapters 3-4) and spectrum sensing methods (Chapters 5-6).

## **Chapter 3      Volume-based                      scheduling algorithm of MU-MIMO downlink channel**

### **3.1 Introduction**

Multuser multiple-input and multiple-output (MU-MIMO) systems have drawn a significant attention in last ten years because MU-MIMO can be used in real wireless systems to enhance performance of wireless networks [D. Gesbert et al., 2007]. To meet the demand of serving multiple users simultaneously in a wireless system with a large number of users, a scheduling scheme is needed to select a group of users in order to achieve a high system sum-rate capacity. The researches on MU-MIMO precoding, feedback, scheduling strategies and different combinations of these strategies have been carried out for the purpose of increased capacity offered by MU-MIMO techniques [T. Yoo and A. Goldsmith, 2006, Q. H. Spencer et al., 2004, L. U. Choi and R. D. Murch, 2004, Z. Shen et al., 2006, C. Lv et al., 2008].

It is well known that dirty paper coding (DPC) can achieve optimal capacity. However, this strategy is difficult to implement in a real wireless system due to its complicated precoding and decoding process [M. Costa, 1983, N. Jindal and A. Goldsmith, 2005]. Block diagonalisation (BD) [Q. H. Spencer et al., 2004] is a less complex and practical strategy. With BD strategy, each user's precoding matrix is formed in such way that it is in the null space of all other users' channels matrix. Compared to DPC, BD is however a suboptimal strategy in terms of achievable sum-rate capacity (bps/Hz). Consider that channel state information (CSI) is known to transmitter and receiver and a system with a large number of users, a good user selection scheme is needed to maximize the system capacity due to the fact that number of simultaneous users to be served is limited by the number of transmit antennas (rank condition in BD) if BD precoding strategy is

used. A semi-orthogonal user selection (SUS) algorithm is proposed in [T. Yoo and A. Goldsmith, 2006] for multiuser MIMO broadcast system and zero forcing beam forming (ZFBF) is applied to the selected active users. The SUS algorithm needs to use Gram-schmidt orthogonalization procedure in each user selection step. Two low-complexity suboptimal user selection algorithms combined with BD precoding for multiuser MIMO systems have been proposed [Z. Shen et al., 2006]. In [Z. Shen et al., 2006], the first algorithm uses a capacity-based user selection algorithm that greedily maximizes the sum-rate capacity in the selected user set, whereas the second algorithm uses the criterion of the Frobenius norm-based algorithm that is based on maximizing the channel energy with optimal combination of selected users. However, the capacity-based user selection algorithm is still computationally demanding because a frequent use of singular value decomposition (SVD) of the channel matrices is needed in the course of selecting each user. The Frobenius norm-based algorithm employs Gram-Schmidt orthogonalization procedure in each user selection step, which still needs a fair amount of computational effort.

In this chapter, we present a novel low complexity suboptimal user selection algorithm called the volume-based scheduling algorithm for a MU-MIMO system based on BD [L. Jin et al., 2009, L. Jin et al., 2011]. The new algorithm defines the channel volume as the product of diagonal elements of an upper-triangular matrix  $\mathbf{R}$  by performing  $\mathbf{QR}$  factorization to the channel matrix of a user set and the volume metric is used for user selection. The benefit of the volume-based algorithm is that the computational complexity is significant less than the capacity-based algorithm because the SVD operation on the channel matrices of selected users is not needed in each user selection step. The proposed algorithm also needs less computational effort in comparison with SUS algorithm.

The outline of the rest of this chapter is as follows. Section 3.2 presents the system model and describes the block diagonalisation (BD)

precoding algorithm and the method of evaluating system sum-rate capacity. Section 3.3 analyses the computational complexity of four **QR** factorization procedures and gives the details of the proposed volume-based algorithm. Section 3.4 presents the computational complexity analysis on volume-based, SUS and capacity-based algorithms. Section 3.5 provides the numerical simulation results and finally the summary is given in Section 3.6.

### **3.2 System model, block diagonalisation (BD) and sum-rate capacity**

In this section, the system model is presented, and BD precoding and capacity calculation are described. Consider a single cell multiuser MIMO broadcast system with a single base station (BS) serving  $K$  users. The BS is equipped with  $M$  transmit antennas, the receiver for user  $k$  is equipped with  $N_k$  antennas and  $K \geq M$  is considered. The BD [Q. H. Spencer et al., 2004, L. U. Choi and R. D. Murch, 2004] precoding method is applied due to the benefit of eliminating inter-user interference in multiuser MIMO downlink system. Each user  $k$  for  $k=1 \dots K$  in the system is characterized by a channel matrix  $\mathbf{H}_k$  with  $N_k \times M$  dimension.  $\mathbf{H}_k \in \mathbb{C}^{N_k \times M}$  with each entry following an independent and identically distributed (i.i.d) complex Gaussian distribution  $\mathcal{CN}(0,1)$ , which is a valid model if the transmit and receive antennas are in rich-scattering environments and antenna spacing is larger than the coherence distance. The transmitted symbol for user  $k$  is denoted as  $\mathbf{x}_k$  which is  $N_k \times 1$  vector. The signal is multiplied by a precoding matrix  $\mathbf{W}_k$  and then is transmitted by the transmit antennas. The received signal  $\mathbf{y}_k$  for user  $k$  can be expressed as

$$\mathbf{y}_k = \mathbf{H}_k \mathbf{W}_k \mathbf{x}_k + \sum_{i=1, i \neq k}^K \mathbf{H}_k \mathbf{W}_i \mathbf{x}_i + \mathbf{n}_k, \quad (3.1)$$

where the first term on the right-hand side of (3.1) is the desired signal for user  $k$ , the second term is the interference from other user signals and  $\mathbf{n}_k$  is the  $N_k \times 1$  additive white Gaussian noise (AWGN) vector for user  $k$  with zero mean and variance  $E[\mathbf{n}_k \mathbf{n}_k^H] = \sigma^2 \mathbf{I}$ .  $(\bullet)^H$  denotes the Hermitian transpose of a matrix in the bracket.

Next the BD precoding method is described. Assuming if  $K$  users can be supported simultaneously, the channel matrix to include  $K$  users is

$$\mathbf{H} = [\mathbf{H}_1, \dots, \mathbf{H}_{k-1}, \mathbf{H}_k, \mathbf{H}_{k+1}, \dots, \mathbf{H}_K]. \quad (3.2)$$

The design of the BD precoding matrix for user  $k$  is to find a matrix  $\mathbf{W}_k$  that meets the following condition:

$$\begin{aligned} \mathbf{W}_k &\in \mathfrak{U}(M, N_k) \\ \mathbf{H}_k \mathbf{W}_i &= 0 \text{ for all } k \neq i \text{ and } 1 \leq k, i \leq K, \end{aligned} \quad (3.3)$$

where  $\mathbf{W}_k$  is a matrix with  $M \times N_k$  dimension,  $\mathfrak{U}(M, N_k)$  stands for the class of  $M \times N_k$  unitary matrix which is a collection of vectors  $(\mathbf{u}_1, \dots, \mathbf{u}_{N_k})$  and the dimension of  $\mathbf{u}_j$  is  $M$  for  $1 \leq j \leq N_k$ ,  $\mathbf{H}_k \mathbf{W}_k$  for user  $k$  is non-zero.

The method to get the desired  $\mathbf{W}_k$  is first to formulate a channel matrix to include all channel matrices from other interference users. The matrix is given by

$$\overline{\mathbf{H}}_k = [\mathbf{H}_1^T, \dots, \mathbf{H}_{k-1}^T, \mathbf{H}_{k+1}^T, \dots, \mathbf{H}_K^T]^T. \quad (3.4)$$

To meet the constraint in (3.3),  $\mathbf{W}_k$  shall be in the null space of  $\overline{\mathbf{H}}_k$ . Let  $\overline{R}_k$  denote the rank of  $\overline{\mathbf{H}}_k$ ,  $\overline{N}_k$  be row size  $(K-1) \times N_k$  and  $\overline{M}$  be column size  $M$ . The row size is less than the column size due to the fact that the maximum supportable users are limited by the number of transmit antennas for BD scheme. Hence  $\overline{R}_k$  takes the value of  $(K-1) \times N_k$ . Performing singular value decomposition (SVD) to  $\overline{\mathbf{H}}_k$ , one has:

$$\overline{\mathbf{H}}_k = \overline{\mathbf{U}}_k \overline{\boldsymbol{\Sigma}}_k \overline{\mathbf{V}}_k^* = \overline{\mathbf{U}}_k \overline{\boldsymbol{\Sigma}}_k \left[ \overline{\mathbf{V}}_k^1 \overline{\mathbf{V}}_k^0 \right]^*, \quad (3.5)$$

where  $\overline{\mathbf{U}}_k$  is a square matrix having the same size as the row of  $\overline{\mathbf{H}}_k$ ,  $\overline{\mathbf{V}}_k^*$  is a square matrix which has the same size as the column of  $\overline{\mathbf{H}}_k$ ,  $\overline{\mathbf{U}}_k$  and  $\overline{\mathbf{V}}_k^*$  are unitary matrices,  $\overline{\mathbf{V}}_k^*$  denotes complex conjugate of  $\overline{\mathbf{V}}_k$ ,  $\overline{\boldsymbol{\Sigma}}_k$  is an  $\overline{N}_k \times \overline{M}$  diagonal matrix of singular values of  $\overline{\mathbf{H}}_k$ ;  $\overline{\mathbf{V}}_k^1$  contains the first  $\overline{R}_k$  right singular vectors and  $\overline{\mathbf{V}}_k^0$  contains the last  $\overline{M} - \overline{R}_k$  right singular vectors of  $\overline{\mathbf{H}}_k$ . The columns in  $\mathbf{W}_k$  are composed from the linear combination of those in  $\overline{\mathbf{V}}_k^0$  because the columns in  $\overline{\mathbf{V}}_k^0$  form a basis set in the null space of  $\overline{\mathbf{H}}_k$ .

Assuming that each user terminal is equipped with same number of antennas  $N$  and transmitter has  $M$  antennas, the maximum simultaneous users,  $\hat{K} = M / N$ , can be supported by BD algorithm [Q. H. Spencer et al., 2004]. Subsequently the system sum-rate capacity is evaluated after precoding matrices are found for all simultaneous users in a subset of users. Consider that  $\hat{K}$  is the maximum number of simultaneously supportable users,  $\kappa = \{1, 2, \dots, K\}$  is the set of all users,  $\beta_i$  is a subset of  $\kappa$  and cardinality of  $\beta_i$  is less than or equal to  $\hat{K}$ ,  $\beta = \{\beta_1, \beta_2, \dots\}$  is the set containing all possible  $\beta_i$  and  $\mathbf{H} = \{\mathbf{H}_1, \mathbf{H}_2, \dots, \mathbf{H}_K\}$  denotes the set of all

users' channels. The achievable system sum-rate capacity under BD scheme is the capacity maximization problem under transmit power constraint  $P$ . The maximum capacity can be expressed as [Q. H. Spencer et al., 2004]

$$C_{BD}(\mathbf{H}, P, \sigma^2) = \max_{\beta_i \in \beta} C_{BD|\beta_i}(\mathbf{H}_{\beta_i}, P, \sigma^2), \quad (3.6)$$

where  $\mathbf{H}_{\beta_i}$  denotes the channel matrix for user set  $\beta_i$  and  $\sigma^2$  denotes Gaussian noise power. The solution for (3.6) is to obtain the maximum sum-rate capacity for user set  $\beta_i$  by SVD operation to  $\mathbf{H}_j \mathbf{W}_j$  for  $j \in \beta_i$  and water-filling on the corresponding singular values.

### 3.3 Novel low complexity scheduling algorithms

This section presents a novel low complexity scheduling scheme called the volume-based scheduling algorithm for MU-MIMO downlink channels.

#### 3.3.1 QR factorization procedures and complexity analysis

As we know, if a matrix  $\mathbf{A}_{m \times n}$  with  $m$  row and  $n$  column has linearly independent columns, it can be uniquely factorized as  $\mathbf{A}_{m \times n} = \mathbf{Q}_{m \times n} \mathbf{R}_{n \times n}$  in which the columns of  $\mathbf{Q}_{m \times n}$  are orthonormal basis for  $\mathbf{R}_{n \times n}$  that is an upper-triangular matrix with positive diagonal entries [C. D. Meyer, 2000]. In our proposed scheduling algorithm, the key operation is to perform **QR** factorization to the channel matrix of a simultaneous user set and obtain the product of the diagonal elements of the upper-triangular matrix.

There are various methods to get the upper-triangular matrix, such as, *Gaussian elimination*, *Gram-Schmidt procedure*, *Householder reduction* and *Given reduction* [C. D. Meyer, 2000]. Table 3.1 compares these **QR**

procedures in terms of the numerical stability and the computational effort if a matrix is a square matrix  $A_{n \times n}$ . In Table 3.1, the computational effort values are approximated by counting only multiplicative operations because the number of multiplicative operations is about the same as the number of additive operations; lower-order terms are also neglected. We can see that *Given reduction* procedure is stable but requires the most computational effort. Compared with *Gram-Schmidt* procedure, *Householder reduction* procedure is not only a stable procedure but also it needs 1/3 less computational effort. Therefore, *Householder reduction* procedure is preferred and it is chosen for the proposed scheduling algorithm.

Table 3.1 Comparison of **QR** procedures

<b>QR procedure</b>	<b>factorization</b>	<b>Numerical stability</b>	<b>Computational effort</b>
<i>Gaussian elimination</i>		Not very stable	$\approx n^3 / 3$
<i>Gram-Schmidt</i> procedure		Not very stable	$\approx n^3$
<i>Householder reduction</i>		Stable	$\approx 2n^3 / 3$
<i>Given reduction</i>		Stable	$\approx 4n^3 / 3$

*Householder reduction* process is described as follows. For a matrix  $A_{m \times n}$ , there exists a unitary matrix  $B$  such that  $BA=T$  has an upper-trapezoidal form. When  $B$  is constructed as a product of elementary reflectors, this process is called *Householder reduction* [C. D. Meyer, 2000]. For  $A_{m \times n} = [a_1, a_2, \dots, a_n]$  where  $a_i$  is a  $m$ -dimensional column vector for  $1 \leq i \leq n$ , the elementary reflector corresponding to column  $i$  takes the form:

$$R_i = I - 2 \frac{u_i u_i^H}{u_i^H u_i}, \quad (3.7)$$

where  $\mathbf{I}$  is an identity matrix, vector  $\mathbf{u}_i \neq 0$  and  $[\cdot]^H$  denotes Hermitian of a matrix. Therefore,  $\mathbf{BA}=\mathbf{T}$  can also be expressed as  $\mathbf{R}_n \cdots \mathbf{R}_2 \mathbf{R}_1 \mathbf{A} = \mathbf{T}$ .

Following is the detailed illustration on the *Householder reduction*. Starts from the first column of  $\mathbf{A}$  and let  $i=1$ . The first elementary reflector is  $\mathbf{R}_1 = \mathbf{I} - 2 \frac{\mathbf{u}_1 \mathbf{u}_1^H}{\mathbf{u}_1^H \mathbf{u}_1}$ , where  $\mathbf{u}_1 = \mathbf{a}_1 \pm \mu_1 \|\mathbf{a}_1\| \mathbf{e}_1$  in which  $\|\mathbf{a}_1\|$  is the norm of vector  $\mathbf{a}_1$ ,  $\mathbf{e}_1$  is the unit vector and  $\mu_1 = \mathbf{a}_1 / \|\mathbf{a}_1\|$ . Applying  $\mathbf{R}_1$  to  $\mathbf{A}$  yields

$$\mathbf{R}_1 \mathbf{A} = [\mathbf{R}_1 \mathbf{a}_1, \mathbf{R}_1 \mathbf{a}_2, \dots, \mathbf{R}_1 \mathbf{a}_n] = \begin{pmatrix} t_{11} & t_{12} & \cdots & t_{1n} \\ 0 & * & \cdots & * \\ \vdots & \vdots & \ddots & \vdots \\ 0 & * & \cdots & * \end{pmatrix} = \begin{pmatrix} t_{11} & \mathbf{t}_1^T \\ 0 & \mathbf{A}_2 \end{pmatrix}, \quad (3.8)$$

where  $\mathbf{A}_2$  is a matrix with dimension of  $(m-1) \times (n-1)$  and  $\mathbf{t}_1^T$  is the vector  $[t_{12} \cdots t_{1n}]$ . Therefore all entries below  $t_{11}$  in the first column of the resulting matrix are annihilated. Applying the same procedure to  $\mathbf{A}_2$  to construct an elementary reflector  $\hat{\mathbf{R}}_2$  that annihilates all entries below the (1,1)-position in  $\mathbf{A}_2$ .

Let the second elementary reflector  $\mathbf{R}_2 = \begin{pmatrix} 1 & 0 \\ 0 & \hat{\mathbf{R}}_2 \mathbf{A}_2 \end{pmatrix}$ , then

$$\mathbf{R}_2 \mathbf{R}_1 \mathbf{A} = \begin{pmatrix} t_{11} & t_{12} & t_{13} & \cdots & t_{1n} \\ 0 & t_{22} & t_{23} & \cdots & t_{2n} \\ 0 & 0 & * & \cdots & * \\ \vdots & \vdots & \vdots & & \vdots \\ 0 & 0 & * & \cdots & * \end{pmatrix} = \begin{pmatrix} t_{11} & t_{12} & \cdots \\ 0 & t_{22} & \mathbf{t}_2^T \\ 0 & 0 & \mathbf{A}_3 \end{pmatrix}. \quad (3.9)$$

Continue this process to build elementary reflector  $\mathbf{R}_i$  until all the rows (when  $m < n$ ) or all the columns (when  $m > n$ ) are exhausted. Hence, the final result of *Householder reduction* process applied to the matrix  $\mathbf{A}$  is expressed as one of the following upper-trapezoidal forms:

$$\mathbf{R}_n \cdots \mathbf{R}_2 \mathbf{R}_1 \mathbf{A} = \begin{pmatrix} t_{11} & t_{12} & \cdots & t_{1n} \\ 0 & t_{22} & \cdots & t_{2n} \\ 0 & \vdots & \ddots & \vdots \\ 0 & 0 & \cdots & t_{mm} \\ 0 & 0 & \cdots & 0 \\ \vdots & \vdots & & \vdots \\ 0 & 0 & \cdots & 0 \end{pmatrix} \text{ when } m > n, \quad (3.10)$$

$$\mathbf{R}_{m-1} \cdots \mathbf{R}_2 \mathbf{R}_1 \mathbf{A} = \begin{pmatrix} t_{11} & t_{12} & \cdots & t_{1m} & t_{1,m+1} & \cdots & t_{1n} \\ 0 & t_{22} & \cdots & t_{2m} & t_{2,m+1} & \cdots & t_{2n} \\ \vdots & \vdots & \ddots & \vdots & \vdots & \ddots & \vdots \\ 0 & 0 & \cdots & t_{mm} & t_{m,m+1} & \cdots & t_{mn} \end{pmatrix} \text{ when } m < n. \quad (3.11)$$

Note that the elementary reflectors  $\mathbf{R}_i$  for  $1 \leq i \leq n$  are unitary matrices and every product  $\mathbf{R}_k \mathbf{R}_{k-1} \cdots \mathbf{R}_2 \mathbf{R}_1$  is a unitary matrix. The case of  $m > n$  is applicable to the volume-based algorithm because the **QR** operation is implemented on the transpose of the combined channel matrix of the selected user group and the number of transmit antennas should be greater than or equal to the total number of the antennas of the selected user group.

Having explained the *Householder reduction* for the **QR** procedure and it is chosen in our proposed algorithm, we now move on to describe the details of the volume-based scheduling algorithm.

### 3.3.2 Details of the volume-based scheduling algorithm

As described in section 3.2,  $K$  is the total number of users in the downlink system, the number of transmit antennas at the BS be  $M$ , the number of receive antennas for user  $k$  terminal be  $N_k$  and each user  $k$  be assigned a channel matrix  $\mathbf{H}_k$ . The row dimension of the channel matrix depends on the number of antennas in the user terminal, that is, the channel matrix for user  $k$  is expressed as  $\mathbf{H}_k = [\mathbf{h}_1^T, \mathbf{h}_2^T, \cdots, \mathbf{h}_{N_k}^T]^T$  where  $\mathbf{h}_1, \mathbf{h}_2, \cdots, \mathbf{h}_{N_k}$  are row

vectors. The column dimension of the channel matrix for user  $k$  is determined by the number of transmit antennas. Assuming these row vectors  $\mathbf{h}_1, \mathbf{h}_2, \dots, \mathbf{h}_{N_k}$  are linearly independent and  $N_k < M$  which can be satisfied in a real time system due to space constraint on user terminal, these row vectors span a subspace:

$$S_k = \text{span}(\mathbf{h}_1, \mathbf{h}_2, \dots, \mathbf{h}_{N_k}). \quad (3.12)$$

When user  $i$  and user  $j$  are selected, a matrix can be formulated to include two user matrices as

$$\mathbf{H}_{i,j} = [\mathbf{H}_i^T \mathbf{H}_j^T]^T. \quad (3.13)$$

The row vectors in  $\mathbf{H}_{i,j}$  span a subspace:

$$S_{i,j} = \text{span}(\mathbf{h}_{1i}, \mathbf{h}_{2i}, \dots, \mathbf{h}_{N_i i}, \mathbf{h}_{1j}, \mathbf{h}_{2j}, \dots, \mathbf{h}_{N_j j}), \quad (3.14)$$

where  $\mathbf{h}_{nm}$  denotes a  $n^{\text{th}}$  row vector for user  $m$ ,  $m = i, j$  and  $N_i, N_j$  denotes the number of antennas for user  $i$  and  $j$ .

We now implement a **QR** factorization to channel matrix  $\mathbf{H}_{i,j}$  and get the product  $V$  of the diagonal elements of the upper-triangular matrix. The product  $V$  can be intuitively seen as the volume of a parallelepiped with each side being unique row vector in  $S_{i,j}$ . The volume of the parallelepiped generated by the rows of a matrix cannot exceed the volume of a rectangular box whose sides have row length [C. D. Meyer, 2000]. In other words, the maximum value of the volume can be obtained only if all row vectors in the matrix  $\mathbf{H}_{i,j}$  are orthogonal to each other. Therefore, the volume metric is a reasonable choice in our scheduling algorithm because a user set achieving

the maximum value of  $V$  indicates that vectors in the combined channel matrix tend to be orthogonal.

The volume-based algorithm is detailed as following:

### Volume-based scheduling algorithm

1. Initialization:
  - a) Let  $\Omega = \{1, 2, \dots, K\}$  is the user set in which the users are waiting to be served,  $B = \emptyset$  is the selected user set which is empty initially.
  - b) Let  $n=1$ .
  - c) Find a user,  $\omega_1 \in \Omega$ , that satisfies  $\omega_1 = \arg \max_{k \in \Omega} \|\mathbf{H}_k\|_F^2$ , where  $\|\mathbf{H}_k\|_F$  is the Frobenius norm of channel matrix of user  $k$ .
  - d) Move the user  $\omega_1$  to the selected user set, let  $B = B + \{\omega_1\}$  and  $\Omega = \Omega - \{\omega_1\}$ .
2. Let  $K_{\max}$  denote the maximum users can be served.
  - a) for  $n=2: K_{\max}$  for each  $k \in \Omega$ , find a user  $\omega_n$  such that  $\omega_n = \arg \max_{k \in \Omega} Vol(\mathbf{H}_{B+\omega_k})$  where  $\mathbf{H}_{B+\omega_k}$  is the channel matrix of user  $\omega_k$  combined with previous selected users in  $B$  set and  $Vol(\mathbf{H}_{B+\omega_k})$  denotes the channel volume.
  - b) Let  $B = B + \{\omega_n\}$  and  $\Omega = \Omega - \{\omega_n\}$ .
3. Finally, calculate the achievable sum-rate  $C_{BD}(B)$  to the selected user set by applying BD precoding and water filling strategy.

### 3.4 Computational complexity analysis on volume-based, SUS and capacity-based scheduling algorithms

In this section, the computational complexity analysis is based on the assumptions in section 3.2. It is assumed that the total number of users in the system is much greater than the number of users to be served simultaneously, i.e.  $K \gg \hat{K}$ , each user has same number of receive antennas and  $\hat{K} \approx M/N$ . To simplify the analysis, the computational effort is estimated on the channel matrices with real element entries  $A \in \mathbb{R}^{N \times M}$  ( $\mathbb{R}$  represents set of real numbers) and the number of receive antenna is less than the number of transmit antenna  $N < M$ . **Frobenius norm**, **Gram-Schmidt orthogonalization**, **Householder reduction**, **water-filling** and **singular value decomposition (SVD)** are the matrix operations used by the volume-based, SUS and capacity-based suboptimal scheduling algorithms. Therefore, rest of this section reviews the flop count of the matrices operations mentioned above, and then presents the complexity evaluation on these suboptimal scheduling algorithms. Note that only multiplication is considered as the flop count of any matrix operations because the number of multiplication is about the same as the number of the addition.

#### 3.4.1 Complexity of five matrix operations

**Frobenius norm** of  $A_{N \times M}$  is  $\|A_{N \times M}\|_F^2 = \sqrt{\text{Tr}[AA^T]} = \sqrt{\sum_{i=1}^N \sum_{j=1}^M |A_{ij}|^2}$ . This operation needs  $N^2M$  multiplication.

Applying the **singular value decomposition (SVD)** to a real matrix  $A_{N \times M}$ , the computational effort to acquire the unitary matrices  $U_{N \times N}$ ,  $V_{M \times M}$  and diagonal matrix  $D_{N \times M}$  is  $2N^2M + 4NM^2 + 5M^3$ .

Either *classic Gram-Schmidt orthogonalization* or *modified Gram-Schmidt orthogonalization* on matrix  $A_{N \times M}$  takes  $N^2M$  multiplication.

*Householder reduction* in *QR* factorization on matrix  $A_{N \times M}$  needs  $N^2M(1 - \frac{1}{3} \frac{N}{M})$  multiplication.

*Water-filling* on  $N$  eigenmodes of matrix  $A_{N \times M}$  requires up to  $N^2 + 3N$  multiplication.

Table 3.2 summarizes the flop counts of the matrix operations mentioned above.

Table 3.2 Complexity analysis on five matrix operations

<b>Matrix operations</b>	<b>Flop count</b>
<i>Frobenius norm</i>	$N^2M$
<i>SVD</i>	$2N^2M + 4NM^2 + 5M^3$
<i>Gram-Schmidt orthogonalization</i>	$N^2M$
<i>Householder reduction</i> in <i>QR</i> factorization	$N^2M(1 - \frac{1}{3} \frac{N}{M})$
<i>Water-filling</i>	$N^2 + 3N$

### 3.4.2 Complexity of volume-based, SUS and capacity-based scheduling algorithms

#### 3.4.2.1 Volume-based algorithm

Firstly, the volume-based algorithm begins with finding a user with maximum Frobenius norm so the flop count is  $KN^2M$ . Secondly, iteration starts from  $i = 2$  to  $\hat{K}$ , finding a user set that the volume of the combined channel matrix of the user set is maximized in each iteration. The flop count

in each iteration is expressed as  $(K-i+1) \times \left[ (iN)^2 M \left(1 - \frac{1}{3} \frac{iN}{M}\right) + iN \right]$ . Finally, the capacity is calculated by applying BD precoding and water-filling on the channel matrix of the chosen user set. The flop count in the final step can be omitted because the flop count is not related to total number of  $K$  and is relatively small.

We can get the total flops by summing the flop counts contributed from step one and step two, which is

$$F_v = KN^2M + \sum_{i=2}^{\hat{K}} (K-i+1) \times \left[ (iN)^2 M \left(1 - \frac{1}{3} \frac{iN}{M}\right) + iN \right] \quad (3.15)$$

$$\approx O\left(\frac{K}{4} \hat{K}^4 N^3\right)$$

### 3.4.2.2. SUS algorithm

The procedure of the SUS algorithm is that the iteration starts from  $i=1$  to  $\hat{K}$ , in each iteration a new user is added to a chosen user set from previous iteration and then the combined channel matrix of the user set is mapped to an orthogonal subspace spanned by  $\{\mathbf{g}_1, \mathbf{g}_2, \dots, \mathbf{g}_i\}$  via Gram-Schmidt orthogonalization procedure. The user with the maximum Frobenius norm  $\mathbf{g}_i$  is chosen and the flop count in each iteration is  $(iN)^2 M$ . The capacity is computed when the maximum supportable users reached. The computational cost of the SUS algorithm is mainly originated from the iteration step because the final capacity calculation is not dependent on  $K$  and can be neglected. Therefore, the flop count of SUS algorithm is

$$F_s = \sum_{i=1}^{\hat{K}} (K-i+1) \times (iN)^2 M \quad (3.16)$$

$$\approx O\left(\frac{K}{3} \hat{K}^4 N^3\right)$$

### 3.4.2.3 Capacity-based algorithm

The first step of the capacity-based algorithm is to search through  $K$  users. For each user, the SVD operation is implemented on the user's channel matrix and then the water-filling algorithm is applied to the eigenmodes of the diagonal matrix obtained via the SVD operation. Finally the capacity is calculated. Hence the flop count of this step is  $K(2N^2M + 4NM^2 + 5M^3 + N^2 + 5N)$ .

The second step of the algorithm is the iteration from  $i=2$  to  $\hat{K}$ . In each iteration, a new user  $k$  is added to a chosen user set from previous round, precoding matrix  $\mathbf{W}_k$  for the user is obtained by SVD operation and  $\mathbf{H}_k\mathbf{W}_k$  is calculated. Then SVD is applied to  $\mathbf{H}_k\mathbf{W}_k$  and water-filling is implemented on the eigenvalues of the diagonal matrix.

Last step of the algorithm is that the sum-rate capacity is computed. The flop count from this step is

$$i[2(i-1)^2 N^2 M + 4(i-1)NM^2 + 5M^3] + iN^2 M + i(2N^2 M + 4NM^2 + 5M^3) + iN(iN + 3) + iN$$

Therefore, the total flop count of the capacity-based scheduling algorithm is expressed as

$$\begin{aligned} F_C &= K(2N^2M + 4NM^2 + 5M^3 + N^2 + 5N) \\ &+ \sum_{i=2}^{\hat{K}} \{i[2(i-1)^2 N^2 M + 4(i-1)NM^2 + 5M^3] + iN^2 M \\ &+ i(2N^2 M + 4NM^2 + 5M^3) + iN(iN + 3) + iN\} \times (K - i + 1) \\ &\approx O(K\hat{K}^5 N^3) \end{aligned} \quad (3.17)$$

To this end of the complexity analysis, it is found that the capacity-based algorithm has highest complexity whilst the volume-based algorithm

needs the lowest computational effort by comparing (3.15), (3.16) and (3.17). The complexity of the volume-based algorithm is  $\frac{3}{4}$  of the SUS algorithm. The capacity-based algorithm needs  $4\hat{K}$  times of the computational effort of the volume-based algorithm.

### 3.5 Simulation results

This section presents the numeral simulation results by applying the proposed volume-based scheduling algorithm. The performance comparison with the sum-rate of capacity-based user selection algorithm [Z. Shen et al., 2006] and semi-orthogonal user selection (SUS) algorithm [T. Yoo and A. Goldsmith, 2006] is provided. The aim of the simulation was to demonstrate that the proposed low complexity volume-based algorithm can achieve a good sum-rate capacity, comparable with others, if not higher.

Figure 3.1 and Figure 3.2 show the sum-rate capacity of the proposed volume-based algorithm compared with the SUS and capacity-based algorithms in the case of MISO antenna configuration. The total system capacity shown in Figure 3.1 and Figure 3.2 is the ergodic sum-rate capacity averaged over 1000 channel realization. The upper bound of sum-rate capacity that can be achieved by optimal DPC strategy is also shown in two figures, which is obtained by using the scaling laws of the sum-rate of DPC in [M. Sharif and B. Hassibi, 2007]. The scaling laws of DPC in [M. Sharif and B. Hassibi, 2007] states that when the number of transmit antennas  $M$  is fixed, the sum-rate scales like  $M \log \log KN$  as number of users  $K$  grows to infinity and for any number of receive antennas  $N$ , no matter  $N$  whether grows to infinity or not.

Figure 3.1 demonstrates the sum-rate capacity versus the number of users when the number of transmit antennas is 8 and all users' terminal has one antenna. The signal-to-noise-ratio (SNR) for each user is 20dB and the

maximum number of simultaneous supportable users is 8. Figure 3.2 provides the sum-rate capacity when the number of transmit antennas is 4 and all users' terminal has one antenna. The signal-to-noise-ratio (SNR) for each user is 20dB and the maximum number of supportable users is 4. The curve from DPC scheme is the result from the theoretical calculation that demonstrates the upper bound of the sum-rate capacity of the system. The results demonstrate that the performances of capacity-based, SUS and volume-based algorithms are close to the upper bound of sum-rate capacity achievable via DPC when there is a large number of users in the system. Figure 3.1 shows that the proposed volume-based algorithm achieves the equivalent performance compared with the capacity-based algorithm and the SUS-based algorithm. As discussed in section 3.4, the advantage of the volume-based algorithm has less computational complexity. The proposed algorithm needs 1/4 less computational effort than the SUS algorithm. The capacity-based algorithm needs the most computational effort because of the vigorous SVD operations in each user selection step. The capacity-based algorithm is  $4\hat{K}$  times of computational complexity in comparison with volume-based algorithm. Figure 3.2 confirms the similar performance result when the number of transmit antenna is 4.

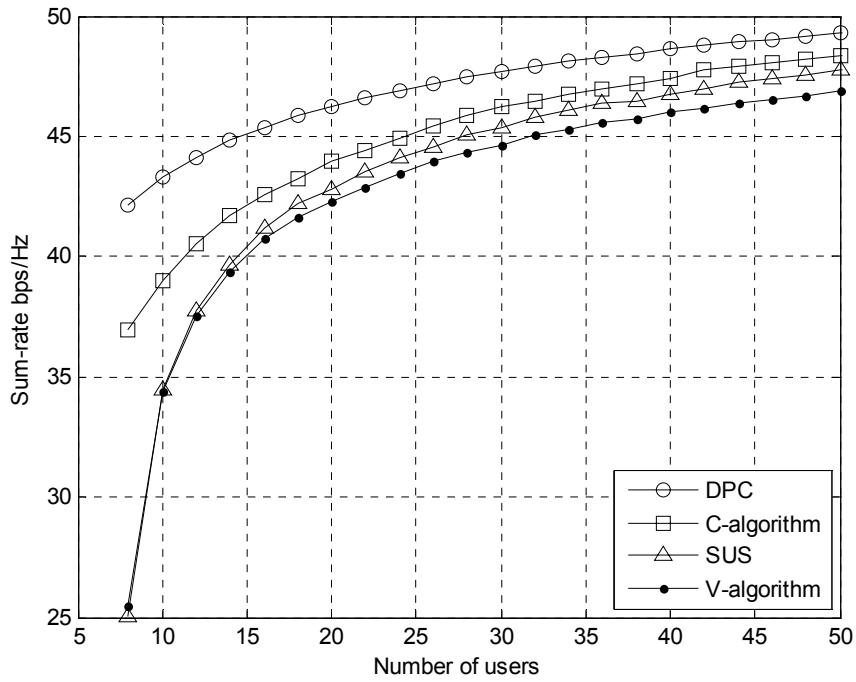


Figure 3.1 Sum-rate capacity versus the number of users. 8x1 MISO configuration.

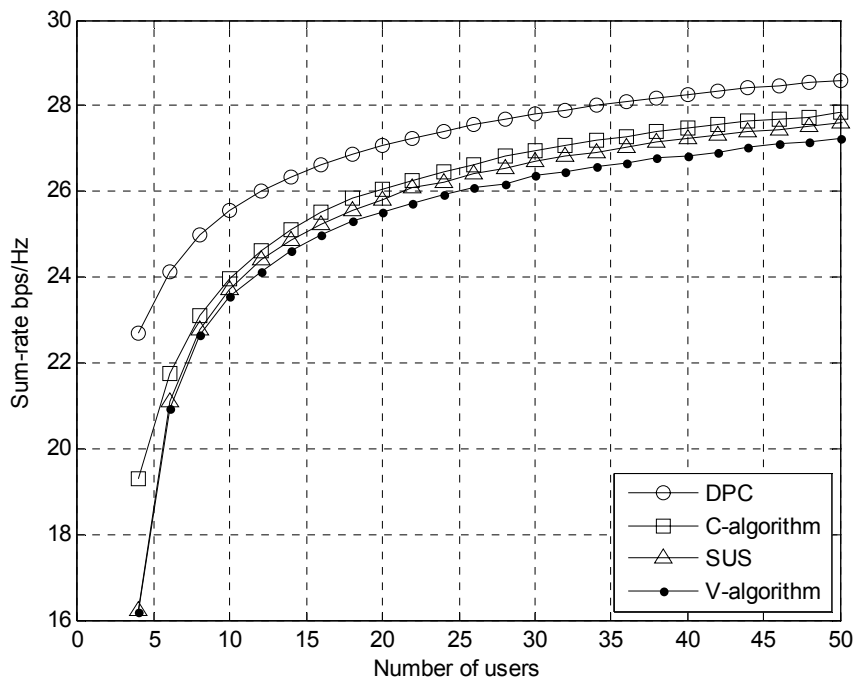


Figure 3.2 Sum-rate capacity versus number of users. 4x1 MISO configuration.

Next, we will show the performance results in the case of multiple receive antennas. The performance comparison with capacity-based user selection algorithm [Z. Shen et al., 2006] and semi-orthogonal user selection (SUS) algorithm [T. Yoo and A. Goldsmith, 2006] is provided. The system capacity shown in the result graphs is the ergodic sum-rate capacity averaged over 3000 channel realizations. In addition, the average simulation time of the volume-based algorithm is compared with the average simulation time of the existing capacity-based and SUS algorithms to validate that the proposed algorithm is indeed the least complex scheduling strategy.

Figure 3.3 shows the performance result when the number of transmit antennas is 4 and the number of receive antennas for each user is 2. In this scenario, the maximum number of simultaneous supportable users is 2. The signal-to-noise-ratio (SNR) for each user is 20dB. The result presented in Figure 3.3 reveals that the performance of the volume-based algorithm is comparable with the SUS and the capacity-based algorithms. The advantage of the volume-based algorithm is that it has less computational complexity. The proposed algorithm needs 1/4 less computational effort than the SUS algorithm. In addition, the volume-based algorithm displays slight better performance than the SUS algorithm. In comparison with the volume-based algorithm, the capacity-based algorithm shows a small increment of the sum-rate capacity; however it needs much more computational effort because of the vigorous SVD operations in each user selection step. The capacity-based algorithm is  $4\hat{K}$  times of the computational complexity of the volume-based algorithm.

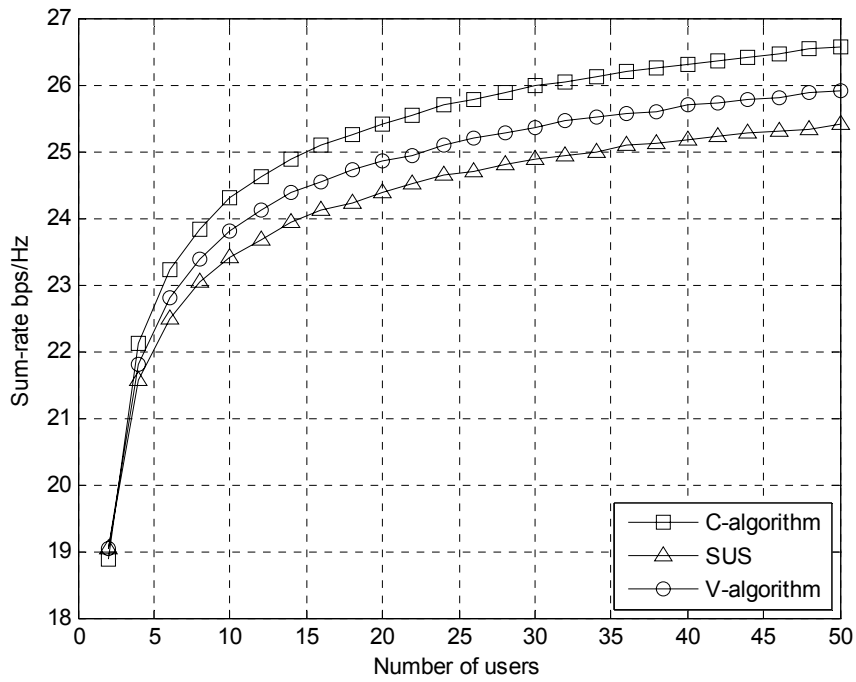


Figure 3.3 Sum-rate capacity versus the number of users. 4x2 MIMO configuration.

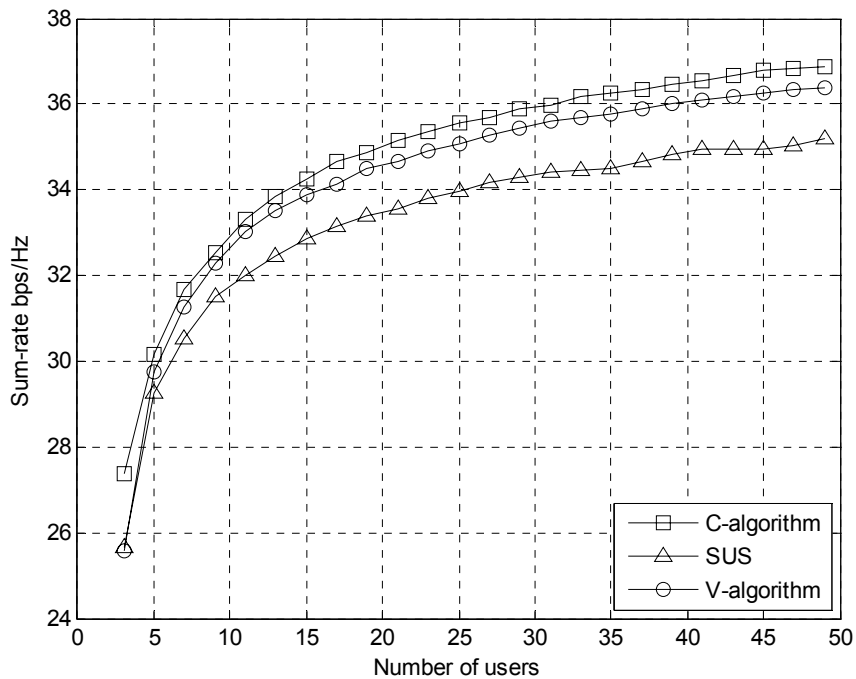


Figure 3.4 Sum-rate capacity versus the number of users. 6x2 MIMO configuration.

Figure 3.4 is the performance result when the transmit and receive antennas configuration is  $6 \times 2$ . The maximum number of simultaneous supportable users is 3 in this case. The signal-to-noise-ratio (SNR) for each user is 20dB. Comparing figure 3.4 to figure 3.3, it is evident that the sum-rate capacity of the volume-based algorithm is closer to the sum-rate capacity acquired via the capacity-based algorithm and the proposed algorithm outperforms the SUS algorithm as the number of transmit antenna increases.

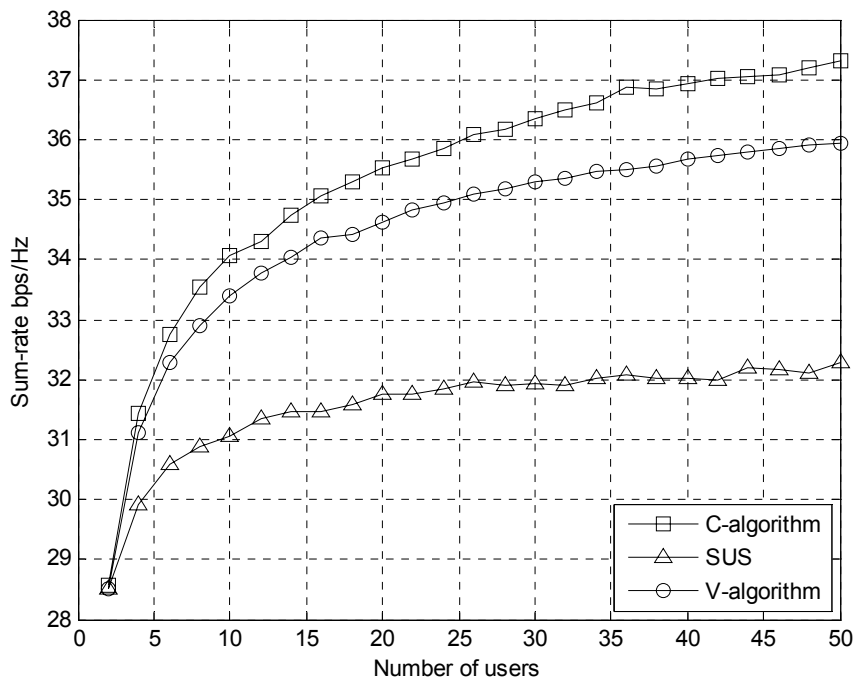
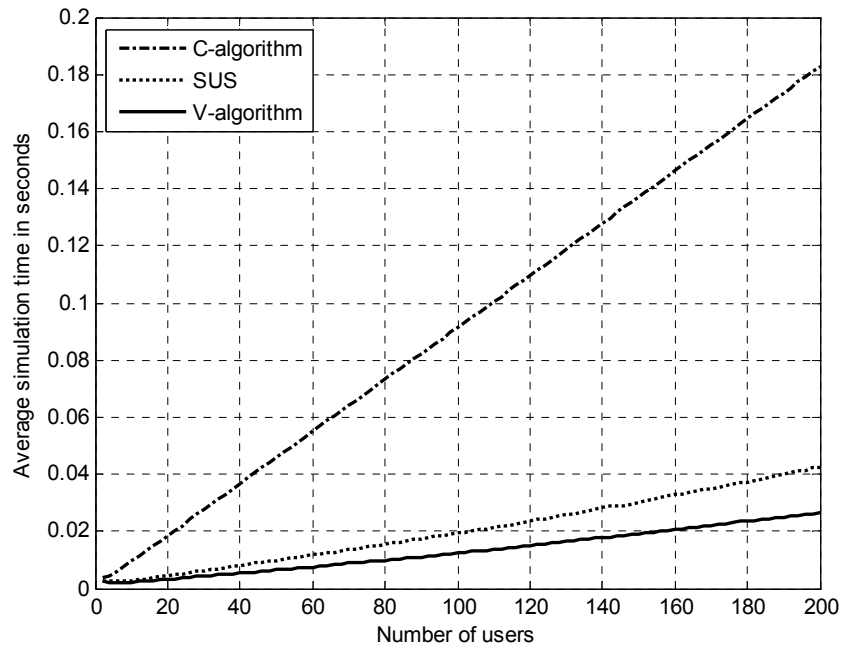


Figure 3.5 Sum-rate capacity versus the number of users.  $6 \times 3$  MIMO configuration.

Figure 3.5 demonstrates the result of the sum-rate capacity versus the number of users when the number of transmit antenna is 6 and the number of receive antennas for each user terminal is 3. The signal-to-noise-ratio (SNR) for each user is 20dB and the maximum number of simultaneous supportable users is 2. It clearly shows that the volume-based algorithm surpasses the SUS algorithm. The proposed algorithm achieves slight less sum-rate capacity than the capacity-based algorithm but with

much reduced computational complexity. Furthermore, by comparing Figure 3.4 and Figure 3.5, the results demonstrate that the volume-based algorithm works better than the SUS algorithm when the number of transmit antennas is kept same at 6 and the number of receive antennas increases from 2 to 3.

To prove that the volume-based strategy is the least complex among these three scheduling schemes, the actual simulation time of the volume-based, SUS and capacity-based algorithms versus number of users is presented in Figure 3.6. The system configuration for Figure 3.6 is the same as that for the previous result shown in Figure 3.5. It is clearly shown in Figure 3.6 that the average simulation time increases linearly with the number of users, which coincides with the computational complexity analysis expressed in equation (3.15), (3.16) and (3.17) in section 3.3. The result curves also demonstrate that capacity based algorithm needs much longer simulation time than that for the volume-based algorithm. The simulation time of the capacity-based algorithm is around 7 times of the simulation time needed for the volume-based algorithm when number of users is 200. Likewise, the simulation time of the SUS algorithm is greater than that of the volume-based algorithm. The simulation time is about 1.7 times of the simulation time of the proposed algorithm when the number of users is 200. The simulation result validates the theoretical computational complexity analysis presented in section 3.4.2 although the simulation result does not match completely with the mathematical analysis due to other factors, such as channel matrix entry being complex element in the simulation instead of real element.



**Figure 3.6 Average simulation time versus the number of users.  $6 \times 3$  MIMO configuration.**

The results presented in this section confirm that the proposed scheduling strategy is superior to the capacity-based algorithm in terms of reducing the simulation time for user selection up to 7~8 fold in a MU-MIMO wireless system with a large number of users. Therefore, this performance gain of the volume-based scheme can be significant in a real MU-MIMO system with a large number of users although a slight capacity loss is observed for the proposed algorithm. Both volume-based and SUS are low complexity algorithms, the capacity gain of the volume-based algorithm is noticeable in comparison with the SUS algorithm, such as, the sum-rate gain shown in Figure 3.5 is about 12 percent when the number of users is 50 in the  $6 \times 3$  MIMO scenario. In addition, the computational complexity of the proposed algorithm is less than the SUS algorithm.

### **3.6 Summary**

In this chapter, a new suboptimal volume-based scheduling algorithm for MU-MIMO downlink system with block diagonalisation (BD) is presented [L. Jin et al., 2009, L. Jin et al., 2011]. The rule of the algorithm is to select a subset of users whose channel matrix provides maximum volume in a subspace spanned by the row vectors of the channel matrix. The sum-rate capacity of the proposed algorithm is evaluated in order to demonstrate that the proposed algorithm not only attains the reduced complexity, but also achieves a good performance. The simulation results show that the performance of our proposed low complexity algorithm is comparable to the performance obtained by the capacity-based and the SUS algorithms that suffer from higher computational complexity. An additional benefit of the volume-based algorithm is that it can achieve an even higher sum-rate capacity than that obtained by the SUS algorithm in the case of multiple receive antennas. Compared with the capacity-based algorithm, the proposed volume-based algorithm does not require SVD and water-filling operation in each user selection iteration, which greatly simplifies the operation of the proposed algorithm. Compared with the SUS algorithm, our algorithm does not need to perform Gram-Schmidt orthogonalization procedure in each user selection step, which is complex and not stable operation. The volume-based algorithm achieves the lowest computation complexity, which may be considered in a wireless MU-MIMO downlink system for the purpose of simplifying system design.

## **Chapter 4 Sum-rate gain for MU-MIMO downlink system with limited feedback and feedback resource constraint**

### ***4.1 Introduction***

Recent researches on MU-MIMO technology in wireless communication have extended from under the condition of perfect channel state information at the transmitter and receiver (CSIT and CSIR) to the situation when the channel state information is not known to the transmitter. The drive behind this is that the channel information is not available to the transmitter in practice, whereas this channel information is needed to enable most of the precoding design or scheduling algorithms to work. Limited feedback in wireless communication systems conveys the channel information from the receiver to the transmitter. The system performance can benefit from this technique even if with a small number of bits feedback of the channel information. A review paper in [D. Love et al., 2008] provides an overview on the limited feedback in the MU-MIMO wireless communication system.

Compared with single user multiple-input and multiple-output (SU-MIMO) system [A. Narula et al., 1998, D. J. Love et al., 2003, K.K. Mukkavilli et al., 2003, W. Wiroonsak and M. Honig, 2009], the quality of the limited feedback in a MU-MIMO system can significantly affect the signal-to-interference-plus-noise ratio (SINR) of each user because accurate channel state information of one user results in accurate precoding matrix design and, therefore transmitted signal to the user will have less interference to other users.

Studies on MU-MIMO broadcast channels with limited feedback was reported in [N. Jindal, 2006], it is assumed that each receiver in a system has perfect channel knowledge and the transmitter receives

quantized information of the channel instantiation from the receiver. Zero-forcing (ZF) precoding is applied. The scheduling is not needed in a system with a small number of users and Rayleigh fading channel model is considered. Each user's codebook is acquired by random vector quantization (RVQ) [W. Santipach and M. Honig, 2005, W. Santipach and M. Honig, 2004]. It is found that the feedback rate per mobile must be increased linearly with the signal-to-noise ratio (SNR) (in decibels) in order to achieve the full multiplexing gain. The result is in sharp contrast to point-to-point multiple-input multiple-output (i.e. SU-MIMO) systems, in which it is not necessary to increase the feedback rate as a function of the SNR. In [N. Jindal, 2006], it also shows that the general results from the RVQ analysis holds for any choice of the quantization codebooks: fixed feedback rate systems achieve only a bounded sum-rate capacity, and feedback rate must be increased proportionally to the system SNR in order to achieve the full multiplexing gain. Other methods of generating quantization codebook can be Generalized Lloyds algorithm (GLA), LBG algorithm [Y. Linde et al., 1980], LBG algorithm with splitting procedure and tree search VQ algorithm [N. Benvenuto et al., 2007]. Tree-Structured RVQ is the modified RVQ vector quantization proposed in [W. Santipach, 2008].

P. Ding [P. Ding et al., 2007] analyzed the performance limit for the wireless downlink system with feedback when there is no user selection scheme is applied. Two models for partial channel state information feedback from each receiver to the transmitter were considered. One is the shape feedback model where the normalized channel vector of each user is available at the base station. The other is the limited feedback model where each user quantizes its channel vector according to a rotated codebook. The precoding strategies applied are zero-forcing dirty paper coding (ZFDPC) and channel inversion (CI). Same result as Jindal's was found that utilizing a fixed codebook in the circumstance of limited feedback leads to a sum rate ceiling for both schemes for asymptotically high SNR.

N. Ravindran [N. Ravindran and N. Jindal, 2008] studied MU-MIMO downlink system with limited feedback where each receiver has perfect channel state information and the transmitter gains the channel knowledge by a finite number of channel feedback bits from each receiver. Both BD precoding and ZF beamforming are used and the user selection is not applied. The sum-rate capacity loss due to imperfect channel knowledge as a function of the feedback level is analyzed. It is shown that scaling the number of feedback bits linearly with the system SNR is sufficient to maintain a bounded rate loss. It is also demonstrated that the superiority of quantized feedback by comparing the quantization strategy to an analogue feedback scheme.

C. Peel [C. Peel et al., 2005] introduced a simple encoding algorithm that achieves near-capacity at sum-rates of tens of bits/channel use for a downlink MU-MIMO wireless system. The algorithm is a variation on channel inversion (ZF beamforming), which regularizes the inverse and uses a “sphere encoder” to perturb the data to reduce the power of the transmitted signal. The poor performance of channel inversion due to the large spread in the singular values of the channel matrix, the regularization can improve the condition of the inverse and maximize the signal-to-interference-plus-noise ratio at the receivers. It is assumed that the transmitter has  $M$  antennas and each user terminal has one antenna. Suppose that the transmitter and receiver have perfect channel state information. Regularization enables sum-rate grow linearly with  $\min(M,K)$  and works especially well at low signal-to-noise ratios (SNRs). In addition, after the regularization of the channel inverse, a certain perturbation of the data using a “sphere encoder” can further reduce the energy of the transmitted signal. Excellent performance at all SNR’s can be achieved with the perturbation.

A limited feedback system with regularized block diagonalisation (RBD) precoding is considered in [B. Song et al., 2008]. It is assumed that each receiver has perfect channel state information (CSI) and the transmitter

receives the quantized CSI with a finite number of feedback bits from each receiver. Similar result as other authors mentioned above is found that linearly increasing the number of feedback bits with the system SNR can maintain a sum-rate capacity loss less than a given value. A dominant eigenvector based LBG (DE-LBG) vector quantization scheme is proposed, which is applied to an OFDM-based multiuser MIMO system.

T. Yoo [T. Yoo et al., 2007] analyzed the sum-rate capacity of a MU-MIMO downlink system with a large number of users and hence scheduling algorithm applied, the transmitter gaining partial channel knowledge via finite rate feedback. It is shown that more multiuser diversity can be exploited if the channel direction information (CDI) and channel quality information (CQI) such as channel magnitude are known at the transmitter. Signal-to-Interference-plus-noise-Ratio (SINR) as CQI is also investigated because SINR captures both channel magnitude and quantization error. The relationship between the SINR distribution and the sum-rate is examined. The tradeoffs between the number of feedback bits, the number of users, and the SNR are observed. It is found that having more users reduces feedback load for a target performance.

In [M. Trivellato et al., 2008], the MU-MIMO broadcast channel is also considered and the CSIT is obtained through limited feedback from the receivers that index a set of precoding vectors contained in a predefined codebook. Transceiver architecture based on zero-forcing beamforming and linear receiver combining is proposed. The receiver combining and quantization for CSIT feedback are jointly designed in order to maximize the expected SINR for each user. An analytic characterisation of the achievable sum-rate capacity in the case of many users is provided. It is shown how additional receive antennas or higher multiuser diversity can reduce the required feedback rate to achieve a target capacity. In addition, a design methodology is proposed for generating codebooks tailored for arbitrary spatial correlation statistics. A tree structured codebook can be

utilized in time-correlated MIMO channels to significantly reduce feedback overhead.

In [M. Kountouris et al., 2008], a downlink MU-MIMO system with an  $M$ -antenna base station and  $K$  single-antenna users is considered. A limited feedback-based scheduling and precoding scenario is considered that builds on the multiuser random beamforming (RBF). The work in [M. Kountouris et al., 2008] is to find a solution to solve the problem that RBF yields degraded performance for low to moderate  $K$  values. A two-stage framework is proposed to decouple the scheduling and beamforming in which RBF is exploited to identify good, spatially separable, users in a first stage then the initial random beams are refined based on the available feedback to offer improved performance toward the selected users. Also a proposed technique is the beam power control that the direction of the second-stage beams is not changed, and therefore the reduced feedback and performance tradeoffs can be achieved.

R. Zakhour [R. Zakhour and D. Gesbert, 2007] studied the MU-MIMO downlink system with a single cell containing a base station having multiple antennas and  $K$  single-antenna mobile terminals. The research considers the more realistic case of having an intermediate state of CSI. It utilizes an idea that the allotted feedback are divided and used for two stages: A first stage devoted to scheduling followed by a second stage for precoder design for the selected users. The investigation emphasizes on how to determine the splitting of the feedback rate so as to maximize performance.

In this chapter, we present a new scheduling algorithm which is designed for the MU-MIMO downlink system with a large number of users and total feedback bits constraint. The new scheduling algorithm adopts an approach that the users are selected by using low bits feedback and then the precoding vectors are designed based on the high bits feedback. The

volume-based scheduling algorithm described in chapter 3 [L.Jin et al., 2009] is used in the user selection and the block diagonalisation (BD) precoding is adopted for signal transmission. We derive the sum-rate capacity expression of the MU-MIMO system by using the scheduling algorithm proposed. It is found that the sum-rate capacity can be improved significantly when SNR is at high value. The details are presented in following sections. Section 4.2 describes the system model; section 4.3 presents the details of the proposed scheduling algorithm; performance analysis and math manipulation are given in section 4.4; and finally Monte Carlo simulation results and summary are shown in section 4.5 and section 4.6.

## **4.2 System model**

The system model is presented in this section. A single cell MU-MIMO broadcast system is considered, which has one base station (BS) serving  $K$  users. The BS is equipped with  $M$  transmit antennas, the receiver for user  $k$  is equipped with  $N_k$  antennas and  $K \geq M$  is considered. Block Diagonalization (BD) [Q. H. Spencer et al., 2004, L. U. Choi and R. D. Murch, 2004] precoding is applied to the transmitted signal. The BD precoding is a method that the inter-user interference can be eliminated in multiuser MIMO downlink system and if the channel information is known to the transmitter and the receiver. Each user  $k = 1 \cdots K$  in the system is characterized by a channel matrix  $\mathbf{H}_k$  with dimension of  $N_k \times M$ .  $\mathbf{H}_k \in \mathbb{C}^{N_k \times M}$  with each entry following an independent and identically distributed (i.i.d.) complex Gaussian distribution  $\mathcal{CN}(0,1)$ , which is a valid model if the transmit and receive antennas are in rich-scattering environments and antenna spacing is larger than the coherence distance. The transmitted symbol for user  $k$  is denoted as  $\mathbf{x}_k$  which is  $N_k \times 1$  vector. The signal is multiplied by a precoding matrix  $\mathbf{W}_k$  and then is transmitted by the

transmit antennas. Assume that maximum  $K$  users can be served simultaneously. Then the received signal  $\mathbf{y}_k$  for user  $k$  can be expressed as

$$\mathbf{y}_k = \mathbf{H}_k \mathbf{W}_k \mathbf{x}_k + \sum_{i=1, i \neq k}^K \mathbf{H}_k \mathbf{W}_i \mathbf{x}_i + \mathbf{n}_k, \quad (4.1)$$

where the first term on the right-hand side of (4.1) is the desired signal for user  $k$ , the second term is the interference from other user signals and  $\mathbf{n}_k$  is the additive white Gaussian noise (AWGN) column vector with  $N_k$  elements for user  $k$  with zero mean and variance  $E[\mathbf{n}_k \mathbf{n}_k^H] = \sigma^2 \mathbf{I}$ .

#### 4.2.1 Perfect channel information at the transmitter and the receiver

The details of BD precoding are described as follows. Assuming if  $K$  users can be supported simultaneously, the channel matrix to include  $K$  users is

$$\mathbf{H} = [\mathbf{H}_1, \dots, \mathbf{H}_{k-1}, \mathbf{H}_k, \mathbf{H}_{k+1}, \dots, \mathbf{H}_K]. \quad (4.2)$$

The design of the BD precoding matrix for user  $k$  is to find a matrix  $\mathbf{W}_k$  that meets the following condition:

$$\begin{aligned} \mathbf{W}_k &\in \mathfrak{U}(M, N_k) \\ \mathbf{H}_k \mathbf{W}_i &= 0 \text{ for all } k \neq i \text{ and } 1 \leq k, i \leq K, \end{aligned} \quad (4.3)$$

where  $\mathbf{W}_k$  is a matrix with  $N_k \times M$  dimension,  $\mathfrak{U}(M, N_k)$  stands for the class of  $M \times N_k$  unitary matrix which is a collection of vectors  $(\mathbf{u}_1, \dots, \mathbf{u}_{N_k})$  and the dimension of  $\mathbf{u}_j$  is  $M$  for  $1 \leq j \leq N_k$ ,  $\mathbf{H}_k \mathbf{W}_k$  for user  $k$  is non-zero.

The method to get the desired  $\mathbf{W}_k$  is first to formulate a channel matrix to include all channel matrices from other interference users. The matrix is given by

$$\bar{\mathbf{H}}_k = [\mathbf{H}_1^T, \dots, \mathbf{H}_{k-1}^T, \mathbf{H}_{k+1}^T, \dots, \mathbf{H}_K^T]^T. \quad (4.4)$$

To meet the constraint in (4.3),  $\mathbf{W}_k$  shall be in the null space of  $\bar{\mathbf{H}}_k$ . Let  $\bar{R}_k$  denote the rank of  $\bar{\mathbf{H}}_k$ ,  $\bar{N}_k$  is row size and  $\bar{M}$  is column size. Performing singular value decomposition (SVD) to  $\bar{\mathbf{H}}_k$ , one has:

$$\bar{\mathbf{H}}_k = \bar{\mathbf{U}}_k \bar{\boldsymbol{\Sigma}}_k \bar{\mathbf{V}}_m^* = \bar{\mathbf{U}}_k \bar{\boldsymbol{\Sigma}}_k \begin{bmatrix} \bar{\mathbf{V}}_k^1 & \bar{\mathbf{V}}_k^0 \end{bmatrix}^*, \quad (4.5)$$

where  $\bar{\mathbf{U}}_k$  is a square matrix having the same size as the row of  $\bar{\mathbf{H}}_k$ ,  $\bar{\mathbf{V}}_m^*$  is a square matrix which has the same size as the column of  $\bar{\mathbf{V}}_m^*$ ,  $\bar{\mathbf{U}}_k$  and  $\bar{\mathbf{V}}_m^*$  are unitary matrices,  $\bar{\mathbf{V}}_m^*$  denotes complex conjugate of  $\bar{\mathbf{V}}_m$ ,  $\bar{\boldsymbol{\Sigma}}_k$  is an  $\bar{N}_k \times \bar{M}$  diagonal matrix of singular values of  $\bar{\mathbf{H}}_k$ ;  $\bar{\mathbf{V}}_k^1$  contains the first  $\bar{R}_k$  right singular vectors and  $\bar{\mathbf{V}}_k^0$  contains the last  $\bar{M} - \bar{R}_k$  right singular vectors of  $\bar{\mathbf{H}}_k$ . The columns in  $\mathbf{W}_k$  are composed from the linear combination of those in  $\bar{\mathbf{V}}_k^0$  because the columns in  $\bar{\mathbf{V}}_k^0$  form a basis set in the null space of  $\bar{\mathbf{H}}_k$ .

Assuming that each user terminal is equipped with the same number of antennas  $N$  and transmitter has  $M$  antennas, the maximum simultaneous users,  $\hat{K} = M / N$ , can be supported by BD algorithm [Q. H. Spencer et al., 2004]. Subsequently the system sum-rate capacity should be evaluated after precoding matrices are found for all simultaneous users in a subset of users. Consider that  $\hat{K}$  is the maximum number of simultaneously supportable users,  $\kappa = \{1, 2, \dots, K\}$  is the set of all users,  $\beta_i$  is a subset of  $\kappa$  and

cardinality of  $\beta_i$  is less than or equal to  $\hat{K}$ ,  $\beta = \{\beta_1, \beta_2, \dots\}$  is the set containing all possible  $\beta_i$  and  $\mathbf{H} = \{\mathbf{H}_1, \mathbf{H}_2, \dots, \mathbf{H}_K\}$  denotes the set of all users' channels. The achievable system sum capacity under BD scheme is the capacity maximization problem under transmit power constraint  $P$ . The maximum capacity can be expressed as [Q. H. Spencer et al., 2004]

$$C_{BD}(\mathbf{H}, P, \sigma^2) = \max_{\beta_i \in \beta} C_{BD|\beta_i}(\mathbf{H}_{\beta_i}, P, \sigma^2), \quad (4.6)$$

where  $\mathbf{H}_{\beta_i}$  denotes the channel matrix for user set  $\beta_i$  and  $\sigma^2$  denotes Gaussian noise power. The solution for (4.6) is to obtain maximum sum capacity for user set  $\beta_i$  by SVD operation to  $\mathbf{H}_j \mathbf{W}_j$  for  $j \in \beta_i$  and water-filling on the corresponding singular values.

#### 4.2.2 Perfect channel information at the receiver and the channel knowledge is available to the transmitter via feedback channel from the receiver to the transmitter

In the case of that perfect channel state information is known to the receiver and it is not known to the transmitter, the limited feedback from the receiver to the transmitter through an uplink feedback channel is a method to convey the channel information from the receiver to the transmitter so as to the scheduling and BD precoding strategy can be utilized and multiuser diversity and multiplexing gain can be explored. Figure 4.1 shows the MU-MIMO downlink system with  $B$  bits feedback for each user. The figure shows that each user terminal only has one antenna, the transmitter has  $M$  antennas and therefore maximum  $M$  users can be served simultaneously; the channel matrix is  $\mathbf{H} = [\mathbf{h}_1^T, \mathbf{h}_2^T, \dots, \mathbf{h}_M^T]^T$  where  $\mathbf{h}_i$  for  $i=1:M$  is the column channel vector with  $M$  dimensions for user  $i$ .

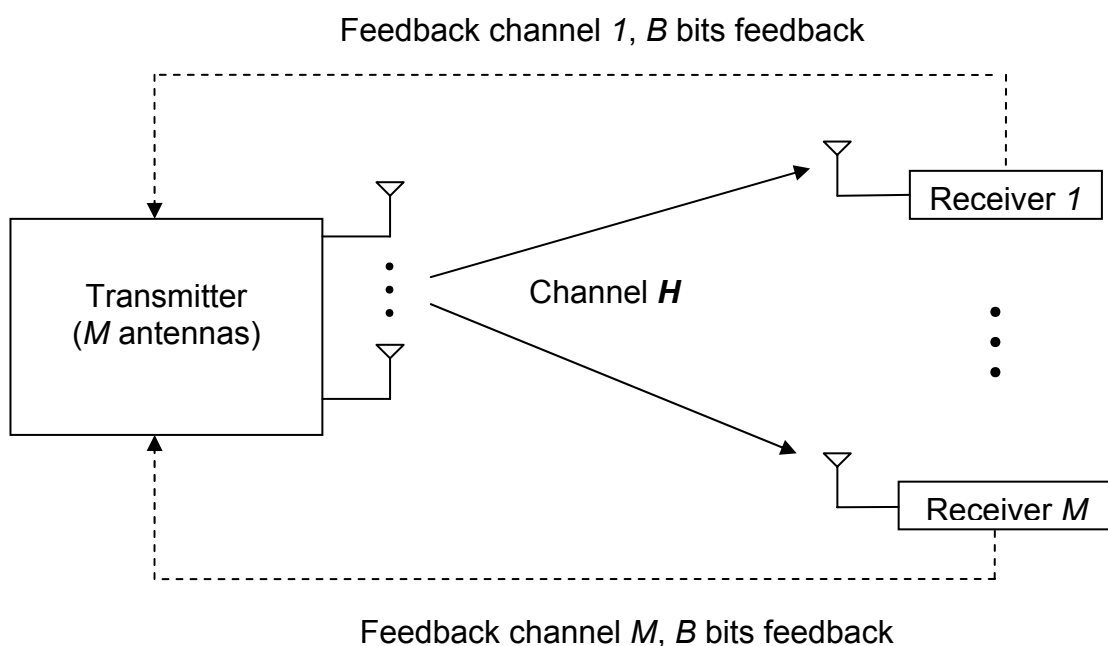


**Figure 4.1** MU-MIMO downlink system with limited feedback. The transmitter has  $M$  antennas and each user terminal has one antenna. Each user has  $B$  feedback bits.

In the case of limited feedback and BD precoding applied and the maximum number of  $K$  users can be served, the precoding vector for user  $k$  is obtained by using the quantized channel vectors, then (4.1) becomes

$$\mathbf{y}_k = \mathbf{H}_k \mathbf{W}_{q,k} \mathbf{x}_k + \sum_{i=1, i \neq k}^K \mathbf{H}_k \mathbf{W}_{q,i} \mathbf{x}_i + \mathbf{n}_k, \quad (4.7)$$

where  $\mathbf{W}_{q,k}$  is the precoding vector for user  $k$  and  $\mathbf{W}_{q,i}$  for  $i=1$  to  $K, i \neq k$ . Obviously, the second term on the right hand side in above equation can not be zero because  $\mathbf{W}_{q,i}$  obtained on quantized channel is different in some degree from  $\mathbf{W}_i$  obtained on real channel. Therefore, interference from other users could not be completely cancelled. The capacity under the limited feedback could not achieve the capacity obtained under the perfect CSIT.

### **4.2.3 The two-step scheduling algorithm proposed for MU-MIMO downlink system with limited feedback and power allocation**

In this chapter, a two-step scheduling algorithm is proposed for a limited feedback MU-MIMO system. The aim of the algorithm design is to alleviate the total feedback load on the feedback channels and to obtain a reasonable higher system capacity if there is a feedback constraint on the MU-MIMO downlink system. The first step of the algorithm is that users are selected by using the volume-based algorithm [L.Jin et al., 2009]. The quantized channel information is gained by using low bits codebook stored at the transmitter and the receiver. The second step is that only selected users feedback their channel information by using higher bits codebook stored at the transmitter and receiver. Then the BD precoding matrices for the selected users are designed and are applied to the selected users. The maximum capacity achieved by this strategy can be expressed by equation (4.6) and the result is the well-known water-filling strategy. However we only consider that the transmit power are evenly allocated to the selected users in the following performance analysis.

### 4.3 The details of new two-step scheduling algorithm

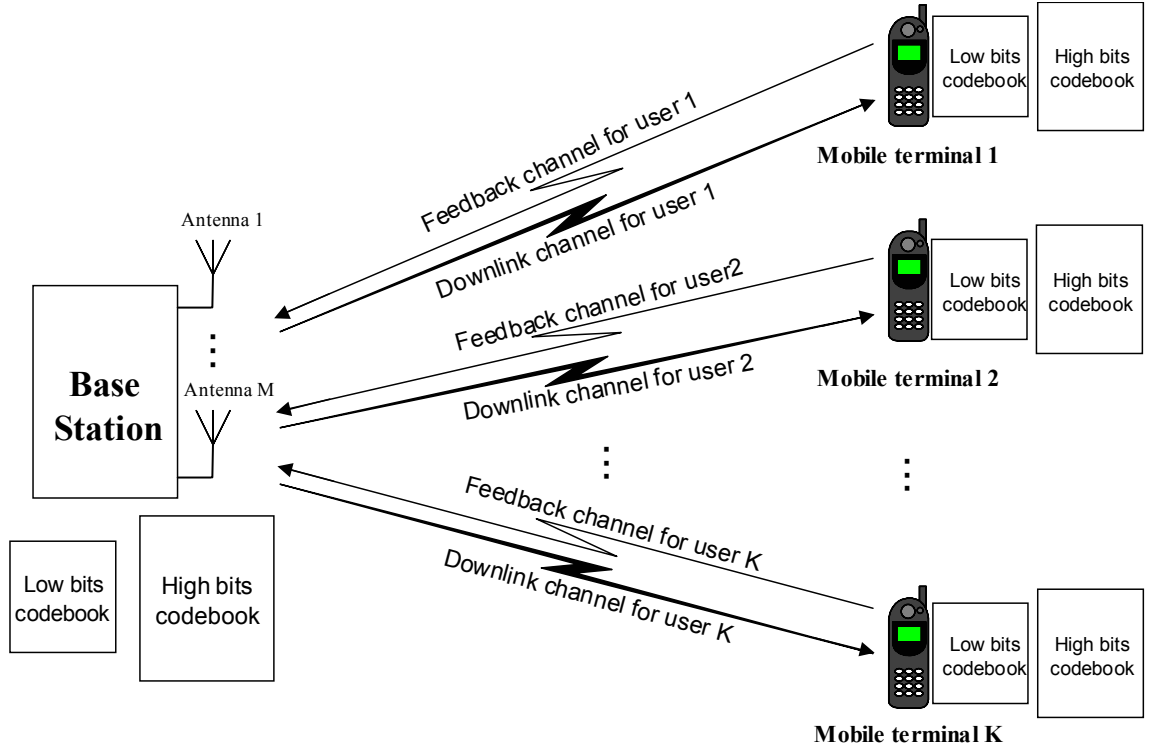


**Figure 4.2 MU-MIMO downlink system with limited feedback. Two versions of the codebook are stored at the transmitter and the receiver.**

Figure 4.2 shows a MU-MIMO system with limited feedback. Assume that two versions of codebooks are stored on each user terminal; one version is a codebook with low bits  $B_l$  and the other version is a codebook with high bits  $B_h$ . The number of codeword in the low bits codebook is  $2^{B_l}$  and the number of codeword in the high bits codebook is  $2^{B_h}$ . These codebooks are also stored on the base station.

Assume that each terminal has one antenna and each user  $k$  has perfect channel knowledge at the receiver (CSIR). In this case each user's channel matrix is a row vector  $\mathbf{h}_k$  with  $M$  dimensions. At the receiver, its normalized channel, also called the direction of the channel (CDI),  $\tilde{\mathbf{h}}_k = \mathbf{h}_k / \|\mathbf{h}_k\|$  is quantized to a unit norm row vector  $\mathbf{h}_{kq}$  with  $M$  dimensions.

The quantized vector  $\mathbf{h}_{kq}$  is chosen from the codebook that is a unitary matrix with unit norm row vector, i.e. codeword, and codebook size is  $2^B$ , i.e. number of rows. The codebook is expressed as

$$C_k = \{\mathbf{c}_{k1}, \mathbf{c}_{k2}, \dots, \mathbf{c}_{kN}\}, \quad N = 2^B. \quad (4.8)$$

The codeword  $\mathbf{c}_{kn}$  is chosen as the quantization vector  $\mathbf{h}_{kq}$  by the minimum chordal distance criterion [A. Narula et al., 1998, D. J. Love et al., 2003, K.K. Mukkavilli et al., 2003]

$$n = \arg \min_{1 \leq i \leq N} d_c(\tilde{\mathbf{h}}_k, \mathbf{c}_{ki}), \quad (4.9)$$

where  $d_c(\tilde{\mathbf{h}}_k, \mathbf{c}_{ki})$  is the chordal distance between two vectors  $\tilde{\mathbf{h}}_k$  and  $\mathbf{c}_{ki}$ . The relation between the chordal distance and the inner product of  $\tilde{\mathbf{h}}_k$  and  $\mathbf{c}_{ki}$  is as follows [K. K. Mukkavilli et al., 2003]

$$d_c(\tilde{\mathbf{h}}_k, \mathbf{c}_{ki}) = 2(1 - |\langle \tilde{\mathbf{h}}_k, \mathbf{c}_{ki} \rangle|), \quad (4.10)$$

where  $\langle \tilde{\mathbf{h}}_k, \mathbf{c}_{ki} \rangle$  denotes the inner product of  $\tilde{\mathbf{h}}_k$  and  $\mathbf{c}_{ki}$ . The codebook is designed off-line and stored at the transmitter and the receiver. Each user feeds back only the index  $n$  of the codeword representing the channel from the receiver to the transmitter where the codebook for each user is searched and the codeword is obtained.  $B$  bits feedback is required for each user.

#### 4.3.1 Codebook design method: Random Vector Quantization (RVQ) and dominant eigenvector based LBG (DE-LBG) algorithm

There are numerous codebook design methods. We resort Random Vector Quantization (RVQ) scheme [W. Santipach, 2008] and a dominant eigenvector based LBG (DE-LBG) algorithm [B. Song et al., 2008].

#### 4.3.1.1 The Random Vector Quantization (RVQ)

A Random Vector Quantization (RVQ) is a scheme [W. Santipach, 2008] that a codeword is selected from a codebook consisting of  $2^B$  random vectors, which are independent and isotropically distributed in  $\mathbb{C}^{1 \times M}$ . The codebook is known *a priori* at the transmitter and receiver. Each codeword in the codebook is randomly generated from  $M$ -dimensional unit-norm complex Gaussian vectors. It is assumed that the codewords of different users are independent, i.e. the  $n^{\text{th}}$  codewords  $\mathbf{C}_{j_1 n}$  and  $\mathbf{C}_{j_2 n}$  are independent when  $k$  takes different values  $j_1$  and  $j_2$ .

#### 4.3.1.2 Dominant Eigenvector based LBG (DE-LBG)

DE-LBG vector quantization algorithm is a modified LBG vector quantization with splitting algorithm [Y. Linde et al., 1980]. The details of the LBG algorithm for acquiring a codebook with its size  $N = 2^B$  are as follows:

- (1) Firstly, a long vector training sequence  $\mathbf{A} = [\mathbf{x}_1, \mathbf{x}_2, \dots, \mathbf{x}_s]^T \in \mathbb{C}^s$  with  $s$  number of vectors is generated, where  $\mathbf{x}_i$  for  $i = 1, \dots, s$  is an  $M$ -dimensional unit-norm complex Gaussian vector.
- (2) Initialization: Set  $J = 1$  and define  $\hat{\mathbf{A}}_0(1) = \hat{\mathbf{x}}(\mathbf{A})$ , the centroid of the training sequence, i.e., the centroid of one Voronoi region.
- (3) Given the reproduction alphabet  $\hat{\mathbf{A}}_0(J)$  containing  $J$  vectors  $\{\mathbf{y}_i, i = 1, \dots, J\}$ , “split” each vector  $\mathbf{y}_i$  into two close vectors  $\mathbf{y}_i + \varepsilon$  and

$\mathbf{y}_i - \boldsymbol{\varepsilon}$ , where  $\boldsymbol{\varepsilon}$  is a fixed perturbation vector. The collection  $\tilde{\mathcal{A}}$  of  $\{\mathbf{y}_i + \boldsymbol{\varepsilon}, \mathbf{y}_i - \boldsymbol{\varepsilon}; i=1, \dots, J\}$  has  $2J$  vectors. Replace  $J$  by  $2J$ . Find new Voronoi region for each vector in  $\tilde{\mathcal{A}}$  and new centroid for each Voronoi region.  $\tilde{\mathcal{A}}$  is updated with  $\tilde{\mathcal{A}}(J)$ .

(4) Is  $J = N$ ? If so, set  $\hat{\mathcal{A}}_0 = \tilde{\mathcal{A}}(J)$  and halt.  $\tilde{\mathcal{A}}_0$  is then the initial reproduction alphabet for the  $N$ -level quantization algorithm. If not, run the algorithm for an  $P$ -level quantizer on  $\tilde{\mathcal{A}}(J)$  to produce a good reproduction alphabet  $\hat{\mathcal{A}}_0(J)$ , and then return to step (3).

More general description of the algorithm is that one starts with a one-level quantizer consisting of the centroid of entire training sequence. This vector is then split into two vectors and the two-level quantizer algorithm is run on this pair to obtain a good two-level quantizer. Each of these two vectors is then split and the algorithm is run to produce a good four-level quantizer. Finally, one has the quantizers for 1, 2, 4, 8,  $\dots$ ,  $N$  levels.

In LBG algorithm, each Voronoi region is formulated by allocating the vectors  $\mathbf{y}_i$  closest to the centroid  $\mathbf{x}_i$  with minimum distance measure  $d(\mathbf{y}_i, \mathbf{x}_i)$ . New centroid in one region is the mean of all vectors in this region. DE-LBG algorithm modifies the nearest neighbour condition from minimum distance measure to minimum chordal distance when determining each Voronoi region. DE-LBG algorithm also modifies the centroid condition that the new centroid is taken as the dominate eigenvector of the covariance matrix  $\mathbf{R} = \frac{1}{J} \sum_{i=1}^J \mathbf{y}_i \mathbf{y}_i^H$ , where  $H$  in  $\mathbf{y}_i^H$  donates the Hermitian of vector  $\mathbf{y}_i$ . Therefore the modified centroid condition can capture the statistics of the training vectors in a Voronoi region.

In comparison with RVQ, DE-LBG vector quantization algorithm needs more time to find centroids and find their Veronoi regions on a

training sequence. Although the codebook for each user can be obtained off-line, the task to find the codebook with higher bits needs very high computation time. It needs  $2^b \times M$  multiplication to calculate the covariance matrix and about  $10 \times M^3$  multiplication to get the dominate eigenvector of the covariance matrix. Note that the addition is not counted here due to the equal number of addition and multiplication in two matrix operations mentioned above and the multiplication count being sufficient as an indicator of the computational complexity. Only multiplication is used for the computational complexity analysis. Therefore DE-LGB algorithm is not suitable for high bits codebook generation.

### 4.3.2 The new proposed scheduling algorithm

**The proposed scheduling algorithm is as follows:**

1. In a MU-MISO downlink system with  $K$  user, a high bits codebook and a low bits codebook are stored on each user terminal. These codebooks are also stored at the transmitter. The codebooks are designed off-line. Each codeword in a codebook holds the direction of the user channel which is normalized user channel vector. A codebook can be generated via RVQ algorithm or DE-LBG algorithm.
2. Assume that the channel state information is known at the receiver and the channel is characterized as block Rayleigh fading. A user channel condition does not vary from the channel state information being quantized, the index of the quantized channel vector being sent until the transmitted signal being received by the user. Each user uses low bits codebook to find a codeword representing its channel by using minimum chordal distance criterion. If user  $k$  has a low bits codebook  $C_k^l = \{\mathbf{c}_{k1}, \mathbf{c}_{k2}, \dots, \mathbf{c}_{kN_l}\}$  with codebook size  $N_l = 2^{B_l}$ . The codeword  $\mathbf{c}_{kn}$  is chosen as the quantization vector  $\mathbf{h}_{kq}$  of  $\tilde{\mathbf{h}}_k$  and the

index of the codeword is obtained by following equation:

$$n_{ki} = \arg \min_{1 \leq i \leq N_i} d_c(\tilde{\mathbf{h}}_k, \mathbf{c}_{ki}).$$

The codeword index  $n_{ki}$  is sent back to the transmitter. The transmitter receives feedback from  $K$  users.

3. The transmitter selects maximum number of users to serve by using the feedback information, locating the quantized vector from the low bits codebook for each user and finally applying the volume-based algorithm.
4. The transmitter requests the channel information from the selected users. At this stage, each selected user  $k$  terminal quantizes its channel by using high bits codebook  $C_k^h = \{\mathbf{c}_{k1}, \mathbf{c}_{k2}, \dots, \mathbf{c}_{kN_h}\}$  with codebook size  $N_h = 2^{B_h}$ . The feedback bit for a selected user  $k$  is obtained via the minimum chordal distance criterion, which can be expressed as  $n_{k_h} = \arg \min_{1 \leq i \leq N_h} d_c(\tilde{\mathbf{h}}_k, \mathbf{c}_{ki})$ . Because there are  $M$  number of antennas at the transmitter and one receive antenna for each user, total  $M$  number of  $n_{k_h}$  are sent back to the transmitter under BD precoding scheme.
5. The transmitter finds precoding vector for each user under BD scheme and signals for the selected users are sent simultaneously.

#### 4.4 Performance analysis

Limited feedback technique can improve system performance in a MU-MIMO system when transmitter does not know the channel state information. The information conveyed from the receiver through the feedback control channel to the transmitter allows the transmitter to design the precoding matrix for each selected user and makes it possible to serve multiple users simultaneously. Multiuser diversity and the multiplexing gain in the MU-MIMO systems can be exploited by using limited feedback strategy. However, using feedback creates overhead on uplink feedback channel to increase the achievable data rate on the downlink channel. This

overhead can sometimes be significant and can not be ignored. Especially in the MU-MIMO system, many users are sending feedback to a central controller (for example base station) so users are competing for the limited feedback resources via multiple access system. In the situation of that the system is subject to the limited feedback constraint, high bits feedback from all users might not be feasible. The proposed scheduling algorithm is designed to solve this issue. To reduce the feedback load, the first step of the algorithm is to gather each user's channel information from all users in the system by using low bits feedback; then the second step of the algorithm is to congregate only the channel information from those selected users via high bits feedback. The second step is to gain more accurate channel information for the selected users in order to acquire near-orthogonal precoding matrix for signal transmission simultaneously. Because only a small number of users are selected due to the number of transmit antenna constraint of BD precoding, the feedback load on the feedback control channel is low in the second step of the algorithm.

#### 4.4.1 Sum-rate capacity analysis

Let  $P$  be the total transmit power at the base station and  $\rho = P/M$ ,  $\rho$  is the transmit power equally allocated to each user in a selected user set ( $M$  users). For each selected user  $k$ ,  $\mathbf{w}_{kq,l}$  denotes the BD precoding vector obtained by using the low bits feedback whereas  $\mathbf{w}_{kq,h}$  denotes the BD precoding vector obtained by using the high bits feedback,  $\mathbf{h}_k$  is the channel vector which is known to the receiver.

The sum-rate capacity (Ergodic capacity)  $R_{k,l}$  achieved by using the low bits feedback can be expressed as

$$R_{k,l} = E \left[ \log_2 \left( 1 + \frac{\rho |\langle \mathbf{h}_k, \mathbf{w}_{kq,l} \rangle|^2}{1 + \sum_{j=1:M, j \neq k} \rho |\langle \mathbf{h}_k, \mathbf{w}_{jq,l} \rangle|^2} \right) \right], \quad (4.11)$$

where  $E[\cdot]$  denotes the expectation operation,  $\langle \mathbf{a}, \mathbf{b} \rangle$  denotes the inner product of vectors  $\mathbf{a}$  and  $\mathbf{b}$ .  $|\mathbf{a}|$  denotes the absolute value of  $\mathbf{a}$ . The term  $\sum_{j=1:M, j \neq k} |\langle \mathbf{h}_k, \mathbf{w}_{jq,l} \rangle|^2$  in the denominator is the interference from users other than  $k$ .

Similarly, the sum-rate capacity  $R_{k,h}$  achieved by using the high bits feedback can be expressed as

$$R_{k,h} = E \left[ \log_2 \left( 1 + \frac{\rho |\langle \mathbf{h}_k, \mathbf{w}_{kq,h} \rangle|^2}{1 + \sum_{j=1:M, j \neq k} \rho |\langle \mathbf{h}_k, \mathbf{w}_{jq,h} \rangle|^2} \right) \right], \quad (4.12)$$

where  $\sum_{j=1:M, j \neq k} \rho |\langle \mathbf{h}_k, \mathbf{w}_{jq,h} \rangle|^2$  is the interference from users other than  $k$ .

*Theorem 1:* The sum-rate gap  $\Delta R_k$  due to extra step of the proposed scheduling algorithm is

$$\Delta R_k \approx -\log_2 \left\{ 1 + P2^{-\frac{B_h}{M-1}} \right\} + \log_2 \left\{ 1 + P2^{-\frac{B_l}{M-1}} \right\}. \quad (4.13)$$

Proof: the rate gap can be expressed as (4.14)

$$\begin{aligned}
 \Delta R_k &= R_{kh} - R_{kl} \\
 &= E \left[ \log_2 \left( 1 + \frac{\rho |\langle \mathbf{h}_k, \mathbf{w}_{kq,h} \rangle|^2}{1 + \sum_{j \neq k} \rho |\langle \mathbf{h}_k, \mathbf{w}_{jq,h} \rangle|^2} \right) \right] - E \left[ \log_2 \left( 1 + \frac{\rho |\langle \mathbf{h}_k, \mathbf{w}_{kq,l} \rangle|^2}{1 + \sum_{j \neq k} \rho |\langle \mathbf{h}_k, \mathbf{w}_{jq,l} \rangle|^2} \right) \right] \\
 &= E \left[ \log_2 \left( \frac{1 + \sum_{j \neq k} \rho |\langle \mathbf{h}_k, \mathbf{w}_{jq,h} \rangle|^2 + \rho |\langle \mathbf{h}_k, \mathbf{w}_{kq,h} \rangle|^2}{1 + \sum_{j \neq k} \rho |\langle \mathbf{h}_k, \mathbf{w}_{jq,h} \rangle|^2} \right) \right] \\
 &\quad - E \left[ \log_2 \left( \frac{1 + \sum_{j \neq k} \rho |\langle \mathbf{h}_k, \mathbf{w}_{jq,l} \rangle|^2 + \rho |\langle \mathbf{h}_k, \mathbf{w}_{kq,l} \rangle|^2}{1 + \sum_{j \neq k} \rho |\langle \mathbf{h}_k, \mathbf{w}_{jq,l} \rangle|^2} \right) \right] \\
 &\stackrel{(a)}{\approx} E \left[ \log_2 \left( \frac{1 + \rho |\langle \mathbf{h}_k, \mathbf{w}_{kq,h} \rangle|^2}{1 + \sum_{j \neq k} \rho |\langle \mathbf{h}_k, \mathbf{w}_{jq,h} \rangle|^2} \right) \right] - E \left[ \log_2 \left( \frac{1 + \rho |\langle \mathbf{h}_k, \mathbf{w}_{kq,l} \rangle|^2}{1 + \sum_{j \neq k} \rho |\langle \mathbf{h}_k, \mathbf{w}_{jq,l} \rangle|^2} \right) \right] \\
 &\stackrel{(b)}{=} E \left[ \log_2 \left( \frac{1 + \rho \|\mathbf{h}_k\|^2 |\langle \tilde{\mathbf{h}}_k, \mathbf{w}_{kq,h} \rangle|^2}{1 + \rho \|\mathbf{h}_k\|^2 \sum_{j \neq k} |\langle \tilde{\mathbf{h}}_k, \mathbf{w}_{jq,h} \rangle|^2} \right) \right] - E \left[ \log_2 \left( \frac{1 + \rho \|\mathbf{h}_k\|^2 |\langle \tilde{\mathbf{h}}_k, \mathbf{w}_{kq,l} \rangle|^2}{1 + \rho \|\mathbf{h}_k\|^2 \sum_{j \neq k} |\langle \tilde{\mathbf{h}}_k, \mathbf{w}_{jq,l} \rangle|^2} \right) \right]
 \end{aligned} \tag{4.14}$$

where (a) follows since the interference from other users  $\sum_{j \neq k} |\langle \mathbf{h}_k, \mathbf{w}_{jq,h} \rangle|^2 \geq 0$  and  $\sum_{j \neq k} |\langle \mathbf{h}_k, \mathbf{w}_{jq,l} \rangle|^2 \geq 0$  is much smaller and can be ignored in the summation of two nominators; (b) follows because the channel vector  $\mathbf{h}_k = \|\mathbf{h}_k\| \tilde{\mathbf{h}}_k$ .

Let  $\theta_k$  denote the angle between  $\tilde{\mathbf{h}}_k$  and its quantization vector  $\mathbf{h}_{kq}$ , decompose  $\tilde{\mathbf{h}}_k$  into one component in the direction of  $\mathbf{h}_{kq}$  and one component in the direction of  $\mathbf{g}_k$  which is a unitary vector being perpendicular to  $\mathbf{h}_{kq}$ .  $\tilde{\mathbf{h}}_k$  can be written  $\tilde{\mathbf{h}}_k = \cos \theta_k \mathbf{h}_{kq} + \sin \theta_k \mathbf{g}_k$ . Then the equation (4.14) can be expressed as

$$\begin{aligned}
 \Delta R_k &= E \left[ \log_2 \left( \frac{1 + \rho \|\mathbf{h}_k\|^2 \left| \langle \tilde{\mathbf{h}}_k, \mathbf{w}_{kq,h} \rangle \right|^2}{1 + \rho \|\mathbf{h}_k\|^2 \sum_{j \neq k} \left| \langle (\cos \theta_{k,h} \mathbf{h}_{kq,h} + \sin \theta_{k,h} \mathbf{g}_{k,h}), \mathbf{w}_{jq,h} \rangle \right|^2} \right) \right] \\
 &\quad - E \left[ \log_2 \left( \frac{1 + \rho \|\mathbf{h}_k\|^2 \left| \langle \tilde{\mathbf{h}}_k, \mathbf{w}_{kq,l} \rangle \right|^2}{1 + \rho \|\mathbf{h}_k\|^2 \sum_{j \neq k} \left| \langle (\cos \theta_{k,l} \mathbf{h}_{kq,l} + \sin \theta_{k,l} \mathbf{g}_{k,l}), \mathbf{w}_{jq,l} \rangle \right|^2} \right) \right] \\
 &\stackrel{(c)}{=} E \left[ \log_2 \left( \frac{1 + \rho \|\mathbf{h}_k\|^2 \left| \langle \tilde{\mathbf{h}}_k, \mathbf{w}_{kq,h} \rangle \right|^2}{1 + \rho \|\mathbf{h}_k\|^2 \sin^2 \theta_{k,h} \sum_{j \neq k} \left| \langle \mathbf{g}_{k,h}, \mathbf{w}_{jq,h} \rangle \right|^2} \right) \right] \\
 &\quad - E \left[ \log_2 \left( \frac{1 + \rho \|\mathbf{h}_k\|^2 \left| \langle \tilde{\mathbf{h}}_k, \mathbf{w}_{kq,l} \rangle \right|^2}{1 + \rho \|\mathbf{h}_k\|^2 \sin^2 \theta_{k,l} \sum_{j \neq k} \left| \langle \mathbf{g}_{k,l}, \mathbf{w}_{jq,l} \rangle \right|^2} \right) \right]
 \end{aligned} \tag{4.15}$$

where  $h$  in the subscript of  $\theta_{k,h}$ ,  $\mathbf{h}_{kq,h}$ ,  $\mathbf{g}_{k,h}$  denotes the parameters for high bits codebook used;  $l$  in the subscript of  $\theta_{k,l}$ ,  $\mathbf{h}_{kq,l}$ ,  $\mathbf{g}_{k,l}$  denotes the parameters for low bits codebook used. (c) in (4.15) follows because  $\mathbf{w}_{jq,h}$  obtained by using the quantized channel vectors  $\mathbf{h}_{kq,h}$ , in the case of high bits codebook utilized,  $\mathbf{w}_{jq,h}$  and  $\mathbf{h}_{kq,h}$  are orthogonal and the inner-product of the vectors should be zero if  $j \neq k$ . Same applies to the situation when low bits codebook is used so the inner-product of  $\mathbf{h}_{kq,l}$  and  $\mathbf{w}_{jq,l}$  is zero when  $j \neq k$ .

N. Jindal [N. Jindal, 2006] provides the analysis on MU-MIMO broadcast channels with finite-rate feedback. Although the analysis is made to the system with zero-forcing (ZF) beamforming, the result should be applicable to the system with block diagonalisation (BD) precoding. Especially in the case of MISO system, ZF beamforming is equivalent to BD precoding [Q. H. Spencer et al., 2004]. Therefore, some of the results in [N. Jindal, 2006] are referred for our performance analysis. Because vectors  $\tilde{\mathbf{h}}_k$  and  $\mathbf{w}_{kq,h}$  are independent and isotropically distributed in  $\mathbb{C}^{1 \times M}$  when the codebook is generated via RVQ,  $\left| \langle \tilde{\mathbf{h}}_k, \mathbf{w}_{kq,h} \rangle \right|^2$  in the nominator of the first

item of (4.15) can be replaced by  $\beta(1, M-1)$  which is a Beta-distributed random variable with parameters  $(1, M-1)$  [N. Jindal, 2006]. Also in the denominator of the first item of (4.15),  $\mathbf{g}_{k,h}$  and  $\mathbf{w}_{jq,h}$  for any  $j \neq k$  are unit i.i.d. isotropic vectors in the  $(M-1)$  null space of  $\mathbf{h}_{kq,h}$ . The quantity  $\langle \mathbf{g}_{k,h}, \mathbf{w}_{jq,h} \rangle^2$  is  $\beta(1, M-2)$  distributed and independent of  $\sin \theta_{k,h}$  [N. Jindal, 2006, Lemma 2].

Similarly, the second item in the above equation can be manipulated for the case of low bits codebook. Therefore, (4.15) becomes

$$\begin{aligned}
 \Delta R_k &= E \left[ \log_2 \left( \frac{1 + \rho \|\mathbf{h}_k\|^2 \beta(1, M-1)}{1 + \rho \|\mathbf{h}_k\|^2 \sin^2 \theta_{k,h} \sum_{j \neq k} \beta(1, M-2)} \right) \right] \\
 &\quad - E \left[ \log_2 \left( \frac{1 + \rho \|\mathbf{h}_k\|^2 \beta(1, M-1)}{1 + \rho \|\mathbf{h}_k\|^2 \sin^2 \theta_{k,l} \sum_{j \neq k} \beta(1, M-2)} \right) \right] \\
 &= E \left\{ \log_2 \left[ 1 + \rho \|\mathbf{h}_k\|^2 \beta(1, M-1) \right] - \log_2 \left[ 1 + \rho \|\mathbf{h}_k\|^2 \sin^2 \theta_{k,h} \sum_{j \neq k} \beta(1, M-2) \right] \right\} \\
 &\quad - E \left\{ \log_2 \left[ 1 + \rho \|\mathbf{h}_k\|^2 \beta(1, M-1) \right] - \log_2 \left[ 1 + \rho \|\mathbf{h}_k\|^2 \sin^2 \theta_{k,l} \sum_{j \neq k} \beta(1, M-2) \right] \right\} \\
 &= E \left\{ \log_2 \left[ 1 + \rho \|\mathbf{h}_k\|^2 \beta(1, M-1) \right] \right\} - E \left\{ \log_2 \left[ 1 + \rho \|\mathbf{h}_k\|^2 \sin^2 \theta_{k,h} \sum_{j \neq k} \beta(1, M-2) \right] \right\} \\
 &\quad - E \left\{ \log_2 \left[ 1 + \rho \|\mathbf{h}_k\|^2 \beta(1, M-1) \right] \right\} + E \left\{ \log_2 \left[ 1 + \rho \|\mathbf{h}_k\|^2 \sin^2 \theta_{k,l} \sum_{j \neq k} \beta(1, M-2) \right] \right\} \\
 &= -E \left\{ \log_2 \left[ 1 + \rho \|\mathbf{h}_k\|^2 \sin^2 \theta_{k,h} \sum_{j \neq k} \beta(1, M-2) \right] \right\} \\
 &\quad + E \left\{ \log_2 \left[ 1 + \rho \|\mathbf{h}_k\|^2 \sin^2 \theta_{k,l} \sum_{j \neq k} \beta(1, M-2) \right] \right\} \\
 &= -\Delta R_k 1 + \Delta R_k 2
 \end{aligned} \tag{4.16}$$

where

$$\Delta R_k 1 = E \left\{ \log_2 \left[ 1 + \rho \|\mathbf{h}_k\|^2 \sin^2 \theta_{k,h} \sum_{j \neq k} \beta(1, M-2) \right] \right\} \quad (4.17)$$

and

$$\Delta R_k 2 = E \left\{ \log_2 \left[ 1 + \rho \|\mathbf{h}_k\|^2 \sin^2 \theta_{k,l} \sum_{j \neq k} \beta(1, M-2) \right] \right\}. \quad (4.18)$$

(4.16) shows that the rate gain via the two-step scheduling algorithm is determined by the interference from other users due to the channel quantization process.

Applying Jensen's inequality to (4.17), it becomes

$$\begin{aligned} \Delta R_k 1 &\leq \log_2 \left\{ 1 + \rho E(\|\mathbf{h}_k\|^2) E(\sin^2 \theta_{k,h}) E \left[ \sum_{j \neq k} \beta(1, M-2) \right] \right\} \\ &\stackrel{(a)}{=} \log_2 \left\{ 1 + \rho M E(\sin^2 \theta_{k,h}) (M-1) E[\beta(1, M-2)] \right\} \\ &\stackrel{(b)}{=} \log_2 \left\{ 1 + \rho M E(\sin^2 \theta_{k,h}) (M-1) \frac{1}{M-1} \right\} \\ &\stackrel{(c)}{<} \log_2 \left\{ 1 + \rho M 2^{-\frac{B_h}{M-1}} \right\} \\ &= \log_2 \left\{ 1 + P 2^{-\frac{B_h}{M-1}} \right\} \end{aligned} \quad (4.19)$$

where (a) follows since  $E(\|\mathbf{h}_k\|^2) = M$  due to the independence of the channel norm, (b) follows since the expectation of  $\beta(1, M-2)$  random variable is  $\frac{1}{M-1}$  and (c) follows since the upper bound of expected quantization error  $E(\sin^2 \theta_{k,h})$  is  $2^{-\frac{B_h}{M-1}}$  [N. Jindal, 2006, Lemma 1].

Similarly, applying Jensen's inequality to (4.18), it becomes

$$\begin{aligned}
 \Delta R_k 2 &\leq \log_2 \left\{ 1 + \rho E(\|\mathbf{h}_k\|^2) E(\sin^2 \theta_{k,l}) E \left[ \sum_{j \neq k} \beta(1, M-2) \right] \right\} \\
 &\stackrel{(a)}{=} \log_2 \left\{ 1 + \rho M E(\sin^2 \theta_{k,l}) (M-1) E[\beta(1, M-2)] \right\} \\
 &\stackrel{(b)}{=} \log_2 \left\{ 1 + \rho M E(\sin^2 \theta_{k,l}) (M-1) \frac{1}{M-1} \right\} \quad (4.20) \\
 &\stackrel{(c)}{<} \log_2 \left\{ 1 + \rho M 2^{-\frac{B_l}{M-1}} \right\} \\
 &= \log_2 \left\{ 1 + P 2^{-\frac{B_l}{M-1}} \right\}
 \end{aligned}$$

where (a) follows since  $E(\|\mathbf{h}_k\|^2) = M$  due to the independence of the channel norm, (b) follows since the expectation of  $\beta(1, M-2)$  random variable is  $\frac{1}{M-1}$  and (c) follows since the upper bound of expected quantization error  $E(\sin^2 \theta_{k,l})$  is  $2^{-\frac{B_l}{M-1}}$  [N. Jindal, 2006, Lemma 1].

## 4.5 Numerical results

This section presents the simulation results by using the proposed scheduling algorithm. The simulation result in Figure 4.3 shows the sum-rate capacity versus signal-to-noise-ratio (SNR). The scenario setting is that the MISO downlink systems with four transmit antennas on base station and one antenna for each user terminal, i.e.  $4 \times 1$  antenna combination. Assume that the total number of users in the system is 4. In this case, the user selection is not needed and the simulation result can demonstrate that increasing feedback bits improve the system performance. The sum-rate capacity in the graph is the Ergodic capacity, each data point for a SNR value is the sum-rate value averaged over 500 channel realization per user. A codebook for each user is obtained via the codebook design methods of RVQ and DE-LBG. The upper bound of sum-rate capacity by using DPC scheme is also shown in the figure, which is the theoretical calculation result

from [M. Sharif and B. Hassibi, 2007]. The result demonstrates that the sum-rate capacity is improved under the high bits feedback although it is interference limited at high SNR. The curve obtained with 16 bits feedback is closest to the curve attained under the perfect channel condition. It is also shown, in the cases of 4 bits and 8 bits feedback, that there is no difference between the sum-rate capacities when the codebook is acquired either by RVQ or by DE-LBG. However, generating high bits codebook via DE-LBG is time consuming even if it is done off-line. Therefore RVQ is used for creating high bits codebooks.

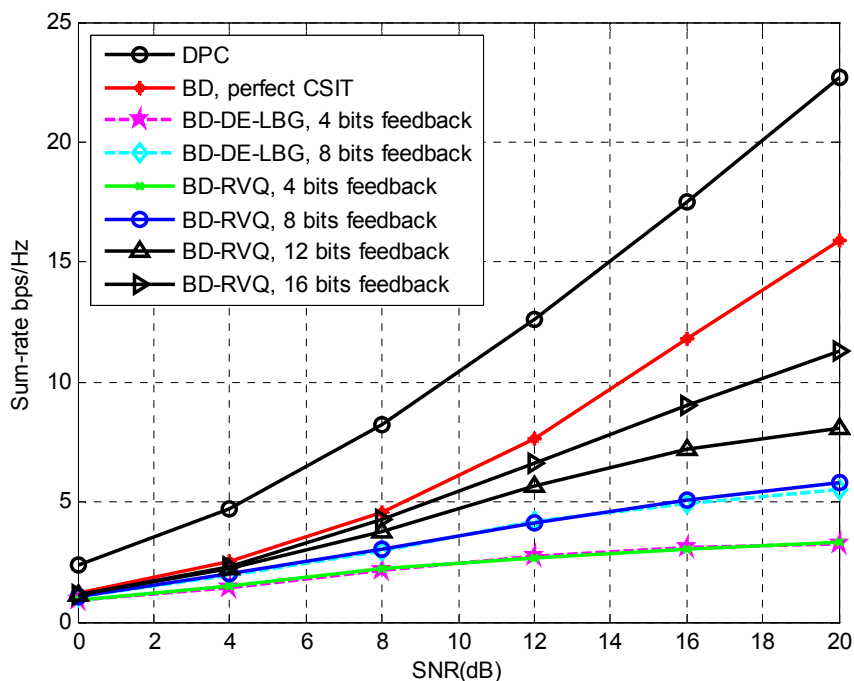


**Figure 4.3** The sum-rate capacity versus SNR. There is total number of 4 users in the system and the user selection algorithm is not needed. 4 transmit antenna and 1 receive antenna per user terminal. BD precoding is applied.

Figure 4.4 shows the sum-rate capacity against SNR when there is a large number of users in the MISO downlink system and the volume-based scheduling algorithm is used [L. Jin et al., 2009]. The antenna combination in the scenario is 4 transmit antennas and 1 receive antenna for each user terminal. The maximum supportable users are 4 and codebook generation

method is RVQ. The sum-rate capacity is Ergodic capacity, each data point for a SNR value is the sum-rate value averaged over 500 channel realization for each user. The upper bound of sum-rate capacity via DPC is also displayed in the figure, which is the theoretical calculation result from [M. Sharif and B. Hassibi, 2007]. The result demonstrates that the system performance is improved under the condition of high bits feedback. The sum-rate capacity achieved by using 8 bits feedback is higher than the capacity obtained via 4 bits feedback. Also in comparison with Figure 4.3, the system with a large number of users and the user selection algorithm being used shows better performance than the system with a small number of users and without user selection algorithm applied. For example, 4bps/Hz better off at SNR 20dB when 8 bits feedback is applied.

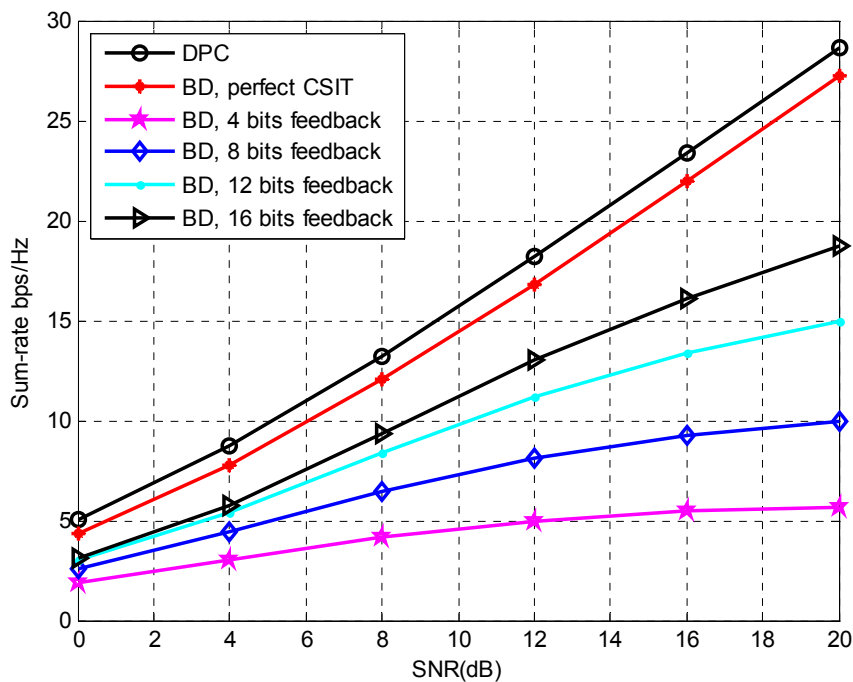


**Figure 4.4** Total number of 50 users is in the MISO downlink system. Antenna combination is 4 transmit antennas and 1 receive antenna per user terminal. The volume-based scheduling algorithm is applied. Maximum supportable users are 4.

Figure 4.5 presents the simulation result when the proposed two-step scheduling algorithm is utilized in the MISO downlinks system. It is assumed that total number of 50 users is in the system. The transmit/receive

antenna combination is  $4 \times 1$  for each user and the volume-based algorithm is applied for user selection. Maximum 4 users can be served simultaneously. The method of codebook generation is RVQ and BD precoding is applied.

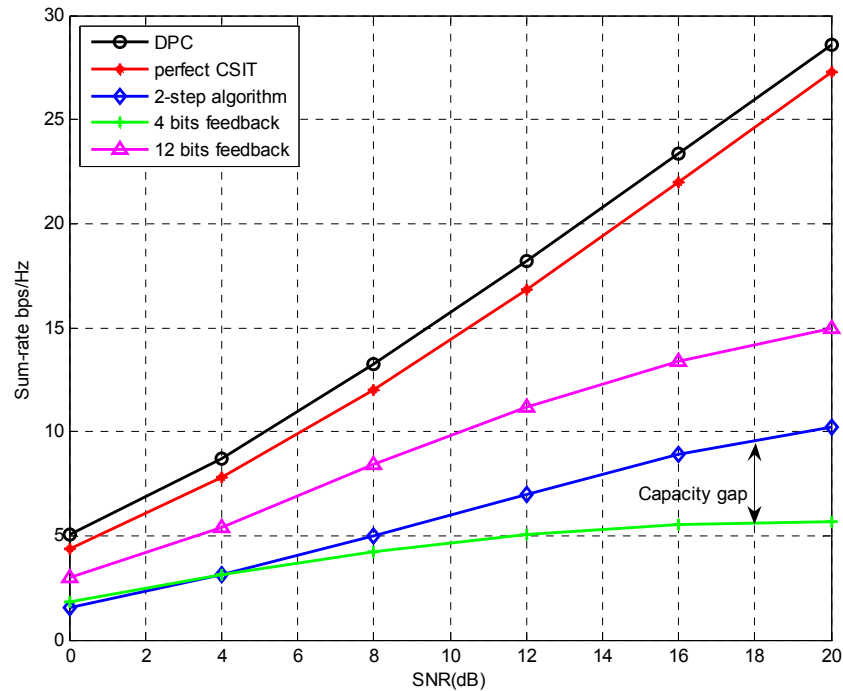
The two-step scheduling algorithm works like this: the maximum 4 users are selected first by using 4 bits feedback channel information, then a BD precoding vector is obtained for each user by using 12 bits feedback channel information and finally the signals for the selected users are transmitted. It is found that the sum-rate capacity acquired by the proposed algorithm is, in general, improved in comparison with the sum-rate capacity obtained only by 4 bits feedback. An improvement is observed when SNR is high from 4dB and beyond ( $SNR > 4dB$ ). The sum-rate gap increases as the SNR increases. This gap increment is as a result of the fact that the interference from the signals transmitted to other users due to non-perfect precoding and non-perfect channel condition is reduced by using additional high bits feedback. However, as shown in the graph, the sum-rate capacity of the algorithm can not achieve as high as that is realized by 12 bits feedback only for user selection and precoding vector obtaining. The benefit of the proposed algorithm is that the sum-rate capacity curve of 4 bits feedback for user selection and then 12 bits feedback for precoding design shows similar trend with the 12 bits feedback only algorithm. With the proposed algorithm, the sum-rate capacity can be raised in the range of high SNR.

Table 4.1 gives total feedback bits required for 4 bits feedback, 12 bits feedback and the proposed scheduling algorithm with 4 bits feedback followed by 12 bits feedback in the system having 50 users. Using 12 bits feedback needs total of 600 bits feedback which is higher than the 200 bits feedback needed by using 4 bits feedback. In the situation that the high bits feedback might not be practical if there are a large number of users in the system and there is feedback resource constraint, the proposed feedback

algorithm can be a potential solution for the problem. The proposed algorithm applies low bits feedback for user selection, then high bits feedback is used to get precoding vector for the selected users. Because the selected user number is much less than the total number of users, the additional step only adds a fraction of feedback load to the system, for example, 1/5 load as indicated in Table 4.1. The extra step in the algorithm can obtain more accurate channel information for the selected users; therefore, the sum-rate at high SNR end can be significantly increased.

Table 4.1 Summary of feedback load

<b>Feedback strategy</b>	<b>Total of feedback bits</b>
4 bits feedback	$4 \times 50 = 200$
12 bits feedback	$12 \times 50 = 600$
Proposed algorithm	$4 \times 50 + 4 \times 12 = 248$



**Figure 4.5** Sum-rate capacity versus SNR. Total number of 50 users is in the MISO downlink system. Antenna combination is 4 transmit antennas and 1 receive antenna per user terminal. The two-step scheduling algorithm is applied. Maximum supportable users are 4.

## 4.6 Summary

In this chapter, a new two-step scheduling algorithm is proposed for optimizing the sum-rate gain in a MU-MIMO downlink system with limited feedback and Block Diagonalisation (BD) precoding [L. Jin et al., 2010]. The two-step algorithm is that the user selection is accomplished via a low bits feedback, and then precoding design is completed by a high bits feedback. Based on the performance analysis and the simulation result in this chapter, the newly proposed algorithm can be a potential solution to a MU-MIMO downlink system with feedback resource constraint. A key finding is that an extra step with a high bits feedback in the proposed algorithm can increase the system capacity, especially when signal-to-noise ratio is at high value.

## **Chapter 5 Signal detection scheme based on free probability theory in MIMO cognitive radio systems**

In previous two chapters, we have investigated suboptimal scheduling strategy in MU-MIMO wireless system to improve the system performance with practical system in mind and the channel state information feedback strategy under the feedback bit constraint in the MU-MIMO system. In this chapter, we will explore the area of applying cognitive radio technology in the MU-MIMO network, which is a hot research topic in recent years to solve the increasing scarce spectrum problem with emergence of new wireless applications and services. The chapter is organised as follows. Section 5.1 introduces the background of cognitive radio, especially in the area of spectrum sensing methods. Section 5.2 presents a new proposed spectrum sensing method based on Free Probability Theory (FPT). The details of the Free Probability Theory, the description of FPT detection method, simulation results and the summary are given in the subsection of section 5.2. Section 5.3 provides the details of the cooperative spectrum sensing strategy in MU-MIMO system by utilising FPT detection method in each user terminal.

### **5.1 Introduction**

With the rapid development of wireless communication over the last decade, the demand for capacity and bandwidth has become increasingly high. As a result, the available resources such as bandwidth and capacity become limited. These resources need to be allocated and distributed effectively. Cognitive radio (CR) [I. Mitola, J. and J. Maguire, G. Q., 1999, J. Mitola, 2000, S. Haykin, 2005] and multiple-input multiple-output (MIMO) [A. Paulraj et al., 2003] have been regarded as two promising techniques to

solve the resource limitation issue. The utmost goals of the cognitive radio technology are to utilize the radio spectrum efficiently and to ensure reliable communications as the radio spectrum becomes a scarce resource. The capacity of a wireless system can be improved through multiplexing gain and diversity gain in a MIMO system. MIMO technology can also mitigate the fading effect characterized in the wireless system.

In cognitive radio communications, spectrum sensing must be performed [T. Yücek and H. Arslan, 2009]. Examples of spectrum sensing methods published in the literatures are energy detector based sensing [H. Urkowitz, 1967], waveform-based sensing [H. Tang, 2005] and matched-filtering [A. Sahai and D. Cabric, 2005]. Different sensing methods are suitable to different circumstances. For example, the waveform-based sensing performs better than energy detector because of the coherent processing that comes from using deterministic signal component if a priori information about the primary user's characteristics is available. Cooperative sensing is a strategy to solve the problem existed in the spectrum sensing due to noise uncertainty, fading, and shadowing. With cooperative sensing, it can also solve hidden primary user problem and it can decrease sensing time. Before introducing our new proposed Free Probability Theory (FPT) spectrum sensing method, we present a review of some of the common spectrum sensing methods in this section.

### **5.1.1 Energy detector based sensing**

Energy detector is the most common spectrum sensing method because of its low computational and implementation complexities [H. Urkowitz, 1967]. The way of energy detection is to compare the output of the energy detector with a threshold which can be set according to the system performance requirement and depends on the noise floor [H. Urkowitz, 1967]. The advantage of the energy detection is that the receivers do not need any

knowledge on the primary users' signal. The drawback of the energy detection is that interference from primary users and noise can not be distinguished. Therefore, it brings the uncertainty to select the threshold for detecting primary users if the noise characteristic is not known to the receiver. The poor performance under low signal-to-noise ratio (SNR) values is observed [H. Tang, 2005]. Energy detectors do not work efficiently for detecting spread spectrum signals either [D. Cabric et al., 2004, T. Yücek and H. Arslan, 2006] since the power of the primary user is distributed over a wide frequency range even though the actual information bandwidth is much narrower. Hence primary users who use spread spectrum signalling are difficult to detect.

Assume SISO case and discrete time system. Let  $x(t)$  represent the signal from the transmitter and  $h(t)$  be the channel response at time  $t$ , the received signal at time  $t$  can be expressed as

$$y(t) = h(t)x(t) + n(t), \quad (5.1)$$

where  $n(t)$  is additive white Gaussian noise (AWGN) with zero mean and variance  $\delta_n^2$ . Assume that the number of observation is  $N$ , then the decision metric for the energy detector is defined as

$$M = \sum_{t=1}^N |y(t)|^2. \quad (5.2)$$

Let  $H_0$  be the hypothesis when signal is absent, and  $H_1$  be the hypothesis when signal is present. The binary hypothesis testing based on the received signal is [C. W. Helstrom, 1968]:

$$H_0 : y(t) = n(t), \quad (5.3)$$

$$H_1 : y(t) = s(t) + n(t), \quad (5.4)$$

where  $s(t) = h(t)x(t)$  is the received signal excluding the noise component. The decision on the occupancy of a band is made on if the decision metric  $M$  is greater than the threshold  $\lambda$  that is chosen according to the performance requirement of the system.

The probability of detection  $P_d$  and the probability of false alarm  $P_f$  are two measures of the performance of the energy detection algorithm:  $P_d$  is the probability of detecting a signal on the considered spectrum when it is present and  $P_f$  is the probability that the test incorrectly decides that the considered spectrum is occupied when it actually is not.  $P_d$  and  $P_f$  can be expressed as

$$P_d = \text{prob}(M > \lambda | H_1), \quad (5.5)$$

$$P_f = \text{prob}(M > \lambda | H_0). \quad (5.6)$$

High probability of detection is desirable and at the same time the probability of false alarm should be low so the frequency band can be utilized efficiently. Because the characteristic of the signal and noise are not known to the receiver, choosing threshold  $\lambda$  can be a challenging task to balance high  $P_d$  and low  $P_f$ . In practice, the threshold is chosen to a predefined false alarm rate [M. J. Lehtomäki et al., 2005]. Hence, knowledge of noise variance is sufficient for selection of a threshold.

Consider that a simple case of the  $s(t)$  is a zero-mean Gaussian distributed variable with variance  $\delta_s^2$  and the noise is white Gaussian noise with zero mean and variance  $\delta_n^2$ . The summation of the  $N$  samples of the received signal in (5.2) follows chi-square distribution with  $2N$  degrees of freedom  $\chi_{2N}^2$ . Therefore, the decision metric in (5.2) can be expressed as

$$M = \begin{cases} \frac{\sigma_n^2}{2} \chi_{2N}^2 & H_0 \\ \frac{\sigma_s^2 + \sigma_n^2}{2} \chi_{2N}^2 & H_1 \end{cases} . \quad (5.7)$$

The expression of probability of detection and the probability of false alarm of the energy detector can be written as [F. Digham et al., 2003]

$$P_f = \frac{\Gamma(u, \frac{\lambda}{2})}{\Gamma(u)} , \quad (5.8)$$

$$P_d = Q_u(\sqrt{2\gamma}, \sqrt{\lambda}) , \quad (5.9)$$

where  $u = TW$  is time bandwidth product if  $T$  is the observation time interval in seconds and  $W$  is one-sided bandwidth in  $Hz$ ,  $\Gamma(a, b)$  represents the incomplete gamma function of variables  $a$  and  $b$  [E. Kreyszig, 1993],  $\gamma$  is signal-to-noise ratio ( $SNR$ ), and  $Q_u(c, d)$  is the generalized Marcum  $Q$ -function of variable  $c$  and  $d$  [J. G. Proakis, 2001]. From (5.8) and (5.9), the pair values of  $P_d$  and  $P_f$  is a function of the threshold value  $\lambda$ . Each pair of values of performance measures  $P_d$  and  $P_f$  corresponds to a chosen threshold value  $\lambda$  if the received signal-to-noise-ratio is fixed. Receiver operating characteristic (ROC) curves can be applied to demonstrate the relationship between the probability of detection and the false alarm rate, which are the sets of curves of  $P_d$  versus  $P_f$  under different  $SNR$  values [P. Varshney, 1996]. It is in general that better performance can be achieved under high  $SNR$  at a fixed threshold value.

### 5.1.2 Waveform based sensing

Waveform based sensing can be applied if the transmitted signal is known to the receiver. We assume that total number of received signal sample is  $N$ ,

transmitted signal is  $x(t)$ , the channel response  $h(t)$  at time  $t$  and  $n(t)$  is the white Gaussian noise, the received signal  $y(t)$  can be expressed as

$$y(t) = h(t)x(t) + n(t). \quad (5.10)$$

The decision metric is defined as

$$M = \text{Re} \left[ \sum_{t=1}^N y(t)x^*(t) \right], \quad (5.11)$$

where  $x^*(t)$  denotes conjugate of  $x(t)$ . If there is no signal coming from the transmitter, the decision metric becomes,

$$M = \text{Re} \left[ \sum_{t=1}^N n(t)x^*(t) \right]. \quad (5.12)$$

Similar to the energy detector, the decision on the presence of a primary user signal is based on if  $M$  is greater than a fixed threshold  $\lambda$ . The probability of detection  $P_d$  and the probability of false alarm  $P_f$  can also be expressed by (5.5) and (5.6). The waveform based sensing performs better than the energy detector based sensing in terms of reliability and convergence time [H. Tang, 2005]. However, the drawback of the waveform based sensing is that the receiver must have the knowledge of the signal from the transmitter.

### 5.1.3 Matched-filtering

Assume SISO case and discrete time system. Consider a signal  $x$  in the presence of additive Gaussian noise  $n$  have zero mean and variance  $\delta_n^2$ . The signal  $y$  at time  $t$  is the summation of  $x$  and  $n$ :

$$y(t) = x(t) + n(t). \quad (5.13)$$

When the signal is filtered with a filter having response  $h_{MF}$ , the output  $z$  of the filter at time  $t$  is the convolution of  $h_{MF}$  and  $y(t)$ , that is,

$$z(t) = h_{MF} * y(t), \quad (5.14)$$

where  $*$  denotes convolution here. If  $z_x(t_0)$  denotes the signal component and  $z_n(t_0)$  is the noise component at time instance  $t_0$  at the output of the filter, the matched filter is to maximize the output signal-to-noise ratio (*SNR*) [N. Benvenuto and G. Cherubini, 2002]

$$h_{MF} : \max_{h_{MF}} = \frac{|z_x(t_0)|^2}{E[|z_n(t_0)|^2]}. \quad (5.15)$$

Assume that the signal  $x(t)$  is known to the receiver and hypothesis testing problem based on  $N$  signal samples, the test statistics for matched filter detector is [Y. Zeng et al., 2010]

$$M = \sum_{t=0}^{N-1} x(t)y(t). \quad (5.16)$$

In next section, we will present a new spectrum sensing method based on free probability theory (FPT) [Ø. Ryan and M. Debbah, 2007] for the MIMO cognitive radio system.

## **5.2 A new signal detection scheme based on free probability theory for multiple-input multiple-output cognitive radio systems**

It is known that a digital communications system can be modelled with random matrices, where the received signal is the summation of the

transmitted signal and the noise. In this case, FPT can be utilized to describe the asymptotic behaviour of the system. More details of the FPT will be provided in Section 5.2.1. We propose a new signal detection algorithm for spectrum sensing using FPT for MIMO cognitive radio systems [L. Jin et al., 2010]. The idea of FPT detection is to estimate the covariance matrices of a large number of observations of the received signals in order to obtain the covariance matrices of the transmitted signals through asymptotic behaviour of random matrices. The performance comparison between the FPT detection and the energy detection will be given because two methods are suitable for the circumstance of the receiver without knowing any information of the signal from the transmitter.

Next four subsections are organized as follows. Section 5.2.1 presents the system model and basics of the free probability theory. Section 5.2.2 describes the new proposed signal detection algorithm based on FPT. Section 5.2.3 provides the simulation results and the summary is given in section 5.2.4. In this thesis, upper boldface is used for matrices and low boldface is used for vectors.  $(\cdot)^*$  denotes conjugate operator,  $(\cdot)^H$  denotes Hermitian transpose,  $\mathbf{I}$  is used for identity matrix and  $E(\cdot)$  denotes expectation operator.

## **5.2.1 MIMO cognitive radio system model and free probability theory**

### **5.2.1.1 MIMO cognitive radio system model**

Figure 5.1 shows a typical cognitive radio system consisting of a primary network and a neighbouring secondary network. Consider that there exist one primary base station and several primary users (PU) in the primary network; one secondary base station serves numbers of secondary users (SU) in the secondary network. Assume that a secondary user attempts to detect if there is a primary user in his vicinity using a frequency band and the SU

without any knowledge of the signals transmitted from the PU. In this case, the PU is regarded as the transmitter and the SU is regarded as the receiver. Suppose that the transmitter is equipped with  $m$  antennas and the receiver is equipped with  $l$  antennas. The channel matrix between the transmitter and the receiver is denoted as  $\mathbf{H}_{l \times m}$  with row size  $l$  (number of receive antennas) and column size  $m$  (number of transmit antennas). In order to know whether a frequency band is used by the PU, the SU needs to detect the signal from the PU so the decision can be made to use the frequency band when it is vacant. Assume that the signal from the PU is a column vector  $\mathbf{x}$  with row size  $m$ . Then the signal  $\mathbf{y}$  received by the SU is

$$\mathbf{y} = \mathbf{H}\mathbf{x} + \mathbf{n}, \quad (5.17)$$

where vector  $\mathbf{n}$  with row size  $m$  is the additive white Gaussian noise (AWGN) vector with zero mean and covariance matrix  $\sigma^2 \mathbf{I}_l$ . Rayleigh fading channel is assumed, therefore each entry in  $\mathbf{H}_{l \times m}$  following an independent and identically distributed (i.i.d.) complex Gaussian distribution.

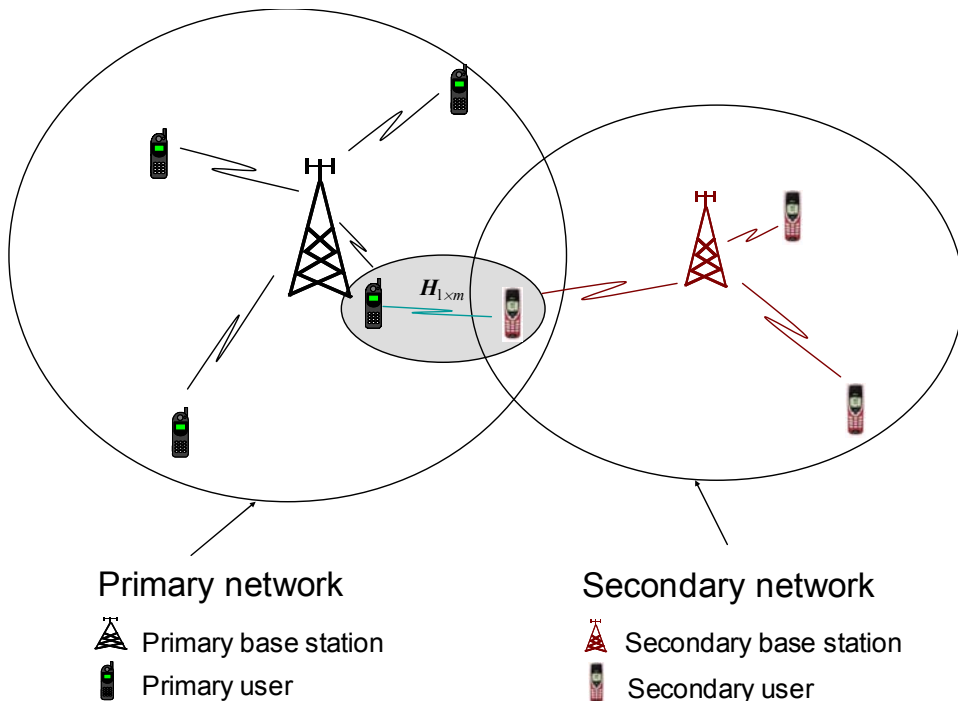


Figure 5.1 Cognitive radio system

### 5.2.1.2 Free probability theory

The FPT is related to the random matrices and what we are interested in this work is the limiting eigenvalue distribution of square random matrices [A. Nica and R. Speicher, 2006]. Random matrices are useful tool for modelling a digital communications system [Ø. Ryan and M. Debbah, 2007]. A typical random matrix model can be used to describe the information-plus-noise model presented in (5.17). Let  $M$  denote the number of samples of the received signals,  $\mathbf{A}$  be the concatenated matrix of  $\mathbf{H}\mathbf{x}$  from  $M$  observations and  $\mathbf{N}$  represents the concatenated noise samples from  $M$  observations, the sample covariance matrix  $\mathbf{W}_l$  is defined as follows:

$$\mathbf{W}_l = \frac{1}{M}(\mathbf{A} + \mathbf{N})(\mathbf{A} + \mathbf{N})^H. \quad (5.18)$$

In the area of classical signal processing, a large number of observations are normally required, that is, the number of samples is much greater than the dimension of matrix  $\mathbf{W}_l$  (i.e.  $M \gg l$ ), therefore (5.18) can be expressed approximately as

$$\mathbf{W}_l = \mathbf{B}_l + \sigma^2 \mathbf{I}_l, \quad (5.19)$$

where  $\mathbf{B}_l$  is the covariance matrix of the received signals excluding the noise component, i.e.,  $\mathbf{B}_l = \frac{1}{M} \mathbf{A} \mathbf{A}^H$ . Hence, the information of  $\mathbf{B}_l$  can be used to extract the transmitted signals. The concept of *free convolution* was developed in [Ø. Ryan and M. Debbah, 2007, Ø. Ryan and M. Debbah, (online), 2007] to provide a method to evaluate  $\mathbf{B}_l$  when  $\mathbf{W}_l$  is known and vice versa. The implementation of the *free convolution* is solely based on the moments of random matrix.

The definition of free probability is analogous to the concept of independence in classical probability [A. Nica and R. Speicher, 2006]. The definition of freeness is as follows: a) The free probability developed as a probability theory can be applied for non-commutative random variables like matrices, b) These random variables are the elements in a *non-commutative probability space* that can be defined by a pair  $(\mathcal{A}, \varphi)$ , where  $\mathcal{A}$  is a unital *\*-algebra* with unit  $\mathbf{I}$ , and  $\varphi$  is a normalized linear functional on  $\mathcal{A}$ . The elements of  $\mathcal{A}$  are called random variables and  $\mathcal{A}$  is composed of  $l \times l$  matrices or random matrices, and c) If  $a$  is denoted a random variable in  $\mathcal{A}$ , then  $\varphi$  is the normalized trace  $tr_l$  for matrices, which is defined as

$$tr_l(a) = \frac{1}{l} \text{trace}(a), \quad (5.20)$$

or  $\tau_l(a)$  for random matrices, which is defined as

$$\tau_l(a) = E(tr_l(a)). \quad (5.21)$$

In the *non-commutative probability space*, the moments approach is to obtain the moments of a random variable which uniquely identifies a probability measure. One important probability measure  $\mu_c$  is Marčhenko-Pastur law [A. M. Tulino and S. Verdo, 2004] which has the density function

$$f^{\mu_c}(x) = (1 - \frac{1}{c})^+ \delta_0(x) + \frac{1}{2\pi cx} \sqrt{(x - (1 - \sqrt{c})^2)^+ ((1 + \sqrt{c})^2 - x)^+}, \quad (5.22)$$

where  $(d)^+ = \max(0, d)$  and  $\delta_0(x)$  is Dirac measure at 0 and  $\mu_c$  depends on the parameter  $c$ . Figure 5.2 shows the density distribution from Marčhenko-Pastur law when  $c=1, 0.3, 0.1$ . One important application of Marčhenko-Pastur law is when it is used to the matrix random variables and the matrices are *Wishart matrices* that have the form  $\frac{1}{q} \mathbf{D}\mathbf{D}^H$  from a random matrix  $\mathbf{D}_{p \times q}$

with each entry following independent standard complex Gaussian distribution, and  $\frac{p}{q} \rightarrow c$ . It is found that the discrepancy between the moments obtained from Marčenko-Pastur law and the empirical eigenvalue distribution of *Wishart matrices* characterized in (5.19) tends to zero when  $q \rightarrow \infty$ . Therefore, Marčenko-Pastur law can be used to depict asymptotic distributions of *Wishart matrices*.

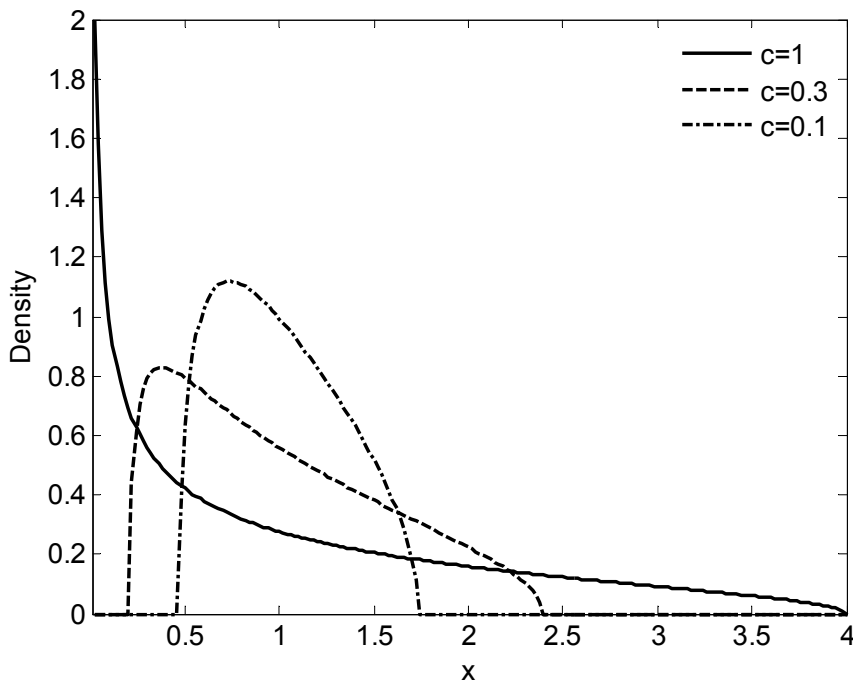


**Figure 5.2** Density function of Marčenko-Pastur law.

Suppose that two random variables  $\mathbf{a}_1$  and  $\mathbf{a}_2$  are matrices in the *non-commutative probability space* and they are free, the probability measures of the distributions of  $\mathbf{a}_1 + \mathbf{a}_2$  and  $\mathbf{a}_1 \mathbf{a}_2$  will depend only on the probability measures associated with  $\mathbf{a}_1$  and  $\mathbf{a}_2$ . Two defined operations of *additive free convolution* and *multiplicative free convolution* are useful, the former is the operation for the sum of free random variables and the later is the operation for the product of the random variables [A. M. Tulino and S. Verdo, 2004].

*Definition 1:* Assume that  $\mathbf{a}_1$  has an eigenvalue distribution which converges to  $\gamma_1$  and  $\mathbf{a}_2$  has an eigenvalue distribution which converges to  $\gamma_2$ , the eigenvalue distribution of  $\mathbf{a}_1 + \mathbf{a}_2$  converges to  $\gamma$  that depends only on  $\gamma_1$  and  $\gamma_2$ . Then the measure  $\gamma$  is said *additive free convolution* of  $\gamma_1$  and  $\gamma_2$  and it is denoted by  $\gamma_1 \boxplus \gamma_2$ .

*Definition 2:* Assume that  $\mathbf{a}_1$  has an eigenvalue distribution which converges to  $\gamma_1$  and  $\mathbf{a}_2$  has an eigenvalue distribution which converges to  $\gamma_2$ , the eigenvalue distribution of  $\mathbf{a}_1 \mathbf{a}_2$  converges to  $\gamma$  (the eigenvalue distribution of  $\mathbf{a}_1^{\frac{1}{2}} \mathbf{a}_2 \mathbf{a}_1^{\frac{1}{2}}$ ) that depends only on  $\gamma_1$  and  $\gamma_2$ . Then the measure  $\gamma$  is termed as *multiplicative free convolution* of  $\gamma_1$  and  $\gamma_2$ , which is denoted by  $\gamma_1 \boxtimes \gamma_2$ .

Associated with the definition 2, *multiplicative free deconvolution* is defined to deal with the situation where if a unique probability measure  $\gamma = \gamma_1 \boxtimes \gamma_2$  is given for the product of two random variables and the probability measure of one of the variables is known, such as  $\gamma_1$ , then the probability measure of the other random variable  $\gamma_2$  can be acquired by the *multiplicative free deconvolution*, which is denoted by  $\gamma_2 = \gamma \boxtimes \gamma_1$ . Similarly related to definition 1, *additive free deconvolution* is defined to get  $\gamma_2$  if a unique probability measure  $\gamma = \gamma_1 \boxplus \gamma_2$  is given for the sum of two random variables and the probability measure of one of the variables  $\gamma_1$  is known. The operation is designated by  $\gamma \boxminus \gamma_1$ .

The concepts of free convolution and free deconvolution are useful since they can be applied to the signal processing of communications systems characterized by (5.17), (5.18) and (5.19). The relation between the covariance of the received signal and the covariance of the input including

real transmitted signal and channel information can be expressed by following equation:

$$\alpha_w \boxtimes \mu_c = (\beta_B \boxtimes \mu_c) \boxplus \delta_{\sigma^2}, \quad (5.23)$$

where  $\beta_B$  is a probability measure that the empirical eigenvalue distribution of  $\mathbf{B}_l = \frac{1}{M} \mathbf{A} \mathbf{A}^H$  converges to,  $\alpha_w$  is a probability measure that the empirical eigenvalue distribution of  $\mathbf{W}_l$  converges to and  $\delta_{\sigma^2}$  is Dirac measure at  $\sigma^2$ . Correspondingly if the covariance of the received signal is known, the covariance of the input  $\beta_B$  can be discovered by the equation:

$$\beta_B = ((\alpha_w \boxtimes \mu_c) \boxminus \delta_{\sigma^2}) \boxtimes \mu_c. \quad (5.24)$$

We will present a new spectrum sensing algorithm for MIMO cognitive radio system by using FPT. The details are given in next section.

## 5.2.2 Free probability theory signal detection algorithm for MIMO cognitive radio systems

We propose to use FPT method to detect signals for a MIMO cognitive radio system [L. Jin et al., 2010]. Assume that the system model can be described by (5.17); in addition, the secondary user lacks any knowledge of the signal character coming from the primary user.

The new signal detection algorithm based on FPT is given below:

1. For the system represented by (5.17), take  $M$  samples of the received signal and  $M \gg l$ .

2. Concatenate the  $M$  samples horizontally and obtain the sample covariance matrix  $\mathbf{W}_l$  which is expressed in (5.18).
3. Calculate the first  $k$  moments of the sample covariance matrix  $\mathbf{W}_l$ , i.e.,  $tr_l(\mathbf{W}_l)^i$  for  $1 \leq i \leq k$ .
4. By applying FPT and using (5.24), obtain corresponding  $k$  moments of  $\mathbf{B}_l$  indicated in (5.19).  $\mathbf{B}_l$  is the covariance matrix of the received signals excluding noise component and it is the approximation of the real covariance of  $(\mathbf{H}\mathbf{x})(\mathbf{H}\mathbf{x})^H = \mathbf{H}\mathbf{x}\mathbf{x}^H \mathbf{H}^H$ .
5. Assume that the antennas are independent to each other in the MIMO cognitive radio system. Rayleigh fading channel is assumed therefore each entry in  $\mathbf{H}_{l \times m}$  following an independent and identically distributed (i.i.d.) complex Gaussian distribution with real and imaginary parts being Gaussian distributed with zero mean and unit variance. From  $\mathbf{B}_l$  and the covariance matrix of channel matrix  $\mathbf{H}$ , it is not difficult to find that the transmit signal power can be retrieved, i.e.

$$\mathbf{P} = \mathbf{x}\mathbf{x}^H = \begin{bmatrix} P_1 & 0 & 0 & 0 \\ 0 & P_2 & 0 & 0 \\ 0 & 0 & \ddots & 0 \\ 0 & 0 & 0 & P_m \end{bmatrix}, \quad (5.25)$$

where  $P_i = x_i x_i^*$  for  $1 \leq i \leq m$  is the allocated signal power on  $i^{\text{th}}$  transmit antenna. However, it is usually the case that the channel information is not known to the SU and, therefore it is not easy to obtain the matrix  $\mathbf{H}\mathbf{H}^H$ . Instead, we will use the estimated covariance matrix  $\sigma_{\mathbf{H}\mathbf{H}^H}^2 \mathbf{I}$ , where  $\sigma_{\mathbf{H}\mathbf{H}^H}^2$  is the variance of the distribution of the entry elements for the matrix  $\mathbf{H}\mathbf{H}^H$ . In theory, if the retrieved power  $\mathbf{P} > \mathbf{0}$ , we can say that the signal is detected and therefore the secondary user can use the frequency band. In practice, we need to set a threshold  $V_r$  and compare  $\mathbf{P}$  with it for following two factors: a) extracted power  $\mathbf{P}$  might not be zero even if the signal is not transmitted due to the estimation error of

the FPT detection method; b) how confident we can be to make our decision based on very small  $\mathbf{P}$  if real signal is transmitted. Hence, It is considered that noise covariance matrix  $\sigma^2\mathbf{I}$  is a reasonable reference value for choosing  $V_T$ .

6. Set the threshold  $V_T$  which should be comparable to the noise covariance matrix  $\sigma^2\mathbf{I}$ . Recall also that signal detection is a test of following two hypotheses [C. W. Helstrom, 1968]:

$$\begin{aligned} H_0 : \mathbf{y}(t) &= \mathbf{n}(t), \\ H_1 : \mathbf{y}(t) &= \mathbf{s}(t) + \mathbf{n}(t), \end{aligned} \tag{5.26}$$

where  $H_0$  is the hypothesis that the received signal  $\mathbf{y}$  at time  $t$  is only contributed by the noise  $\mathbf{n}(t)$ ,  $H_1$  is the hypothesis that the received signal  $\mathbf{y}$  at time  $t$  is contributed by the noise  $\mathbf{n}(t)$  and signal  $\mathbf{s}(t)$  coming from the transmitter through the transmission channel.

7. Finally, the probability of false alarm  $P_f$  for a given threshold  $V_T = \alpha\sigma^2\mathbf{I}$ , where  $\alpha$  is a constant, is given by

$$P_f = \text{prob}(P_i > \alpha\sigma^2 | H_0) \text{ for } 1 \leq i \leq m. \tag{5.27}$$

The probability of detection  $P_d$  is given by

$$P_d = \text{prob}(P_i > \alpha\sigma^2 | H_1) \text{ for } 1 \leq i \leq m. \tag{5.28}$$

Both probability of false alarm  $P_f$  and probability of detection  $P_d$  can measure the performance of the detection algorithm. It is desirable that  $P_d$  has a high value when the signal is truly present on the considered frequency band. On the other hand, the detection algorithm works well if the probability of false alarm  $P_f$  has low value, which means that unoccupied frequency band can be utilized more efficiently. Therefore, the decision

threshold  $V_r$  should be chosen to ensure an optimum balance between  $P_f$  and  $P_d$ . In practice,  $V_r$  is usually selected against the predefined probability of false alarm and  $P_f$  is determined by the noise covariance.

Although the Free Probability Theory (FPT) presented in section 5.2.1.2 seems complex, the detection method based on FPT is actually matrix operation on received signals. The complexity of the FPT detection method depends on how many number of samples that are used.

### 5.2.3 Simulation results

This section presents the simulation results of the spectrum sensing by applying the proposed FPT detection algorithm. The performance comparison of signal detection will be made between the FPT detector and the energy detector [H. Urkowitz, 1967] because these detection methods are suitable for the circumstance of the receiver (the secondary user) without any knowledge of the signal coming from the transmitter (the primary user). The energy detector (ED) based approach is a conventional technique for spectrum sensing, which has the advantage of low computational and implementation complexity. The simplicity of the ED technique is that the decision rule is based on comparing the output of the ED with a threshold depended on the noise floor. However, it does not distinguish real signal from the noise background and it exhibits poor performance when the signal-to-noise-ratio (SNR) is low.

Consider a simulation scenario that in a cognitive radio system, one primary user has four transmit antennas and one secondary user has three receive antennas; each entry of the MIMO channel matrix are following an independent and identically distributed (i.i.d.) complex Gaussian distribution  $\mathcal{CN}(0,1)$ ; the noise component is the additive white Gaussian noise (AWGN) with zero mean and unit variance; equal power allocation on

each transmit antenna is assumed and the receiver without any knowledge of signal transmitted by primary user is presumed. The number of samples taken for the detection scheme is 100 which are considered large enough for the proposed FPT detection algorithm.

Figure 5.3 demonstrates the result that the probability of detection varies with the SNR via the FPT detection algorithm under a set of threshold values. It shows that the performance of the FPT detector is good when SNR is greater than -5dB. Furthermore, the probability of detection increases as the  $P_f$  increases (or  $V_T$  decreases). However, high  $P_f$  is not desirable because the vacant frequency band can not be correctly detected under this condition. On the other hand,  $P_f$  is low when the threshold value is set high, but the low probability of detection under high threshold is also not desirable. Therefore, to detect the signal presence of primary user, the threshold  $V_T$  must be chosen to balance between the predictions of the probability of false alarm and the probability of detection.

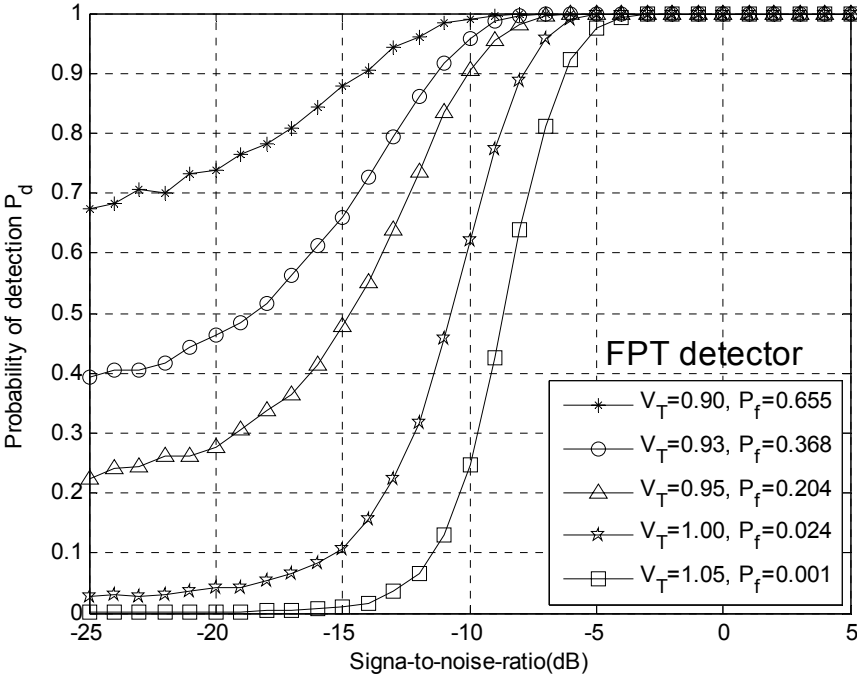
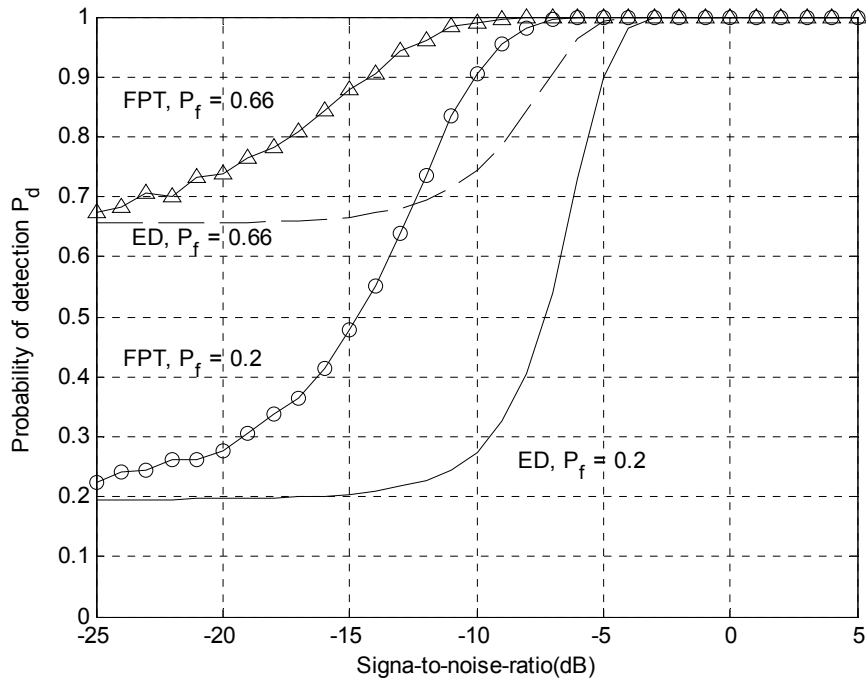


Figure 5.3 The probability of detection versus SNR(dB) via FPT detection algorithm for MIMO cognitive radio system. Thresholds values  $V_T$  are set to 0.90, 0.93, 0.95, 1.0 and 1.05. Corresponding  $P_f$  values to  $V_T$  are 0.655, 0.368, 0.204, 0.024, and 0.001.



**Figure 5.4 Performance comparison between FPT detector and energy detector when probabilities of false alarm are 0.2 and 0.66.**

Figure 5.4 shows the performance comparison of the spectrum sensing between FPT detector and energy detector when the probabilities of false alarm are set to 0.2 and 0.66. The figure illustrates that the FPT detection scheme works better than the energy detection scheme. The detection probability of the FPT detector is higher than that of the energy detector when  $P_f = 0.66$  and the signal-to-noise-ratio is in the range from -25dB to -5dB. Similarly, the FPT detector shows better performance when the probability of false alarm  $P_f$  is set to 0.2 and the signal-to-noise-ratio is in the range from -25dB to -3dB. From the simulation results, we can see that FPT scheme can predict the occupancy of the frequency band more accurately than the ED scheme. Better performance of the FPT method implies that the decision rule of the algorithm can be made more precisely by exploring the free probability property of the random matrices and segregating the real signal from the background noise.

#### **5.2.4 Summary**

The main contribution of section 5.2 is that a new FPT detection scheme for spectrum sensing is proposed for MIMO cognitive radio system. By utilizing the asymptotic behaviour of random matrix based on the free probability theory, the covariance matrix of true signals can be estimated through a large number of observations of the received signals. The real signal power is then extracted. The simulation results demonstrate that the FPT detection algorithm achieves better performance in comparison with the traditional energy detection algorithm. Although the signal power is utilized for the decision rules of FPT detector and energy detector, it is evident that the FPT detection algorithm benefits from the decision rule based on the estimation of real signal power instead of the received signal power (real signal plus noise).

### ***5.3 Cooperative FPT spectrum sensing technique in MIMO cognitive radio system***

#### **5.3.1 Introduction**

As we know that spectrum sensing is the key technology in cognitive radio system from previous section. Our previous work on a spectrum sensing method based on free probability theory (FPT) [Ø. Ryan and M. Debbah, 2007] for the MIMO cognitive radio system is shown in [L.Jin et al., 2010], which demonstrates that the FPT detector outperforms the traditional energy detector [H. Urkowitz, 1967]. The idea of FPT detection is to estimate the covariance matrices of a large number of observations of the received signals in order to obtain the covariance matrices of the transmitted signals through asymptotic behaviour of random matrices because a digital

communications system can be modelled with random matrices, where the received signal is the summation of the transmitted signal and the noise.

In a cognitive radio network, a reliable spectrum sensing can be achieved through cooperation among secondary users [T. Yücek and H. Arslan, 2009]. One of the advantages of cooperative sensing is that different users take their own measurements and therefore the system performance can be improved at low SNR due to the diversity of the measurements. In addition, the hidden-terminal problem can be greatly reduced because the cooperative users are scattered in a wide area of the network and thus the possibility of all users shadowed away from the primary user is relatively small.

Many cooperative spectrum sensing schemes are presented in current research papers. In [J. Unnikrishnan, 2008], it is assumed that the cooperating users use identical energy detectors, the received signals are considered as correlated log-normal random variables and decision fusion strategy is adopted at the fusion centre. The results demonstrate that a proposed linear-quadratic (LQ) fusion strategy, which takes into account the correlation between the nodes, outperforms the Counting Rule (or Voting Rule) [V. Aalo and R. Viswanathan, 1992], which is the fusion rule that is obtained by ignoring the correlation. Counting Rule just counts the number of sensor nodes that vote in favour of  $H_1$  in the case of the hypothesis test ( $H_1$  when signal existing and  $H_0$  with noise only) and compares it with a threshold.

In [part1 and part 2, G. Ganesan, 2007], the evidence shows that the cooperation among multiple cognitive users in the same band can reduce the detection time and thus increase the overall system agility. Two cognitive users' case demonstrates that the agility of the cognitive network can be increased as much as 35% by using the amplify-and-forward (AF) cooperation scheme. For multiple cognitive user networks, a user pairing

cooperation scheme (one weaker user is in a users' set with low received signal power and the other strong user is in users' set with a high received signal power) can achieve a certain degree of the reduction of the detection time, which depends on the relative location of the pairing users. The user pairing cooperation scheme can also improve the probability of detection of the weak user.

A linear cooperation framework for spectrum sensing of CR network is proposed in [Z. Quan et al., 2008]. The idea of the scheme is that the global decision is based on simple energy detection over a linear combination of the local statistics from individual nodes. The sensing problem is treated as a nonlinear optimization problem. A cluster-based method in [C. Sun et al., 2007] is proposed for cooperative spectrum sensing over imperfect reporting channels between the cognitive users and the fusion centre in cognitive radio systems. Two fusion schemes of decision fusion and energy fusion are adopted for the cluster-based cooperative spectrum sensing. Both performance analysis and simulation results show that the sensing performance of the cluster-based method is improved in comparison with conventional spectrum sensing. The error rate can be reduced via the user selection diversity in each cluster under the condition of the fading report channels.

In [J. Ma and Y. Li, 2007], the cooperative spectrum sensing based on energy detection in cognitive radio networks is considered. The idea of soft combination in the paper is that accurate energy values observed by different CR users are combined to make a better decision. Two schemes of the soft combination are maximal ratio combination (MRC) and equal gain combination (EGC). MRC is theoretically proved to be nearly optimal in low signal-to-noise ratio (SNR) region. In comparison with conventional hard combination that CR users exchange only one bit of information regarding whether their observed energy value is above a certain threshold, both MRC and EGC schemes show the performance improvement. Also a proposed softened hard combination scheme with two-bit overhead for each

cognitive user can accomplish a good trade off between detection performance and complexity. An advantage of the cooperation among independent cognitive radio users is that the SNR wall due to the noise power uncertainty can be reduced.

In general, there are two categories of cooperative sensing: centralized sensing and distributed sensing.

**Centralized sensing** – In centralized sensing, a fusion centre receives the sensing data from secondary users and makes final detection decision. Regarding to how to make the final detection decision in a fusion centre, there are two kinds of cooperative spectrum sensing strategies, namely (1) data fusion and (2) decision fusion. The data fusion strategy is that the final decision in the fusion centre is based on the raw data sent by each secondary user. The decision fusion is that the final decision in the fusion centre is made on the decisions sent by each secondary user who process his data individually. More details on this topic can be found in the review paper by Zeng [Y. Zeng, 2010] and the references within.

**Distributed sensing** – In distributed sensing, a central control unit does not exist. Each secondary user accomplishes his spectrum sensing based on his own measurement; however information is shared among secondary users. This sensing strategy appears less complex and cost effective in comparison with the centralized strategy. The system performance also depends on the approach of information sharing and utilization.

In this section, we will discuss cooperative sensing in MIMO cognitive radio system by using FPT detection algorithm.

### 5.3.2 System model

The complexity of a cognitive radio system varies considerably depending on number of primary users and secondary users in the system as well as the geographical area concerned. The simplest form of the cognitive radio system is that only one primary user and a few secondary users are in the area that we are interested in.

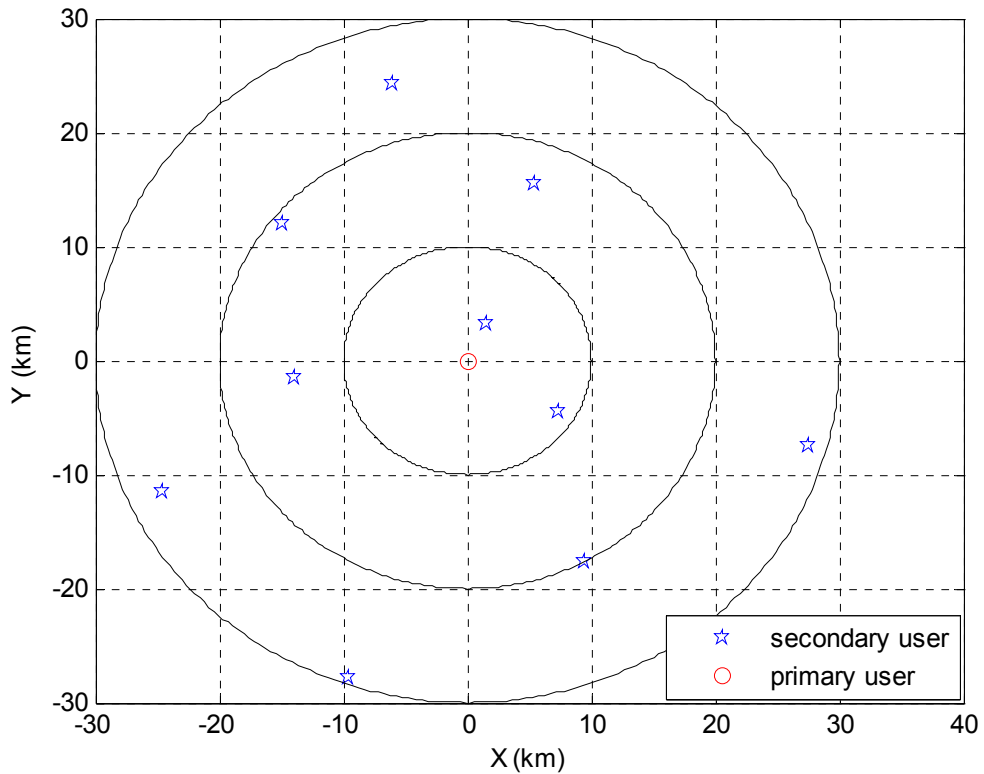


**Figure 5.5 Cognitive radio system.**

Figure 5.5 shows two dimensional geographical distributions of a primary user and secondary users in a cognitive radio system. The figure demonstrates that one primary user is located at the centre of an area with a radius of 30km and  $K$  numbers of secondary users are randomly dotted in the area. Assume that the transmit power from the primary user is  $P$  and the received power for the secondary user  $i$  is  $P_{r,i}$  for  $1 \leq i \leq K$ . If the distance between the PU and  $i^{th}$  SU is  $d_i$ , the path loss is considered and it is represented by the path loss exponent factor  $\beta$ , the received power  $P_{r,i}$  for  $i^{th}$  secondary user is proportional to  $\propto 1/d_i^\beta$ . Depending on the environment in

which the PU and the SU are situated, the value of  $\beta$  is in the range of 2~6 [T. S. Rappaport, 2002]. In the case of free space attenuation,  $\beta$  takes the value of 2.

Suppose that the noise at each SU terminal and PU terminal is independent and identical distributed (i.i.d) and follows the standard Gaussian distribution with zero mean and unit variance (i.e.,  $\sigma^2 = 1$ ) . The signal-to-noise ratio (SNR) at the PU is

$$SNR = 10\log_{10}(P / \sigma^2), \quad (5.29)$$

and SNR at the  $i^{th}$  SU is

$$SNR = 10\log_{10}(P_{r,i} / \sigma^2) \text{ for } 1 \leq i \leq K. \quad (5.30)$$

The SNR measurements at each secondary user will contribute to the considered spectrum sensing algorithm for the cooperation sensing strategy of the cognitive radio system in this chapter.

### 5.3.3 FPT detection and binary hypothesis test

As it is introduced in section 5.2, a spectrum sensing method based on FPT [Ø. Ryan and M. Debbah, 2007] is one of the newly developed spectrum sensing techniques for the cognitive radio system. The FPT spectrum sensing method will be used for each secondary user in the considered cooperative spectrum sensing scheme. Assume that each SU terminal is equipped with number of  $l$  antennas and the transmitter (PU) is equipped with  $m$  antennas. The channel matrix for the link between the primary user and each SU is  $\mathbf{H}_i$  for  $1 \leq i \leq K$  . The sizes of the row and column of the channel matrix  $\mathbf{H}_i$  are  $l$  (number of receive antennas) and  $m$  (number of transmit antennas), respectively. Let  $\mathbf{x}$  be the transmitted signal column

vector with  $m$  dimension;  $\mathbf{n}_i$  for  $1 \leq i \leq K$  be the noise column vector with  $l$  dimension. Then the received signal  $\mathbf{y}_i$  for  $i$ th SU can be expressed as

$$\mathbf{y}_i = \mathbf{H}_i \mathbf{x} + \mathbf{n}_i. \quad (5.31)$$

It is known that signal detection is a test of two hypotheses [C. W. Helstrom, 1968].  $H_0$  is defined as the hypothesis that the received signal  $\mathbf{y}$  at time  $t$  is contributed by the noise  $\mathbf{n}(t)$  only.  $H_1$  is the hypothesis that the received signal  $\mathbf{y}$  at time  $t$  is contributed by the transmitted signal through the channel and the noise component  $\mathbf{n}(t)$ . The test of two hypotheses can be expressed as

$$\begin{aligned} H_0 : \mathbf{y}(t) &= \mathbf{n}(t) \\ H_1 : \mathbf{y}(t) &= \mathbf{H}(t) \mathbf{x}(t) + \mathbf{n}(t) \end{aligned} \quad (5.32)$$

In the signal detection algorithm, the probability of detection  $P_d$  is defined as the probability of detecting a signal on the frequency band when the signal is truly present. The probability of false alarm  $P_f$  is the probability that the test decision declares that the frequency band is occupied by the primary user when the frequency is actually vacant. Both  $P_d$  and  $P_f$  depend on a predefined threshold value  $V_T$ . In the FPT detection algorithm, the threshold value  $V_T$  is the value of the detected signal power predefined under a fixed overall system probability of false alarm  $P_f$ . Rayleigh fading channel is assumed. The probability of false alarm  $P_{f,i}$  for  $i^{\text{th}}$  SU at a given threshold  $V_T$  is

$$P_{f,i} = \text{prob}(P_{r,i} > V_T | H_0) \text{ for } 1 \leq i \leq K. \quad (5.33)$$

The probability of detection  $P_{d,i}$  for  $i^{\text{th}}$  SU at a given threshold  $V_T$  is given by

$$P_{d,i} = \text{prob}(P_{r,i} > V_T | H_1) \text{ for } 1 \leq i \leq K. \quad (5.34)$$

Here, we consider the cooperative spectrum sensing scheme of the cognitive radio system. The assumption of the scheme is that all SUs apply same threshold value  $V_T$  to make their decision. It is also considered that the extracted signal power should be comparable to the noise variance, hence  $V_T$  is set to  $\delta^2$ .

Having examined the MIMO single user FPT spectrum sensing algorithm, we now move on to the cooperative spectrum sensing in a MU-MIMO cognitive radio network. It is known that cooperative sensing in the cognitive radio network can improve system performance of detection and avoid hidden node problem. In the following section, we will consider the cooperative scheme of centralized sensing in the multiuser cognitive radio network. We assume that each user in the cognitive radio network applies FPT detection individually and his detection data or decision is sent to the fusion centre where the final decision is made.

### **5.3.4 Cooperative detection with false alarm rate constraint**

We consider a cognitive radio parallel fusion network and the cooperative detection under the condition that the acceptable probability of false alarm value at the system level is less than a predefined value [P. K. Varshney, 1996]. Figure 5.6 shows the block system diagram of the parallel fusion network for the cognitive radio system. One primary user and  $K$  secondary users are in the system. In this cooperative detection scheme, each secondary user  $i$  detects independently from the received signal  $\mathbf{y}_i$  for  $1 \leq i \leq K$  and makes his decision whether the interested spectrum is occupied by the primary user. Then the decision  $\delta_i$  for  $1 \leq i \leq K$  from all secondary users are sent to a fusion centre where the final decision  $\delta_s$  is made. Both  $\delta_i$  and  $\delta_s$  takes the binary decision  $\{0, 1\}$ , the decision  $0$  declares the primary user being vacant on the band whereas the decision  $1$  says the primary user occupying the band.

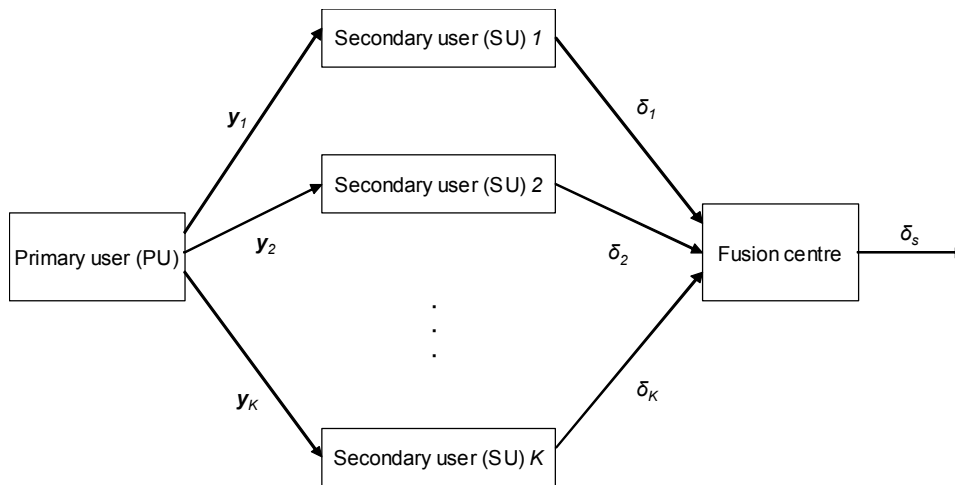


**Figure 5.6 A cognitive radio parallel fusion network**

The system detection depends on the fusion rule at the fusion centre as well as the local decision rule at each secondary user. The aim of the system detection is to maximize the probability of the detection  $P_d$  on the system level and to meet the requirement of the system probability of false alarm  $P_f$  limitation.

There are some fusion rules commonly used, such as the AND fusion rule, the OR fusion rule and “ $k$  out of  $K$ ” fusion rule [P. Varshney, 1996 and Y. Zeng et al., 2010]. The brief descriptions of these decision fusion rules are as follows.

#### **5.3.4.1 AND fusion rule**

The basics of the AND fusion rule is that the system decision value is 1 only if all  $K$  secondary users decision values are 1. In this case, the probability of detection  $P_d$  on the system level is

$$P_d = \prod_{i=1}^K P_{d,i}, \quad (5.35)$$

where  $P_{d,i}$  is the probability of detection for  $i^{\text{th}}$  secondary user. The probability of false alarm  $P_f$  on the system level is

$$P_f = \prod_{i=1}^K P_{f,i}, \quad (5.36)$$

where  $P_{f,i}$  is the probability of false alarm for  $i^{\text{th}}$  secondary user.

### 5.3.4.2 OR fusion rule

For the OR fusion rule, the system decision value takes  $1$  if at least one of  $K$  secondary users takes the decision value  $1$ . Therefore, the probability of detection  $P_d$  on system level under OR fusion rule is expressed as

$$P_d = 1 - \prod_{i=1}^K (1 - P_{d,i}), \quad (5.37)$$

and the probability of false alarm  $P_f$  on the system level is

$$P_f = 1 - \prod_{i=1}^K (1 - P_{f,i}). \quad (5.38)$$

We discuss here the cooperative sensing with false alarm constraint by utilizing FPT detection algorithm for each user and applying OR fusion rule at the fusion centre of the cognitive radio system. Moreover, since each user in the system will have different received SNR, the secondary users with the maximum received SNR are chosen to cooperate. In this way, the higher system probability of detection can be achieved under the system probability of false alarm constraint. It is assumed that all secondary users

apply the same threshold value  $V_T$  to make their decisions. The number of cooperative secondary users will depend on the system false alarm limitation.

### 5.3.4.3 “ $k$ out of $K$ ” fusion rule

Assume that  $1 \leq k \leq K$ , the “ $k$  out of  $K$ ” rule states that if and only if  $k$  decisions or more are  $1$ , the final decision is  $1$ . Two extreme cases are OR rule if  $k=1$  and AND rule if  $k=K$ . It is Majority rule if  $k = K/2$  [P. K. Varshney, 1996].

### 5.3.5 Simulation result

Receiver operating characteristics (ROC) graph, which is a plot of the probability of the detection  $P_d$  against the probability of false alarm  $P_f$ , is often used to describe the performance of a spectrum detection technique. Figure 5.7 is the receiver operating characteristics of the FPT detector when the signal-to-noise ratio at receiver is -10dB, -15dB and -20dB. The ROC curve is obtained under following system parameters. One SU terminal is equipped with 3 receive antennas and one PU terminal has 4 transmit antennas. Rayleigh fading channel is assumed so both real and imaginative parts of each entry in the channel matrix are following Gaussian distribution with zero mean and unit variance. The noise component is an additive white Gaussian noise (AWGN) with zero mean and unit variance. Assuming equal power allocation on each antenna of PU terminal and the SU terminals without any knowledge of signal transmitted from the primary user. The number of samples taken for the detection scheme is 100 which are considered large enough for the FPT detection algorithm. The threshold for FPT detector is set to  $1\text{dBW}$ . The result data in the simulation is acquired via 10000 channel realization.

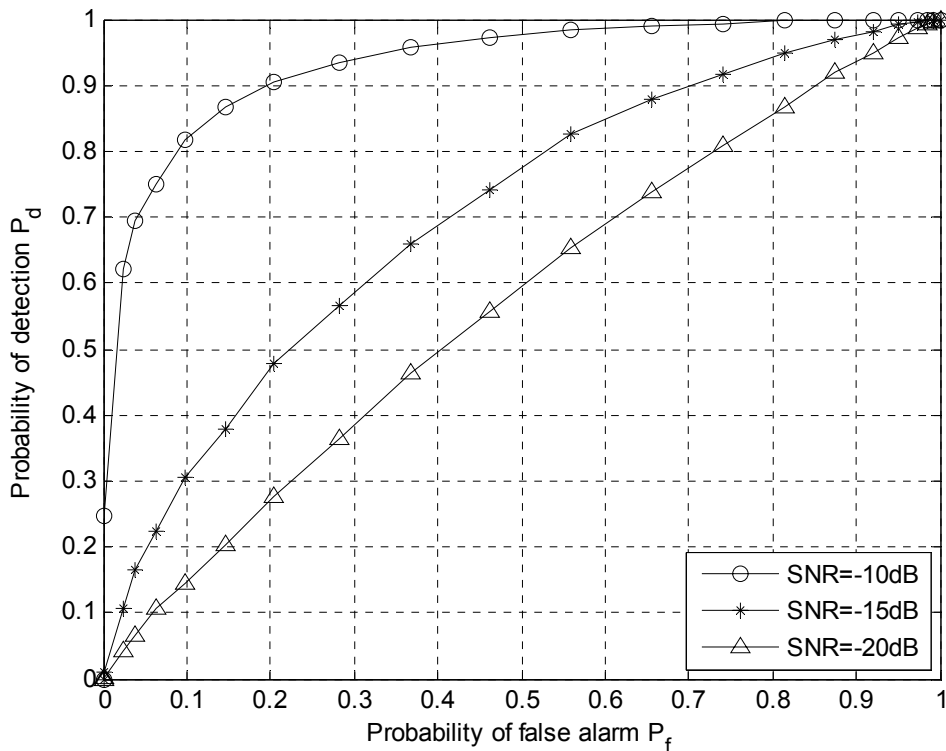
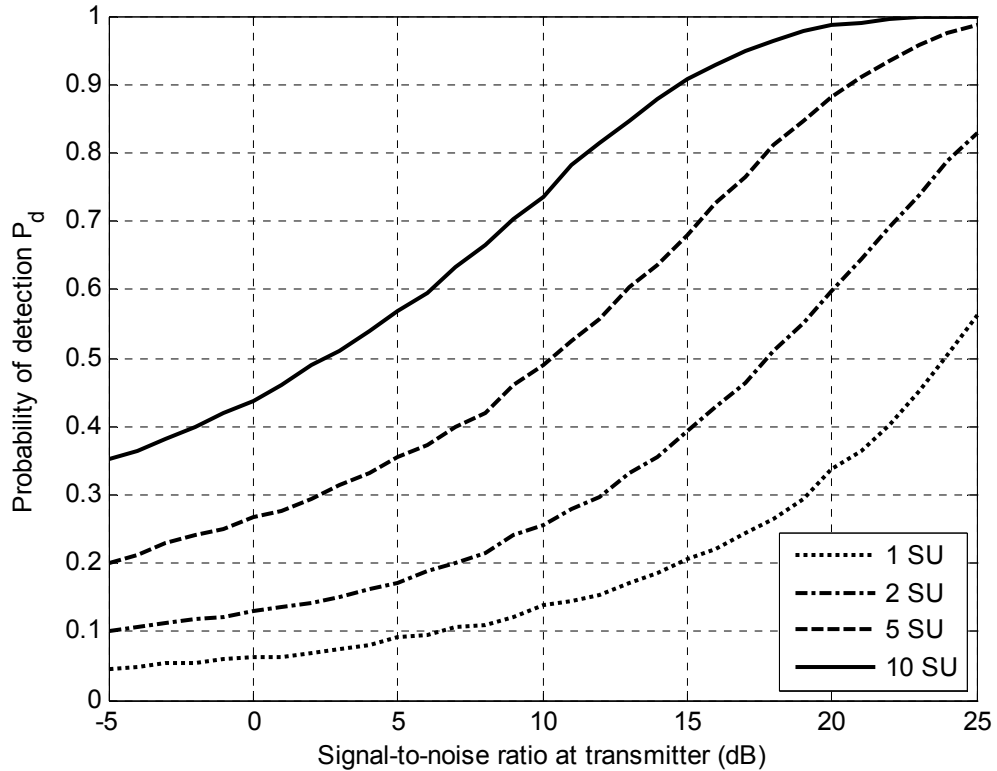


Figure 5.7 ROC graph of FPT detector.

Figure 5.8 shows the probability of detection on the system level  $P_d$  versus SNR at the primary user terminal when numbers of secondary user are 1, 2, 5 and 10. The antennas configuration for each receiver and transmitter pair is  $3 \times 4$  in the simulation. The FPT detection method is utilized and the threshold value for each detector is set to  $V_T = 1$  dBW. Arbitrary choice of different decision fusion rules results in different sensing performances in a designated multiuser CR system. Furthermore, spectrum sensing by using one chosen fusion rule might perform better in one wireless environment setting than in the other. Hence, OR decision rule is only applied in the simulation, that is, the system decision is set to 1 as long as at least one of the binary decisions received from secondary users at the fusion centre is 1. The result graph demonstrates that the system probability of detection  $P_d$  increases as number of cooperative SUs increases at a given SNR value. Hence, the system performance of cognitive radio

system can be improved in terms of the probability of detection via cooperation among secondary users.



**Figure 5.8** Probability of detection versus SNR at transmitter (PU) in a cooperative cognitive radio system.

On the other hand, the system false alarm rate  $P_f$  increases as the number of SUs  $K$  increases under the OR decision rule. If we treat each SU the same and the false alarm rate for each user is represented by an average value  $\bar{P}_{f,i}$  (i.e.,  $P_{f,1} = P_{f,2} \dots = P_{f,K} = \bar{P}_{f,i}$ ), the system false alarm rate in (5.38) becomes  $P_f = 1 - (1 - \bar{P}_{f,i})^K$ . Because  $\bar{P}_{f,i}$  is less than 1.0, the system false alarm rate  $P_f$  increases as  $K$  increases. This reveals that the total number of cooperative users is limited by the system false alarm  $P_f$  constraint. Therefore, a cooperative strategy is to maximize the probability of detection under the limited number of cooperative users determined by the probability of false alarm constraint.

Figure 5.9 shows the system false alarm rate against total number of secondary users in a cognitive radio. The average false alarm rate for each SU is 0.0228 when the threshold for FPT detector is set to  $1$ . It demonstrates that the system false alarm rate  $P_f$  increases as the total number of SUs increases in the system. It raises a question that the total number of cooperative users is limited by the system false alarm  $P_f$  constraint.

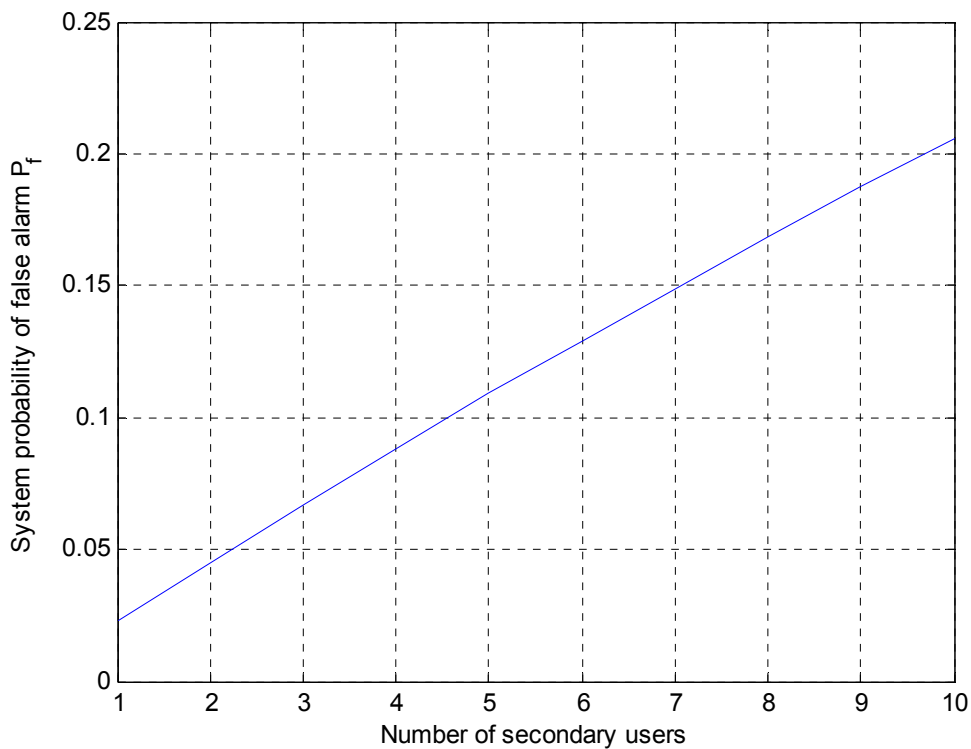


**Figure 5.9 System false alarm rate versus number of secondary users. The false alarm rate for each SU is 0.0228 when the threshold for FPT detector is set to 1.**

We consider a scenario that only a limited number of secondary users  $k$  out of total number of secondary users  $K$  are selected for cooperation under the system false alarm constraint  $P_f$ . This scheme is described as the selective cooperative scheme. The value  $k$  is determined by the system false alarm constraint. Assume that  $k \leq K$  and OR decision rule is applied. In the case of  $k = K$ , all secondary users can participate cooperative sensing and the system probability of false alarm meets the system false alarm constraint.

In the case of  $k < K$ , assume that each secondary user terminal sends to a fusion centre not only its binary decision but also its received SNR. Only  $k$  users with the highest SNR out of  $K$  secondary users are chosen for cooperation. However, the drawback of this scheme is more traffic generated in the channel between the SU and fusion centre due to the detected SNR data sent to the fusion centre. We expect that the system performance can be improved if more secondary users exist in the system and users with the highest SNR are chosen for cooperation. Figure 5.10 shows the system probability of detection  $P_d$  versus SNR at the primary user. It can be seen that the system performance can be improved if the secondary users with the highest SNR out of a large number of secondary users in the system are selected for cooperation. In Figure 5.10, it is assumed that the system false alarm constraint is set to 0.1, therefore the number of cooperative users is limited to 4. The result shows that the cooperation among 4 secondary users with the highest SNR out of total number of 10 secondary users achieves higher system  $P_d$  than the cooperation of 4 secondary users out of total number of 4 secondary users in the system. The result shows that the performance of 4 SUs cooperative scheme out of 10 users is close to the performance of all 10 users cooperation. The benefit of 4 SUs cooperative scheme out of 10 SUs is that the system false alarm constraint can be met while all 10 secondary users cooperation result the probability of false alarm  $P_f=0.2$  over predefined false alarm constraint 0.1.

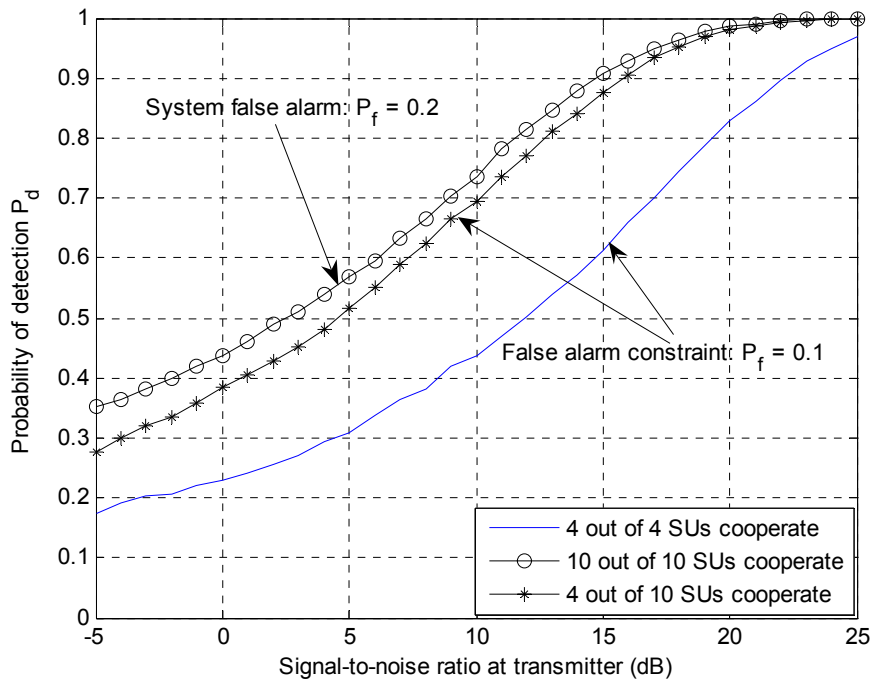


Figure 5.10 Probability of detection  $P_d$  versus SNR at the transmitter (PU).

### 5.3.6 Summary

Section 5.3 presents the cooperative spectrum sensing using Free Probability Theory (FPT) detection method in a MU-MIMO cognitive radio system. The advantage of FPT detection is that it is a blind spectrum sensing method and it performs better than traditional energy detection technique. Maximizing the system probability of detection is a paramount goal under pre-defined system false alarm constraint. High probability of detection under false alarm constraint can be achieved via the selective cooperative spectrum sensing approach. The simulation results demonstrate that the system performance can be improved by such cooperative scheme in the multiuser cognitive radio system.

## **Chapter 6 Spectrum sensing based on higher-order statistics and receiver diversity in SIMO cognitive radio systems**

In this chapter, we present a new spectrum sensing method with higher-order statistics (HOS) and receiver diversity for improved sensing performance in single-input multiple-output (SIMO) cognitive radio (CR) system. In comparison with classic energy detection method that is one of the blind spectrum sensing methods, the HOS spectrum sensing has the advantage of suppressing Gaussian noise. The HOS spectrum sensing works better than the traditional energy detection method when the signal-to-noise (SNR) ratio is low in the CR system [F. Xu et al., 2009]. We consider the SIMO wireless cognitive radio system, where a primary user (PU) is considered as the transmitter with one antenna and a secondary user (SU) is considered as the receiver equipped with multiple antennas. The secondary user detects if the licensed band is occupied by the primary user. The spectrum sensing method proposed combines the third-order statistics (bispectrum) spectrum sensing with receiver diversity in the SIMO wireless cognitive radio system. It is known that multiple-input multiple-output (MIMO) technique can be employed to improve the performance of multiple antenna wireless system [A. J. Paulraj et al., 2004]. The system capacity can be increased via multiplexing gain; the signal-to-noise (SNR) at the receiver can be enhanced due to the diversity gain and array gain in the MIMO system. MIMO technology can also mitigate the channel fading in the wireless system. Therefore, the receiver diversity is also applied in our proposed spectrum sensing algorithm. In the signal detection in our proposed algorithm, the independent fading paths associated with multiple receive antennas are combined to obtain a signal which is then used for bispectrum estimation.

## **6.1 Introduction**

In a cognitive radio system, primary users are the users who have exclusive right to use a frequency band allocated to them; secondary users are those who are not allocated to the frequency band and hence they have no privilege to use the frequency band. Cognitive radio technology [I. Mitola, J. and J. Maguire, G. Q., 1999, J. Mitola, 2000, S. Haykin, 2005] allows secondary users exploit the spectrum that is not occupied by the primary users. To use the frequency band, secondary users must perform the task of spectrum sensing and discover if primary users are present in the band. There are many spectrum sensing methods used in the cognitive radio systems. Examples of the sensing methods are energy detection, matched filtering and free probability theory (FPT) detection, which are introduced in previous chapters, as well as cyclostationary feature detection [T. Yücek and H. Arslan, 2009, L. Jin et al., 2010]. Energy detection method is a blind spectrum sensing method that is a simple detection technique and does not require any knowledge of transmitted signal. In contrast, matched filtering is a detection method applied when the transmitted signal is known to the receiver. Cyclostationary feature detection is a method for detecting primary user transmission by exploiting the cyclostationary features of the received signals. FPT spectrum sensing is a blind detection method that utilizes the asymptotic behaviour of random matrix based on the free probability theory in the wireless communication system. By extracting the information of covariance matrix of received signal excluding noise background, the FPT method performs better than the traditional energy detection.

We here focus on a blind spectrum sensing method based on high-order statistics. The application of higher-order statistics in the signal processing has been studied in past two decades [C. L. Nikias and J. M. Mendel, 1993, C. L. Nikias and M. R. Raghuveer, 1987, J. M. Mendel, 1991]. The benefit of signal detection based on HOS is that this technique can eliminate Gaussian noise in a typical signal-plus-Gaussian noise

wireless system. In recent years, researches on HOS detection applied in a cognitive radio system have been presented in [Y. Sun et al., 2008, F. Xu et al., 2009]. In [Y. Sun et al., 2008], an indirect bispectrum spectrum sensing method is applied to a cognitive radio system. It proves that the bispectrum spectrum sensing can effectively detect the existence of the primary user in low signal-to-noise environment. The sensing method based on the simplified bispectrum slide analysis is presented in [F. Xu et al., 2009]. The result in the paper demonstrates that the sensing method performs better than the traditional energy detection technique in noisy environment. The sensing technique in [F. Xu et al., 2009] appears to be useful to detect wireless broadcast TV signal and wireless microphone signals under low SNR situation.

In this chapter, a new spectrum sensing method is proposed for a multiple antenna receiver cognitive radio system [L. Jin and Z. Hu, 2011]. The sensing method combines bispectrum of higher-order statistics and multiple antenna diversity for a specified SIMO cognitive radio system. In comparison with estimating the first-order and the second-order statistics, the computational complexity to evaluate higher-order statistics (the third-order and fourth-order statistics etc) is much higher. Therefore, the SIMO cognitive radio system is considered in this chapter in order to focus on spectrum sensing at receiver side. The work presented in this chapter can be extended to MIMO cognitive radio system. The simulation result demonstrates that the new proposed spectrum sensing method achieves high performance of signal detection under the condition of low SNR. High probability of detection of the proposed method can be achieved through multiple antennas diversity at the receiver and Gaussian noise suppression inherited from the bispectrum sensing technique. Furthermore, cooperative spectrum sensing in multiuser cognitive radio network by using the proposed detection method is discussed in the chapter.

The remaining of the chapter is organized as follows. Firstly, section 6.2 presents spectrum sensing method based on HOS and receive diversity. Section 6.2.1 presents the system model of the SIMO cognitive radio system. Section 6.2.2 depicts the definitions of the higher-order statistics and the method to estimate the third-order statistics (bispectrum). Section 6.2.3 presents the algorithm of the proposed spectrum sensing method. The simulation results are presented in section 6.2.4 and the summary is in the section 6.2.5. Secondly, section 6.3 presents cooperative spectrum sensing by utilizing proposed spectrum sensing method based on HOS and receive diversity in a multiuser cognitive radio system. Section 6.3.1 depicts the system models of multiuser CR system with either a small number of users or a large number of users. Section 6.3.2 describes the concept of hypothesis test. Section 6.3.3 presents cooperation detection algorithms in the cases of multiuser CR networks with a small number of users and a large number of users. The simulation results are in section 6.3.4 and the summary is given in section 6.3.5.

## **6.2 Spectrum sensing based on HOS**

### **6.2.1 SIMO cognitive radio system model**

Assume that a primary network and a secondary network coexist in a cognitive radio system, as shown in Figure 6.1. Consider that the primary network has a primary base station and multiple primary users; the secondary network contains one secondary base station which serves numbers of secondary users. The task of a secondary user is to detect if a frequency band concerned is occupied by a primary user nearby in the system. Therefore, the PU is regarded as the transmitter and the SU is seen as the receiver. A single-input multiple-output (SIMO) scenario is considered, that is, PU is perceived as a transmitter with single antenna and SU is observed as a receiver with  $m$  antennas. The channel matrix between the transmitter and the receiver is denoted as a column vector  $\mathbf{h}$  with  $m$

elements (number of receive antennas). In order to know whether a frequency band is used by the PU, the SU needs to detect the signal from the PU so the decision can be made to use the frequency band when it is vacant. Assume that the signal from the PU is  $x$ , then the signal  $y$  received by the SU is

$$\mathbf{y} = \mathbf{h}x + \mathbf{n}, \quad (6.1)$$

where  $\mathbf{y}$  is a column vector with  $m$  dimension; vector  $\mathbf{n}$  with row size  $m$  is the additive white Gaussian noise (AWGN) vector with zero mean and variance  $\sigma^2$ . Rayleigh fading channel is assumed, therefore each entry in  $\mathbf{h}$  following an independent and identically distributed (i.i.d.) complex Gaussian distribution.

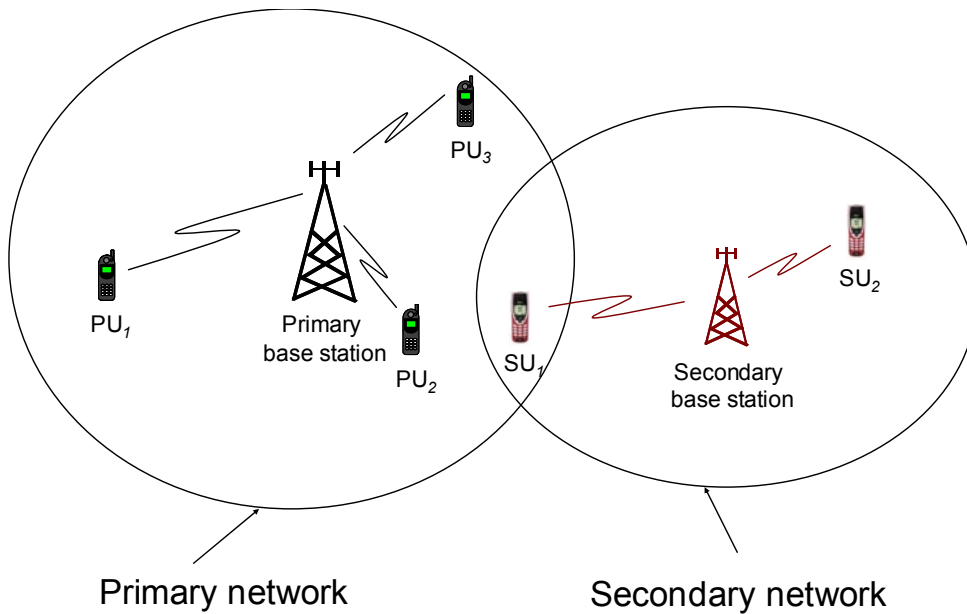


**Figure 6.1 Cognitive radio system**

Figure 6.2 shows receiver diversity of SIMO antenna system. In the receiver diversity, the independent fading paths associated with  $m$  receive

antennas are combined to obtain a signal that is then processed for signal detection. The linear combining techniques are commonly used, that is, the output of the combiner is a weighted sum of the different fading paths. The receiver diversity with linear combining technique in the SIMO system will be considered in the proposed spectrum sensing method.

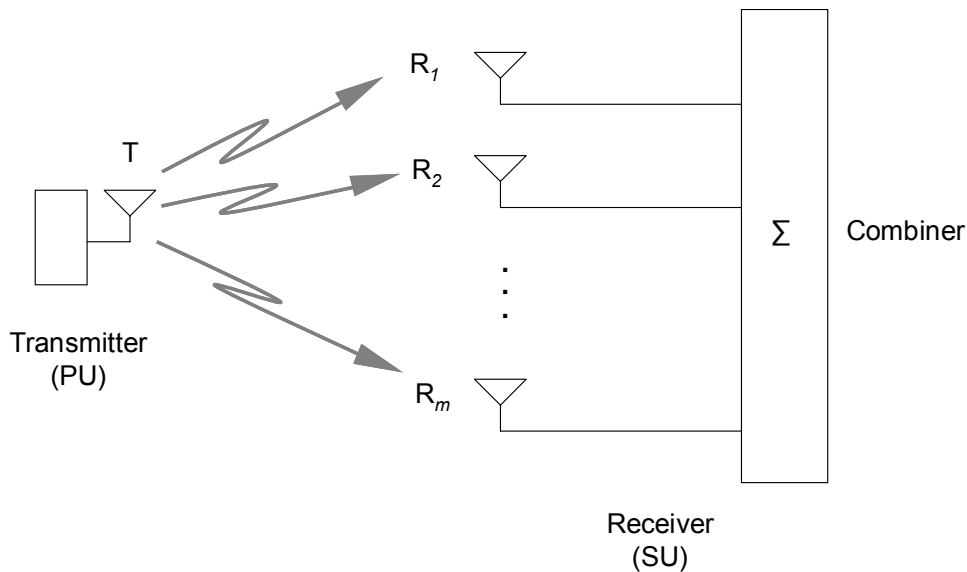


Figure 6.2 SIMO system and receiver diversity.

T – transmitter antenna,  $R_1, R_2, \dots, R_m$  – receive antennas

### 6.2.2 Higher-order statistics

In this section, we describe high-order statistics. The earlier work on signal processing based on high-order statistics, i.e. cumulants, can be found in [C. L. Nikias and J. M. Mendel, 1993, C. L. Nikias and M. R. Raghuveer, 1987, J. M. Mendel, 1991]. Two special cases of higher-order spectra are the second-order spectrum and the third-order spectrum. The second-order spectrum is the power spectrum of a signal while the third-order spectrum is

defined as the Fourier transform of the third-order statistics of a stationary signal. The third-order spectrum is also termed as bispectrum. To detect a signal, a simple method is to evaluate the power spectrum of the signal. If the signal is a Gaussian signal, the information obtained in the power spectrum is normally sufficient to describe the statistical feature of the signal. In this case, the relations between frequency components are suppressed. However, if the signal does not completely conform to Gaussian character, the power spectrum of a signal alone can not describe the signal sufficiently. Under this circumstance, the third-order spectrum can be used to extract the information that represents the deviations from Gaussian character and presence of phase relations between frequency components. In our proposed spectrum sensing algorithm, bispectrum method is utilized since the random process of channel condition is non-symmetrically distributed for the Rayleigh channel assumed [J. M. Mendel, 1991]. It is anticipated that the performance of signal detection will be improved by using the bispectrum information obtained in the sensing method. The details of the third-order spectrum (bispectrum) are presented at the end of this section. The bispectrum will be utilized in the proposed spectrum sensing algorithm in this chapter.

The definition of higher-order spectra will be introduced in next two subsections. Firstly the definition of higher-order moment and cumulant of one dimensional random variable is introduced in section 6.2.2.1.1. Then the details of the definition of higher-order moment and cumulant of high dimensional random variables are given in section 6.2.2.1.2. Finally, the polyspectra of zero-mean  $q$ th-order stationary random process is presented in section 6.2.2.2. The third-order spectrum (the bispectrum) will be used in the proposed spectrum sensing.

### 6.2.2.1 The definition of higher-order spectra

#### 6.2.2.1.1 Definition of higher-order moment and cumulant for one dimensional random variable

In the realm of signal processing, let  $x$  be a random variable in the time domain, angular frequency  $\omega = 2\pi f$  be a random variable in the frequency domain and  $f$  be the frequency. The first characteristic function of  $x$  is defined as

$$\psi(\omega) = E(e^{j\omega x}) = \int_{-\infty}^{\infty} e^{j\omega x} p(x) dx, \quad (6.2)$$

where  $E(\cdot)$  denotes the expectation operator and  $p(x)$  denotes probability density function of the random variable  $x$ . The  $k$ th-order moment can be expressed as

$$m^k = E(x^k) = \int_{-\infty}^{\infty} x^k p(x) dx. \quad (6.3)$$

Assume that the first characteristic function of  $x$  can be expanded in a Taylor series about the point  $\omega = 0$ ,  $\psi(\omega)$  can be written as [J. G. Proakis, 2001]

$$\psi(\omega) = \sum_{k=0}^{\infty} m^k \frac{(j\omega)^k}{k!} = 1 + \sum_{k=1}^{\infty} m^k \frac{(j\omega)^k}{k!}. \quad (6.4)$$

If there exists up to  $n$ th-order moment, i.e.  $m^k, k=1,2,\dots,n$ , the equation above can be approximated as

$$\psi(\omega) \approx \sum_{k=0}^n m^k \frac{(j\omega)^k}{k!} = 1 + \sum_{k=1}^n m^k \frac{(j\omega)^k}{k!}. \quad (6.5)$$

The  $p$ th-order cumulants  $c^p$  of the random variable  $x$  are defined via the cumulant-generating function

$$\phi(\omega) = \sum_{p=1}^{\infty} c^p \frac{(j\omega)^p}{p!}. \quad (6.6)$$

The cumulant generating function is also defined as the natural logarithm of the first characteristic function, which is also called the second characteristic function. The expression of the cumulant generating function is given below

$$\phi(\omega) = \ln \psi(\omega) = \ln E(e^{j\omega x}). \quad (6.7)$$

If the Taylor series of the expansion of (6.7) exists, (6.7) can be expressed as

$$\phi(\omega) = -\sum_{p=1}^{\infty} \frac{1}{p} (1 - E(e^{j\omega x}))^p = -\sum_{p=1}^{\infty} \frac{1}{p} \left( -\sum_{k=1}^{\infty} m^k \frac{(j\omega)^k}{k!} \right)^p. \quad (6.8)$$

Then the relationship between  $p$ th-cumulant  $c^p$  and the  $k$ th-moment  $m^k$  can be found.

If the random variable  $x$  is Gaussian distributed with zero mean and variance  $\sigma^2$ , the probability density function of  $x$  is as follows

$$p(x) = \frac{1}{\sqrt{2\pi}\sigma} e^{-\frac{x^2}{2\sigma^2}}. \quad (6.9)$$

The cumulants  $c^p$  for  $p=1,2,\dots$  of  $x$  are  $c^1=0, c^2=\sigma^2, c^p=0, p>2$ . Therefore, the higher-order cumulants of Gaussian random variable  $x$  are zero.

### **6.2.2.1.2 Definition of higher-order moment and cumulant of high dimensional random variables**

Let angular frequency  $\boldsymbol{\omega}$  a  $q$ -dimensional random variables  $(\omega_1, \omega_2, \dots, \omega_q)$  and  $\mathbf{x}$  a  $q$ -dimensional random variables  $(x_1, x_2, \dots, x_q)$ . The  $q$ -dimensional characteristic function is defined as [John G. Proakis, 2001]

$$\psi(\boldsymbol{\omega}) = \psi(j\omega_1, j\omega_2, \dots, j\omega_q) = E \left[ \exp \left( j \sum_{i=1}^q \omega_i x_i \right) \right]. \quad (6.10)$$

From (6.10), the higher-order moments can be generated. For example, the two-dimensional characteristic function is

$$\begin{aligned} \psi(\boldsymbol{\omega}) &= \psi(j\omega_1, j\omega_2) = E \left[ \exp \left( j \sum_{i=1}^2 \omega_i x_i \right) \right], \\ &= \int_{-\infty}^{\infty} \int_{-\infty}^{\infty} e^{j(\omega_1 x_1 + \omega_2 x_2)} p(x_1, x_2) dx_1 dx_2 \end{aligned} \quad (6.11)$$

where  $p(x_1, x_2)$  is the joint probability of density function of two dimensional variable  $(x_1, x_2)$ . The joint moment of  $(x_1, x_2)$  can be obtained by partial derivatives of  $\psi(j\omega_1, j\omega_2)$  with respect to  $\omega_1$  and  $\omega_2$ , that is,

$$E(x_1, x_2) = - \left. \frac{\partial^2 \psi(j\omega_1, j\omega_2)}{\partial \omega_1 \partial \omega_2} \right|_{\omega_1 = \omega_2 = 0}. \quad (6.12)$$

The second characteristic function, which is also called the cumulant generating function, is defined as

$$\phi(\boldsymbol{\omega}) = \ln \psi(\boldsymbol{\omega}) = \ln E \left[ \exp \left( j \sum_{i=1}^q \omega_i x_i \right) \right]. \quad (6.13)$$

If the Taylor series expansion of the cumulant-generating function exists, the  $q$ th-order cumulant of these random variables is defined as the coefficient of  $(\omega_1 \omega_2 \dots \omega_q)$  in the Taylor series expansion of  $\phi(\boldsymbol{\omega})$ . Therefore the  $q$ th-order

cumulant is defined in terms of its joint moments of orders up to  $q$ . The details of relationship between cumulants and moments can be found in [J. M. Mendel, 1991].

### 6.2.2.2 Polyspectra of zero-mean $q$ th-order stationary random process

Consider  $\{x(t)\}$  is a zero mean  $q$ th-order stationary random process. The  $q$ th-order cumulant is defined as the joint  $q$ th-order cumulant of the random variables  $x(t), x(t + \tau_1), x(t + \tau_2), \dots, x(t + \tau_q)$ , which is expressed as

$$\begin{aligned} C_{q,x}(\tau_1, \tau_2, \dots, \tau_{q-1}) \\ = \text{cum}(x(t), x(t + \tau_1), x(t + \tau_2), \dots, x(t + \tau_{q-1})) \end{aligned} \quad (6.14)$$

where  $\tau_i$ , for  $i=1, 2, \dots, q-1$  denotes the  $i$ th time lag,  $C_{q,x}(\tau_1, \tau_2, \dots, \tau_{q-1})$  denotes  $q$ th-order cumulant and  $\text{cum}(\cdot)$  denotes the joint  $q$ th-order cumulant of the random variables in the bracket.

Polyspectra are related to the higher-order spectra in terms of cumulants and their Fourier transforms. Assuming that  $C_{q,x}(\tau_1, \tau_2, \dots, \tau_{q-1})$  is absolutely summable, the  $q$ th-order polyspectrum denoted as  $S_{q,x}(\omega_1, \omega_2, \dots, \omega_{q-1})$  is defined as the  $(q-1)$ -dimensional discrete-time Fourier transform of the  $q$ th-order cumulant, which can be expressed as

$$\begin{aligned} S_{q,x}(\omega_1, \omega_2, \dots, \omega_{q-1}) \\ = \sum_{\tau_1=-\infty}^{+\infty} \cdots \sum_{\tau_{q-1}=-\infty}^{+\infty} C_{q,x}(\tau_1, \tau_2, \dots, \tau_{q-1}) \times \exp \left[ -j \sum_{i=1}^{q-1} \omega_i \tau_i \right]. \end{aligned} \quad (6.15)$$

In this chapter, one special case is considered when  $q=3$ . Let  $S_{3,x}(\omega_1, \omega_2)$  denote as the third-order spectrum (bispectrum), which can be expressed as

$$S_{3,x}(\omega_1, \omega_2) = \sum_{\tau_1=-\infty}^{+\infty} \sum_{\tau_2=-\infty}^{+\infty} C_{3,x}(\tau_1, \tau_2) \times \exp(-j\omega_1\tau_1 - j\omega_2\tau_2). \quad (6.16)$$

It is known [J. M. Mendel, 1991] that first-order cumulant  $C_{1,x}$  is the mean value of  $\{x(t)\}$  and the second-order cumulant  $C_{2,x}(\tau_1)$  is the autocorrelation of  $\{x(t)\}$  and  $\{x(t+\tau_1)\}$ . The important feature of the third-order cumulant  $C_{3,x}(\tau_1, \tau_2)$  is that it can be used to extract the information that differs from the Gaussian random process with same second-order statistics as  $\{x(t)\}$ . Therefore, the third-order spectrum can be used to gain the information of the transmitted signal immersed in the Gaussian noise in the digital communication system. The third-order spectrum is a simple form of polyspectra and it is applied to the proposed spectrum sensing algorithm for the SIMO cognitive radio system in this chapter.

The methods to estimate the bispectrum are presented in [C. L. Nikias and M. R. Raghuveer, 1987]. The indirect method is adopted to evaluate the bispectrum in this thesis. Assume that  $\{X(1), X(2), \dots, X(N)\}$  is the data set of the received signals. For the SIMO case, the data set is the summation of the signals received from each antenna of the receiver. The details of the method are given below:

1. Segment the data  $N$  into  $K$  records of  $M$  samples each, i.e.,  $N=KM$ .
2. Substrate the average value of each record.
3. For each segment  $i=1,2,\dots,K$ , the data set is expressed as  $\{x^i(k), k=1,2,\dots,M\}$  where  $x^i(k)$  denotes  $i$ th record and  $k$ th sample.

Obtain an estimation of the third-order cumulant sequence

$$C_{3x}^i(\tau_1, \tau_2) = \frac{1}{M} \sum_{k=s_1}^{s_2} x^i(k)x^i(k+\tau_1)x^i(k+\tau_2), \text{ where } s_1 = \max(0, -\tau_1, -\tau_2)$$

and  $s_2 = \min(M-1, M-1-\tau_1, M-1-\tau_2)$ .

4. Average  $C_{3x}^i(\tau_1, \tau_2)$  over all segments  $C_{3x}(\tau_1, \tau_2) = \frac{1}{K} \sum_{i=1}^K C_{3x}^i(\tau_1, \tau_2)$ .
5. Generate the bispectrum estimation  $B_x(\omega_1, \omega_2) = \sum_{\tau_1=-\infty}^{\infty} \sum_{\tau_2=-\infty}^{\infty} C_{3x}(\tau_1, \tau_2) w(\tau_1, \tau_2) \exp(-j\omega_1\tau_1 - j\omega_2\tau_2)$ , where  $w(\tau_1, \tau_2)$  is two-dimensional window function.

### 6.2.3 Proposed spectrum sensing based on third-order spectrum and receiver diversity

In this section, we will describe the proposed algorithm of spectrum sensing based on third-order spectrum and receiver diversity in SIMO cognitive radio system. The details of the algorithm are given below:

1. Apply receiver diversity and obtain the signal for bispectrum estimation by utilizing linear combining technique to the received signals from all antennas of the receiver. It is assumed that the SU has no knowledge of the signal from the PU. Therefore, equal weight is applied to each antenna of the receiver. The signal for calculation of bispectrum is the summation of the signals from all antennas.
2. Calculate the bispectrum of the signal by using the indirect method stated in the section above.
3. Compare the amplitude of bispectrum to the predefined threshold  $\lambda$ . Then the occupancy of the frequency band by the primary user is decided if the amplitude of bispectrum is greater than the threshold. Otherwise, the frequency band is empty.

The choice of the threshold  $\lambda$  depends on the requirement of the probability of false alarm in the system considered. Large threshold value results in low probability of false alarm whereas the small threshold value results in high

probability of false alarm. To avoid harmful interference to the primary user, high threshold value should be chosen and therefore low false alarm probability is assured. In this case, the probability of detection of PU is low as well. On the other hand, if the detection of the vacant band is paramount, low threshold value should be chosen. In this case, high probability of detection of PU is achieved. Therefore, the aim of choosing threshold  $\lambda$  is to balance  $P_d$  and  $P_f$  as required in the design of signal detection.

#### 6.2.4 Simulation result

In the simulation, the transmitted signal is BPSK signal with carrier frequency 4 MHz, signal sample rate is  $1024 \times 10^5$  sps (sample per second). Two-dimensional window function is Parzen window for bispectrum estimation and the number of cumulant lags is 100. The channel is frequency-flat Rayleigh fading channel with maximum Doppler shift 10Hz. The noise is additive white Gaussian noise.

Figure 6.3 shows the probability of detection  $P_d$  versus the received SNR in the case of one SU by using the proposed detection method. The result compares the probabilities of detection when number of receive antenna is 1, 2 and 3; the false alarm rate is set to  $P_f = 0.04$ . It demonstrates that receiver with three antennas achieves higher probability of detection than the receiver with two antennas in the range of  $SNR = -16\text{dB}$  to  $SNR = -6\text{dB}$ . Similarly, the receiver with two antennas attains higher probability of detection than the receiver with one antenna in the range of  $SNR = -16\text{dB}$  to  $SNR = -3\text{dB}$ . The receiver with three antennas achieves the highest probability of detection in the range of low SNR. The result demonstrates that the HOS spectrum sensing method performs well in the range of low received SNR. The performance of HOS detection method is improved significant by utilizing the multiple receive antenna diversity in the SIMO CR system.

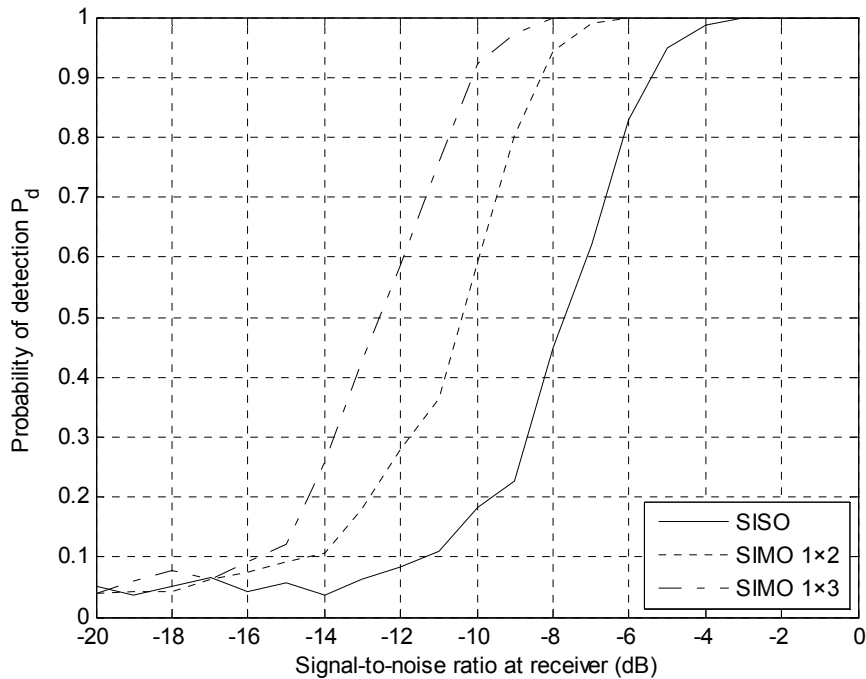


**Figure 6.3** Probability of detection  $P_d$  versus SNR at receiver,  $P_f=0.04$

Figure 6.4 shows the image of the bispectrum magnitude of the received signal at the receiver by using the proposed spectrum sensing method. The axes  $f_0$  and  $f_1$  in the figure are the normalized signal sample frequencies. Figure 6.4 (a) – (c) demonstrate the images of the bispectrum magnitudes of the received signal at the receiver when number of receive antenna increases. Figure 6.4 (a) is the SISO case when received SNR = -10dB. Both Figure 6.4 (b) and Figure 6.4 (c) are the SIMO cases with received SNR = -10dB. The number of receive antenna for Figure 6.4 (b) and Figure 6.4 (c) is 2 and 3 respectively. Figure 6.4 (d) shows the image of bispectrum magnitude of the received signal when received SNR is at high value of 20dB; which serves as a reference image that the pattern of the bispectrum magnitude of the received signal is mainly contributed by the transmitted signal. In comparison with Figure 6.4 (d), the data points contributed by the transmitted signal itself in Figure 6.4 (a) are not clearly

seen and are submerged in the data points contributed by the noise background. In the case of two receive antennas, the data points due to the transmitted signal itself become more visible by comparing Figure 6.4(b) to Figure 6.4 (a). The data points originated from the transmitted signal are more observable in Figure 6.4 (c) by comparing the image to Figure 6.4 (a) and (b). The result demonstrates that the image of bispectrum magnitude is more close to the image of bispectrum magnitude at high SNR value when the number of antennas at receiver increases. In other words, the probability of detection in a cognitive radio system can be improved if multiple receive antennas are utilized at the secondary user. Therefore, the proposed spectrum sensing method can further improve the performance of signal detection based on the bispectrum estimation at low received SNR value due to receiver diversity.

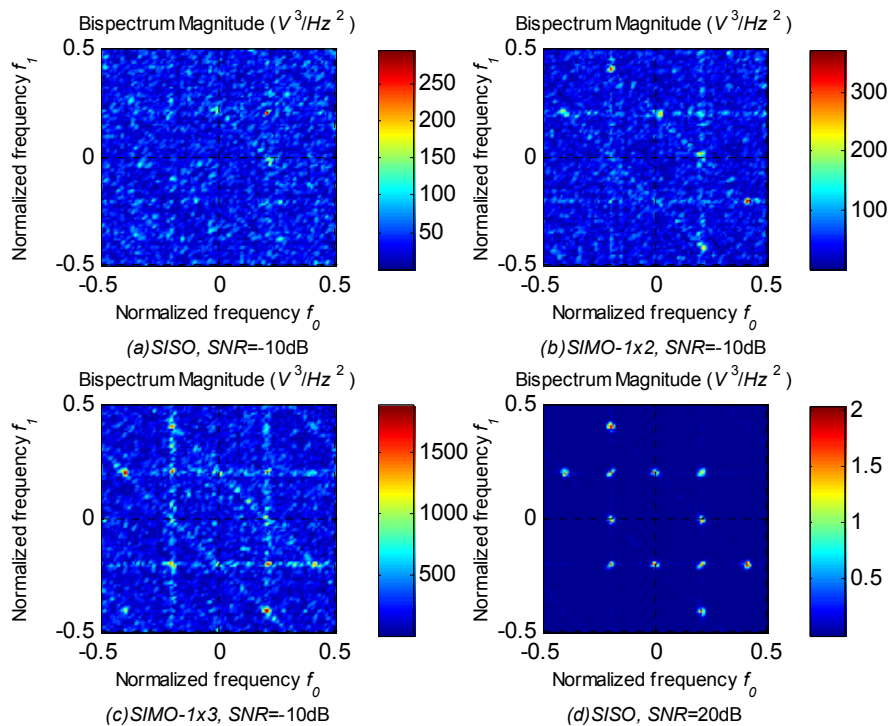


Figure 6.4 Image of bispectrum magnitude of BPSK signal, carrier frequency is 4MHz.

### **6.2.5 Summary**

In section 6.2 of this chapter, a new spectrum sensing method is proposed for a SIMO cognitive radio system. The detection scheme utilizing higher-order statistics and receiver diversity of multiple antenna system demonstrates high performance of signal detection under low SNR condition. The feature of the proposed scheme is two-fold: (1) the sensing method inherits the character of higher-order statistics spectrum sensing; (2) depending on the number of receive antennas, the effect of the receiver diversity of secondary user can increase the received signal  $SNR$ . The new detection scheme performs better than the HOS spectrum sensing without receive diversity. Therefore, the proposed scheme can enhance the probability of detection in the cognitive radio system at the expense of the increased number of receive antenna at the SU terminal. The new method can improve the efficiency of the spectrum utilization in the cognitive radio system.

### **6.3 Cooperative detection based on HOS in SIMO cognitive radio systems**

In this section, we present cooperative spectrum sensing by using the proposed spectrum sensing method based on higher-order statistics (HOS) and receive diversity in multiuser SIMO cognitive radio (CR) system. As being described in section 6.2, the spectrum sensing scheme based on HOS and receiver diversity is a blind detection method and has the advantage of suppressing Gaussian noise. In the SIMO cognitive radio system, a primary user (PU) is considered as the transmitter with one antenna and a secondary user (SU) is considered as the receiver equipped with multiple antennas. The secondary user detects if the licensed band is occupied by the primary user.

In a cognitive radio network, a reliable spectrum sensing can be achieved through cooperation among secondary users. One of the advantages of cooperative sensing is that different users take their own measurements and therefore the system performance can be improved at low SNR due to the diversity of the measurements. In addition, the hidden-terminal problem can be greatly reduced because the cooperative users are scattered in a wide area of the CR network and thus the possibility of all users shadowed away from the primary user is relatively small [Y. Zeng et al., 2010]. We consider cooperative spectrum sensing that is regarded as the centralized detection problem with false alarm constraint in multiuser SIMO CR system. Each SU will apply the spectrum sensing method based on HOS and receive diversity for detecting the existence of PU in a frequency band. The final detection decision is made in the fusion centre by applying OR decision fusion rule to the detect decision received from all secondary users. In the case of cognitive radio network with a small number of secondary users, we consider two cases. The first case is that each SU only sends his detection decision to the fusion centre. The second case is that each SU not only reports his detect decision to the fusion centre but also send measured SNR value to the fusion centre. Assume that the CR network is under system-level false alarm constraint, the system-level probability of detection can be improved via choosing the secondary users with the high SNR values to cooperate. In the case of CR network with a large number of SUs, all users reporting to central fusion centre may not be most efficient because large amount of network resources can be consumed. To solve this problem, the considered geographical area of CR network can be divided into many sub-areas. Assume that the users in a sub-area form a cluster and each cluster has a cluster head that serves as a local fusion centre. The users in the cluster send their detection decision to the cluster head where the detection decision is made for the cluster. All cluster heads will send their decisions to the central fusion where final detection decision is made. More details will be presented in following sections.

Following sections are organized as this. Section 6.3.1 presents the system model of the SIMO CR system. Section 6.3.2 presents the hypothesis test by applying the proposed spectrum sensing method. Section 6.3.3 describes cooperative spectrum sensing in multiuser CR system. The simulation results are presented in section 6.3.4 and the summary is in section 6.3.5. Low boldface is used for vectors.  $E(\cdot)$  denotes expectation operator.

### **6.3.1 Multiuser cognitive radio system model**

We consider two models of multiuser cognitive radio system. Firstly consider multiuser CR network with a small number of users. Secondly consider multiuser network with a large number of users. The details are given below in next two sections.

#### **6.3.1.1 Multiuser CR network with a small number of users**

Figure 6.5 shows two dimensional geographical distribution of users in a cognitive radio network that comprise one primary user and a small number of secondary users. This case can be extended to three dimensional user distribution in a CR network. In this thesis, we only consider two dimensional distribution of users in the network. It is assumed that one primary user is located at the centre of an area with a radius of 20km and  $K$  numbers of secondary users are randomly dotted in the area. The transmit power from the primary user is  $P$  and the received power for the secondary user  $i$  is  $P_{r,i}$  for  $1 \leq i \leq K$ . Consider that the signal from the PU experiences path loss, the received power for  $i^{th}$  secondary user can be expressed as

$$P_{r,i} = \frac{P}{1 + \alpha d_i^\beta} \quad \text{for } 1 \leq i \leq K, \quad (6.17)$$

where  $d_i$  is the distance between the PU and the SU  $i$ ,  $\alpha$  is a scalar and  $\beta$  is the path loss exponent factor. Depending on the environment in which the PU and the SU are situated, the value of  $\beta$  is in the range of 2~6 [T. S. Rappaport, 2002]. In this paper,  $\beta$  takes the value of 2 and  $\alpha$  takes the value 0.07. The constant value '1' is added in the denominator of (6.17) to accommodate the extreme case where  $d_i$  is zero or tends to zero. Since the secondary users are spread in a very large area, the difference between (6.17) and the path loss expression ( i.e.  $P_{r,i} = \frac{P}{\alpha d_i^\beta}$  ) commonly found in the wireless reference articles can be ignored. In the extreme case of very small  $d_i$ , the received signal power at  $i$ th SU is equivalent to the transmitted signal power at the PU since the path loss can be ignored.

Suppose that the noise at each SU terminal is i.i.d (independent and identically distributed) and follows standard Gaussian distribution with zero mean and unit variance ( $\delta^2 = 1$ ). The path loss can be ignored when the distance between a SU and the PU is near zero. Let the received signal-to-noise ratio of SU at the location of PU be defined as

$$SNR_i = 10 \log_{10}(P / \delta^2). \quad (6.18)$$

If  $d_i$  is large enough and the path loss has to be considered, the received signal-to-noise ratio for the  $i^{th}$  SU is defined as

$$SNR_i = 10 \log_{10}(P_{r,i} / \delta^2) , \text{ for } 1 \leq i \leq K. \quad (6.19)$$

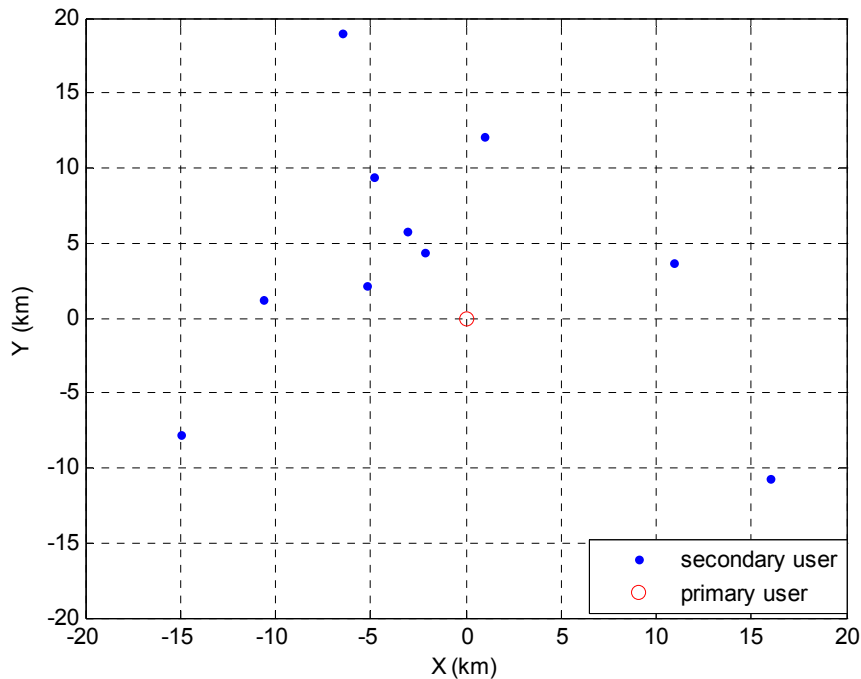


**Figure 6.5** Cognitive radio network with one primary user and a small number of secondary users.

Assume that the spectrum sensing method based on the HOS and receive diversity is applied at each SU. Consider that the PU terminal is equipped with single antenna and each SU terminal is equipped with  $m$  antennas. The channel matrix between the transmitter and the  $i$ th receiver is denoted as a column vector  $\mathbf{h}_i$  for  $1 \leq i \leq K$  with  $m$  elements. Assume that the signal from the PU is a scalar  $x$ , the signal  $\mathbf{y}_i$  for  $1 \leq i \leq K$  received by the  $i$ th SU is

$$\mathbf{y}_i = \mathbf{h}_i x + \mathbf{n}_i \text{ for } 1 \leq i \leq K, \quad (6.20)$$

where  $\mathbf{y}_i$  is a column vector with  $m$  dimension; vector  $\mathbf{n}_i$  for  $1 \leq i \leq K$  with row size  $m$  is the additive white Gaussian noise (AWGN) vector with zero mean and variance  $\delta^2$  at the  $i$ th SU. Rayleigh fading channel is assumed therefore each entry in  $\mathbf{h}_i$  following an independent and identically

distributed (i.i.d.) complex Gaussian distribution. The detection method explores receive diversity at each receiver. The signals from the independent fading paths associated with  $m$  receive antennas are combined to obtain a signal that is then processed for signal detection. The linear combining techniques are commonly used, that is, the combined signal at the receiver is a weighted sum of different fading paths. The channel information is usually not known to the SU in the CR system, therefore equal weight will be applied to each receive antenna.

Consider that the spectrum sensing based on third-order spectrum and utilizing receive diversity is used in the multiuser SIMO cognitive radio system. The details of the algorithm are described in section 6.2.3. Assume that same threshold  $\lambda$  is set at all SU terminals and the signal attenuation is fast in large area of the SU distribution as shown in Figure 6.5. Hence weak signal powers are received at the secondary users who are distant from the PU, which may well below the threshold  $\lambda$  at those SU terminals. Only the secondary users near the PU can receive strong signals from PU, which may be above the threshold value  $\lambda$ .

### **6.3.1.2 Multiuser CR network with a large number of users**

In the scenario described here, consider that a large number of secondary users  $K$  are in a region that is a square area with edge length 40km. Assume that each secondary user represents as a spectrum sensor and detects independently by utilizing HOS spectrum sensing method. The spectrum sensors are independent and identically and uniformly distributed in the region. Suppose that one primary user is in the region and secondary users detect cooperatively if the primary user is occupying the frequency band. Supposing the noises at all secondary users are i.i.d and follow Gaussian distributed with zero mean and unit variance. There exists a central fusion centre in the region.

Since the area of the secondary users' distribution is very large, the strength of the received signal at a detector varies with the distance between the PU and SU due to large scale path loss. It is more likely that the secondary users near the PU have high received signal-to-noise ratio, the secondary users are distant from the PU having low received SNR and a group of secondary users close by will have similar detection decisions. It is not an efficient way to send all local decisions from all secondary users to a central fusion centre when there are a large number of users in the system. To solve this problem, we can adopt an approach of dividing the area into several sub-regions, as shown in Figure 6.6. The sensors in each sub-region form a cluster and each cluster has its own cluster head that serves as local fusion centre.

We accept all symbol definitions described in section 6.3.1.1 for path loss, if the transmit power from the primary user is  $P$  and the received power for the secondary user (SU)  $i$  is  $P_{r,i}$  for  $1 \leq i \leq K$ . The received power for  $i^{th}$  secondary user can also be expressed by (6.17). The received SNR at  $i^{th}$  SU can be expressed as (6.19). The channel model for signal transmission for each SU expressed as (6.20) is applied here. The HOS detection method described in 6.3.1.1 will also be applied here.

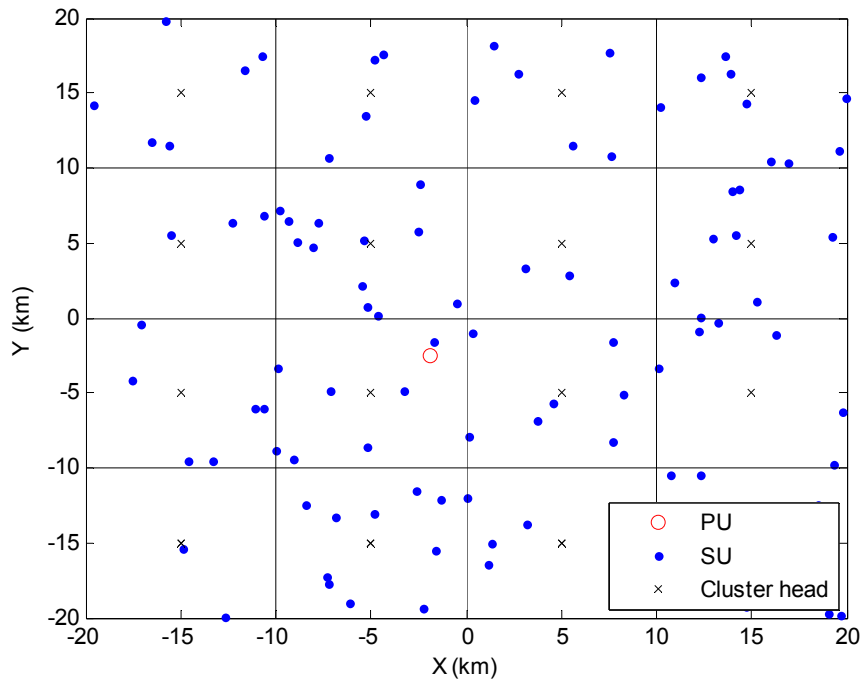


Figure 6.6 Cognitive Radio system with a large number of users. The SUs form a cluster in each sub-region and the cluster head in a sub-region serves as local fusion centre.

### 6.3.2 Hypothesis test at each secondary user

Since (6.20) represents the signal received by the  $i$ th SU  $y_i$  for  $1 \leq i \leq K$ , the signal detection at  $i$ th SU is a test of following two hypotheses [C. W. Helstrom, 1968]:

$$\begin{aligned} H_0^i : y_i(t) &= n_i(t) \\ H_1^i : y_i(t) &= h_i(t)x_i(t) + n_i(t) \end{aligned} \quad \text{for } 1 \leq i \leq K, \quad (6.21)$$

where  $H_0^i$  is the hypothesis that the received signal  $y_i(t)$  at time  $t$  is only contributed by the noise  $n_i(t)$ ,  $H_1^i$  is the hypothesis that the received signal  $y_i(t)$  at time  $t$  is the summation of the noise and the transmitted signal

experienced path loss and channel fading. Rayleigh fading channel is assumed. The probability of false alarm  $P_{f,i}$  at a given threshold  $\lambda$  is

$$P_{f,i} = \text{prob}(B_i > \lambda | H_0^i), \quad (6.22)$$

where  $B_i$  is the amplitude of bispectrum obtained by using the proposed detection method. The probability of detection  $P_{d,i}$  at a given threshold  $\lambda$  is given by

$$P_{d,i} = \text{prob}(B_i > \lambda | H_1^i). \quad (6.23)$$

The threshold value  $\lambda$  is in general determined by predefined false alarm  $P_{f,i}$  constraint.

### 6.3.3 Cooperative detection

#### 6.3.3.1 All SU detect in a small network

Assume that there exists a fusion centre in a multiuser CR network with a small number of secondary users. To detect if a frequency band is occupied by a primary user, each secondary user detects independently by applying HOS spectrum sensing method and sends his detect decision to the fusion centre. The final detection decision at fusion centre is made upon receiving the detection decision from all secondary users. Suppose that the OR fusion rule is utilized at the fusion centre.

For the system model with a small number of SUs described in section 6.3.1.1, assume that one primary user and  $K$  secondary users are in the system and the distribution of the SUs is shown in Figure 6.5. The parallel fusion network is demonstrated in Figure 6.7. We consider that all secondary users detect, each SU  $i$  detects independently from the received

signal  $y_i$  for  $1 \leq i \leq K$  and makes his decision whether the interested spectrum band is occupied by the PU. Then all decisions  $\delta_i$  for  $1 \leq i \leq K$  are sent to a fusion centre where the final decision  $\delta_s$  is made.

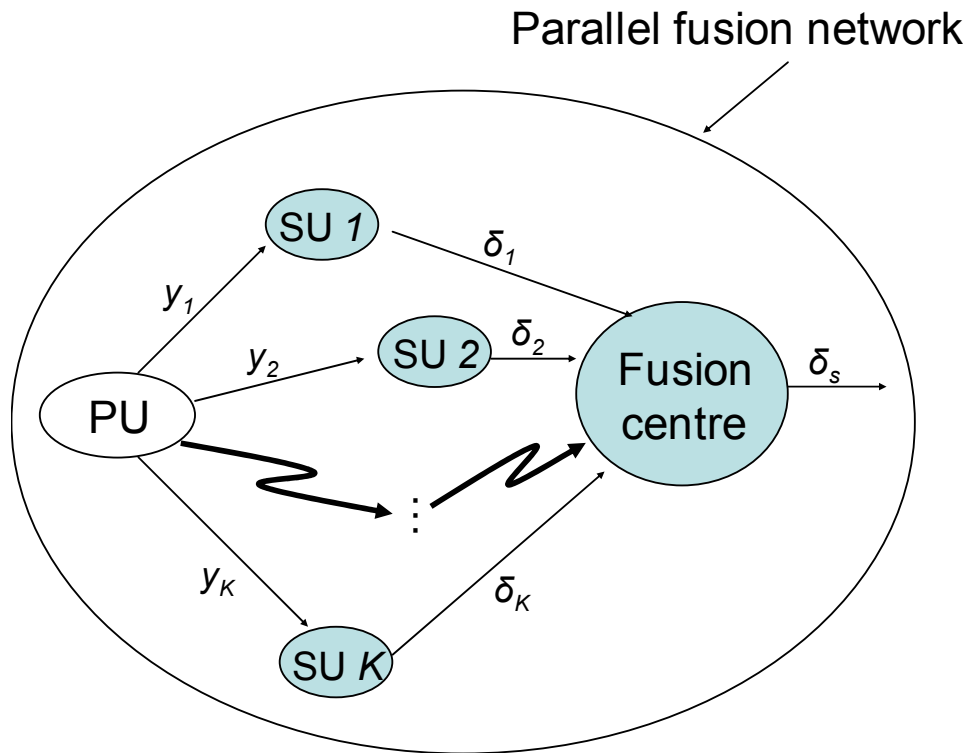


Figure 6.7 A cognitive radio parallel fusion network

Depending on the requirement of system-level probability of false alarm, the cooperative detection problem is the Neyman-Pearson detection formulation of the binary hypothesis testing problem [P. K. Varshney, 1996]. The Neyman-Pearson detection is to maximize the system detection probability under a constant false alarm rate constraint. The aim of the system detection is to design the fusion rule and the local decision rules to maximize the probability of the detection  $P_d$  at the fusion centre and to meet the requirement of the system probability of false alarm  $P_f$  constraint. Assume that each secondary user sends only binary decision  $\delta_i = \{1, 0\}$  for  $1 \leq i \leq K$ , the fusion rule at the fusion centre takes the form

$$\delta_s = \begin{cases} 1, & \text{if } \text{prob}(\boldsymbol{\delta}|H_1) > T\text{prob}(\boldsymbol{\delta}|H_0) \\ 0, & \text{if } \text{prob}(\boldsymbol{\delta}|H_1) < T\text{prob}(\boldsymbol{\delta}|H_0) \end{cases}, \quad (6.24)$$

where  $H_0$  is the hypothesis that the received signal at any time is only contributed by the noise;  $H_1$  is the hypothesis that the received signal at any time is when the signal is present;  $\boldsymbol{\delta} = (\delta_1, \dots, \delta_k)$  is the decision vector containing the local decisions;  $\text{prob}(\boldsymbol{\delta}|H_1)$  is the probability of  $\boldsymbol{\delta}$  under hypothesis  $H_1$  and  $\text{prob}(\boldsymbol{\delta}|H_0)$  is the probability of  $\boldsymbol{\delta}$  under hypothesis  $H_0$ ;  $T$  is the threshold value at the fusion centre for the Neyman-Pearson detection problem. Therefore, the final system detection performance is the collective result of local decision rule at each SU and the fusion rule at the fusion centre.

In this chapter, we only consider the OR fusion rule applied at the fusion centre. For the OR fusion rule, the probability of detection  $P_d$  on the system level is expressed as

$$P_d = 1 - \prod_{i=1}^K (1 - P_{d,i}) \text{ for } 1 \leq i \leq K, \quad (6.25)$$

and the probability of false alarm  $P_f$  on the system level is

$$P_f = 1 - \prod_{i=1}^K (1 - P_{f,i}) \text{ for } 1 \leq i \leq K. \quad (6.26)$$

### **6.3.3.2 $k$ out of $K$ SUs ( $k < K$ ) cooperative detection in a CR network with a small number of users**

Additional to the system model described in previous section, we consider that the system-level detection performance is under false alarm constraint.

Assume that all secondary users not only detect and send their detect decision to the fusion centre, but also send their detected  $SNR$  to the fusion centre, as shown in Figure 6.8. If same threshold is applied to all HOS detectors, all detectors will have same probability of false alarm value. Suppose that the system-level of probability of false alarm will be over the false alarm constraint if the detection decisions from all secondary users are used for final decision at the fusion centre. Based on the  $SNR$  values received at the fusion centre, the  $k$  secondary users with the highest  $SNR$  values are selected to contribute to the final system-level detection decision. This strategy can ensure high system-level probability of detection and to meet the requirement of system false alarm constraint.

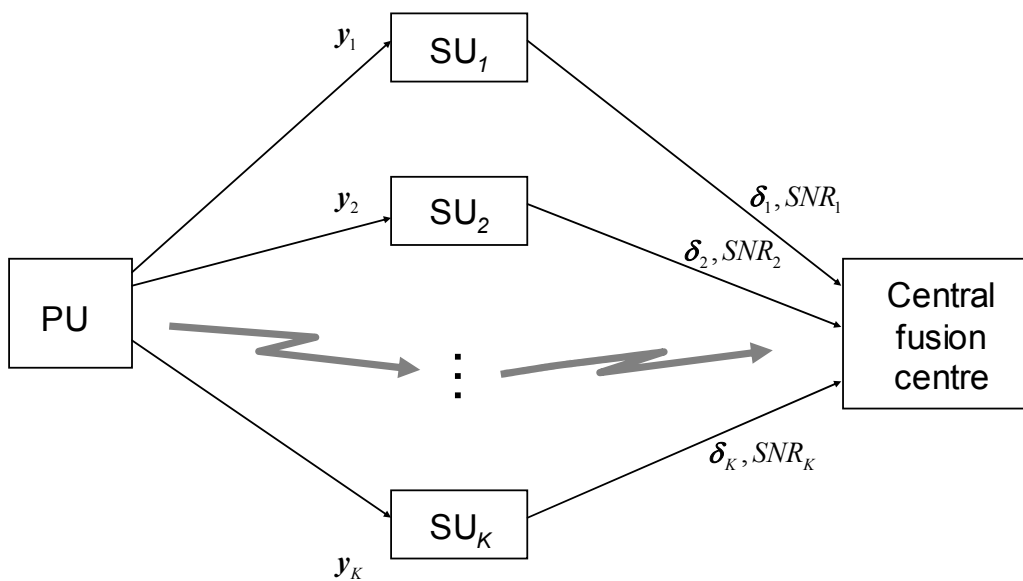


**Figure 6.8** A cognitive radio parallel fusion network, each SU sends his detection decision and detected  $SNR$  to central fusion centre.

### 6.3.3.3 Cooperative detection in a CR network with a large number of users

In a CR network with a large number of users, consider that there exists a central fusion centre and the CR network region is divided into sub-regions. The secondary users in each sub-region form a cluster in which there exists a cluster head. The cluster head is also used as a local fusion centre. The SUs in each cluster send their detection decisions to their cluster head where local detect decision is made. Then all cluster heads send their decisions to the central fusion centre where final system-level detection decision is made.

Assume that total number of  $Z$  cluster heads are in the network, which are represented as  $CH_i$  for  $1 \leq i \leq Z$ . Figure 6.9 shows that the local detection decision in each cluster is made at the cluster head upon receiving the detection decision from all SUs in the cluster. Then, the cluster heads will send their decisions  $\delta_{CH_i} = \{0,1\}$  for  $1 \leq i \leq Z$  to the central fusion centre where final detection decision  $\delta_s$  will be made if the PU occupies a frequency band. Assume that OR fusion rule is implemented at all cluster heads and central fusion centre.

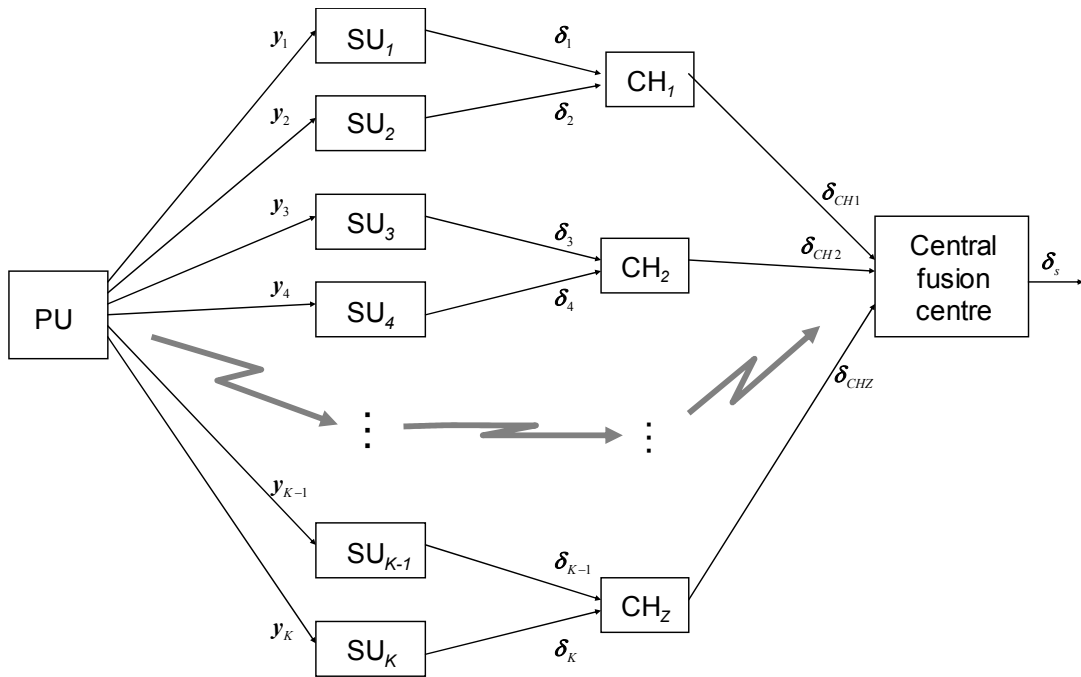


**Figure 6.9** CR network with a large number of users.  $CH_i$  for  $1 \leq i \leq Z$  - cluster head.  $\delta_i = \{0,1\}$  for  $1 \leq i \leq K$  - detect decision from  $i$ th SU.  $\delta_{CH_i} = \{0,1\}$  for  $1 \leq i \leq Z$  - detect decision from  $i$ th cluster head.  $\delta_s = \{0,1\}$  - final detection decision from central fusion centre.

### 6.3.4 Simulation Result

This section presents the simulation results. In the simulation, the transmitted signal is BPSK signal with carrier frequency 4 MHz, signal sample rate is  $1024 \times 10^5$  sps (sample per second). Two-dimensional window function is Parzen window for bispectrum estimation and the number of cumulant lags is 100. The channel is frequency-flat Rayleigh fading channel with maximum Doppler shift 10Hz. The noise is additive white Gaussian noise. In the CR system described in section 6.3.1, the distance between a SU (receiver) and a PU (transmitter) is a variable that depends on the location of the SU in the area considered at a given time  $t$ . The received  $SNR$

at each SU varies with the distance between the transmitter and receiver and the path loss suffered in the channel. To compare the system performance of the signal detection in the cooperative CR system, it is more meaningful to show the probability of detection of the system  $P_d$  versus transmit power (in dBW) at the PU in our result curves below.

Figure 6.10 shows the probability of detection of CR system versus the transmit power at the transmitter in a CR network with a small number of SUs. The result curves are obtained by setting the threshold value of each HOS detector according to the predefined probability of false alarm  $P_f=0.04$ . All SUs detect and send their detect decisions to the central fusion centre. Final system-level decision is based on the decision obtained by applying OR decision rule to the decisions received from all SUs at the central fusion centre. In each scenario of 4, 8 and 16 SUs in the CR network, the result demonstrates that the system-level  $P_d$  obtained in the case of multiple receive antennas is higher than the system  $P_d$  achieved in the case of single receive antenna. The simulation result also shows that more SUs cooperation results in high system-level probability of detection.

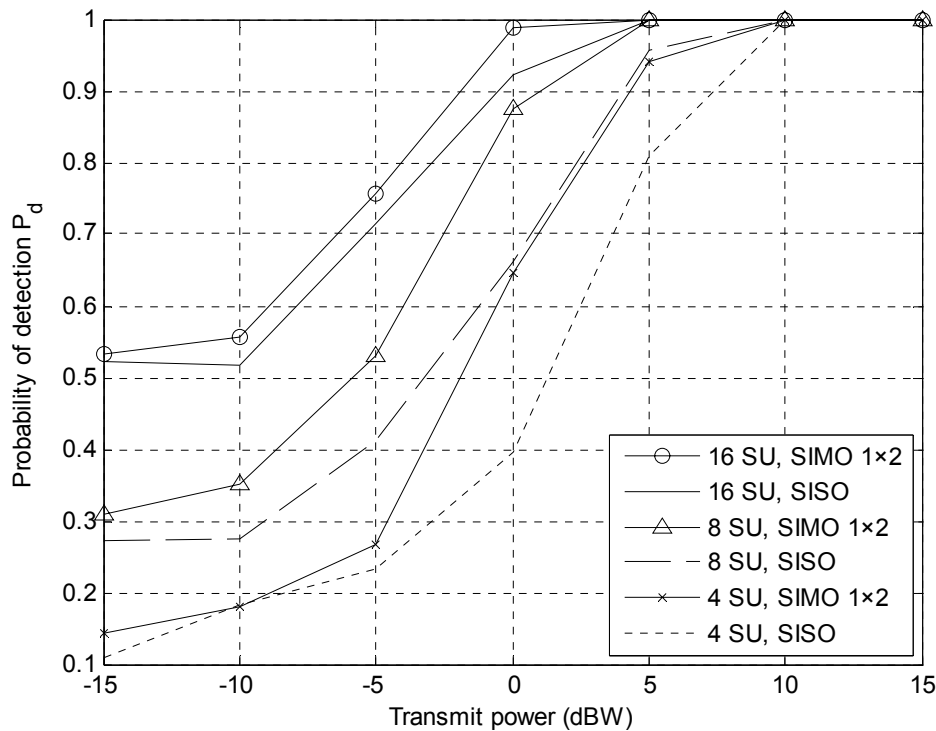


**Figure 6.10** Probability of detection versus transmit power at transmitter (PU) in a CR network with a small number of users. All SUs detect and contribute to the final system-level detect decision.

Figure 6.11 demonstrates the system-level probability of detection versus the transmit power at the transmitter in a CR network with a small number of users. The result curves are obtained by setting the threshold value of each HOS detector according to the predefined probability of false alarm  $P_f=0.04$ . OR decision rule is applied at the central fusion centre in the simulation. In addition, the system-level probability of false alarm constraint is set to 0.1. The fact is that the system-level false alarm rate  $P_f$  increases as the number of SUs  $K$  increases under the OR decision rule. If we treat each SU the same, the false alarm rate for each user is represented by an average value  $\bar{P}_{f,i}$ , for  $i=1,2,\dots,K$ . From the  $P_f$  expression  $P_f = 1 - \prod_{i=1}^K (1 - P_{f,i})$ , we can decide that maximum number of SUs can contribute to the final detect decision making under OR fusion rule and fixed system-level false alarm

constraint. In the simulation, assume that all SUs send their detect decisions as well as detected  $SNR$  data to the central fusion centre, two users with highest  $SNR$  values are selected to contribute to final system detect decision. Figure 6.11 demonstrates that the system probability of detection  $P_d$  increases as the number of SUs in CR network increases at a given  $SNR$  value. Hence, the system performance for CR system can be improved in terms of  $P_d$  via the cooperative spectrum sensing among SUs.

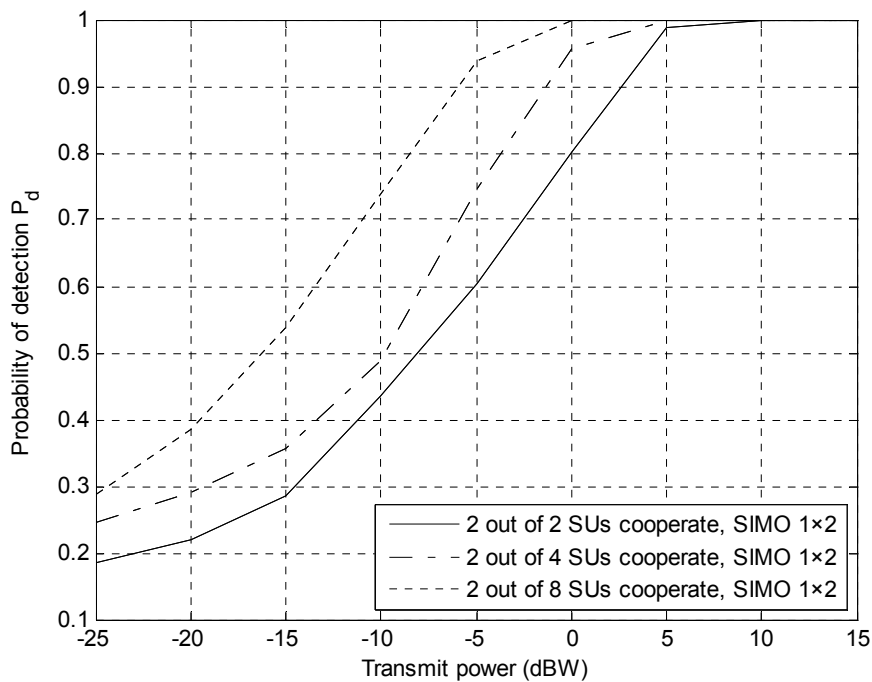


**Figure 6.11** Probability of detection versus transmit power at transmitter (PU) in the CR network with 2, 4, 8 secondary users. 2 users with highest received  $SNR$  are selected and contributed to the final system-level detect decision.

Figure 6.12 is the result graph of system-level  $P_d$  versus transmit power at PU in a multiuser network with a large number of users. The system model is described in section 6.3.1.2. Assume that there are 32 secondary users in the system, the geographical area of  $40km \times 40km$  are divided into 16 sub-areas (clusters). There exist one central fusion centre in the system and one cluster head in each cluster. The result curves are obtained by setting the threshold value of each HOS detector according to

the predefined probability of false alarm  $P_f=0.04$ . The first step of the cooperative detection algorithm is that the users in each cluster report their detect decisions to their cluster head. Then all cluster heads send their local decisions to the central fusion centre where the final detection decision is made. OR fusion rule is implemented at each cluster head and central fusion centre. Figure 6.12 shows that system-level probability of detection  $P_d$  is above 0.7 with cooperative detection of 32 users when transmit power is greater than -15dBW. Furthermore, HOS detector with two receive antennas achieves better probability of detection in comparison with HOS detector with single receive antenna.

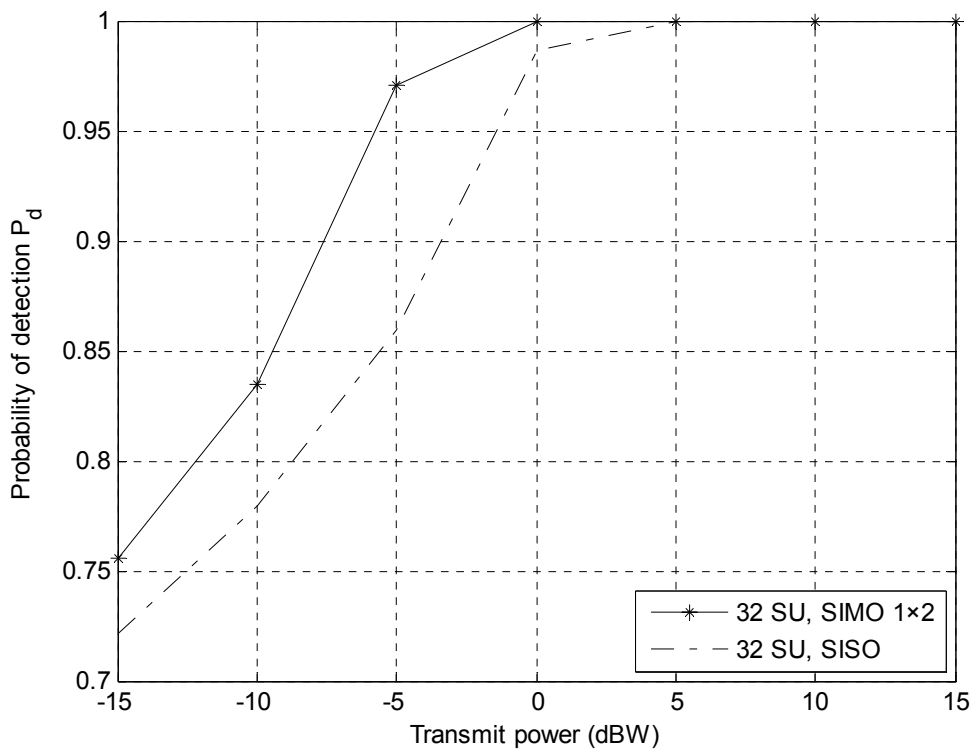


Figure 6.12 System-level  $P_d$  versus transmit power at PU in a multiuser network with a large number of users.

### 6.3.5 Summary

In section 6.3, we discussed cooperative spectrum sensing in multiuser cognitive radio network with a small or a large number of users [L. Jin and

Z. Hu, 2011]. The spectrum sensing method utilized is the proposed spectrum sensing method based on higher-order statistics and receiver diversity, which is described in section 6.2. The performance of new detection scheme can be enhanced when the number of receive antennas increases. We considered three simulation scenarios: (A) multiuser CR network with a small number of users, all users contribute to final system-level detect decision. (B) Multiuser CR network with a small number of users, only  $k$  users with highest  $SNR$  out of all SUs are selected for participating final system-level detect decision. (C) Multiuser CR network with a large number of users, the secondary users are grouped into number of clusters according to their geographical locations. Each cluster has a cluster head and all users in the cluster report their detect decisions to the cluster head. One central fusion centre in the network collects the detect decisions from all cluster heads and make final system-level detect decision. OR fusion rule is applied either at cluster heads or central fusion centre. All simulation results show that cooperative detection among secondary users can further increase the probability of detection of the system and improve the efficiency of the spectrum utilization in the cognitive radio system.

## Chapter 7 Conclusions & future work

To improve two performance measures of capacity and efficient use of spectrum, main contributions of this thesis in the research area of MU-MIMO system are:

- We have developed a new volume-based scheduling algorithm under the perfect conditions of CSIR and CSIT in MU-MIMO system. The scheduling algorithm offers low computational complexity and it can also achieve high system sum-rate capacity. The volume-based scheduling algorithm can be used in a practical MU-MIMO system with a large number of users.
- We have developed a two-step scheduling algorithm under perfect CSIR and the transmitter gaining channel state information via limited feedback in MU-MIMO system. This two-step scheduling algorithm is designed for a MU-MIMO system that is under the feedback resource constraint and has a large number of users. The algorithm uses low bits feedback to select users before the precoding vectors are generated for the selected users, which can significantly reduce feedback load in the feedback control channels.
- We have developed a Free Probability Theory (FPT) spectrum sensing method for cognitive radio MU-MIMO system. The FPT method utilizes the asymptotic behaviour of random matrix based on FPT. The method performs better than traditional energy spectrum sensing method. The FPT method is easy to be implemented and can be applicable in real MU-MIMO CR systems.
- We have developed a spectrum sensing method based on higher-order statistics (HOS) and receive diversity in SIMO CR system. This method can be used to detect the signal that the signal statistical feature differs from Gaussian character. We demonstrate that the sensing performance can be improved considerably via receive diversity.

- We have also considered cooperative spectrum sensing by using either FPT method or HOS method in MU-MIMO CR system. Our study demonstrates that cooperative spectrum sensing can improve the performance of spectrum sensing. High probability of detection can be achieved if the users with the best received SNR are chosen to perform cooperative sensing when the system is under false alarm constraint.

In this thesis, we have investigated the methods that can be used to improve the system performance of MU-MIMO wireless communication channels. The studies are focused on two broad areas: (1) Explore multiuser nature and multiple antennas character of the MU-MIMO wireless system. A new volume-based scheduling algorithm is proposed for MU-MIMO downlink wireless system. The system transmission strategy is designed to find users with best channel conditions. The channels of chosen users are virtually orthogonal as a result of applying BD precoding matrices to the channels of these users. Therefore the signals to chosen users can be transmitted concurrently. The new scheduling algorithm is efficient in terms of less computational complexity and high achievable sum-rate capacity. (2) We investigated spectrum sensing methods in cognitive radio technology in MU-MIMO wireless network, namely Free Probability Theory (FPT) spectrum sensing and Higher-Order Statistics (HOS) spectrum sensing. We combine these methods with multiple antennas feature in the MU-MIMO system. It is found that these methodologies can improve the system sensing performance. We also studied the benefit of cooperative sensing in such network. It is found that CR user cooperation can enhance the system-level detection performance.

In searching for an efficient transmission scheme to multiple users in a MU-MIMO downlink system, we found that DPC [M. Costa, 1983] scheme can achieve theoretically maximum capacity limit while RBF [M. Kountouris et al., 2008] attain only data rate which is very much lower than the ideal upper bound system capacity limit. However, DPC strategy is

complex to be implemented and might be impractical in a real system. The advantage of the RBF is that it is simple and the fairness to users is considered, and therefore each user has equal chance to be served. These two strategies represent two extreme cases of transmission scheme for MU-MIMO system reported in research papers. In view of this and with feasibility of a proposed scheduling scheme in mind, we propose the scheduling algorithm called volume-based scheduling algorithm for MU-MIMO downlink system with the aim of achieving as high as possible system data rate with reduced implementation complexity. The algorithm is presented in Chapter 3. The volume-based scheduling algorithm belongs to the category of suboptimal scheduling algorithm. First, the design of the volume-based algorithm is realized under the assumption of perfect channel information and BD precoding is applied in a cellular downlink system. Because number of users served concurrently is limited by the number of antennas of a transmitter due to BD precoding employed, the users to be served in the MU-MIMO system with a large number of users must be selected according to the criterion that these selected users appear to have best channel conditions. The criterion is that the first user selected must have the maximum Frobenius norm; the second user is selected when QR factorization via *householder reduction* is performed to the combined channel matrix from these two users, and the multiplication of diagonal elements of the upper triangular matrix is maximised; continue this process via using the criterion the same as selecting the second user until final user is selected. Once user selection is complete, the signals to the selected users are transmitted simultaneously. The channels of selected users are virtually orthogonal when BD precoding is applied. Therefore, the signal from one user does not cause interference to other users and multiuser multiplexing gain can be explored. Furthermore, transmit power to users is allocated by using water-filling algorithm. Our study demonstrates that the volume-based scheduling algorithm can achieve good performance in terms of high data rate achievement and low computational complexity in comparison with the capacity-based scheduling algorithm and SUS scheduling algorithm. The

contribution of this study is that the volume-base scheduling algorithm can be suitable to use in a real wireless MU-MIMO system.

Most of the scheduling algorithms function properly under the assumption of both transmitter and receiver having perfect channel state information. However, the channel state information in wireless channel is not so accessible for a transmitter while the receiver may gain channel information via direct measurement. In order to send the channel state information from the receiver to the transmitter, a feedback channel can be established between the transmitter and receiver. However, multiple feedback channels may cause resource constraint of uplink channels in the wireless system with a large number of users. In view of this, we have proposed a two-step scheduling algorithm presented in chapter 4. The algorithm can be used in a MU-MIMO wireless system under the assumption of perfect channel state information at the receiver and the channel state information made available to a transmitter through feedback channel between the transmitter and receiver. Assuming that two copies of codebooks generated via RVQ are stored at one transmitter and each receiver, one copy of low bits codebook and one copy of high bits codebook. Each codeword in a codebook mimics any instant channel condition between each transmitter and receiver pair. The codeword in the high bits codebook represents more accurately the channel conditions between one transmitter and one receiver. The proposed algorithm works in two steps. (1) By using the channel information acquired through the feedback link and using the low bits codebook, select users with best channel conditions out of a large number of users via volume-based scheduling algorithm. The number of users served is limited by the number of transmit antennas in BD precoding scheme. (2) By using the high bits codebook, find a codeword representing instant channel condition of one transmitter and one selected user pair. This process applies to all selected users. The signals are transmitted concurrently to the selected users via BD precoding. This two-step scheduling algorithm can be used for wireless system under feedback

channel resource constraint because it requires less feedback resource during user selection stage. Furthermore, the system data rate can be improved by using the high bits codebook.

Then we moved on to the area of cognitive radio technique that can be applied in MU-MIMO wireless communication system. In particular, we focused our studies on finding a new spectrum sensing method with the goal that the new method can achieve high signal detection performance and better spectrum utilization. There are numerous spectrum sensing methods reported in current research papers. Some works are based on the assumption of detector knowing the information of transmitted signals and noise component. Others work when only partial knowledge of the signal and noise interference. The rest of spectrum sensing methods function without need of any information of transmitted signal and noise. In chapter 5, we present a new proposed spectrum sensing method called Free Probability Theory (FPT) signal detection. The FPT spectrum sensing method is a blind signal detection method. The technique exploits the fact that FPT can be used to describe asymptotic behaviour of random matrix of a digital communication system. We can estimate the covariance matrices of a large number of observations of the received signals, and then obtain the covariance matrices of the transmitted signals through asymptotic behaviour of random matrices. Our results demonstrate that the performance of the FPT spectrum sensing method is better than the conventional energy detection method. This FPT method is easy to implement at a secondary user terminal in a cognitive radio network. Also by utilizing multiple antennas feature in a secondary user terminal, the spectrum sensing performance can be improved significantly since combined signal from received signals of multiple antennas effectively increase the SNR value detected. Moreover, multiuser cooperative spectrum sensing can improve signal detection in MU-MIMO cognitive radio system. A scenario is assumed that (a) primary network and secondary network coexist, (b) secondary users detect if a portion of spectrum is occupied by a primary

user and (c) in secondary network, there is a central fusion centre where the sensing data from all secondary are received and OR fusion rule is applied. It is demonstrated that cooperative sensing can enhance probability of detection on the system level in multiuser wireless network. One benefit of the cooperative sensing is that channel fading and shadowing effect in wireless channels can be mitigated due to different geographical location of users. Furthermore, assuming the system under the probability of false alarm constraint, the sensing performance can be improved if central fusion centre can accept the SNR raw data detected from secondary users and make final system detection decision based on the decisions from SUs with the highest SNR values.

Finally a spectrum sensing algorithm based on third-order statistics (bispectrum) and multiple antennas is proposed in Chapter 6. The second-order and third-order statistics are two simplest forms among the definition of higher-order statistics of a stationary signal. The second-order spectrum is the power spectrum of a signal, the information obtained in the power spectrum is normally sufficient to describe the statistical feature of a Gaussian signal. However, if the signal does not completely conform to Gaussian character, the third-order spectrum can be used to extract the information that represents the deviations from Gaussian character and presence of phase relations between frequency components. In our proposed spectrum sensing algorithm, bispectrum method is utilized to describe the random process of channel condition of the Rayleigh channel assumed. We have also examined the benefit of multiple receive antennas in a secondary user terminal for spectrum sensing in SIMO wireless system. Multiple antennas on receiver can increase received SNR values and therefore can improve probability of detection of spectrum sensing. Cooperative spectrum sensing is discussed for the cognitive radio SIMO system in the case of a small number of users as well as a large number of users. The simulation results demonstrate that user cooperative sensing can improve system-level probability of detection. If system is under probability of false alarm

constraint, system-level probability of detection can be improved if users with the highest received SNR are selected for the cooperative detection.

### **Future work**

In our work presented in this thesis, the interference from other users was not considered when we investigate the spectrum sensing in cognitive radio network. To deal with more realistic scenario where inter-user signal interference is inevitable, we can extend our work of spectrum sensing in future by taking into account of the interference from other users. More efficient user cooperation can also be considered in terms of reducing the effect of inter-user interference. The aim of future work in considering the interference from other users is to increase the accuracy of signal detection and to enhance system performance of MU-MIMO cognitive radio network.

We considered that the HOS spectrum sensing method is applied to the SIMO wireless system. This work can be extended to the MIMO system.

We utilized the OR fusion rule in the area of cooperative spectrum sensing of multiuser cognitive radio system. It is known that commonly used fusion rules are the OR fusion rule, the AND fusion rule and the Majority rule [P.K. Varshney, 1996]. The choice of the fusion rule depends on the circumstances of the applications. These rules are optimum only for certain ranges of parameter values. OR fusion rule is that the final system detect decision is  $1$  if at least one of the users takes the detect decision  $1$ . However, this method might not be reliable if one of the users experiences strong signal interference from other sources in the wireless system and falsely detect the signal. On the contrary, AND fusion rule is that the final system detect decision is  $1$  if the detect decisions from all users are  $1$ . The signal can not be detected if one of the users can not detect the signal due to channel impairment, such as shadowing effect. In view of this, We can extend our work of the cooperative spectrum sensing by using “ $k$  out of  $K$ ”

rule, such as  $1 < k < K$  or  $k = K/2$  (Majority rule). The aim of the future work is to improve the reliable system spectrum sensing performance in real system by using the “ $k$  out of  $K$ ” rule.

## Appendix

### List of publications

#### Journal paper

1. L. Jin, X. Gu and Z. Hu, "Low Complexity Scheduling Strategy for Wireless Multiuser Multiple-Input Multiple-Output Downlink System," IET Communication Journal, Vol. 5, Iss. 7, pp. 990-995, May 2011.

#### Conference Paper

2. L. Jin, Z. Hu and X. Gu, "A New Scheduling Algorithm with Low Complexity for Multiuser Multiple-Input Multiple-Output Downlink System," 2009 International Conference on Wireless Communications and Signal Processing (WCSP 2009), Nanjing, China, pp. 1-5, Nov. 2009.
3. L. Jin, X. Gu, and Z. Hu, "A Novel Volume-Based Scheduling Scheme for Multiuser Multiple-Input Multiple-Output Downlink System," 2010 IEEE Radio & Wireless Symposium, Sheraton hotel, New Orleans, LA, pp. 448-451, Jan. 2010.
4. L. Jin, Z. Hu, X. Gu, "A New Signal Detection Scheme Based on Free Probability Theory for Multiple-Input Multiple-Output Cognitive Radio Systems," in Proceedings of the 2010, 7th International Symposium on Wireless Communication Systems (ISWCS' 10), University of York, York, UK, pp.746-750, Sep. 2010.
5. L. Jin, Z. Hu, X. Gu, "Analysis of Sum-rate Gain for Multiuser MIMO Downlink System with Limited Feedback and Feedback Resource Constraint," European Microwave Week 2010, CNIT La Défence, Paris, France, in Proceeding of the 3rd European Wireless Technology conference, 2010 European, pp 73-76, Issue date: 27-28 Sep. 2010.
6. L. Jin and Z. Hu, "Spectrum Sensing Using Higher-Order Statistics and Receive Diversity and Cooperative Detection in SIMO Cognitive Radio System," 2011 IET International Communication Conference on Wireless Mobile & Computing ( IET CCWMC2011), Shanghai, China, pp. 247-253, 14-16 Nov. 2011.

## Reference

- [1] 802.22 Working Group, "IEEE 802.22 D1: draft standard for wireless regional area networks," March 2008. [Online]. Available: <http://grouper.ieee.org/groups/802/22/>.
- [2] A. Ghasemi and E. S. Sousa, "Collaborative spectrum sensing for opportunistic access in fading environments," in IEEE Int. Symp. New Frontiers Dyn. Spectrum Access Netw (DySPAN 2005), Baltimore, Md, USA, pp. 131-136, Nov. 2005.
- [3] A. Goldsmith, *Wireless Communications*, Cambridge University Press, New York, USA, 2005.
- [4] A. Goldsmith, S. Jafar, I Maric and S. Srinivasa, "Breaking Spectrum Gridlock with Cognitive Radios: An Information Theoretic Perspective," in Proc. IEEE, Vol. 97, No. 5, pp. 894-914, May 2009.
- [5] A. Goldsmith, S. Jafar, N. Jindal, and S. Vishwanath, "Capacity limits of MIMO channels," IEEE J. Sel. Areas Commun., Vol. 21, No. 5, pp. 684–702, Jun. 2003.
- [6] A. J. Paulraj, D. A. Gore, R. U. Nabar and H. Bölcskei, "An overview of MIMO communications-A key to gigabit wireless," in Proc. IEEE, Vol. 92, No. 2, pp. 198-218, Feb. 2004.
- [7] A. M. Tulino and S. Verdo, *Random Matrix Theory and Wireless Communications* (2004). [Online]. Available: [www.nowpublishers.com](http://www.nowpublishers.com).
- [8] A. Narula, N. J. Lopez, M.D. Trott, and G.W. Wornell, "Efficient use of side information in multiple-antenna data transmission over fading," IEEE J. Sel. Areas Commun., Vol. 16, No 8, pp. 1423-1436, Oct. 1998.
- [9] A. Nica and R. Speicher, *Lectures on the Combinatorics of Free Probability*, Cambridge University Press, 2006.
- [10] A. Paulraj, R. Nabar, and D. Gore, *Introduction to Space-Time Wireless Communications*, Cambridge University Press, Cambridge, UK, 2003.
- [11] A. Sahai and D. Cabric, "Spectrum sensing: fundamental limits and practical challenges," in IEEE International Symposium on New Frontiers in Dynamic Spectrum Access Networks (DySPAN '05), Baltimore, Md, USA, Nov. 2005.
- [12] A. Sahai, N. Hoven, S. M. Mishra, and R. Tandra, *Fundamental tradeoffs in robust spectrum sensing for opportunistic frequency reuse* (Mar.2006). [Online]. Available: <http://www.eecs.berkeley.edu/~sahai/Papers/CognitiveTechReport06.pdf>.
- [13] B. Song, F. Roemer, and M. Haardt, "Efficient channel quantization scheme for multi-user MIMO broadcast channels with RBD precoding," in Proc. IEEE Int. Conf.

## Reference

---

- Acoust., Speech and Sig. Proc. (ICASSP 2008), Las Vegas, NV, pp. 2389-2392, March- April 2008.
- [14] B. Suard, G. Xu, H. Liu, and T. Kailath, "Uplink Channel Capacity of Space-Division-Multiple-Access Schemes," *IEEE Trans. Info. Theory*, Vol. 44, No. 4, pp.1468-1476, Jul. 1998.
- [15] C. D. Meyer, *Matrix Analysis and Applied Linear Algebra*, (SIAM, 2000).
- [16] C. E. Shannon, "A mathematical theory of communication," *Bell System Technical Journal*, Vol. 27, pp. 379-423 and 623-656, Jul. and Oct. 1948.
- [17] C. Etielle et al., "Transmitter directed, multiple receivers system using path diversity to equatably maximize throughput," patent, Sep. 10, 2002.
- [18] C. L. Nikias and J. M. Mendel, "Signal processing with higher-order spectrum," *IEEE Signal Processing Magazine*, Vol. 10, pp. 10-37, Jul. 1993.
- [19] C. L. Nikias and M. R. Raghuveer, "Bispectrum estimation: a digital signal processing framework," *Proc. IEEE*, Vol. 75, pp. 869-891, Jul. 1987.
- [20] C. Lv, S. Zhou, Y. Li, and T. Wang, "Low complexity scheduling technique for multiuser MIMO systems," *Vehicular Technology Conference (VTC-2008 Spring)*, Marina Bay, Singapore, pp. 1345-1349, 2008.
- [21] C. Peel, B. Hochwald, and A. Swindlehurst, "A Vector-Perturbation Technique for Near-Capacity Multiantenna Multiuser Communication-Part I: Channel Inversion and Regularization," *IEEE Trans. Commun.*, Vol. 53, No. 1, pp. 195-202, Jan. 2005.
- [22] C. Stevenson, G. Chouinard, Z. D. Lei, W. D. Hu, S. Shellhammer, and W. Caldwell, "IEEE 802.22: the first cognitive radio wireless regional area network standard," *IEEE Communications Magazine*, Vol. 47, No. 1, pp. 130-138, Feb. 2009.
- [23] C. Sun, W. Zhang, and K. B. Letaief, "Cluster-based cooperative spectrum sensing in cognitive radio systems," in *Proceedings of the 18th International Symposium on Personal, Indoor and Mobile Radio Communications (PIMRC '07)*, Athens, Greece, pp. 2511-2515, Sep. 2007.
- [24] C. W. Helstrom, *Statistical Theory of Signal Detection*, Pergamon Press, 2nd edition, 1968.
- [25] C.-B. Chae, D. Mazzarese, and R.W. Heath Jr., "Coordinated beamforming for multiuser MIMO systems with limited feedforward," in *Proc. Asilomar Conf. Sign., Syst. Computers*, Pacific Grove, CA, pp. 1511-1515, Oct.–Nov. 2006.

## Reference

---

- [26] D. Cabric, S. Mishra, and R. Brodersen, "Implementation issues in spectrum sensing for cognitive radios," in Proc. Asilomar Conf. on Signals, Systems and Computers, Pacific Grove, California, USA, Vol. 1, pp. 772–776, Nov. 2004.
- [27] D. Gesbert, M. Kountouris, R. W. Heath Jr. and Chan-Byoung Chae, "Shifting the MIMO Paradigm: From single-user to multiuser communications," IEEE Signal Processing Magazine, Vol. 24, No. 5, pp. 36-46, Oct. 2007.
- [28] D. J. Love, R. W. Heath Jr. and T. Strohmer, "Grassmannian beamforming for multiple-input multiple-output wireless systems," IEEE Trans. Inf. Theory, Vol. 49, No. 10, pp. 2735-2747, Oct. 2003.
- [29] D. Love, R. Heath Jr, V. Lau, D. Gesbert, B. Rao, and M. Andrews, "An Overview of Limited Feedback in Wireless Communication Systems," IEEE J. Sel. Areas Commun., Vol. 26, No. 8, pp. 1341-1365, Oct. 2008.
- [30] D. Tse and P. Viswanath, Fundamentals of Wireless Communication, Cambridge University Press, Cambridge, UK, 2005.
- [31] E. Kreyszig, Advanced Engineering Mathematics, 7th edition, JOHN WILEY & SONS, INC., New York, 1993.
- [32] E. Larsson and P. Stoica, Space-Time Block Coding for Wireless Communications, Cambridge University Press, Cambridge, UK, 2nd edition, 2003.
- [33] E. Telatar, "Capacity of Multi-antenna Gaussian Channels," Euro. Trans. Telecommun., Vol. 10, No. 6, pp. 585-596, Nov. 1999.
- [34] F. Digham, M. Alouini, and M. Simon, "On the energy detection of unknown signals over fading channels," in Proc. IEEE Int. Conf. Commun., Seattle, Washington, USA, Vol. 5, pp. 3575- 3579, May 2003.
- [35] F. Xu, J. Hui, X. Zheng, and Z. Zhou, "Accurate Blind Spectrum Sensing Based on High Order Statistical Analysis in Cognitive Radio System," IEEE Int. Conf. Commun. Tech. App. (ICCTA '09), Beijing, China, pp. 386-391, 2009.
- [36] Federal Communications Commission, "Notice of proposed rule making and order: Facilitating opportunities for flexible, efficient, and reliable spectrum use employing cognitive radio technologies," ET Docket No. 03-322, Dec. 2003. [Online]. Available: [http://hraunfoss.fcc.gov/edocs\\_public/attachmatch/FCC-03-322A1.pdf](http://hraunfoss.fcc.gov/edocs_public/attachmatch/FCC-03-322A1.pdf).
- [37] G. Caire and S. Shamai, "On the achievable throughput of a multiantenna Gaussian broadcast channel," IEEE Trans. Inf. Theory, Vol. 49, No. 7, pp. 1691-1706, Jul. 2003.
- [38] G. G. Raleigh and J. M. Cioffi, "Spatio-temporal coding for wireless communication," IEEE Trans. Commun., Vol. 46, No. 3, pp. 357-366, Mar. 1998.

## Reference

---

- [39] G. G. Raleigh and J. M. Cioffi, "Spatio-temporal coding for wireless communications," Proc. IEEE Global Telecommunications Conf. (GLOBECOM '96), Vol. 3, pp. 1809-1814, Nov. 18-22, 1996.
- [40] G. Ganesan and Y. Li, "Cooperative spectrum sensing in cognitive radio-part II: multiuser networks," IEEE Trans. Wireless Commun., Vol. 6, pp. 2214-2222, Jun. 2007.
- [41] G. Ganesan and Y. Li, "Agility improvement through cooperative diversity in cognitive radio," in Proc. IEEE Global Commun. Conf. (GLOBECOM '05), Vol. 5, pp. 2505-2509, Nov.-Dec. 2005.
- [42] G. Ganesan and Y. Li, "Cooperative spectrum sensing in cognitive radio-part I: two user networks," IEEE Trans. on Wireless Commun., Vol. 6, pp. 2204-2213, Jun. 2007.
- [43] G. J. Foschini and M. J. Gans, "On limits of wireless communications in a fading environment when using multiple antennas," Wireless Pers. Commun., Vol. 6, pp. 311-335, Mar. 1998.
- [44] H. Tang, "Some physical layer issues of wide-band cognitive radio systems," in Proc. IEEE Int. Symposium on New Frontiers in Dynamic Spectrum Access Networks, Baltimore, Maryland, USA, pp. 151-159, Nov. 2005,
- [45] H. Urkowitz, "Energy Detector of Unknown Deterministic Signals," Proc. IEEE, Vol. 55, No. 4, pp. 523-531, Apr. 1967.
- [46] I. Akyildiz, W. Lee, M. Vuran, and S. Mohanty, "NeXt generation/dynamic spectrum access/cognitive radio wireless networks: A survey," Computer Networks, Vol. 50, No. 13, pp. 2127-2159, Sep. 2006.
- [47] I. Mitola, J. and J. Maguire, G. Q., "Cognitive radio: making software radios more personal," IEEE Personal Commun. Mag., Vol. 6, No. 4, pp. 13-18, Aug. 1999.
- [48] J. G. Proakis, Digital Communications, McGraw-Hill, New York, 4th ed., 2001.
- [49] J. Ma and Y. Li, "Soft combination and detection for cooperative spectrum sensing in cognitive radio networks," in Proc. IEEE Global Communications Conference (GlobeCom '07), Washington, DC, USA, pp. 3139-3143, Nov. 2007.
- [50] J. Mitola, "Cognitive radio: An integrated agent architecture for software defined radio," Doctor of Technology, Royal Inst. Technol. (KTH), Stockholm, Sweden, 2000.
- [51] J. Unnikrishnan and V. V. Veeravalli, "Cooperative sensing for primary detection in cognitive radio," IEEE J. Sel. Topics in Signal Process., Vol. 2, No. 1, pp. 18-27, 2008.

## Reference

---

- [52] J. Winters, "On the Capacity of Radio Communication Systems with Diversity in a Rayleigh Fading Environment," *IEEE J. Sel. Areas in Commun.*, Vol. SAC-5, No. 5, pp. 871-878, Jun. 1987.
- [53] J. M. Mendel, "Tutorial on Higher-Order Statistics (Spectra) in Signal Processing and System Theory: Theoretical Results and Some Applications," *Proc. IEEE*, Vol. 19, No. 3, pp. 279-305, Mar. 1991.
- [54] K. K. Mukkavilli, A. Sabharwal, E. Erkip, and B. Aazhang, "On beamforming with finite rate feedback in multiple-antenna systems," *IEEE Trans. Inf. Theory*, Vol. 49, No 10, pp. 2562-2579, Oct. 2003.
- [55] L. U. Choi and R. D. Murch, "A transmit precoding technique for multiuser MIMO systems using a decomposition approach," *IEEE Trans. Wireless Commun.*, Vol. 3, No. 1, pp. 20-24, Jan. 2004.
- [56] L. Jin, Z. Hu and X. Gu, "A New Scheduling Algorithm with Low Complexity for Multiuser Multiple-Input Multiple-Output Downlink System," 2009 International Conference on Wireless Communications and Signal Processing (WCSP 2009), Nanjing, China, pp. 1-5, Nov. 2009.
- [57] L. Jin, X. Gu, and Z. Hu, "A Novel Volume-Based Scheduling Scheme for Multiuser Multiple-Input Multiple-Output Downlink System," 2010 IEEE Radio & Wireless Symposium, Sheraton hotel, New Orleans, LA, pp. 448-451, Jan. 2010.
- [58] L. Jin, Z. Hu, X. Gu, "A New Signal Detection Scheme Based on Free Probability Theory for Multiple-Input Multiple-Output Cognitive Radio Systems," in Proceedings of the 2010, 7th International Symposium on Wireless Communication Systems (ISWCS' 10), University of York, York, UK, pp.746-750, Sep. 2010.
- [59] L. Jin, Z. Hu, X. Gu, "Analysis of Sum-rate Gain for Multiuser MIMO Downlink System with Limited Feedback and Feedback Resource Constraint," European Microwave Week 2010, CNIT La Défence, Paris, France, in Proceeding of the 3rd European Wireless Technology conference, 2010 European, pp 73-76, Issue date: 27-28 Sep. 2010.
- [60] L. Jin and Z. Hu, "Spectrum Sensing Using Higher-Order Statistics and Receive Diversity and Cooperative Detection in SIMO Cognitive Radio System," 2011 IET International Communication Conference on Wireless Mobile & Computing ( IET CCWMC2011), Shanghai, China, pp. 247-253, 14-16 Nov. 2011.
- [61] L. Jin, X. Gu and Z. Hu, "Low Complexity Scheduling Strategy for Wireless Multiuser Multiple-Input Multiple-Output Downlink System," *IET Communication Journal*, Vol. 5, Iss. 7, pp. 990-995, May 2011.

## Reference

---

- [62] M. Cooper and M. Goldberg, "Intelligent antennas: Spatial division multiple access," *ArrayComm: Annu. Rev. Commun.*, pp. 999–1002, 1996.
- [63] M. Costa, "Writing on dirty paper," *IEEE Trans. Inf. Theory*, Vol. 29, No. 3, pp. 439-441, May 1983.
- [64] M. Gudmundson, "Correlation model for shadow fading in mobile radio systems," *Elec. Lett.*, Vol. 27, No. 23, pp. 2145-2146, Nov. 1991.
- [65] M. J. Lehtomäki, M. Juntti, H. Saarnisaari, and S. Koivu, "Threshold setting strategies for a quantized total power radiometer," *IEEE Signal Proc. Lett.*, Vol. 12, No. 11, pp. 796–799, Nov. 2005.
- [66] M. J. Feuerstein, K. L. Blackard, T. S. Rappaport, S. Y. Seidel, and H. H. Xia, "Path Loss, Delay Spread, and Outage Models as Functions of Antenna Height for Microcellular System Design," *IEEE Trans. Veh. Tech.*, Vol. 43, No. 3, pp. 487-498, Aug. 1994.
- [67] M. Jankiraman, *Space-time codes and MIMO systems*, ARTECH House, INC., Norwood, MA, 2004.
- [68] M. Jiang and L. Hanzo, "Multiuser MIMO-OFDM for Next-Generation Wireless Systems," *Proc. IEEE*, Vol. 95, No. 7, pp.1430-1469, Jul. 2007.
- [69] M. Kountouris, David Gesbert, and T. Sälzer, "Enhanced Multiuser Random Beamforming: Dealing With the Not So Large Number of Users Case," *IEEE J. Sel. Areas Commun.*, Vol. 26, No. 8, pp. 1536-1545, Oct. 2008.
- [70] M. Sharif and B. Hassibi, "A Comparison of Time-Sharing, DPC, and Beamforming for MIMO Broadcast Channels with Many Users," *IEEE Trans. on Commun.*, Vol. 55, No. 1, pp. 11-15, Jan. 2007.
- [71] M. Sharif and B. Hassibi, "On the capacity of MIMO broadcast channel with partial side information," *IEEE Trans. Inf. Theory*, Vol. 51, No. 2, pp. 506–522, Feb. 2005.
- [72] M. Trivellato, F. Boccardi and H. Huang, "On Transceiver Design and Channel Quantization for Downlink Multi-user MIMO Systems with Limited Feedback," *IEEE J. Select. Areas Commun.*, Vol.26, No. 8, pp. 1494-1504, Oct. 2008.
- [73] N. Benvenuto and G. Cherubini, *Algorithms for Communications Systems and their Applications*, John Wiley & Sons, Ltd, Chichester, England, UK, 2002.
- [74] N. Benvenuto, E. Conte, S. Tomasin, and M. Trivellato, "Joint Low-Rate Feedback and Channel Quantization for the MIMO Broadcast Channel," *Proc. IEEE Africon'07*, Windhoek, Namibia, pp. 1-7, Sep. 2007.

## Reference

---

- [75] N. Jindal and A. Goldsmith, "Dirty-paper coding versus TDMA for MIMO broadcast channel," *IEEE Trans. Info. Theory*, Vol. 51, No. 5, pp. 1783-1794, May 2005.
- [76] N. Jindal, "MIMO Broadcast Channels with Finite-Rate Feedback," *IEEE Trans. Inf. Theory*, Vol. 52, No. 11, pp. 5045-5060, Nov. 2006.
- [77] N. Jindal, U. Mitra, and A. Goldsmith, "Capacity of ad-hoc networks with node cooperation," in *Proc. IEEE Int. Symp. Inf. Theory*, p. 271, Jun. 2004.
- [78] N. Ravindran and N. Jindal, "Limited Feedback-Based Block Diagonalization for the MIMO Broadcast Channel," *IEEE J. Sel. Areas Commun.*, Vol. 26, No. 8, pp. 1473-1482, Oct. 2008.
- [79] National Telecommunications and Information Administration, "United States Frequency Allocations – The Radio Spectrum," Oct. 2003. [Online]. Available: <http://www.ntia.doc.gov/osmhome/allochrt.pdf>.
- [80] Ø. Ryan and M. Debbah, "Free Deconvolution for Signal Processing Applications," *Inf. Theory*, 2007, *IEEE International Symposium on (ISIT2007)*, Nice, France, pp. 1846-1850, Jun. 2007.
- [81] Ø. Ryan and M. Debbah, "Multiplicative free convolution and information-plus-noise type matrices," 2007. [Online]. Available: <http://arxiv.org/abs/math.PR/0702342>. Feb. 2007.
- [82] O. S. Shin and K.B. Lee, "Antenna assisted round-robin scheduling for MIMO cellular systems," *IEEE Commun. Letters*, Vol. 7, No. 3, pp. 109-111, Mar. 2003.
- [83] Ofcom, "United Kingdom Frequency Allocation Table," issue no. 15, 2008. [online]. Available: <http://www.ofcom.org.uk/radiocomms/isu/ukfat/ukfat08.pdf>.
- [84] Ofcom, "Cognitive Radio," [Online]. Available: [http://www.ofcom.org.uk/research/technology/research/emer\\_tech/cograd/](http://www.ofcom.org.uk/research/technology/research/emer_tech/cograd/).
- [85] P. Ding, D. Love, and M. Zoltowski, "Multiple antenna broadcast channels with shape feedback and limited feedback," *IEEE Trans. Signal Process.*, Vol. 55, No. 7, pp. 3417-3428, Jul. 2007.
- [86] P. K. Varshney, *Distributed Detection and Data Fusion*, Springer, New York, NY, USA, 1996.
- [87] P. Vishwanath and D. N. C. Tse, "Sum capacity of the vector Gaussian broadcast channel and uplink-downlink duality," *IEEE Trans. Inf. Theory*, Vol. 49, No. 8, pp. 1912-1921, Aug. 2003.

## Reference

---

- [88] P. Viswanath, D. Tse, and R. Laroia, "Opportunistic beamforming using dumb antennas," *IEEE Trans. Inf. Theory*, Vol. 48, No. 6, pp. 1277-1294, Jun. 2002.
- [89] Q. H. Spencer, A. L. Swindlehurst, and M. Haardt, "Zeroforcing methods for downlink special multiplexing in multi-user MIMO channels," *IEEE Trans. Signal Process.*, Vol. 53. No.2, pp. 461-471, Feb. 2004.
- [90] R. H. Clark, "A Statistical Theory of mobile-Radio Reception," *Bell Systems Technical Journal*, Vol. 47, pp. 957-1000, 1987.
- [91] R. S. Ranasinghe, L. Andrew, D. A. Hayes, and D. Everitt, "Scheduling disciplines for multimedia WLANs: Embedded round robin and wireless dual queue," *IEEE Int. Conf. Commun. (ICC 2001)*, Helsinki, Finland, Vol. 4, pp. 1243-1248, Jun. 2001.
- [92] R. Zakhour and D. Gesbert, "A Two-Stage Approach To Feedback Design In Multi-user MIMO Channels With Limited Channel State Information," in the 18th Annual IEEE International Symposium on Personal, Indoor and Mobile Radio Communications (PIMRC'07), Athens, Greece, pp. 1-5, Sep. 2007.
- [93] Roke, "The UK Frequency Allocations," 2007. [Online]. Available: <http://www.roke.co.uk/resources/datasheets/UK-Frequency-Allocations.pdf>.
- [94] S. Alamouti, "A simple transmit diversity technique for wireless communications," *IEEE J. Sel. Areas Comm.*, Vol. 16, No. 8, pp. 1451-1458, Oct. 1998.
- [95] S. Haykin, "Cognitive Radio: Brain-Empowered Wireless Communication," *IEEE J. Sel. Areas Comm.*, Vol. 23, No. 2, pp. 201-220, Feb. 2005.
- [96] S. M. Mishra, A. Sahai, and R. W. Brodersen, "Cooperative sensing among cognitive radios," in *Proc. IEEE Int. Conf. Commun.*, Vol. 4, pp. 1658-1663, Jun. 2006.
- [97] S. Vishwanath and N. Jindal, and A. J. Goldsmith, "Duality, achievable rates, and sum-rate capacity of Gaussian MIMO broadcast channels," *IEEE Trans. Inf. Theory*, Vol. 49, No. 10, pp. 2658-2568, Oct. 2003.
- [98] T. Cover and J. Thomas, *Elements of Information Theory*, John Wiley & Sons, INCNew York, 2nd edition, 1991.
- [99] T. Lo, "Maximal ratio transmission," *IEEE Trans. Commun.*, Vol. 47, No. 10, pp. 1458-1461, Oct. 1999.
- [100] T. Yoo and A. Goldsmith, "On the optimality of multiantenna broadcast scheduling using zero-forcing beamforming," *IEEE J. Sel. Areas Commun.*, Vol. 24, No. 3, pp. 528-541, Mar. 2006.

## Reference

---

- [101] T. Yoo, N. Jindal, and A. Goldsmith, "Multi-Antenna Downlink Channels with Limited Feedback and User Selection," *IEEE J. Sel. Areas Commun.*, Vol. 25, No. 7, pp. 1478-1491, Sep. 2007.
- [102] T. Yücek and H. Arslan, "Spectrum characterization for opportunistic cognitive radio systems," in *Proc. IEEE Military Commun. Conf.*, Washington, D.C., USA, pp. 1-6, Oct. 2006.
- [103] T. S. Rappaport, *Wireless Communications Principles and Practice*, Prentice Hall PTR, New Jersey, 2nd edition, 2002.
- [104] Tevfik Yücek and Hüseyin Arslan, "A Survey of Spectrum Sensing Algorithms for Cognitive Radio Applications," *IEEE Communications. Surveys & Tutorials*, Vol. 11, No. 1, pp. 116-130, first quarter 2009.
- [105] V. Aalo and R. Viswanathan, "Asymptotic performance of a distributed detection system in correlated Gaussian noise," *IEEE Trans. Signal Process.*, Vol. 40, pp. 211-213, 1992.
- [106] V. Erceg, L. J. Greenstein, S. Y. Tjandra, S. R. Parkoff, A. Gupta, B. Kylic, A. A. Julius, and R. Bianchi, "An empirically based path loss model for wireless channels in suburban environments," *IEEE J. Sel. Areas Commun.*, Vol. 17, no.7, pp. 1205-11, Jul 1999.
- [107] W. Santipach and M. Honig, "Signature optimization for CDMA with limited feedback," *IEEE Trans. Info. Theory*, Vol. 51, No. 10, pp. 3475-3492, Oct. 2005.
- [108] W. Santipach and M. Honig, "Asymptotic capacity of beamforming with limited feedback," in *Proc. IEEE Int. Symp. Information Theory*, Chicago, IL, pp. 290, Jun./Jul. 2004.
- [109] W. Santipach, "Asymptotic performance of DS-CDMA with linear MMSE receiver and limited feedback," in *Proc. IEEE Int. Conf. on Commun. (ICC 08)*, Beijing, China, pp. 1393-1397, May 2008.
- [110] W. Wiroonsak and M. Honig, "Capacity of a Multiple-Antenna Fading Channel With a Quantized Precoding Matrix," *IEEE Trans. Inf. Theory*, Vol. 55, No. 3, pp. 1218-1234, Mar. 2009.
- [111] W. Yu, and J. M. Cioffi, "Sum Capacity of Gaussian Vector Broadcast Channels," *IEEE Trans. Inf. Theory*, Vol. 50, No. 9, pp. 1875-1892, Sep. 2004.
- [112] Wireless Innovation Alliance. [Online]. Available: <http://www.wirelessinnovationalliance.com/2008>.
- [113] Y. Linde, A. Buzo, and R. M. Gray, "An algorithm for vector quantizer design," in *Proc. IEEE Trans. Commun.*, Vol. 50, No. 1, pp. 195-202, Jan. 1980.

## Reference

---

- [114] Y. Sun, Y. Liu, and X. Tan, "Spectrum Sensing for Cognitive Radio based on Higher-Order Statistics," 4th International Conference on Wireless Communications, Networking and Mobile Computing, WiCOM '08, Dalian, China, pp. 1-4, 12-14 Oct. 2008.
- [115] Y. Zeng, Y. Liang, A. Hoang, and R. Zhang, "A review on Spectrum Sensing for Cognitive Radio: Challenges and Solutions," EURASIP Journal on Advances in Signal Processing, Volume 2010, 2010.
- [116] Z. Quan, S. Cui, and A. H. Sayed, "Optimal linear cooperation for spectrum sensing in cognitive radio networks," IEEE J. Sel. Topics in Signal Process., Vol. 2, No. 1, pp. 28-40, Feb. 2008.
- [117] Z. Shen, R. Chen, J. Andrews, R. Heath, and B. Evans, "Low complexity user selection algorithms for multi-user MIMO Systems with block diagonalization," IEEE Trans. Signal Process., Vol. 54, No. 9, pp. 3658-3663, Sep. 2006.
- [118] Z. Tian and G. B. Giannakis, "A wavelet approach to wideband spectrum sensing for cognitive radios," in Proceedings of the 1st International Conference on Cognitive Radio Oriented Wireless Networks and Communications (CROWNCOM '06), Mykonos, Greece, pp. 1-5, June 2006.